ABUNDANCE AND DISTRIBUTION OF MUSHROOM CORALS (SCLERACTINIA: FUNGIIDAE) ON A CORAL REEF AT EILAT, NORTHERN RED SEA

S. Goffredo and N. E. Chadwick-Furman

ABSTRACT

Mushroom corals (Scleractinia: Fungiidae) are important components of Indo-Pacific coral reefs, yet little is known about their patterns of abundance and distribution in the Red Sea. On a fringing reef at Eilat, northern Red Sea, mushroom corals were found to be common on the reef flat and shallow slope at <10 m depth, where they occurred at densities of up to 15 individuals m^{-2}, but were rare on the mid to deep reef slope at 10–50 m depth. Eleven species were observed, a 27% increase in the recorded species diversity of this coral family at Eilat. Individuals of two species were limited to the reef flat and shallow reef slope, and members of five other species also occurred mainly on the shallow slope, but had wide depth ranges. Individuals of an additional four mushroom coral species were found mainly on the lower reef slope at low densities. In shallow water, most fungiids occurred in shaded reef habitats such as caves or holes, while at >20 m depth, they mainly occupied open, unshaded habitats. This study documents differences in habitat use between species of mushroom corals on a fringing reef, and substantial migration by the adult free-living polyps of some species out of shaded reef habitats, down the reef slope, and onto soft substratum.

Mushroom corals comprise one of the more diverse families of reef-building corals in the tropical Indo-Pacific region, with 41 known species in the family Fungiidae (Hoeksema 1992, 1993a,b). They are unique among scleractinians in that the individuals of most species are able to move from one habitat to another during their benthic phase. Juvenile mushroom corals (= the anthocaulus stage) grow attached to hard substratum, but after reaching a few cm diameter, the cap-shaped polyps of most species actively dissolve their skeletal attachment to the stalk-like base (Yamashiro and Yamazato, 1996, and references therein), detach from the reef, and become free-living polyps (= the anthocyathus stage) that may migrate onto soft substratum or down the reef slope (Chadwick-Furman and Loya, 1992). The adults of most species form solitary, mobile disks that are among the largest known scleractinian coral polyps (Hoeksema, 1989). The free-living adults sexually produce planktonic planula larvae that settle and metamorphose into attached anthocaulus polyps, which in turn may successively bud off a limited number of anthocyathi (Yamashiro, 1992), thus forming small clones of unconnected, mobile adults (Wells, 1966; Hoeksema, 1989). In addition, the members of some species reproduce asexually from adult polyps after injury (Krupp et al., 1992; Kramarsky-Winter and Loya, 1998). Members of a single clone may disperse over the reef or, if the source anthocaulus is inside a hole or reef depression, may remain aggregated (Hoeksema, 1988; Chadwick-Furman and Loya, 1992). Young fungiid corals suffer high mortality immediately after detachment from the stalk, so that only a small percentage of all anthocyathi that originally detach eventually reach sexual maturity and maximal adult size (Chadwick-Furman et al., 1999). Members of some fungiid genera (*Cantharellus*, *Lithophyllon* and *Podabacia*) have not developed the mobile anthocyathus stage, and remain in the sessile phase during their entire lifespan (Hoeksema, 1989).

Fungiid corals are conspicuous and common members of many Indo-Pacific coral reefs. They contribute to reef-building, and have recently been discovered to construct large patch reefs (Littler et al., 1997). The mobile adults are important colonizers of sandy substratum, in contrast to most other scleractinians which are confined to hard substratum (Chadwick-Furman and Loya, 1992). When fungiid corals die, their calcareous skeletons may remain on the sandy bottom and serve as a base for the adherence of the larvae of other corals, thus becoming nuclei for the formation of new patch reefs and for the extension of coral reefs over sandy areas (Sheppard, 1981).

Little is known about patterns of abundance and distribution on coral reefs by members of this family. Evidence of segregation among species by depth has been found on reefs in Indonesia (Hoeksema, 1990) and at Fanning Island in the central Pacific (Maragos, 1974). However, almost no quantitative information is available concerning their abundance or spatial distribution in the Red Sea. A diverse assemblage of 21 mushroom coral species occurs on Red Sea coral reefs (Sheppard and Sheppard, 1991), and they are conspicuous members of the reef-building coral fauna of Eilat (Loya and Slobodkin, 1971; Chadwick-Furman and Loya, 1992). Twenty of these species also occur at the center of scleractinian coral diversity in Indonesia, and one (*Cantharellus doederleini*) is endemic to the Gulf of Aqaba in the northern Red Sea (Hoeksema, 1989).

We present here information on the abundance, distribution, and habitat use of mushroom corals on a fringing reef at Eilat, northern Red Sea. We increase the number of fungiid species recorded at Eilat to 11, and extend the range of one species (*Fungia paumotensis*) approximately 700 km north from its previously known limit in the central Red Sea (Hoeksema, 1989, 1993b). Our observations document that the detached polyps of some mushroom corals migrate down the reef slope, onto sand and out of reef caves, probably due in part to low light levels in caves at depth.

This study presents the first comprehensive description of distributional patterns and habitat use of mushroom corals on a Red Sea coral reef. As such, it contributes important new information to understanding the biology of solitary reef-building corals.

Materials and Methods

The present study was conducted during January to April 1996, at Eilat, Gulf of Aqaba, northern Red Sea. We examined fungiid corals at a fringing coral reef site known locally as the Japanese Gardens. The depth profile and overall coral community structure at this site have been described by Loya and Slobodkin (1971). We quantified the abundance of fungiid corals within a series of 1-m^2 quadrats (n = 25) in a band parallel to shore at each of 12 depths on this reef: on the inner edge of the reef flat, on the outer edge of the reef flat (both at 1 m depth), and at 2, 3, 6, 9, 12, 15, 21, 27, 33, and 40 m depth on the reef slope (after Hoeksema, 1990, 1991). We also made qualitative observations on the presence of mushroom corals outside of the quadrats at all depths, especially on the deep reef slope at 41–55 m depth where quadrats were not examined.

Within each quadrat, we identified all mushroom corals to species after Hoeksema (1989). Individuals of *Fungia (Danafungia) horrida* and *F. (Danafungia) scruposa* have both been found to occur at Eilat, and differ only in the presence of perforations in the corallum wall (Chadwick-Furman and Loya, 1992). We were unable to distinguish this trait on live polyps in the field, so the corals of these two species were grouped as *F. (Danafungia)* spp. (after Chadwick-Furman and Loya, 1992). For each mushroom coral observed, we determined the type of substratum occupied (hard vs soft), life history phase (attached anthocaulus vs detached anthocyathus stage), and microhabitat (shaded vs open habitat). Shaded habitats were quantified as those exposed to <10% (range

= 2.0–9.8%) of the light level measured in adjacent open reef habitats, using a submersible light meter (LiCor Instruments, San Diego, California). We also estimated the percent cover of hard substratum within each quadrat, and the percent coveroccupied by fungiid corals, to the nearest 5%.

Results

We observed 11 species of mushroom corals at our study site in Eilat, northern Red Sea (Figs. 1,2). They varied widely in both their overall abundance and in depth distribution, with the members of most species occurring over a wide depth range on the reef slope (Fig. 2). As a group, mushroom corals were most common on the reef flat and shallow slope to 6 m depth, where they reached a maximal abundance of approximately 15 ind m^{-2} and covered up to 5% of the substratum (Fig. 3). They were rare on the mid to deep slope, even though % cover of hard substratum on the deep slope was high (Fig. 3).

Examination of the depth distribution of attached versus free-living phases revealed that attached juveniles occurred almost entirely on the shallow reef slope at <10 m depth, while the adult free-living individuals of some species also were found deeper on the reef (Fig. 4). In most fungiids, free-living adults were more common than the attached juveniles (Fig. 4B–E), except in *Fungia scutaria* (Fig. 4A). Both phases of *F. scutaria* occurred almost entirely on the reef flat at this site, with a median recorded depth of only 1 m (Figs. 1A, 2). On the outer reef flat, they reached abundances of up to eight attached plus four free-living ind m^{-2} (Fig. 4A). Of 469 *F. scutaria* individuals, only 1.1% were found at >3 m depth on the reef (Fig. 4A). Individuals of the elongate fungiid *Ctenactis echinata* (Fig. 1B) also were limited to shallow water at this site, and were not found at >8 m depth even during extensive qualitative surveys down to 55 m depth on the reef slope (Fig. 2). They were common at 2–6 m depth, where they occurred at an abundance of up to two ind m^{-2} (Fig. 4B). Members of five additional species of mushroom corals (*F. fungites*, *F. granulosa*, two species of *F. (Danafungia)*, and *Herpolitha limax*) all had wide depth ranges, but also were most common on the shallow slope, with median depths at 2–9 m (Fig. 2). Of these, members of the two species grouped together under *F. (Danafungia)* spp. were the most abundant (Fig. 2), with up to four ind m^{-2} at 2–3 m depth (Fig. 4E). Both *F. fungites* and *F. granulosa* also were common (Fig. 2), occurring at approximately three and one individual m^{-2} respectively on the shallow reef slope (Fig. 4C,D). The elongate, polystomatous fungiid *Herpolitha limax* was rare at our study site, with only six individuals observed at shallow depths inside the quadrats, and other individuals found scattered deeper on the reef slope (Figs. 1H and 2). Members of the four final species of mushroom corals (*Cantharellus doederleini*, *Fungia costulata*, *F. paumotensis* and *Podabacia crustacea*) were relatively rare, and occurred mainly on the deep reef slope (Figs. 1E,G,2). Only *Cantharellus doederleini* occurred in high enough numbers to assess depth-abundance patterns (Fig. 2). Individuals of this permanently-attached, endemic fungiid were most common at >15 m depth, occurring at approximately 0.3 ind m^{-2} on the deep reef slope (Fig. 4F).

All fungiids in the attached phase were observed to occur on hard substratum. Similarly, most free-living individuals also remained on hard substratum (= 99.5% of *Fungia scutaria* (n = 186), 93.7% of *F. fungites* (n = 190), 88.0% of two species of *F. (Danafungia)* (n = 333), and 93.1% of *C. echinata* (n = 102)). Only in *F. granulosa*, a substantial proportion of free-living polyps (=35.6%, n = 118) moved off the reef and onto the surrounding soft substratum (Fig. 1C).

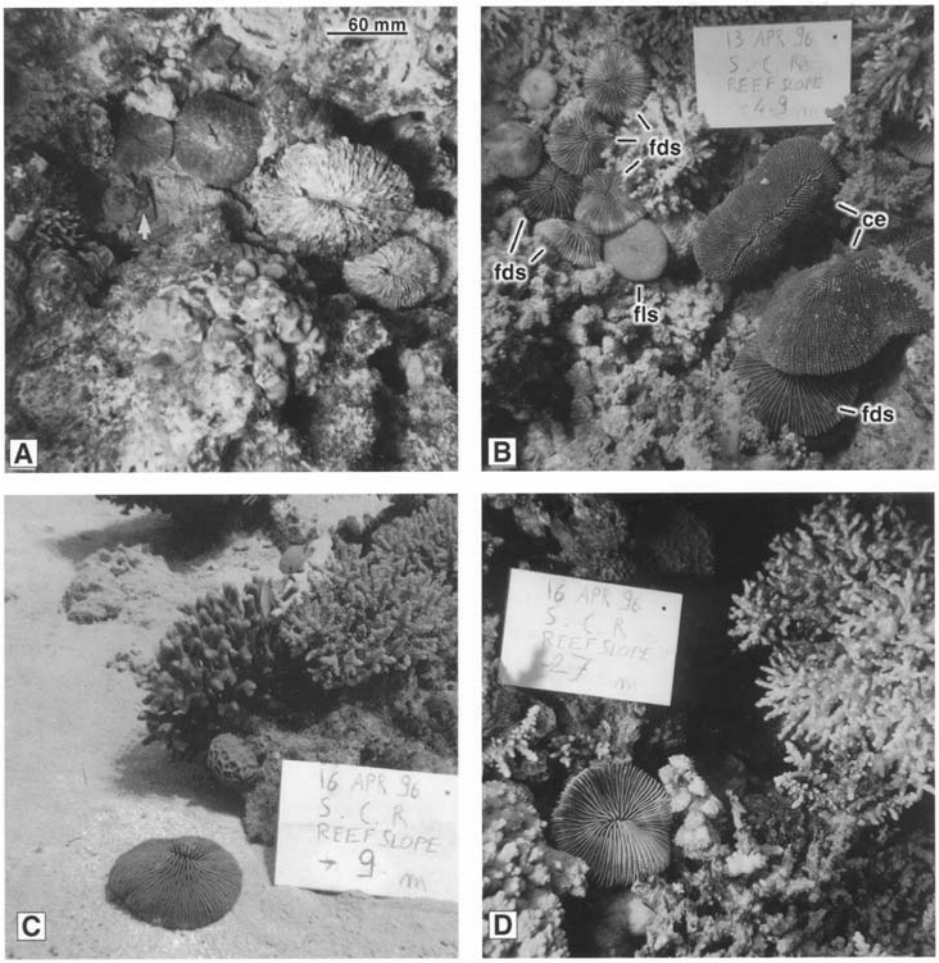

Figure 1. Mushroom corals and typical habitats on a fringing reef at Eilat, northern Red Sea. Scale is indicated by a white slate (15 cm long × 10 cm wide) or a scale bar (6 cm long). (A) Solitary polyps of *Fungia scutaria* in a depression on the reef flat at 1 m depth. Note small attached polyps (arrow) and dead adult corals. (B) Mixed aggregation on hard substratum on the shallow reef slope at 4.9 m depth (fds = *F. (Danafungia)* spp., fls = *F. scutaria*, ce = *Ctenactis echinata*). (C) Patch reef and free-living polyp of *Fungia granulosa* on soft substratum on the mid reef slope at 9 m depth. (D) Free-living polyp of *F. (Danafungia)* sp. on hard substratum on the deep reef slope at 27 m depth. ***(opposite page)*** (E) Large, permanently-attached individual of *Podabacia crustacea* on the deep reef slope at 40 m depth. Colony = 60 cm diameter. (F) Mixed aggregation on the deep reef slope at 50 m depth (fds = *Fungia (Danafungia)* spp.; fff = *F. fungites*, fsp = *Fungia* sp.). (G) Two free-living polyps of *F. paumotensis* on the deep reef slope at 45 m depth. (H) A free-living polystomatous individual of *Herpolitha limax* (hl) and a polyp of *Fungia fungites* (fff) on coral rubble on the deep reef slope at 55 m depth.

At shallow depths of <20 m, most attached individuals occurred in shaded reef habitats such as reef caves or holes (Table 1). In contrast, the proportion of free-living individuals that remained in shaded habitats varied widely between species (Table 1). In both *Ctenactis echinata* and *F. granulosa*, a substantial proportion of the individuals (approx 65 and 45%, respectively) moved out into open, unshaded reef areas once they became free-living (Table 1). Individuals of only *F. (Danafungia)* spp. and *C. doederleini* occurred at

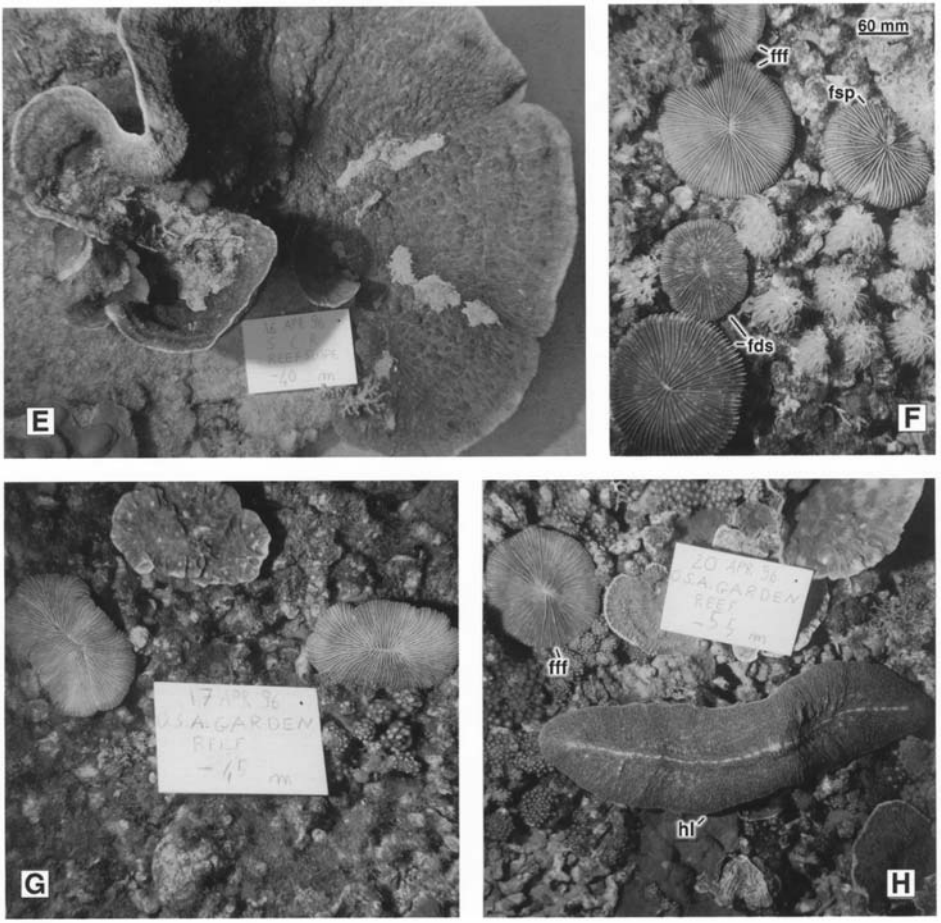

sufficient abundance on the deep reef slope to assess changes in the use of shaded habitat with depth (Fig. 4E,F). In these corals, significantly lower proportions of polyps were found in shaded habitats in deep than in shallow areas of the reef (Table 1) (G test of independence, G = 21.77, 17.31 and 37.97 for *C. doederleini*, attached and free-living *Fungia (Danafungia)* spp., respectively, $P < 0.01$ for all). Fungiids did not abruptly change their habitat use at a given depth, but appeared to gradually decrease the proportion of polyps occurring in shaded habitats with depth on the reef (Fig. 5). As a group, mushroom corals in shaded habitats decreased from 74.6% of individuals at <10 m depth to only 17.2% of individuals at >30m depth (Fig. 5).

Discussion

We demonstrate here that mushroom corals varied widely among species in their patterns of depth distribution, abundance and habitat use on a coral reef in the Red Sea. These differences may relate to variation between the species in their morphologies and life history strategies. The observed patterns of space use also indicate that the free-living

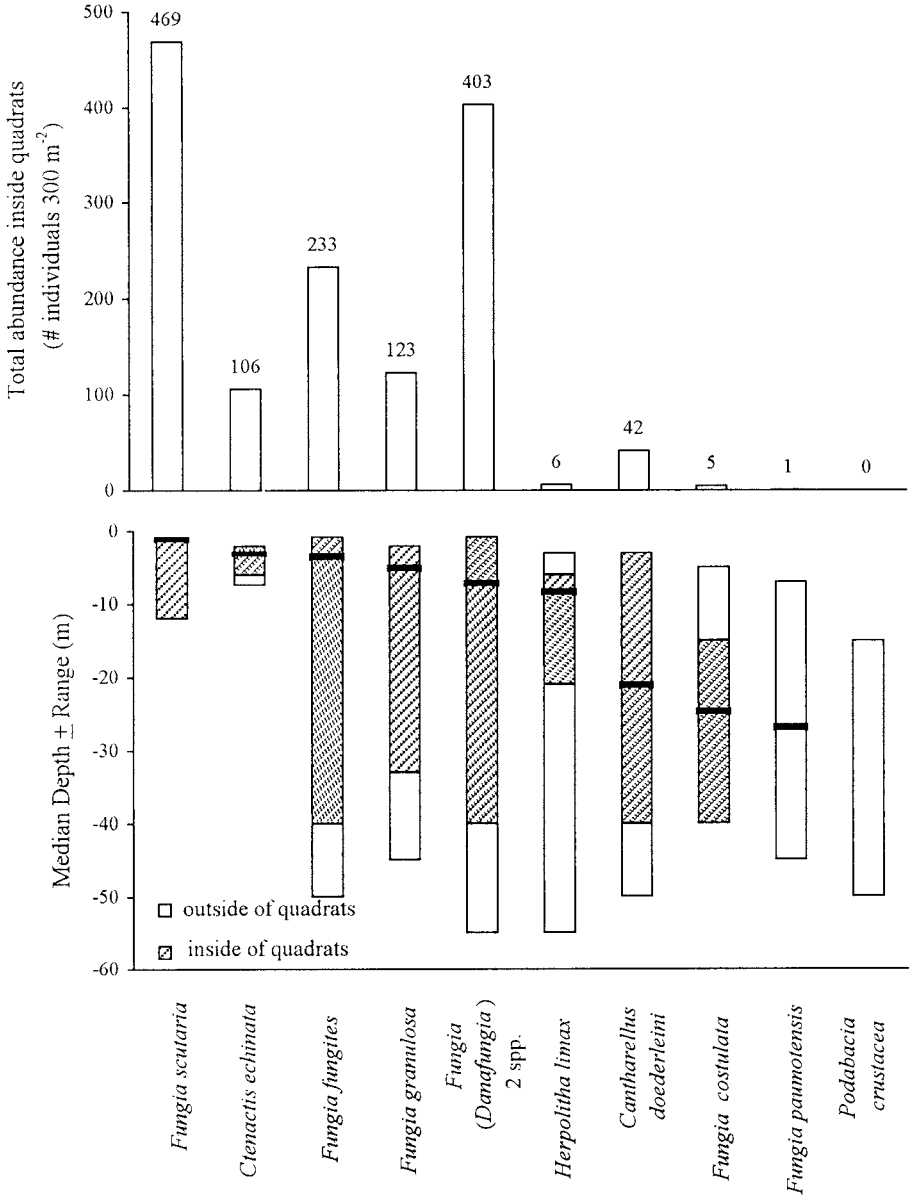

Figure 2. Depth ranges and relative abundances of members of 11 species of mushroom corals on a fringing reef at Eilat, northern Red Sea. Coral abundance was quantified at 0–40 m depth inside quadrats, and the presence of each species also was recorded outside of quadrats at 0–55 m depth. A total area of 300 m^2 was examined inside quadrats (= 1-m^2 quadrats [n = 25] per depth × 12 depths examined).

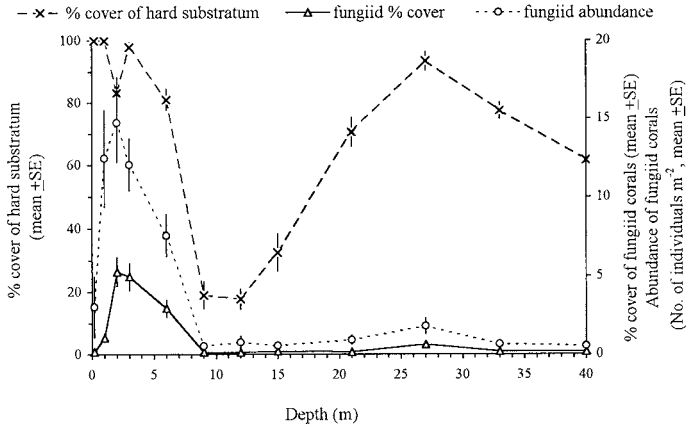

Figure 3. Variation in the percent cover of hard substratum, and the percent cover and abundance of mushroom corals with depth on a fringing coral reef at Eilat, northern Red Sea. n = 25 quadrats of 1-m^2 each were examined at each depth. For clarity, the inner reef flat is presented as 0 m depth and the outer reef flat as 1 m depth.

individuals of some species migrated down the reef slope, onto soft substratum, and out of shaded areas on the reef slope (Figs. 4,5, Table 1). The ability of fungiid corals to actively and passively migrate on the reef has been documented previously (Hoeksema, 1988; Chadwick-Furman and Loya, 1992). Several species of fungiids also are known to move actively toward light (Yamashiro and Nishihira, 1995), a form of positive phototaxis that may explain in part their increased occurrence in open rather than shaded habitats following the end of the attached phase during their life history (Table 1). The present study is the first detailed analysis of abundance and distributional patterns of mushroom corals on a Red Sea coral reef, and substantially increases the recorded species diversity for this group at Eilat.

We found 11 species of mushroom corals at Eilat, in contrast to only six species recorded by Loya and Slobodkin (1971), and eight by Chadwick-Furman and Loya (1992). This increase in observed diversity is due in part to a recent taxonomic revision of the family Fungiidae (Hoeksema, 1989), and also likely due to deep water research on the members of rare species (Fig. 2). Our observation of *F. paumotensis* is the first confirmed record of this species in the Gulf of Aqaba, and extends its range from Yambu, Saudi Arabia in the central Red Sea, a northward extension of 700 km (Hoeksema, 1989, 1993b). The total diversity of fungiid corals in the Gulf of Aqaba, now 15 species, is remarkably high, given the position of this area at the northwestern edge of the Indo-Pacific region, far from the center of scleractinian coral diversity in southeast Asia, where 39 fungiid species occur (Hoeksema, 1992). The relatively high number of fungiid corals at Eilat corresponds to a high diversity of scleractinian corals in general at this site (Loya, 1972).

The depth distributions of fungiids recorded here may relate to some unique features of our study site. For example, their low abundance on the mid reef slope corresponded to a lack of hard substratum and an abundance of sandy habitat at this depth (Fig. 3). Other reefs that do not display such wide variation in hard substratum availability with depth might have different zonation patterns of fungiid corals. Some mushroom corals are able to colonize sandy substratum, but the abundance of most species is higher on reef slopes

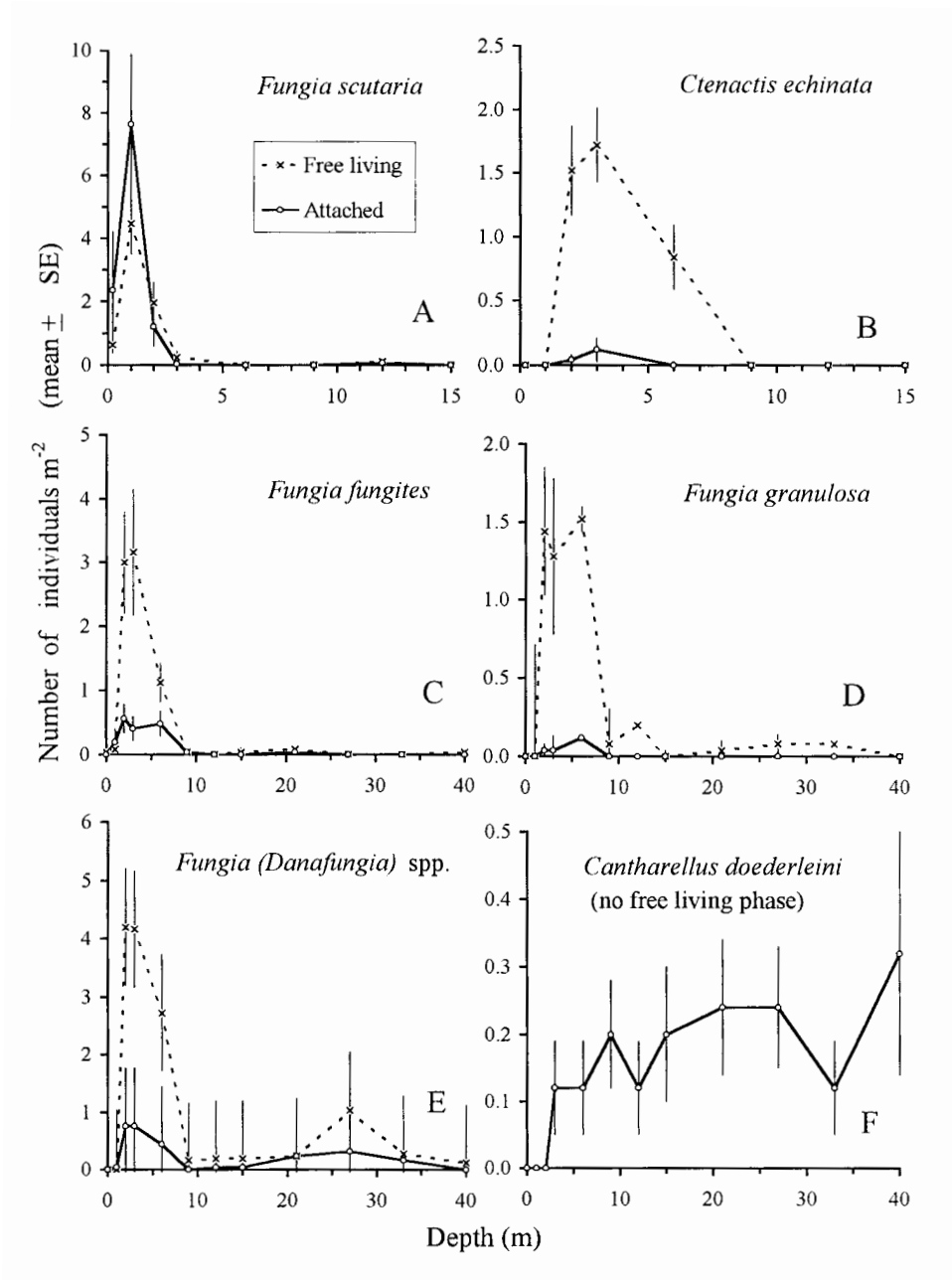

Figure 4. Variation in the abundance of attached versus free-living stages with depth among common species of fungiid corals on a fringing reef at Eilat, northern Red Sea. n = 25 quadrats of 1-m^2 each were examined at each depth. For clarity, inner reef flat presented as 0 m depth and outer reef flat as 1 m depth. Note the differences in scale between graphs.

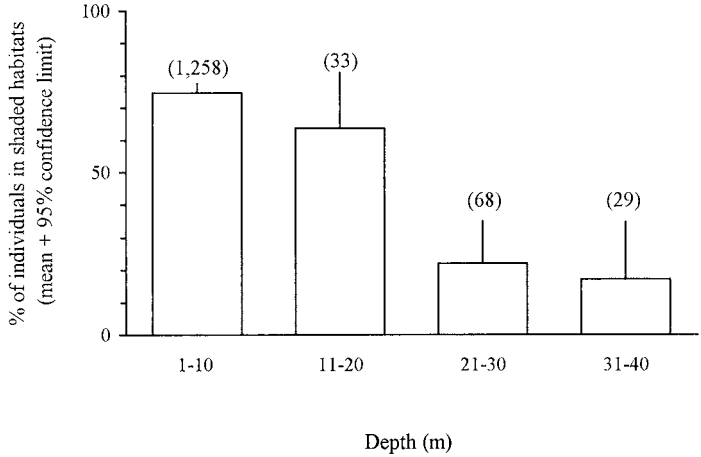

Figure 5. Variation in the occupation of shaded reef habitats with depth by mushroom corals on a fringing reef at Eilat, northern Red Sea. Sample sizes are given in parentheses. Shown are data for all fungiid corals observed inside transects; note that most individuals occurred in shallow water.

with hard substratum than on adjacent slope areas with mainly sediment cover (Hoeksema, 1990). At a nearby site in Eilat that contained only patch reefs and rocky rubble, a similar depth distribution pattern was observed for *F. scutaria* (range = 0.5–5 m depth), but not for *F. granulosa* (range = 5–25 m depth, but maximum abundance at 15–25 m depth) (Kramarsky-Winter and Loya, 1998; compare with Fig. 2). This difference probably is due to between-site variation in substratum characteristics, and to the special ability of *F. granulosa* to invade sandy and rubble habitats (see Results).

Despite localized differences due to reef topography and substratum type, the depth distributions of some of the fungiids measured here were similar to those observed on

Table 1. Variation among mushroom coral species in the percentage of individuals that occurred in shaded habitats on a coral reef at Eilat, northern Red Sea. Sample sizes are given in parentheses. Data are given for both major life history stages within each species.

	Percent of individuals that occurred in shaded habitat during:	
Species	attached stage	free-living stage
Ctenactis echinata	100% (4)	35.3% (102)
Fungia scuriata	96.8% (283)	82.8% (186)
F. fungites	100% (43)	72.1% (190)
F. granulosa	100% (5)	55.1% (118)
F. (Danafungia) (2 species)*		
shallow (0–20 m)	82.9% (52)	60.8% (291)
deep (21–40 m)	27.8% (18)	11.9% (42)
*Cantharellus doederleini**		
shallow (0–20 m)	100% (19)	**
deep (21–40 m)	39.1% (23)	**

* Shallow and deep areas shown separately for these species because they were the only ones common at both deep ranges.
** Does not have a free-living stage during the life cycle.

reefs in Indonesia (Hoeksema, 1990). Most mushroom corals reached maximal abundances at shallower depths at Eilat (Fig. 2) than in Indonesia (Hoeksema, 1990), possibly due to the relatively protected location and low levels of water motion at Eilat, which is located at the northern end of an enclosed sea (Chadwick-Furman and Loya, 1992; Genin et al., 1994). Other possible explanations, such as low light penetration or temperature levels due to the high latitude of reefs in Eilat, do not explain these differences: light penetration is known to be high in the northern Red Sea, and temperatures remain practically constant with depth on reefs in Eilat (Fricke and Schuhmacher, 1983). Three species (*F. scutaria*, *F. fungites* and *C. echinata*) were found to be shallow-water corals at both sites, occurring mainly on the intertidal reef flat and upper reef slope (Hoeksema, 1990; Fig. 4). However, two other species (*F. paumotensis* and *Podabacia crustacea*) were common shallow-water fungiids in Indonesia (Hoeksema, 1990), but were rare and deep at the site examined in Eilat (Fig. 2). Interestingly, the sister species of *Fungia (Danafungia) horrida* and *F. (D.) scruposa* were observed to have almost identical depth distributions in Indonesia (Hoeksema, 1990), so the pattern recorded here for the two species grouped under *F. (Danafungia)* spp. (Figs. 2,4) may accurately reflect the depth distributional pattern for members of the subgenus *Danafungia* at Eilat.

The depth ranges observed here also were shallower than for fungiid corals examined on a reef at Fanning Island in the central Pacific (Maragos, 1974; Fig. 2). At Fanning Island, both *F. fungites* and *F. scutaria* occurred at 6–20 m depth, and were the shallowest of the five fungiid corals recorded there (Maragos, 1974). In contrast, at Eilat, these two species also were among the shallowest, but reached their peak abundances at only 1–3 m depth (Fig. 2). These differences again appear related to levels of water motion. The reef at Fanning Island is exposed to large oceanic swells which generate high levels of water motion at shallow depths (Maragos, 1974), while the sheltered reef examined in Eilat, as noted above, experiences relatively low levels of water motion during most of the year (Chadwick-Furman and Loya, 1992), with a mean current speed of only 5.5 cm s^{-1} (Genin et al., 1994). Due to their free-living life style, shallow water fungiids on exposed reefs are transported downslope by wave action (Hoeksema, 1988), resulting in possibly deeper distributions than for those occurring on protected reefs.

Individuals of *F. scutaria* are unique among mushroom corals in that often they are limited to reef flats in very shallow water, as observed in Papua New Guinea (Claereboudt, 1988), Indonesia (Hoeksema, 1988; 1990), Hawaii (Krupp et al., 1992 and references therein), and Eilat (Chadwick-Furman and Loya, 1992; Kramarsky-Winter and Loya, 1996, 1998; Figs. 2,4). Members of this species possess traits suited for life in shallow turbulent waters and exposure to frequent physical disturbances such as low tides and fresh-water runoff. The polyps have a bowl-like shape that passively rights itself when overturned by water motion, and a dense skeleton that resists abrasion (Jokiel and Cowdin, 1976). The septa of *F. scutaria* have fine, sharp spines that are unable to resist tissue damage due to sedimentation, and thus are not suited for life on soft substratum (Schuhmacher, 1977). The dense skeleton and convex shape of *F. scutaria* may hinder movements by anchoring the corals in crevices on the reef flat instead of allowing them to migrate downslope or onto sand (Hoeksema, 1988). Finally, if adult polyps of *F. scutaria* are partially killed by low-tide events or other disturbances, their remaining tissues rapidly regenerate many small polyps (Krupp et al., 1992; Jokiel et al., 1993). Damaged individuals of *F. scutaria* produce >10× more buds per polyp than do those of other fungiid species (Kramarsky-Winter and Loya, 1996). This high rate of asexual reproduction leads to a proliferation of

numerous juvenile anthocauli attached to the dead parent coralla of *F. scutaria*, and thus a population structure dominated by young, attached individuals on reef flats at both Eilat (Loya, 1975; Figs. 1A,4A) and Hawaii (Krupp et al., 1992). At Eilat, disturbances in the form of catastrophic low tides and oil pollution in the early 1970s killed most of the stony corals on the reef flat at the Japanese Gardens site (Loya, 1975). These disturbances apparently facilitated the proliferation of many small fungiids by (1) creating open space for colonization, and (2) damaging the tissues of adult mushroom corals, which responded by asexually budding new polyps (Loya, 1975; Krupp et al., 1992; Kramarsky-Winter and Loya, 1996, 1998). The result was a large increase in the abundance of mushroom corals on the reef flat in the mid 1970s (Loya, 1975). We propose that the high abundance of *F. scutaria* polyps today at this site (Fig. 2) is a consequence of severe physical disturbance, followed by a lack of coral recovery during the last 20 yrs (Loya, 1990) and subsequent lack of spatial competition with other corals. Likewise, the proliferation of *F. scutaria* on reef flats in Kaneohe Bay, Hawaii, appears related to catastrophes in the form of freshwater flooding (Krupp et al., 1992; Jokiel et al., 1993).

The four other common mushroom corals on the shallow reef slope at Eilat (*C. echinata*, *F. fungites* and two species of *F. (Danafungia)*) (Fig. 2), all possess morphologies that are well-suited to life on the hard substratum of reef slopes. They all possess large costal spines on their aboral surfaces, that serve to anchor them and reduce downward migration to the deep slope (Hoeksema, 1988). They also have sharp, narrow septa on the oral surface, which do not protect tissues from damage by extensive sedimentation, and thus are not suited to living on fine sand (Schuhmacher, 1977). At Eilat, almost all free-living individuals of these species remained on hard substratum on the shallow reef slope, and did not migrate out onto the surrounding sand (see Results).

In contrast, polyps of *F. granulosa* appear to be adapted for life on soft substratum adjacent to the reef. They have relatively porous, lightweight skeletons with small, granular aboral spines that allow for rapid migration from the reef onto sand (Hoeksema, 1988; Chadwick-Furman and Loya, 1992). They also possess broad granular septa that resist tissue damage during sedimentation and burial in sand, and thus the polyps are able to rapidly unearth themselves if buried (Schuhmacher, 1977). At Eilat, our current and previous studies have shown that polyps of *F. granulosa* migrate faster on the reef (Chadwick-Furman and Loya, 1992) and move more frequently onto sand (see Results, Fig. 1C) than do those of other, co-existing mushroom corals.

The use of shaded habitats by attached mushroom corals (Table 1) also has been documented by Chadwick-Furman and Loya (1992) and Dinesen (1983). Attached fungiids may prefer shaded reef habitats because they provide favorable conditions for juvenile coral survival, due to relatively low levels of competition (Dinesen, 1983), sedimentation, predation (Sammarco, 1991 and references therein), and damaging ultraviolet radiation (Hoeksema, 1991). The disadvantages of cave-dwelling increase with depth for zooxanthellate corals, in part because light levels available for photosynthesis decrease exponentially with depth in open reef habitats at Eilat, to 10% of surface light at 50 m depth, and only 1% of surface light at 100 m depth (Fricke and Schuhmacher, 1983, and references therein). In shaded habitats containing fungiid corals, light levels were >10× lower than on the open reef (see Materials and Methods), resulting in very low light levels available to corals occurring in the shade at depth. The fungiids observed here gradually switched from shaded to open habitats with depth (Fig. 5), a pattern that also has been observed for juvenile stony corals in Australia (Sammarco, 1991). The mechanisms con-

tributing to this pattern may include: (1) preferential settlement by coral larvae on open rather than shaded surfaces on deep reefs, (2) higher coral mortality in shaded areas, and (3) active movement by mushroom corals out of caves once they become free-living, facilitated by their positive phototactic behavior (Yamashiro and Nishihira, 1995). At Eilat, light levels are apparently high enough (10% of surface light at 50 m depth) on the open reef for some free-living fungiids to occur down to 55 m depth (Fig. 2) and even deeper (Fricke and Schuhmacher, 1983).

We conclude that morphological traits (aboral surface smoothness, septal morphology, skeletal density) explain in part the occurrence of some fungiid corals in sandy habitats, while others remain on hard substratum on the reef. In addition, the reproductive traits of at least one species (*F. scutaria*) allow it to survive and proliferate in the unique, frequently-disturbed environment of the shallow reef flat (Kramarsky-Winter and Loya, 1998). Both types of strategies (morphological and reproductive) allow mushroom corals to persist on coral reefs that are dominated by colonial attached corals (Maragos, 1974). Finally, the migratory behavior of mushroom corals reduces competition on the reef, and allows some of them to make use of sandy habitats that are not available to most other corals (Chadwick-Furman and Loya, 1992). Thus, their unique life histories and morphological and behavioral adaptations appear to explain the persistence and diversity of fungiids on reefs dominated by larger, attached colonial corals.

Acknowledgements

This research was conducted at the Interuniversity Institute for Marine Science in Eilat. We thank the staff of the Interuniversity Institute for Marine Science in Eilat for technical support, especially K. Tarnaruder for preparing the graphics. We also thank A. Balderman, S. Bensur, T. Feldstein, O. Langmead, E. Snider and D. Torovetzky for assistance during the field work, and G. Galli for photographic advice. Comments by J. Feingold, T. Telò, H. Yamazato, and F. Zaccanti greatly improved the manuscript. Funding was provided to S.G. by Scuba Schools International of Italy.

Literature Cited

Chadwick-Furman, N. and Y. Loya. 1992. Migration, habitat use, and competition among mobile corals (Scleractinia: Fungiidae) in the Gulf of Eilat, Red Sea. Mar. Biol. 114: 617–623.

Chadwick-Furman, N. E., S. Goffredo and Y. Loya. 1999. Growth and population dynamic model of the reef coral *Fungia granulosa* Klunzinger, 1879 at Eilat, northern Red Sea. (submitted to J. Exp. Mar. Biol. Ecol.)

Claereboudt, M. R. 1988. Spatial distribution of fungiid corals population on exposed and sheltered reef slopes in Papua New Guinea. Proc. 6th Int'l. Coral Reef Symp., Townsville 2: 653–660.

Dinesen, Z. D. 1983. Shade-dwelling corals of the Great Barrier Reef. Mar. Ecol. Prog. Ser. 10: 173-185.

Fricke, H. W. and H. Schuhmacher. 1983. The depth limits of Red Sea stony corals: an ecophysiological problem. P.Z.N.I. Mar. Ecol. 4: 163–194.

Genin, A., L. Karp and A. Miroz. 1994. Effects of flow on competitive superiority in scleractinian corals. Limnol. Oceanogr. 39: 913–924.

Hoeksema, B. W. 1988. Mobility of free-living fungiid corals (Scleractinia), a dispersion mechanism and survival strategy in dynamic reef habitats. Proc. 6th Int'l. Coral Reef Symp., Townsville 2: 715–720.

_____. 1989. Taxonomy, phylogeny and biogeography of mushroom corals (Scleractinia: Fungiidae). Zool. Verh. Leiden 254: 1–295.

_____. 1990. Systematics and ecology of mushroom corals (Scleractinia: Fungiidae). Doctoral dissertation, Leiden University, Leiden, The Netherlands. 471 p.

_____. 1991. Control of bleaching in mushroom coral populations (Scleractinia: Fungiidae) in the Java Sea: stress tolerance and interference by life history strategy. Mar. Ecol. Prog. Ser. 74: 225–237.

_____. 1992. The position of northern New Guinea in the center of marine benthic diversity: a reef coral perspective. Proc. 7th Int'l. Coral Reef Symp., Guam 2: 710–717.

_____. 1993a. Mushroom corals (Scleractinia: Fungiidae) of Madang Lagoon, northern Papua New Guinea: an annotated check-list with the description of *Cantharellus jebbi* spec. nov. Zool. Med. Leiden 67: 1–19.

_____. 1993b. Historical biogeography of *Fungia (Pleuractis)* spp. (Scleractinia: Fungiidae), including a new species from the Seychelles. Zool. Med. Leiden 67: 639–654.

Jokiel, P. L. and H. P. Cowdin. 1976. Hydromechanical adaptation in the solitary free-living coral *Fungia scutaria*. Nature 262: 212-213.

_____, C. L. Hunter, S. Taguchi and L. Waterai. 1993. Ecological impact of a fresh water 'reef kill' in Kaneohe Bay, Oahu, Hawaii. Coral Reefs 12: 177–184.

Kramarsky-Winter, E. and Y. Loya. 1996. Regeneration versus budding in fungiid corals: a trade-off. Mar. Ecol. Prog. Ser. 134: 179–185.

_____. 1998. Reproductive strategies of two fungiid corals from the northern Red Sea: environmental constraints? Mar. Ecol. Prog. Ser. 174: 175–182.

Krupp D. A., P. L. Jokiel and T. S. Chartrand. 1992. Asexual reproduction by the solitary scleractinian coral *Fungia scutaria* on dead parent coralla in Kaneohe Bay, Oahu, Hawaiian Islands. Proc. 7th Int'l. Coral Reef Symp., Guam 1: 527–534.

Littler, M. M., D. S. Littler, B. L. Brooks and J. F. Koven. 1997. A unique coral reef formation discovered on the Great Astrolabe Reef, Fiji. Coral Reefs 16: 51–54.

Loya, Y. 1972. Community structure and species diversity of hermatypic corals at Eilat, Red Sea. Mar. Biol. 13: 100–123.

_____. 1975. Environmental predictability in relation to life histories of reef corals. Proc. 6th Scient. Conf. Israel Ecol. Soc. 1: 215–223.

_____. 1990. Changes in a Red Sea coral community structure: a long-term case history study. Pages 369–384 *in* G. M. Woodwell, ed. The earth in transition: patterns and processes of biotic impoverishment. Cambridge Univ. Press, Cambridge. 525 p.

_____ and L. B. Slobodkin. 1971. The coral reefs of Eilat (Gulf of Eilat, Red Sea). Symp. Zool. Soc. Lond. 28: 117–139.

Maragos, J. E. 1974. Coral communities on a seaward reef slope, Fanning Island. Pac. Sci. 28: 257–278.

Sammarco, P. W. 1991. Geographically specific recruitment and post settlement mortality as influences on coral communities: The cross-continental shelf transplant experiment. Limnol. Oceanogr. 36: 496–514.

Schuhmacher, H. 1977. Ability of fungiid corals to overcome sedimentation. Proc. 3rd Int'l. Coral Reef Symp., Miami 1: 503–509.

Sheppard, C. R. C. 1981. The reef and soft-substrate coral fauna of Chagos, Indian Ocean. J. Nat. Hist. 15: 607–621.

_____ and A. L. S. Sheppard. 1991. Corals and coral communities of Arabia. Fauna Saudi Arabia 12: 1–170.

Wells, J.W. 1966. Evolutionary development in the scleractinian family Fungiidae. Symp. Zool. Soc. Lond. 16: 223–246.

Yamashiro, H. 1992. Skeletal dissolution by scleractinian corals. Proc. 7th Int'l. Coral Reef Symp., Guam 2: 1142–1146.

_____ and K. Yamazato. 1996. Morphological studies of the soft tissues involved in skeletal dissolution in the coral *Fungia fungites*. Coral Reefs 15: 177–180.
_____ and M. Nishihira. 1995. Phototaxis in Fungiidae corals (Scleractinia). Mar. Biol. 124: 461–465.

DATE SUBMITTED: March 18, 1999. DATE ACCEPTED: September 27, 1999.

ADDRESSES: (S.G.) *Department of Evolutionary and Experimental Biology, University of Bologna, Via F. Selmi 3, I-40126 Bologna, Italy;* (N.E.C.-F.) *Interuniversity Institute for Marine Science, P.O. Box 469, Eilat, Israel, and Faculty of Life Sciences, Bar Ilan University, Ramat Gan, Israel.* CORRESPONDING AUTHOR: (N.E.C.-F.) *Interuniversity Institute for Marine Science, P.O. Box 469, Eilat, Israel, email <furman@mail.biu.ac.il>.*

ELSEVIER

Journal of Experimental Marine Biology and Ecology
249 (2000) 199–218

JOURNAL OF EXPERIMENTAL MARINE BIOLOGY AND ECOLOGY

www.elsevier.nl/locate/jembe

Growth and population dynamic model of the reef coral *Fungia granulosa* Klunzinger, 1879 at Eilat, northern Red Sea

Nanette E. Chadwick-Furman[a,b,*], Stefano Goffredo[c], Yossi Loya[d]

[a]*Interuniversity Institute for Marine Science, P.O. Box 469, Eilat, Israel*
[b]*Faculty of Life Sciences, Bar Ilan University, Ramat Gan, Israel*
[c]*Department of Evolutionary and Experimental Biology, University of Bologna, via Selmi 3, I-40126 Bologna, Italy*
[d]*Department of Zoology, The George S. Wise Faculty of Life Sciences, and the Porter Super-Center for Ecological and Environmental Studies, Tel Aviv University, Tel Aviv, Israel*

Received 18 August 1999; received in revised form 10 February 2000; accepted 9 March 2000

Abstract

The lack of population dynamic information for most species of stony corals is due in part to their complicated life histories that may include fission, fusion and partial mortality of colonies, leading to an uncoupling of coral age and size. However, some reef-building corals may produce compact upright or free-living individuals in which the above processes rarely occur, or are clearly detectable. In some of these corals, individual age may be determined from size, and standard growth and population dynamic models may be applied to gain an accurate picture of their life history. We measured long-term growth rates (up to 2.5 years) of individuals of the free-living mushroom coral *Fungia granulosa* Klunzinger, 1879 at Eilat, northern Red Sea, and determined the size structure of a population on the shallow reef slope. We then applied growth and population models to the data to obtain estimates of coral age, mortality rate, and life expectancy in members of this species. In the field, few *F. granulosa* polyps suffered partial mortality of $>10\%$ of their tissues. Thus, the majority of polyps grew isometrically and determinately, virtually ceasing growth by about 30–40 years of age. Coral ages as revealed by skeletal growth rings were similar to those estimated from a growth curve based on field data. The frequency of individuals in each age class on the reef slope decreased exponentially with coral age, indicating high mortality rates when corals were young. The maximum coral age observed in the field population (31 years) was similar to that estimated by application of a population dynamic model (30 years). Calculated rates of growth, mortality and life expectancy for *F. granulosa* were within the range of those known for other stony corals. Our results reveal a young, dynamic population of this species on Eilat reefs, with high turnover rates and short lifespans. Such information is important for understanding

*Corresponding author. Tel.: +972-7-636-0101; fax: +972-7-637-4329.
E-mail address: furman@mail.biu.ac.il (N.E. Chadwick-Furman)

0022-0981/00/$ – see front matter
PII: S0022-0981(00)00204-5

recovery of coral reefs from disturbances, and for application to the management of commercially exploited coral populations.

Keywords: Fungiidae; Growth model; Mushroom coral; Population ecology; Red Sea; Reef management; Scleractinia

1. Introduction

Processes of population turnover among stony reef-building corals are important in that they influence how rapidly and to what extent coral reefs recover from disturbances (Connell, 1973). Patterns of larval survival, juvenile recruitment, somatic growth, sexual reproduction and mortality vary widely among species of corals, and play a decisive role in species succession on developing reefs (Grigg and Maragos, 1974; Hughes and Jackson, 1985). Some scleractinians, such as species of the branching corals *Stylophora* and *Pocillopora*, have been classified as r-strategists in that they produce a large number of propagules over a long season each year, grow rapidly, and are among the first to colonise newly created space on reefs (Grigg and Maragos, 1974; Loya, 1976a,b; Connell et al., 1997). Others, in particular those with massive hemispherical growth forms such as some species of *Porites* and *Platygyra*, may be K-strategists in that they reproduce only during a short period each year and grow slowly (Babcock, 1991; Shlesinger and Loya, 1991), and thus may take several years to colonize new substrata, but once established are able to dominate reefs via effective defense of living space (Grigg and Maragos, 1974). Thus, the life history characteristics of each coral species may explain in large part the observed variation in coral community structure between patches with different disturbance histories on shallow reefs.

The current lack of basic population dynamic information for most stony corals is due in part to a distortion of the relationship between colony size, age and genetic origin, because many colonies may experience fission, fusion, or partial mortality (Hughes and Jackson, 1985; Babcock, 1991). Thus, studies on foliaceous and encrusting corals have relied on long-term observations of individual colonies in order to determine their history and origins, and have used size-based rather than age-based models of population dynamics (Hughes, 1984; Hughes and Jackson (1985), but see Babcock (1991) for a combination of models). However, some corals on reefs grow in distinct forms that rarely undergo fission or fuse, and in which partial mortality is clearly detectable by distortions of the regular growth form. These include stony corals that build compact branching colonies, such as *Pocillopora* (Grigg, 1984; Ross, 1984) and *Stylophora* (Loya, 1976a), some with massive hemispherical growth forms such as *Platygyra* and *Goniastrea* (Babcock, 1991), and free-living corals such as *Fungia* (Chadwick and Loya, 1990), *Manicina* (Johnson, 1992) and *Siderastrea* (Lewis, 1989). In some of these corals, individuals may be aged reliably, thus standard age-based growth and population dynamic models may be applied to understand their demography.

The population dynamic model developed for fisheries by Beverton and Holt has been applied successfully to many marine invertebrates (reviewed by Clasing et al. (1994)),

including the scleractinian corals *Pocillopora verrucosa* (Grigg, 1984; Ross, 1984) and *Balanophyllia europaea* (Goffredo, 1999). This model also has been proposed for use in managing exploited populations of stony reef corals in the Philippines (Ross, 1984). The Beverton Holt model characterises the population dynamics of a given species based on the size frequency distribution of individuals in the field, individual growth rates, and the relationship between individual mass and length. The most important constraint of this model is the assumption that a population is in steady state, in other words that no major disturbance has recently altered population size structure. For species of short-lived corals, or those in relatively deep or stable environments, this may not be a serious limitation (Fadlallah, 1983; Grigg, 1984; Ross, 1984; Mistri, 1995). This is a cohort-based model, in which a cohort of recruits is estimated to gain biomass until an age–size point at which losses to the cohort due to mortality overtake gains in biomass due to individual growth. After this point, as the cohort ages, its biomass declines to zero, as very few individuals of large size remain in the population. The individual size that corresponds to the age at peak cohort biomass is the minimum size of individuals that can be removed from the population in a sustainable manner, without decimating it.

In order to apply this population model to corals, growth rate data must be converted to age–size relationships. In corals that grow indeterminately, if processes of partial mortality or fragmentation do not interfere, age is a linear function of individual length (Loya, 1976a; Grigg, 1984; Ross, 1984; Babcock, 1991). However, in reef-building corals with size-dependent growth, age–size relationships must be estimated using a growth curve, because growth rate decreases as the individuals age. The von Bertalanffy growth curve (von Bertalanffy, 1938) models size-dependent growth, and has been applied widely to estimate age–size relationships in various invertebrates (reviewed by Stokes (1996)). This model curve also has been used to describe growth patterns in cnidarians, including some gorgonians (Grigg, 1974; Mistri and Ceccherelli, 1993, 1994) and solitary scleractinians (Gerrodette, 1979; Bablet, 1985; Goffredo, 1995).

Population dynamic and growth models are important tools for understanding patterns of turnover and change among stony corals on reefs. Such models also are increasingly needed to manage the sustainable harvest of reef corals for the ornamental aquarium industry (Ross, 1984), and to assess the health of exploited reefs (Bak and Meesters, 1998). Until the late 1980s, coral reefs in the Philippines produced most of the world's stony corals for ornamental use (Ross, 1984). More recently, an increasing proportion of stony corals are being collected from reefs in Indonesia (Bentley, 1998). Harvesting of corals from reef populations resulted in imports of scleractinians to the United States alone averaging about $1 million annually during 1975 to 1980 (Grigg, 1984), and continuing at about 1 million pieces imported per year in the 1990s (Bentley, 1998). Coral resources may be managed successfully by the application of population models to determine a maximum sustainable yield for each species, based on a minimum size or age for collection (Grigg, 1984).

Most members of the scleractinian family Fungiidae (mushroom corals) form unique free-living polyps on coral reefs, and are particularly vulnerable to overexploitation. In many mushroom corals, small attached polyps actively dissolve the skeleton near the polyp base, and become detached, free-living individuals (reviewed by Hoeksema (1989) and Yamashiro (1992)). Due to their mobility, many mushroom corals move off

the reef and colonize the sandy base, where they may serve as nuclei for the formation of new patch reefs (Chadwick-Furman and Loya (1992) and references therein). Thus, mushroom corals are initiators of reef growth, and sometimes are major components of reef flats (Kramarsky-Winter and Loya, 1998) and slopes (Goffredo and Chadwick-Furman, 2000). Because they also reproduce asexually, the members of some species recover rapidly after disturbances (Loya, 1975), and may even build large patch reefs consisting only of mushroom corals (Littler et al., 1997).

Mushroom corals also are one of the major components of international trade in ornamental corals (Bentley, 1998). They constituted $>60\%$ of the coral fishery in the Philippines in the 1980s, where they far outnumbered all other types of stony corals collected (Ross, 1984). Even though the coral curio industry has shifted to Indonesian reefs, mushroom corals remain in high commercial demand (Bentley, 1998) due to their large polyp size, ease of collection, and popularity among consumers. Thus, the development of accurate models of population turnover and growth in fungiid corals is important in order to understand basic reef processes, and for application to the management of exploited reef coral populations. Finally, fungiids may serve as an ideal group for the application of population dynamic models, because in many species, age and size are directly related. In the free-living polyps of many mushroom corals, shape is constant over the lifespan, fission and fusion are rare, and evidence of partial mortality is clearly visible on the disk due to its shape (Hoeksema, 1989; Chadwick and Loya, 1990).

Individuals of the mushroom coral *Fungia granulosa* Klunzinger, 1879 are a common component of the stony coral assemblage on reefs at Eilat, northern Red Sea (Kramarsky-Winter and Loya, 1998; Goffredo and Chadwick-Furman, 2000). Members of this species form dioecious polyps that spawn gametes during July to August each year (Kramarsky-Winter and Loya, 1998). The duration of the larval phase is unknown, but polyps appear to recruit at 2–9 m depth at Eilat, and then to detach actively and migrate down to at least 33 m depth as adults (Goffredo and Chadwick-Furman, 2000). The goals of the present study were to determine patterns of individual shape and size, long-term growth, and field population structure in *F. granulosa*, and then to apply population and growth models (see above) to estimate rates of mortality, population turnover and lifespan. We also compare here the life history characteristics of this species with those known for other scleractinians, and discuss the application of population models to the management of commercially exploited stony corals on tropical reefs.

2. Materials and methods

This study was conducted on reefs adjacent to the Interuniversity Institute for Marine Science (IUI) at Eilat, northern Red Sea. Growth rates of 131 individuals of *Fungia granulosa* were measured at 5–7 m depth on the reef slope during September 1992–March 1995. This depth was chosen because it contains many individuals of this species (Goffredo and Chadwick-Furman, 2000). Each coral was measured for 0.5–2.5 years. The period of measurement varied between individuals, because corals that died were

replaced by others of similar size during the study. The measured polyps were contained in wide, flat baskets (30 cm long × 20 cm wide × 4 cm high) on the reef slope in order to prevent their dispersal and loss during the growth study. The bottom of each basket was attached to a cement brick for stability, and ~10 polyps spanning the size range for *F. granulosa* were placed inside. The baskets were open on top, in order to simulate a small natural depression in the reef, and to minimize any artifacts of altered water flow, light, or predation patterns on the corals. The polyps in each basket were individually recognisable due to their sizes and individual markings (color pattern, polyp outline, after Chadwick-Furman and Loya (1992)). Each 3 months during the study, all polyps were examined in situ, and their length (along the mouth axis), width (perpendicular to the mouth axis, after Abe (1940) and Bablet (1985)), and polyp condition (% tissue mortality) were recorded. We include here data only for polyps that had < 10% tissue mortality throughout the study, thus the growth rates reported here represent maximal values for polyps in each size class.

The skeletons of polyps that died naturally during the study ($N = 35$) were removed from the sea, dried at 400°C for 24 h, and their length and dry skeletal mass obtained. We also counted circular rings that were externally visible on the aboral surface of each skeleton (Fig. 1). These rings have been shown to correspond to annual growth in the congener *F. actiniformis* (Abe, 1940). Growth rings were counted only on relatively small corals (< 60 mm length), because on larger individuals they were too close together to distinguish externally.

The population size structure of *F. granulosa* was determined by examining polyps on the Japanese Gardens fringing reef, ~500 m north of the IUI. This reef area was chosen for population sampling because it is a well-developed fringing reef with many mushroom corals (Goffredo and Chadwick-Furman, 2000), its coral community structure has been well-studied (reviewed by Loya, 1990), and it occurs inside a fenced, inaccessible portion of the Coral Beach Nature Reserve of Eilat, thus being largely protected from human impacts to coral populations on the reef slope. A belt transect (1 × 25 m) was deployed parallel to shore on the reef slope at each of five depths: 2, 3, 6, 9, and 12 m, thus encompassing the depth range of most of the *F. granulosa* population on the Japanese Gardens reef (Goffredo and Chadwick-Furman, 2000; but see Kramarsky-Winter and Loya (1998) for a different depth range on other reefs). Within each transect, all *F. granulosa* polyps were examined, and their length, width (as defined above), and attached versus free-living status were recorded.

We then used mathematical models to describe patterns of growth and population dynamics for *F. granulosa* at Eilat, by applying the von Bertalanffy growth function and the Beverton Holt population dynamics model (see above).

3. Results

As expected for a disc-shaped coral, mass increased exponentially with length in individuals of *Fungia granulosa* (Fig. 2A). Width varied linearly with length (Fig. 2B), and the width:length ratio of polyps remained constant throughout the lifespan (Fig. 2C), indicating that the corals did not change shape as they aged, and thus that growth was

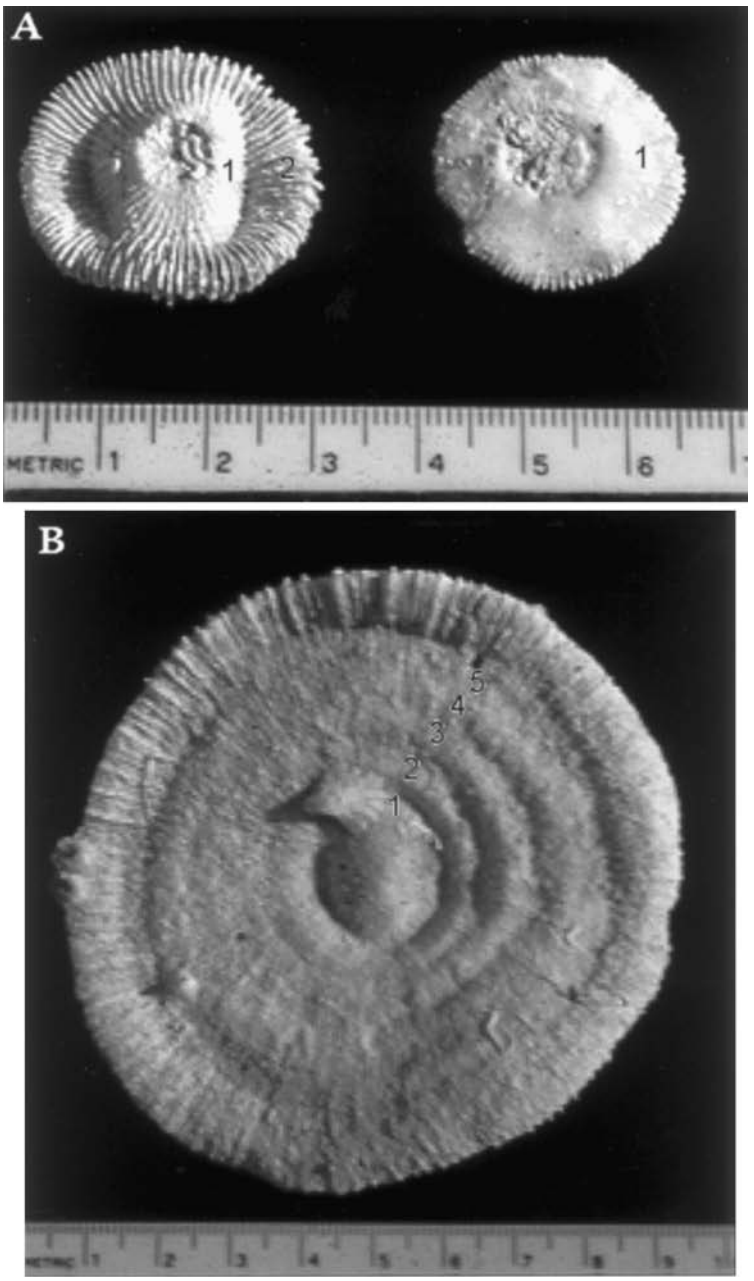

Fig. 1. Aboral view of skeletons of the mushroom coral *Fungia granulosa*, showing externally-visible growth rings. Each number denotes a ring, corresponding to a year of growth. Scale is in cm. (A) Coral on left is ~2 years old, coral on right is between 1 and 2 years old. (B) Coral is at least 7 years old. After about 6 years of growth, the rings became too close together to distinguish externally.

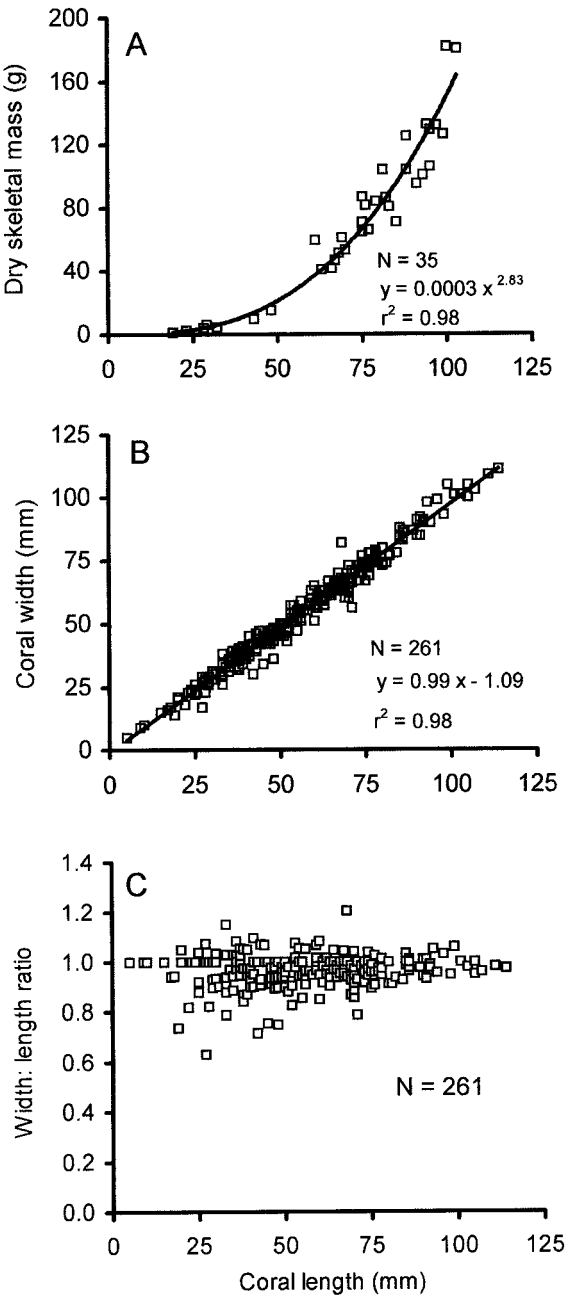

Fig. 2. Dependence of biometric parameters on individual length in the mushroom coral *Fungia granulosa*. (A) Dry skeletal mass. (B) Width. (C) Polyp shape (width:length ratio).

isometric. A width:length ratio of 0.96±0.06 (mean±S.D., $N = 261$ polyps) indicated that the polyps were slightly oblong in shape (Fig. 2B and C).

The growth rate of individuals of *F. granulosa* decreased linearly with increasing coral size (Fig. 3). According to the von Bertalanffy growth function (see above), the rate of this decrease may be symbolized as a growth constant *K*, which is the slope of the linear regression line, with sign reversed. Thus, for the examined population of *F. granulosa*, the growth constant $K = 0.1095$ (Fig. 3). Maximum expected coral length in this population (L_∞) corresponded to the coral length at which growth rate became zero, or where the growth regression line intercepted the *x*-axis. Thus, for *F. granulosa* at Eilat, the maximum expected coral length $L_\infty = 118$ mm (Fig. 3).

From the above data, a lifetime growth curve for this population, according to the von Bertalanffy growth model, may be expressed by the following formula:

$$L_t = L_\infty(1 - e^{-Kt})$$

where L_t is the coral length at age *t*, L_∞ is the asymptotic length (maximum expected coral length), *K* is the growth constant, and *t* is the coral age.

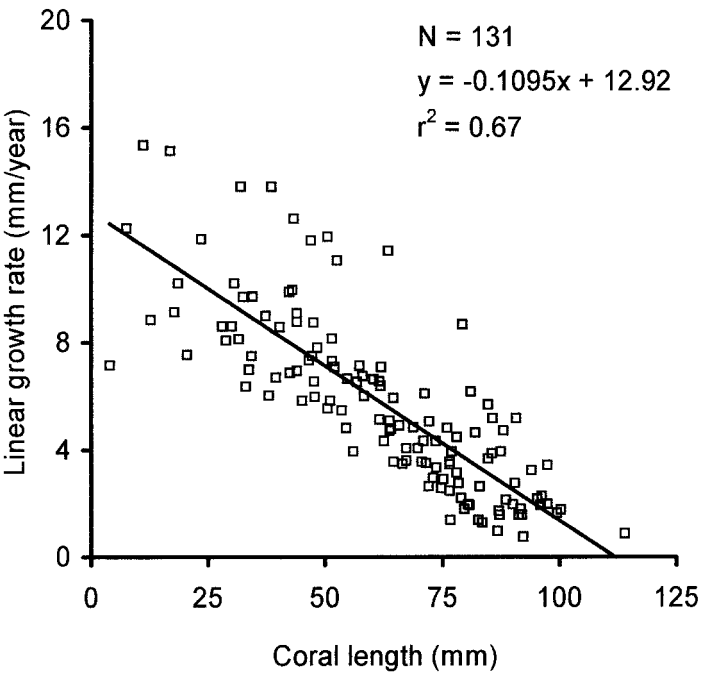

Fig. 3. Variation in linear growth rate among individuals of the mushroom coral *Fungia granulosa*. From in situ field measurements of individual corals during 0.5–2.5 years on a reef slope at Eilat, northern Red Sea. Note that linear growth rate decreases with coral size. The annual growth constant (*K*) is equal to the slope of the regression line, with sign reversed.

Using the values obtained above for K and L_∞, the growth curve for *F. granulosa* in Eilat was:

$$L_t\,(\text{mm}) = 118(1 - e^{-0.1095t(\text{years})}).$$

According to this growth curve, individuals of *F. granulosa* reached maximal individual length at ~35 years of age (Fig. 4A). When young (0–5 years old), the corals grew relatively rapidly (mean±S.D.=9.9±1.7 mm year^{-1}), but as they aged their growth rate decreased, and by the time they were 30–35 years old, grew at imperceptible rates of only 0.4±0.1 mm year^{-1} (Fig. 4A). Over the entire period of active growth (0–35 years of age), growth rate was ~3.4±3.3 mm year^{-1}. The above growth curve was based on estimated growth for each size class, and thus individual growth varied somewhat around the curve (Fig. 3 and 4A). For young corals <7 years in age, the growth curve produced similar age–size relationships as those obtained from skeletal growth rings; after this age, growth was so slow that growth rings became externally indistinguishable and thus unusable (Figs. 1 and 4A).

The growth curve for changes in mass with age in *F. granulosa* had a sigmoidal shape (Fig. 4A), due to the exponential relationship between length and mass, in which body mass was very small when corals were young (Fig. 2A). For corals 0 to 35 years old, the mean growth rate of skeletal mass was 6.2±3.3 g year^{-1} (mean±S.D.).

The size-frequency of individuals observed in the field population, when converted to an age-frequency distribution using the above age–size relationships, revealed a population dominated by young, small individuals (Fig. 4B). More than 95% of the population was <15 years old (<95 mm in individual length), and the largest individual observed was estimated to be 31 years old (=114 mm length). The mean age of corals in this sample was 7 years old. During the first year of life, most individuals occurred in the attached phase, but this proportion decreased until, by the third year, most individuals became free-living, detached polyps (Fig. 4B). Relatively few individuals in the attached phase were found in the field population, but once they became free-living, young individuals were observed at high frequencies (Fig. 4B).

From the above age-frequency distribution, the Beverton Holt model (see above) estimated the instantaneous mortality rate of individuals at each age, expressed as a function of the natural logarithm of the decrease in individual frequency with age:

$$N_t = N_0\, e^{-Zt}$$

where N_0 is the initial number of individuals at age zero (new recruits), N_t is the number of individuals remaining at age t, Z is the instantaneous rate of annual mortality and t is the coral age.

Upon fitting this expression to the field data on age frequencies, we obtained the following relationship:

$$N_{t(\text{years})} = 51.94e^{-0.17t(\text{years})}.$$

This function represented a best fit to the data in Fig. 4B, and yielded an exponential regression coefficient of $r^2=0.76$. The age classes of 0–2 years were excluded from this analysis (Fig. 4B), because they are known to be underrepresented in field samples of

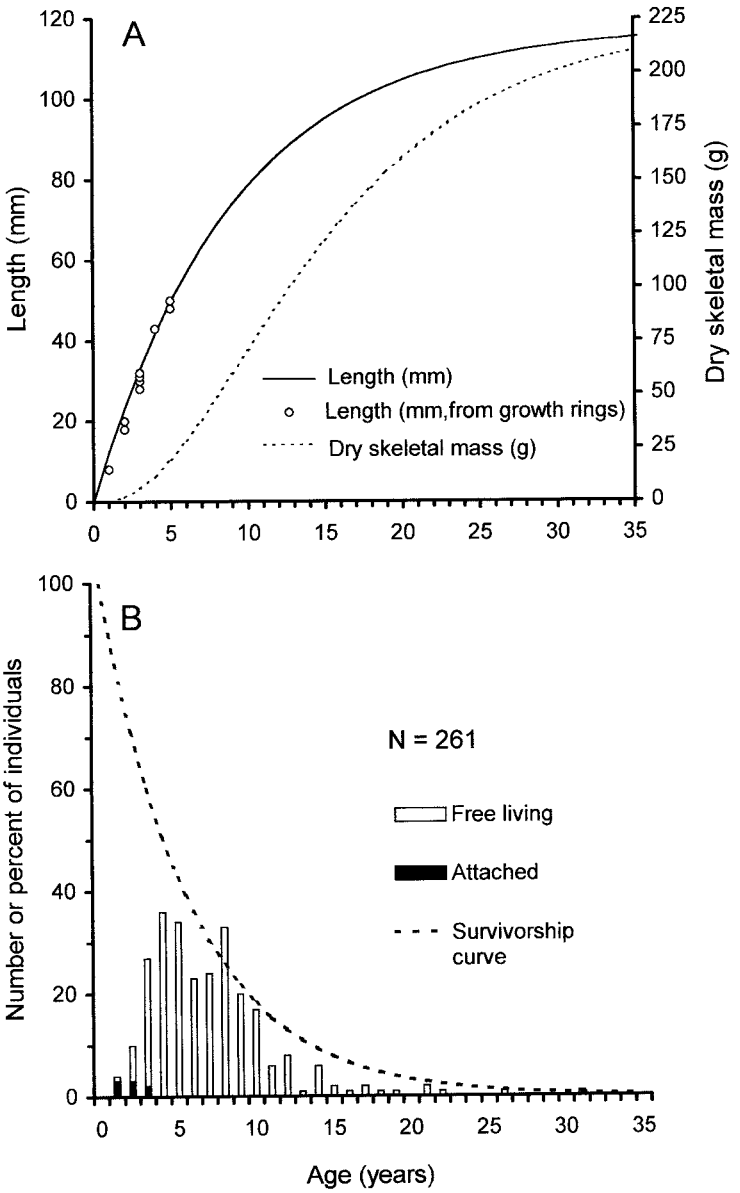

Fig. 4. Sizes and numbers of individuals of different ages in a population of the mushroom coral *Fungia granulosa*. (A) Age-specific growth curves obtained from application of a growth model to linear extension rates measured in the field, with comparative data from skeletal rings. (B) Age-frequency structure (bars, number of individuals) and survival curve (dotted line, percent of individuals) for corals on a reef slope at Eilat, northern Red Sea.

Table 1
Age, survival and yield of the mushroom coral *Fungia granulosa* on a reef slope at Eilat, northern Red Sea. Shown in bold are the age at sexual maturity (=6 years, calculated from Kramarsky-Winter and Loya, 1998), and the age at maximum yield (=9–10 years)

Age (years)	Length (mm)	Skeletal mass (g)	Survival	Yield (g/rec)
0	0	0.0	1.000	0.00
1	12	0.4	0.844	0.34
2	23	2.2	0.712	1.57
3	33	6.1	0.600	3.66
4	42	11.8	0.507	5.98
5	50	19.3	0.427	8.24
6	**57**	**28.2**	**0.361**	**10.18**
7	63	38.1	0.304	11.58
8	69	48.6	0.257	12.49
9	**74**	**59.5**	**0.217**	**12.91**
10	**79**	**70.5**	**0.183**	**12.90**
11	83	81.4	0.154	12.53
12	86	92.1	0.130	11.97
13	90	102.4	0.110	11.26
17	100	138.6	0.056	7.76
21	106	165.8	0.028	4.64
25	110	185.0	0.014	2.59
29	113	198.2	0.007	1.39
33	115	207.0	0.004	0.83

corals (Grigg, 1984; Babcock, 1991). Thus, the survival curve for members of this population, as given by the above function, estimated the mean age of individuals to be 6 years, and the oldest individual to be about 30 years old (Fig. 4B). Individuals had a high mortality rate when young, and the few surviving large, old individuals experienced low mortality (Fig. 4B).

The above data were used to calculate the yield, in terms of skeletal mass per recruit, of *F. granulosa* individuals at Eilat (Table 1). Cohort yield (=individual mass×percent survival) increased rapidly when the polyps were young, due to their rapid increases in size. Yield became maximal at age 9–10 years, after which losses due to mortality overtook gains due to individual growth. The age at maximum yield occurred 3–4 years after the polyps reached sexual maturity at 6 years of age (=60 mm length, Table 1). By the age of 33 years, <1% of polyps remained in the population.

4. Discussion

4.1. General

We show here that growth in the mushroom coral *Fungia granulosa* is size-dependent, with virtual cessation of growth after about 35 years of age. We also demonstrate that the mortality rate of these corals in a natural population decreases exponentially with coral

age, and thus that maximum biomass of the population is achieved by the time a cohort is about 9–10 years old. These data demonstrate that the sampled population is young and dynamic, and that there is a high turnover rate of these fungiid corals on Eilat reefs. Our results are the first attempt to model the life history and population dynamics of a mushroom coral, and have important implications for reef conservation management.

4.2. Coral shape and size parameters

Assessment of coral shape parameters in *F. granulosa* revealed that the corals have a slightly elongated discal shape (width:length ratio = 0.964), which they do not change as they grow (Fig. 2). An essential condition of the von Bertalanffy growth function employed here is that individual shape does not change with age, in other words, that mass is proportional to the cube of length throughout the lifespan, and thus that growth in mass is isometric (von Bertalanffy, 1938). Individuals of *F. granulosa* grow isometrically, in that mass is a cubed function of length, and the width:length ratio remains constant throughout life (Fig. 2). This condition occurs only in fungiid corals that retain a circular discal shape, and do not become elongated or bud polyp mouths along the disk's central axis, as occurs in the fungiid genera *Herpolitha* and *Ctenactis* (Hoeksema, 1989). Isometric growth in mass also has been demonstrated for the almost-circular solitary individuals of *Fungia actiniformis*, whose width:length ratio remains constant throughout life, at 0.927–0.942 depending upon locality (Abe, 1940). In contrast, the solitary polyps of *F. paumotensis* elongate as they grow, their width:length ratio decreasing from 0.810 to 0.639 as the individuals age (Bablet, 1985). Thus, due to less active skeletal secretion across the polyp's width over time, adult individuals of *F. paumotensis* have a smaller surface area compared to those of *F. granulosa* and *F. actiniformis* of equal length.

4.3. Growth rate and models

Many reef-building corals are known to grow indeterminately, and thus theoretically to have unlimited body size (reviewed in Hughes and Jackson, 1985; Bak and Meesters, 1998). However, the paradigm of unlimited growth in stony corals does not apply to all reef-building species. Despite their essentially 2-dimensional tissues and thus lack of surface area to volume constraints on growth, some corals are known to reduce their growth rate as they age. Scleractinian corals with size-dependent growth include some species that form branching colonies (*Pocillopora bulbosa* (Stephenson and Stephenson, 1933), *P. cespitosa* (Tamura and Hada, 1932), and *P. meandrina* (Grigg and Maragos, 1974)), massive colonies (*Goniastrea aspera* (Motoda, 1940; Sakai, 1998)), attached solitary polyps (*Balanophyllia elegans* and *Paracyathus stearnsii* (Gerrodette, 1979)) free-living colonies (*Manicina areolata* (Johnson, 1992)), and free-living solitary polyps (the mushroom corals *Ctenactis echinata* (Goffredo, 1995), *Diaseris distorta* (Yamashiro and Nishihira, 1998), *Fungia actiniformis* (Tamura and Hada, 1932), *F. fungites* (Stephenson and Stephenson, 1933), *F. granulosa* (present study, Figs. 3 and 4), and *F. paumotensis* (Bablet, 1985)). In free-living corals, which often colonise soft substratum, a genetic limitation on maximum size may represent an adaptation to avoid

sinking (Chadwick-Furman and Loya, 1992). Among attached corals, other constraints may influence maximal size, such as the biomechanics of a skeleton with highly branched architecture, or the physiology of a solitary polyp with a single mouth.

The pattern of size-dependent growth observed here in *F. granulosa* appears to fit the von Bertalanffy growth function (Figs. 3 and 4). The maximum individual length predicted by the model ($L_\infty = 118$ mm) is similar to that observed in the field population sampled at Eilat (maximum observed length is 114 mm for a coral 31 years of age, Fig. 4). In addition, the age–size curve derived from the model closely fits the age–size relationship obtained from analysis of annual skeletal growth rings in the corals, at least for young individuals (Fig. 4A). The external growth rings visible on the aboral skeleton of fungiid corals are a unique feature for the non-destructive aging of these corals, and also have been used to accurately age individuals of *F. actiniformis* (Abe, 1940). Our growth curves indicate that individuals of *F. granulosa* grow rapidly in length when young, increasing their mass more slowly, and reach a plateau for both mass and length sometime between 30 and 40 years of age, at which point they effectively stop growing (Fig. 4A).

Life history characters such as growth rate, maximum adult size and life expectancy vary widely between species of mushroom corals, and between populations within species (Table 2). According to our field data, members of three fungiid species examined in the northern Red Sea appear to take longer to reach maximum size (as described by the growth constant K) and to live longer than do members of the four species examined thus far in the tropical-equatorial Pacific (Table 2). Individual *F. actiniformis* that were investigated at a port entrance in Palau grew much more slowly than did all other fungiids studied in the tropical-equatorial Pacific (Table 2), possibly because they were exposed to anthropogenic stress. In contrast, growth rates of the fungiid coral *Diaseris distorta* measured at Okinawa (sub-tropical Pacific) were relatively high, but were obtained under optimal laboratory conditions (Table 2) which may not reflect growth in the natural environment. In general, the values for growth rate, adult size, and life expectancy that we obtained here for *Fungia granulosa* were within the range of those known for other fungiids in habitats throughout the Indo-Pacific (Table 2).

4.4. Population dynamics

The size and age structure of the examined population showed an exponential decrease in the frequency of individuals with age (Fig. 4B). This structure indicates a population in steady state, in that no age cohorts were missing or over represented, as would be the case if a major disturbance event had recently altered recruitment patterns (Grigg, 1977, 1984; Santangelo et al., 1993). In contrast to this population on the reef slope, fungiid corals occurring on the shallow reef flat at Eilat are occasionally impacted by extreme low tide disturbances, and their population structure reflects a non-steady state (Loya, 1975). Eilat is located at the northern end of an enclosed sea, and thus corals on the reef slope occur in a relatively stable environment (Chadwick-Furman and Loya, 1992; Kramarsky-Winter and Loya, 1998), which may explain their steady state condition (Fig. 4B). Other coral populations known to occur in a steady state include

Table 2
Estimated maximum length (L_∞, mm), growth rate constant (K, annual), mean linear growth rate (M, mm year^{-1}) and life expectancy (E, years) of mushroom corals (Scleractinia: Fungiidae)

Species	Reference	Locality	Environment	Depth (m)	L_∞	K	M	E
Ctenactis echinata	Goffredo, 1995	Sharm el Sheikh (northern Red Sea)	Natural field	6–12	323	0.1086	9	34
Diaseris distorta	Yamashiro and Nishihira, 1998	Okinawa (subtropical Pacific)	Aquarium	–	19	0.3600	2	10
Fungia actiniformis	Tamura and Hada, 1932	Caroline Islands (tropical-equatorial Pacific)	Natural field	0–10	106	0.2199	6	17
	Abe, 1940	Palao (tropical-equatorial Pacific)	Port entrance	0–2	195	0.0839	4	44
F. fungites	Stephenson and Stephenson, 1933	Great Barrier Reef (tropical-equatorial Pacific)	Natural field	0–3	133	0.2150	8	17
	Goffredo, 1995	Sharm el Sheikh (northern Red Sea)	Natural field	6–11	107	0.0878	3	42
F. granulosa	Present study	Eilat (northern Red Sea)	Natural field	6	118	0.1095	4	35
F. paumotensis	Bablet, 1985	Mururoa, Tahiti (tropical-equatorial Pacific)	Natural field	10	147	0.4041	16	9

those of the stony reef-builder *Pocillopora verrucosa* (Grigg, 1984; Ross, 1984), the gorgonians *Muricea californica* (Grigg, 1977) and *Lophogorgia ceratophyta* (Mistri, 1995), and the commercially important precious corals *Corallium rubrum* (Santangelo et al., 1993), *C. secundum* and *Anthipathes dichotoma* (Grigg, 1984).

According to population dynamic models, the rate of instantaneous mortality (Z) equals the inverse of the mean age of the animals in a population, and hence is equal to their turnover rate, or annual production:biomass ratio (P/B) (Clasing et al., 1994). The turnover time for *F. granulosa* at Eilat is 5.88 years (calculated as the reciprocal of Z), indicating rapid turnover in this population of reef corals. Our estimates of mortality rate and life expectancy for *F. granulosa* appear to be reasonable, in that values derived from the survival curve closely reflect the field observations (Fig. 4B). Annual mortality rate and individual life expectancy are known to vary widely between the few species of anthozoans examined thus far (Table 3). In *F. granulosa*, values for both of these life history traits are within the range of those known for other stony reef corals (Table 3).

We observed relatively few 1–2-year-old individuals of *F. granulosa* in the field at Eilat (Fig. 4B). Two phenomena may explain this pattern. Firstly, newly settled individuals may be underrepresented because of the difficulty in locating them. Young, attached juveniles of fungiids and other reef corals may occur mainly in cryptic environments on the reef (reviewed in Chadwick-Furman and Loya (1992), Goffredo and Chadwick-Furman (2000)), and so the youngest age classes of corals are usually excluded from population dynamic analyses (Grigg, 1984; Babcock, 1991). In addition, fungiid corals have a life-history feature that further complicates the relationship between small and large individuals. When a young disk-shaped mushroom coral detaches from the reef, it leaves behind a stalked base that contains live tissue, and which may produce a small number of additional polyps (Hoeksema, 1989). Long-term field observations on the tagged stalks of fungiid corals at Eilat indicate that they may produce new free-living individuals at a rate of approximately one each year (mean$\pm$S.D.$=13.0\pm5.5$ months, range$=9$–23 months, $N=10$ stalks; Chadwick-Furman, unpublished data). The height of the stalk indicates how many polyps were previously released, with each release represented by a ring on the stalk (Hoeksema, 1989; Yamashiro, 1992). A maximum of five rings were found on the stalked bases of *F. granulosa* observed at Eilat (mean$\pm$S.D.$=2.0\pm1.4$ rings, $N=7$ stalks), suggesting that only a few polyps are released by each stalk before it ceases to produce. Thus, a given number of attached stalks of *F. granulosa* potentially produces up to five times as many free-living disk-shaped polyps (Fig. 4B). In other fungiid species, a maximum of only three polyps have been observed to be released from each stalk (Yamashiro, 1992). Due to this asexual proliferation, the ages of individual fungiid corals, as estimated by growth functions or skeletal rings, are best thought of as age since detachment from the stalked anthocaulus phase. Recruitment to a population of free-living fungiids is actually a combination of larval settlement and the repeated production of individuals by attached stalks on the reef. This combination of sexual and asexual reproduction in mushroom corals leads to the formation of small clones of unconnected, dispersed individuals (Yamashiro, 1992). This life history feature need not invalidate the use of models to describe and manage populations of mushrooms corals, as long as standard definitions of coral age and recruitment are clearly understood to be modified or altered in members of

Table 3
Mortality rates (*Z*, annual) and life expectancies (*E*, years) known for anthozoans

Taxon	Reference	Locality	Depth (m)	*Z*	*E*
Gorgonacea					
Muricea californica	Grigg, 1977	La Jolla (southern California)	14–20	0.06	90
M. fruticosa	Grigg, 1977	La Jolla (southern California)	14–20	0.14	39
Paramuricea clavata	Mistri and Ceccherelli, 1994	Messina (Mediterranean)	30–38	0.12	46
Leptogorgia hebes	Mitchell et al., 1993	Northeastern Gulf of Mexico	22	1.14	6
	Mitchell et al., 1993	Northeastern Gulf of Mexico	27	0.23	25
L. virgulata	Mitchell et al., 1993	Northeastern Gulf of Mexico	1–1.5	0.54	11
Lophogorgia ceratophyta	Mistri, 1995	La Spezia Gulf (Mediterranean)	19–22	0.07	77
Corallium rubrum	Santangelo et al., 1993	Calafuria (Mediterranean)	20–45	0.56	11
C. secundum	Grigg, 1976	Makapuu (Hawaii)	350–475	0.07	77
Antipatharia					
Antipathes dichotoma	Grigg, 1976	Maui (Hawaii)	44–58	0.07	77
Scleractinia					
Goniastrea aspera	Babcock, 1991	Great Barrier Reef (Australia)	0–3	0.12	46
	Babcock, 1991	Great Barrier Reef (Australia)	0–3	0.16	35
Platygyra sinensis	Babcock, 1991	Great Barrier Reef (Australia)	0–3	0.09	60
Pocillopora verrucosa	Ross, 1984	Cebu (Philippines) (On a reef with a coral fishery)	1–10	0.61	10
	Ross, 1984	Cebu (Philippines)	1–11	0.34	17
Balanophyllia elegans	Fadlallah, 1983	Pacific Grove (central California)	10–15	0.80	8
	Gerrodette, 1979	Pacific Grove (central California)	9	0.15	37
	Gerrodette, 1979	Pacific Grove (central California)	21	0.12	45
	Gerrodette, 1979	La Jolla (southern California)	19	0.11	50
	Gerrodette, 1979	Pt. Loma (southern California)	14	0.06	91
	Gerrodette, 1979	Pt. Loma (southern California)	18	0.07	79
B. europaea	Goffredo, 1999	Tyrrenian Sea (Mediterranean)	1–13	1.17	6
Paracyathus stearnsii	Gerrodette, 1979	La Jolla (southern California)	19	0.05	99
	Gerrodette, 1979	La Jolla (southern California)	35	0.01	590
	Gerrodette, 1979	Pacific Grove (central California)	21	0.03	213
Fungia granulosa	Present study	Eilat (northern Red Sea)	6	0.17	33

this group. Finally, members of some fungiid coral species are known to proliferate extensively via active fragmentation of the free-living disc (reviewed by Yamashiro and Nishihira, 1998) or by the budding of polyps from the damaged or dying tissues of detached adults (Kramarsky-Winter and Loya, 1998). In species where these forms of reproduction dominate, different types of models need to be applied in order to understand processes of population turnover and structure.

4.5. Applications to coral reef management

Use of the Beverton Holt yield per recruit model to describe population dynamics in *F. granulosa* has important implications for stony coral fishery management. This model has been applied previously to manage stocks of precious corals in Hawaii (Grigg, 1984) and the Mediterranean (Caddy, 1993), and of reef-building stony corals in the Philippines (Ross, 1984). According to our estimates, the minimum size of *F. granulosa* individuals that can be fished without eventually decimating the local population (=size at maximum yield) is 74–79 mm in length, reached at ~9–10 years of age (Table 1). Polyps of *F. granulosa* at Eilat are known to reach sexual maturity at 55 mm in length (Kramarsky-Winter and Loya, 1998), corresponding to an age of about 6 years (Table 1). Thus, a minimum size limit of 74–79 mm would allow a 3–4 year buffer during which individuals could reproduce sexually before harvest. The growth model we employed here probably estimates accurately the age at sexual maturity, because it provides an appropriate description of prematurity growth (Day and Taylor, 1997), as corroborated by skeletal rings (Figs. 1 and 4).

According to our survival curve data, the percent of sexually mature individuals in this population is 43% (Table 1). In our field sample of the population, this value is slightly higher (57%), due to under representation of the 0–2 year age classes (Fig. 4B). The short time to maximum yield in *F. granulosa* (9–10 years, Table 1) is similar to that of the stony coral *Pocillopora verrucosa*, which reaches maximum yield at only 6 years of age (Grigg, 1984; Ross, 1984). In comparison, cohorts of antipatharians and gorgonians reach their maximum yield at much older ages of 28–40 years (Grigg, 1976, 1984; Caddy, 1993).

In Hawaii, the Beverton Holt model has been applied to sustainably manage the precious coral fishery for the production of jewelry and art objects (Grigg, 1984). Although this model likely will not be applied at Eilat, where coral harvest is prohibited, our work provides population dynamic information for a fungiid coral in the Red Sea, that may be compared with populations elsewhere. More widespread application of this type of model to fisheries of reef-building corals, especially in southeast Asia (Bentley, 1998), would reduce over-harvesting and the rapid depletion of stony coral populations in economies that depend upon this important natural resource.

Acknowledgements

We thank the staff of the Interuniversity Institute for Marine Science for their administrative and technical assistance, especially K. Tarnaruder for help with the

graphics. We are also grateful to Prof. F. Zaccanti of the University of Bologna for valuable advice on data elaboration and models. A. Balderman, S. Bensur, T. Feldstein, O. Langmead, E. Snider and D. Torovetzky assisted during the field work. This study was partially supported by an immigrant scientist fellowship from the Israeli Ministry of Science to N.E. Chadwick-Furman, funds from Scuba Schools International (Italy) to S. Goffredo, and funds to Y. Loya from the Porter Super-Center for Ecological and Environmental Studies, Tel Aviv University. [AU]

References

Abe, N., 1940. Growth of *Fungia actiniformis* var. *palawensis* Doederlein and its environmental conditions. Palao Trop. Biol. Station Stud. 2, 105–145.

Babcock, R.C., 1991. Comparative demography of three species of scleractinian corals using age- and size-dependent classifications. Ecol. Monogr. 61, 225–244.

Bablet, J.P., 1985. Report on the growth of a scleractinia (*Fungia paumotensis*). In: Proceedings 5th International Coral Reef Symposium, Tahiti, Vol. 4, pp. 361–365.

Bak, R.P.M., Meesters, E.H., 1998. Coral population structure: the hidden information of colony size-frequency distributions. Mar. Ecol. Prog. Ser. 162, 301–306.

Bentley, N., 1998. An overview of the exploitation, trade and management of corals in Indonesia. Traffic Bull. 17, 67–78.

Caddy, J.F., 1993. Background concepts for a rotating harvesting strategy with particular reference to the Mediterranean red coral *Corallium rubrum*. Mar. Fish. Rev. 55, 10–18.

Chadwick, N.E., Loya, Y., 1990. Regeneration after experimental breakage in the solitary reef coral *Fungia granulosa* Klunzinger, 1879. J. Exp. Mar. Biol. Ecol. 142, 221–234.

Chadwick-Furman, N., Loya, Y., 1992. Migration, habitat use, and competition among mobile corals (Scleractinia: Fungiidae) in the Gulf of Eilat. Red Sea Mar. Biol. 114, 617–623.

Clasing, E., Brey, T., Stead, R., Navarro, J., Asencio, G., 1994. Population dynamics of *Venus antiqua* (Bivalvia: Veneracea) in the Bahia de Yaldad, Isla de Chiloe, Southern Chile. J. Exp. Mar. Biol. Ecol. 177, 171–186.

Connell, J.H., 1973. Population ecology of reef building corals. In: Jones, O.A., Endean, R. (Eds.), Biology and Geology of Coral Reefs, Vol. II, Academic Press, New York, pp. 271–324.

Connell, J.H., Hughes, T.P., Wallace, C.C., 1997. A 30-year study of coral abundance, recruitment, and disturbance at several scales in space and time. Ecol. Monogr. 67, 461–488.

Day, T., Taylor, P.D., 1997. Von Bertalanffy growth equation should not be used to model age and size at maturity. Am. Nat. 149, 381–393.

Fadlallah, Y.H., 1983. Population dynamics and life history of a solitary coral, *Balanophyllia elegans*, from Central California. Oecologia 58, 200–207.

Gerrodette, T., 1979. Ecological Studies of Two Temperate Solitary Corals, University of California, San Diego, Ph.D. Thesis.

Goffredo, S., 1995. Studio dell'accrescimento di *Ctenactis echinata* (Pallas, 1766) e di *Fungia fungites* (Linnaeus, 1758) (Madreporaria, Fungiidae) nella barriera corallina di Sharm el Sheikh, Sud Sinai, Egitto, University of Bologna, Bologna, Italy, M.Sc. Thesis; in Italian, with English summary.

Goffredo, S., 1999. Population Dynamics and Reproductive Biology of the Solitary Coral *Balanophyllia europaea* (Anthozoa, Scleractinia) from the Northern Tyrrhenian Sea. In: University of Bologna, Bologna, Italy, Ph.D. Thesis; in Italian, with English summary.

Goffredo, S., Chadwick-Furman, N.E., 2000. Abundance and distribution of mushroom corals (Scleractinia: Fungiidae) on a coral reef at Eilat, northern Red Sea. Bull. Mar. Sci. 66, 241–254.

Grigg, R.W., 1974. Growth rings: annual periodicity in two gorgonian corals. Ecology 55, 876–881.

Grigg, R.W., 1976. Fishery management of precious and stony corals in Hawaii. In: University of Hawaii Sea Grant Report #77-03, p. 48.

Grigg, R.W., 1977. Population dynamics of two gorgonian corals. Ecology 58, 278–290.

Grigg, R.W., 1984. Resource management of precious corals: a review and application to shallow water reef building corals. P.S.Z.N.I. Mar. Ecol. 5, 57–74.

Grigg, R.W., Maragos, J.E., 1974. Recolonization of hermatypic corals on submerged lava flows in Hawaii. Ecology 55, 387–395.

Hoeksema, B.W., 1989. Taxonomy, phylogeny and biogeography of mushroom corals (Scleractinia: Fungiidae). Zool. Verh. Leiden 254, 1–295.

Hughes, T.P., 1984. Population dynamics based on individual size rather then age: a general model with a reef coral example. Am. Nat. 123, 778–795.

Hughes, T.P., Jackson, J.B.C., 1985. Population dynamics and life histories of foliaceous corals. Ecol. Monogr. 55, 141–166.

Johnson, K.G., 1992. Population dynamics of a free-living coral: recruitment, growth and survivorship of *Manicina areolata* (Linnaeus) on the Caribbean coast of Panama. J. Exp. Mar. Biol. Ecol. 164, 171–191.

Kramarsky-Winter, E., Loya, Y., 1998. Reproductive strategies of two fungiid corals from the northern Red Sea: environmental constraints? Mar. Ecol. Prog. Ser. 174, 175–182.

Lewis, J.B., 1989. Spherical growth in the Caribbean coral *Siderastrea radians* (Pallas) and its survival in disturbed habitats. Coral Reefs 7, 161–167.

Littler, M.M., Littler, D.S., Brooks, B.L., Koven, J.F., 1997. A unique coral reef formation discovered on the Great Astrolabe Reef, Fiji. Coral Reefs 16, 51–54.

Loya, Y., 1975. Environmental predictability in relation to life histories of reef corals. In: Proceedings Sixth Scientific Conference of the Israeli Ecological Society, Jerusalem, pp. 215–223.

Loya, Y., 1976a. Settlement, mortality and recruitment of a Red Sea scleractinian coral population. In: Mackie, G.O. (Ed.), Coelenterate Ecology and Behavior, Plenum Press, New York, pp. 89–100.

Loya, Y., 1976b. The Red Sea coral *Stylophora pistillata* is an r strategist. Nature 259, 478–480.

Loya, Y., 1990. Changes in a Red Sea coral community structure: a long-term case history study. In: Woodwell, G.M. (Ed.), The Earth in Transition: Patterns and Processes of Biotic Impoverishment, Cambridge University Press, Cambridge, pp. 369–384.

Mistri, M., 1995. Population structure and secondary product of the Mediterranean octocoral *Lophogorgia ceratophyta* (L. 1758). P.S.Z.N.I. Mar. Ecol. 16, 181–188.

Mistri, M., Ceccherelli, V.U., 1993. Growth of the Mediterranean gorgonian *Lophogorgia ceratophyta* (L., 1758). P.S.Z.N.I. Mar. Ecol. 14, 329–340.

Mistri, M., Ceccherelli, V.U., 1994. Growth and secondary production of the Mediterranean gorgonian *Paramuricea clavata*. Mar. Ecol. Prog. Ser. 103, 291–296.

Mitchell, N.D., Dardeau, M.R., Schroeder, W.W., 1993. Colony morphology, age structure, and relative growth of two gorgonian corals, *Leptogorgia hebes* (Verril) and *Leptogorgia virgulata* (Lamark), from the northern Gulf of Mexico. Coral Reefs 12, 65–70.

Motoda, S., 1940. The environment and the life of massive reef coral, *Goniastrea aspera* Verrill, inhabiting the reef flat in Palao. Palao Tropical Biological Station Studies 2, 41–80.

Ross, M.A., 1984. A quantitative study of the stony coral fishery in Cebu, Philippines. P.S.Z.N.I. Mar. Ecol. 5, 75–91.

Sakai, K., 1998. Delayed maturation in the colonial coral *Goniastrea aspera* (Scleractinia): whole-colony mortality, colony growth and polyp egg production. Res. Popul. Ecol. (Kyoto) 40, 287–292.

Santangelo, G.M., Abbiati, M., Caforio, G., 1993. Age structure and population dynamics in *Corallium rubrum* (L). In: Cicogna, F., Cattaneo-Vietti, R. (Eds.), Red Coral in the Mediterranean Sea: Art, History, and Science, Min. Ris. Agr. Al. For, Rome, pp. 131–157.

Shlesinger, Y., Loya, Y., 1991. Larval development and survivorship in the corals *Favia favus* and *Platygyra lamellina*. Hydrobiologia 216–217, 101–108.

Stephenson, T.A., Stephenson, A., 1933. Growth and sexual reproduction in corals. Great Barrier Reef Expedition 1928–29. Sci. Rep. 3, 167–217.

Stokes, M.D., 1996. Larval settlement, post-settlement growth and secondary production of the Florida lancelet (=amphioxus) *Branchiostoma floridae*. Mar. Ecol. Prog. Ser. 130, 71–84.

Tamura, T., Hada, Y., 1932. Growth rate of reef building corals inhabiting in the South Sea Island. Sci. Rep. Tohoku Imp. Univ., 4th Ser., Biology 6, 433–455.

von Bertalanffy, L., 1938. A quantitative theory of organic growth (Inquiries on growth laws. II). Hum. Biol. 10, 181–213.

Yamashiro, H., 1992. Skeletal dissolution by scleractinian corals. In: Proceedings 7th International Coral Reef Symposium, Guam, Vol. 2, pp. 1142–1146.

Yamashiro, H., Nishihira, M., 1998. Experimental study of growth and asexual reproduction in *Diaseris distorta* (Michelin, 1843), a free-living fungiid coral. J. Exp. Mar. Biol. Ecol. 225, 253–267.

Marine Biology (2003) 142: 411–418
DOI 10.1007/s00227-002-0980-9

S. Goffredo · N.E. Chadwick-Furman

Comparative demography of mushroom corals (Scleractinia: Fungiidae) at Eilat, northern Red Sea

Received: 25 March 2002 / Accepted: 12 October 2002 / Published online: 30 November 2002

Abstract The population structure and growth rates of stony corals may provide important information concerning their processes of turnover and recovery on coral reefs, yet for most corals such information is lacking. We quantify here the population dynamics of solitary free-living mushroom corals on a fringing reef at Eilat, northern Red Sea. Population models were applied to estimate growth, mortality, and lifespan in members of four common taxa: *Ctenactis echinata*, *Fungia scutaria*, *F. fungites*, and the subgenus *F.* (*Danafungia*) spp. Individuals of *C. echinata* and *F. scutaria* grew allometrically: their oral disc length increased more rapidly than width, leading to an oval body shape. Individuals of *F. fungites* and *F.* (*Danafungia*) spp. grew isometrically, retaining a circular body shape. A population of *F. scutaria* on the intertidal reef flat was characterized by young individuals (mean age = 2 years), with high mortality and short lifespan (13 years). In contrast, populations of the other three mushroom coral taxa on the reef slope consisted of older individuals (mean age = 4–9 years), with lower mortality and longer lifespans (24–46 years). Demographic patterns appeared to vary with species characteristics, and possibly with the level of disturbance in each reef habitat. Minimum sizes at which these mushroom corals may be removed sustainably from the populations range from 7 to 22 cm polyp diameter (5–14 years of age). We conclude that the Beverton and Holt population dynamic model is applicable to the management of stony corals with solitary or compact, upright growth forms that rarely fragment.

Communicated by R. Cattaneo-Vietti, Genova

S. Goffredo (✉)
Department of Evolutionary and Experimental Biology,
University of Bologna, Via F. Selmi 3,
40126 Bologna, Italy

E-mail: sgoff@tin.it
Fax: +39-051-251208

N.E. Chadwick-Furman
Interuniversity Institute for Marine Science,
P.O. Box 469, Eilat, Israel

N.E. Chadwick-Furman
Faculty of Life Sciences, Bar Ilan University,
Ramat Gan, Israel

Introduction

Understanding the population dynamics of reef-building corals is important for the management of coral reef resources, and for assessment of reef recovery rates following disturbances (Grigg 1984; Ross 1984; Wilkinson 1993; Meesters et al. 2001). Demographic parameters also reveal relationships between organisms and their environment, and contribute to assessment of habitat stability (Grigg 1975; Bak and Meesters 1998; Meesters et al. 2001). In addition, information on population turnover in reef-building corals may contribute to techniques for the restoration of damaged or degraded coral reefs (Connell 1973; Rinkevich 1995; Chadwick-Furman et al. 2000).

Scattered information is available on the population dynamics of scleractinian corals. Connell (1973) reviewed the modest amount of data that had been collected as of 30 years ago, and described parameters such as growth and survivorship. Since then, demographic processes have been described for some coral species in the Red Sea (Loya 1976a,b; Goffredo 1995; Chadwick-Furman et al. 2000), northeastern Pacific (Gerrodette 1979; Fadlallah 1983), Caribbean Sea (Hughes and Jackson 1985; Johnson 1992; Meesters et al. 2001), Great Barrier Reef of Australia (Babcock 1988, 1991), and Mediterranean Sea (Goffredo 1999). The paucity of information on population dynamics in most species of scleractinian corals may in part be attributed to a distortion of age–size relationships in this group, resulting from processes of fragmentation, fusion, and partial colony mortality (Hughes and Jackson 1985; Hughes and Connell 1987; Babcock 1991; Hughes et al. 1992). These phenomena, characteristic of clonal modular organisms (Hughes 1989), prevent the application of traditional growth and population dynamic

models based on organism age, and reveal highly complex demographic patterns (Hughes and Jackson 1985). A recent analysis of 13 Caribbean coral species used a size-based rather than age-based assessment of population structure, due to the above complexities of colony growth patterns (Meesters et al. 2001). In some cases, it is possible to overcome this barrier to coral age determination by selecting model species, whose individuals rarely fragment or fuse, and in which partial mortality is discernable by anomalies in the regular growth pattern (Chadwick-Furman et al. 2000). Corals that form discrete, upright branching colonies that rarely fragment in certain environments, such as *Pocillopora* and *Stylophora*, are suitable for this analysis (Grigg 1984). In addition, in some solitary corals, age estimates may be obtained from growth rings that are visible externally (Abe 1940; Chadwick-Furman et al. 2000) or detectable by x-ray analysis (Goffredo et al., unpublished data). Growth-ring analysis has been used more widely to age colonial scleractinian and gorgonian corals (Knuston et al. 1972; Buddemeir and Maragos 1974; Grigg 1974; Logan and Anderson 1991; Mistri and Ceccherelli 1993; Mitchell et al. 1993). As such, growth and population dynamic models based on age may be applied to certain growth forms of scleractinian corals to elucidate demographic characteristics (Nisbet and Gurney 1982; Grigg 1984; Ross 1984; Bak and Meesters 1998; Chadwick-Furman et al. 2000).

Solitary, free-living mushroom corals are conspicuous members of reef coral assemblages in the Indo-Pacific region (Hoeksema 1990; Goffredo and Chadwick-Furman 2000). They contribute to reef building, and in some areas build patch reefs consisting entirely of mushroom corals (Littler et al. 1997). Of particular interest are coral reefs at Eilat in the northern Red Sea, where mushroom corals are abundant on the reef flat and shallow slope (Kramarsky-Winter and Loya 1998; Goffredo and Chadwick-Furman 2000). Populations of mushroom corals at Eilat appear to meet the assumptions of standard population dynamic models, in that they occur in stable environmental conditions at the northern end of an enclosed sea, so their population structure appears to be stable, with no large recent changes in recruitment or mortality rates (Chadwick-Furman et al. 2000).

We describe here the comparative demography of mushroom corals at Eilat, by applying the population dynamic model of Beverton and Holt (1957) to four common taxa: *Ctenactis echinata* (Pallas, 1876), *Fungia scutaria* Lamarck, 1801, *F. fungites* (Linnaeus, 1758), and *F.* (*Danafungia*) spp. Wells, 1966. In combination with previous work on *F. granulosa* (Chadwick-Furman et al. 2000), we thus define population characteristics of the major mushroom corals in this reef area.

Materials and methods

This study was conducted during January–April 1996 at the Japanese Gardens fringing reef site at Eilat, northern Gulf of Aqaba, Red Sea. The coral community structure and reef profile at this site have been described in detail by Loya and Slobodkin (1971) and Loya (1990). To assess mushroom coral population structure, we deployed a 1×25 m belt transect parallel to shore at each of 12 depths: 1 m (inner margin of the reef flat), 1 m (outer margin of the reef flat) and at 2, 3, 6, 9, 12, 15, 21, 27, 33, and 40 m, thus encompassing the depth range of most mushroom corals at this site. A total area of 300 m^2 was surveyed (i.e. 25 m^2 per depth×12 depths surveyed, after Hoeksema 1990, 1991a; Goffredo and Chadwick-Furman 2000). Within each transect, we identified all mushroom corals to species according to Hoeksema (1989). Individuals of *Fungia* (*Danafungia*) *horrida* and *F.* (*Danafungia*) *scruposa* were grouped under the subgenus name *F.* (*Danafungia*) (see Hoeksema 1989), because the only trait distinguishing them was the presence of perforations in the corallum wall, which were not discernable in live polyps in the field (after Chadwick-Furman and Loya 1992; Goffredo and Chadwick-Furman 2000). Data on population dynamics of these two species grouped together were included here, because: (1) both species appear to be abundant at Eilat based on skeletal examination of dead polyps (N.E. Chadwick-Furman, personal observations), (2) both are known to have similar distribution and abundance patterns on reef slopes (Hoeksema 1990), and (3) no discontinuities were detected in their growth patterns, including mass–length relationships (see Fig. 1). The following information was recorded for each live mushroom coral observed: life history phase (attached anthocaulus or free-living anthocyathus), length (along axis of the oral disc parallel to the stomodeum's major diameter), and width (along axis of the oral disc perpendicular to the stomodeum's major diameter, after Abe 1940; Bablet 1985). Here we present data for four of the most common taxa, *Ctenactis echinata*, *F. scutaria*, *F. fungites*, and *F.* (*Danafungia*) spp., because too few individuals were observed of the other mushroom coral species to assess their population dynamics (Goffredo and Chadwick-Furman 2000).

To establish the relationship between polyp length and dry skeletal mass, we used a non-destructive method (after Chadwick-Furman et al. 2000) in compliance with coral conservation regulations of the Nature and Parks Authority of Israel. Skeletons of recently dead polyps found in the field were collected, observed under a dissecting microscope to eliminate any sediments or epifauna, dried at 400°C for 24 h, and weighed. Based on growth rings visible on the external aboral surface of live polyps observed underwater, and of skeletons examined in the laboratory, we established the relationship between age and length for polyps of each taxon (after Abe 1940; Chadwick-Furman et al. 2000). The growth rings visible on each polyp were counted several times to ensure accuracy.

Growth was expressed according to the von Bertalanffy function (von Bertalanffy 1938):

$$L_t = L_m\left(1 - e^{-Kt}\right)$$

where L_t is individual length at age t, L_m is asymptotic length (maximum expected length), K is a growth constant, and t is individual age. The parameters L_m and K were determined via application of a von Bertalanffy plot to age–length relationships obtained by growth-ring analysis (after Pauly 1984; Sparre et al. 1989). The Fisheries Program "Fishparm" (Prager et al. 1989) was used for parameter estimation. Maximum expected skeletal mass, expressed as asymptotic mass (W_m), or the mass corresponding to asymptotic length L_m, was calculated for each taxon based on the relationship between polyp length and dry skeletal mass.

►

Fig. 1A–C Patterns of individual growth in four taxa of mushroom corals at Eilat, northern Red Sea. Variation with individual length in: **A** width, **B** width:length ratio, and **C** dry skeletal mass. Relationships between linear parameters (columns A and B) were obtained from live polyps observed in the field; relationships between length and mass (column C) were obtained from recently dead polyps collected from the field. Equations are shown for the regression line in each graph

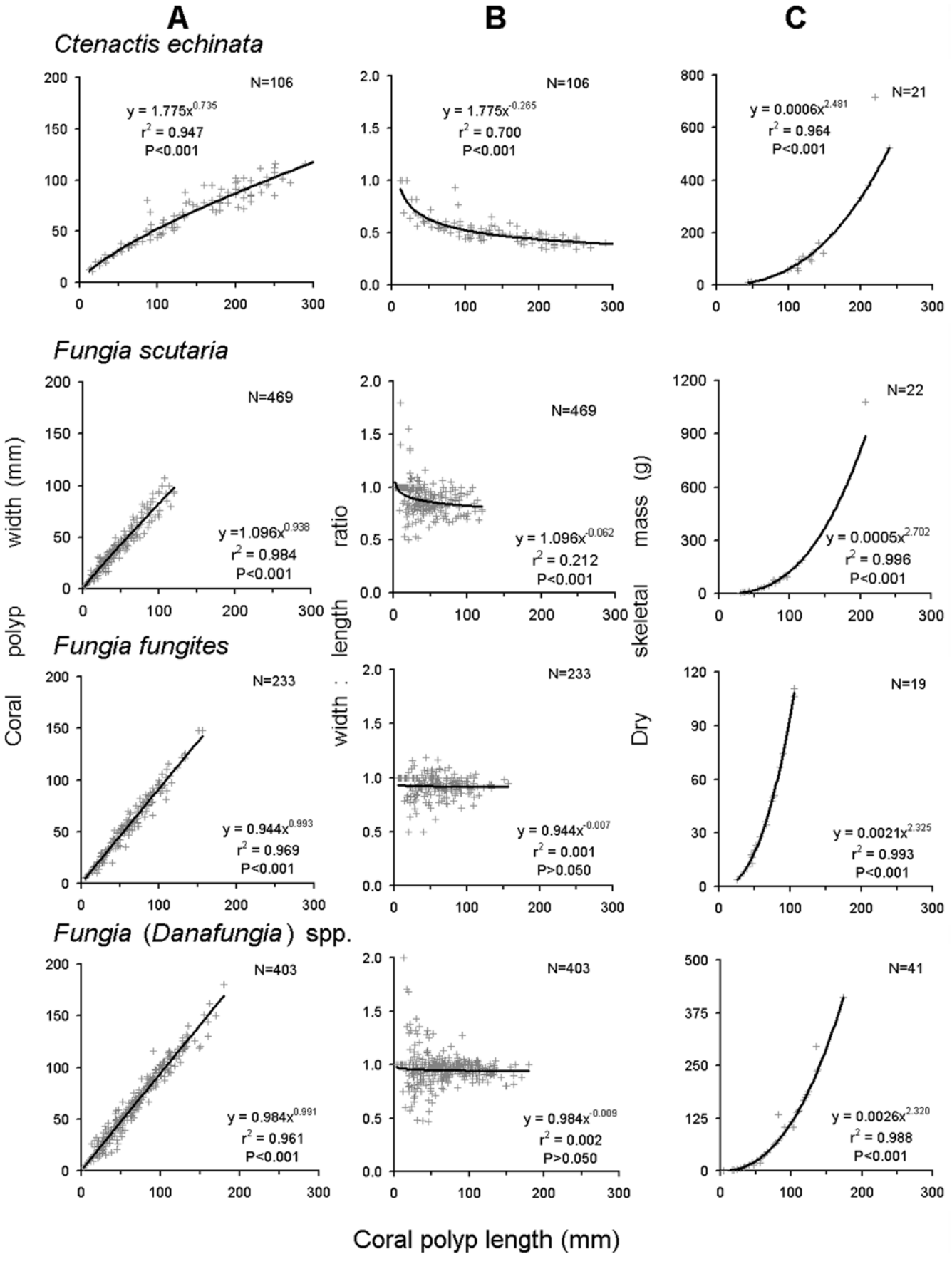
A
B
C
Ctenactis echinata
N=106
y = 1.775x^0.735
r² = 0.947
P<0.001
N=106
y = 1.775x^-0.265
r² = 0.700
P<0.001
N=21
y = 0.0006x^2.481
r² = 0.964
P<0.001
Fungia scutaria
N=469
y =1.096x^0.938
r² = 0.984
P<0.001
N=469
y = 1.096x^-0.062
r² = 0.212
P<0.001
N=22
y = 0.0005x^2.702
r² = 0.996
P<0.001
Fungia fungites
N=233
y = 0.944x^0.993
r² = 0.969
P<0.001
N=233
y = 0.944x^-0.007
r² = 0.001
P>0.050
N=19
y = 0.0021x^2.325
r² = 0.993
P<0.001
Fungia (Danafungia) spp.
N=403
y = 0.984x^0.991
r² = 0.961
P<0.001
N=403
y = 0.984x^-0.009
r² = 0.002
P>0.050
N=41
y = 0.0026x^2.320
r² = 0.988
P<0.001
Coral polyp width (mm)
Coral polyp width : length ratio
Dry skeletal mass (g)
Coral polyp length (mm)

The age structure of each population was determined from the population size structure, using the above length–age function. The instantaneous rate of mortality (Z) was expressed as a numeric reduction of the corals over time (i.e. survivorship curve):

$$N_t = N_0 e^{-Zt}$$

where N_t is the number of individuals at age t, N_0 is the number of individuals at age 0, Z is the instantaneous rate of mortality, and t is individual age (after Grigg 1984; Pauly 1984; Sparre et al. 1989; Chadwick-Furman et al. 2000). The age classes of 0–2 years were excluded from mortality-rate analysis because they are known to be under-represented in field samples of corals (Grigg 1984; Babcock 1991). According to the Beverton and Holt (1957) model, an age-specific curve expressing the cohort yield in skeletal mass was generated using the growth curve of skeletal mass and the survival curve of the individuals (after Grigg 1984; Ross 1984; Chadwick-Furman et al. 2000). Maximum individual lifespan was calculated as the age at which $< 0.5\%$ of the population was still surviving, based on survival curves (after Sparre et al. 1989).

Results

Individual growth patterns

The mushroom corals grew in two distinct forms, as shown by analysis of their shape parameters (Fig. 1). The first growth form, seen in *Fungia scutaria* and *Ctenactis echinata*, was characterized by an inverse exponential relationship between individual length and width:length ratio, with this ratio changing as the coral grew (Fig. 1A, B). This changing proportion indicated allometric growth, in that oral disc length increased more rapidly than width, resulting in an oval body shape. The second growth form occurred in *F. fungites* and *F.* (*Danafungia*) spp., and was characterized by a linear relationship between oral disc width and length, indicating isometric growth and the retention of a circular body shape (Fig. 1A, B). In terms of mass–length relationships, the corals characterized by allometric growth (*F. scutaria* and *C. echinata*) had higher exponent values and lower constant values than those with isometric growth [*F. fungites* and *F.* (*Danafungia*) spp., Fig. 1C].

In all taxa, very few individuals ($< 0.5\%$) were observed with partial mortality of their tissues, or with distorted body shapes indicating previous skeletal fragmentation, fusion, or restriction of growth by location.

Growth curves

Members of all four mushroom coral taxa grew determinately, as revealed by analysis of their growth rings and maximum individual sizes (L_m) in field populations (Fig. 2A). It was possible to assess age from skeletal growth rings only in young corals, because the rings became too close together to distinguish in older corals, due to the slowing of coral growth rate with age (Fig. 2A). The largest corals that we were able to age using external growth rings were 220 mm polyp length for *C. echinata* (12 years old), 118 mm for *F. scutaria* (9 years old), 77 mm for *F. fungites* (7 years old), and 66 mm for *F.* (*Danafungia*) spp. (6 years old) (Fig. 2A). Due to the exponential relationship between polyp length and mass (Fig. 1C), the growth curves for skeletal mass were sigmoidal (Fig. 2A).

Survivorship

Population age structure varied widely between the taxa examined (Fig. 2B). Mean coral age varied from 2 years in the population of *F. scutaria*, to 4 years in *F. fungites*, 5 years in *F.* (*Danafungia*) spp., and 9 years in *C. echinata* (arrows in Fig. 2B). During the first and second years of life, most of the individuals in each taxon occurred in the attached phase, but this proportion decreased, until by 3–5 years of age, all individuals became free living (Fig. 2B).

The instantaneous rate of mortality (Z) was two to four times higher for *F. scutaria* than for the other three taxa examined (Fig. 2B). Estimated survival curves indicated individual lifespans of about 13 years for *F. scutaria*, 24 years for *F. fungites*, 30 years for *F.* (*Danafungia*) spp., and 46 years for *C. echinata* (Fig. 2C).

Population yield

All taxa exhibited rapid early growth in population mass, followed by a peak as losses due to mortality overcame gains due to individual growth. Subsequently, population mass decreased for older specimens due to their low survival rate (Fig. 2C). Population yield curves for *F. fungites* and *F.* (*Danafungia*) spp. were similar, with peaks in population skeletal mass at 8 and 10 years, respectively. The population of *F. scutaria* peaked in mass at a much younger individual age of 5 years, and that of *C. echinata* at a much older age of 14 years (Fig. 2C).

Discussion

General

We demonstrate here that populations of mushroom corals on a coral reef at Eilat are highly dynamic: mean

►

Fig. 2A–C Population dynamic parameters of four taxa of mushroom corals at Eilat, northern Red Sea. **A** Growth curves (age–length and age–mass relationships) (*open circles* age–length data from growth rings; L_m asymptotic length; K growth constant; W_m asymptotic mass; N_{GRA} number of corals examined for growth ring analysis; *SE* standard error). **B** Population age structure [*arrows* indicate mean coral age in each population; N sample size; Z instantaneous rate of mortality; r^2 coefficient of determination of the semi-log regression from which the Z-value has been estimated (after Pauly 1984)]. **C** Survivorship curves and population yield in dry skeletal mass

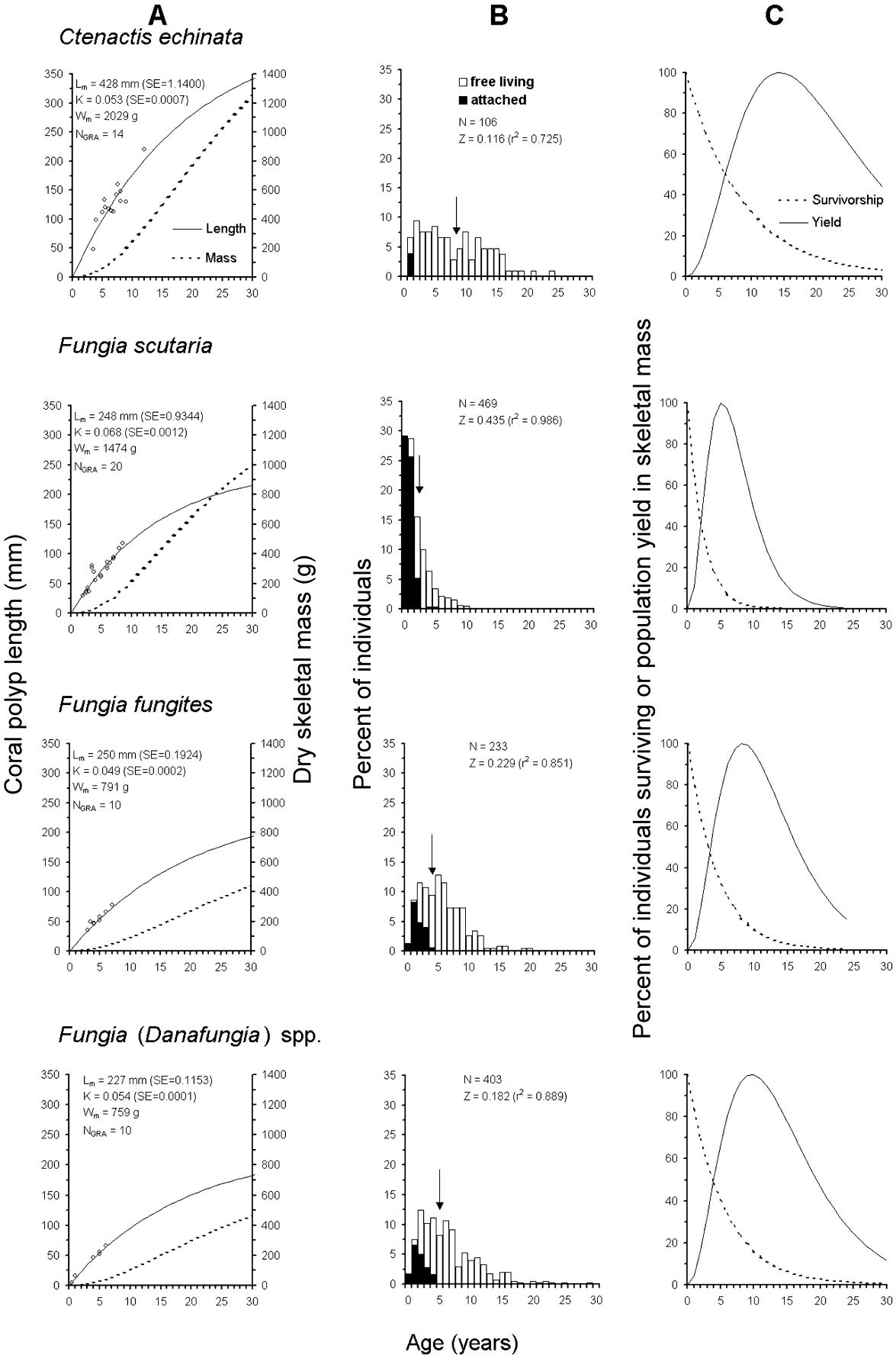
A
B
C
Ctenactis echinata
Fungia scutaria
Fungia fungites
Fungia (Danafungia) spp.
Coral polyp length (mm)
Dry skeletal mass (g)
Percent of individuals
Percent of individuals surviving or population yield in skeletal mass
Age (years)
Length
Mass
free living
attached
Survivorship
Yield
L∞ = 428 mm (SE=1.1400)
K = 0.053 (SE=0.0007)
W∞ = 2029 g
NGRA = 14
N = 106
Z = 0.116 (r2 = 0.725)
L∞ = 248 mm (SE=0.9344)
K = 0.068 (SE=0.0012)
W∞ = 1474 g
NGRA = 20
N = 469
Z = 0.435 (r2 = 0.986)
L∞ = 250 mm (SE=0.1924)
K = 0.049 (SE=0.0002)
W∞ = 791 g
NGRA = 10
N = 233
Z = 0.229 (r2 = 0.851)
L∞ = 227 mm (SE=0.1153)
K = 0.054 (SE=0.0001)
W∞ = 759 g
NGRA = 10
N = 403
Z = 0.182 (r2 = 0.889)

coral age in all populations was estimated at < 10 years, indicating a high turnover rate among individuals. In addition, polyps of *Fungia scutaria*, which live mainly on the intertidal reef flat (Goffredo and Chadwick-Furman 2000), had much higher mortality and faster turnover than did mushroom corals living on the reef slope. Comparison of demographic traits among the four taxa reveals different potential recovery rates of each taxon from physical disturbances.

Individual growth patterns

Isometric polyp growth likely represents the ancestral growth form for scleractinian corals (Wells 1956). Isometric growth occurs in all coral polyps with a circular adult shape, and has been demonstrated among mushroom corals in *F. actiniformis* (Abe 1940), *F. fungites* (Goffredo 1995; present paper), *F. granulosa* (Chadwick-Furman et al. 2000), and *F.* (*Danafungia*) spp. (present paper). In contrast, allometric growth is probably a derived trait, in which circular juvenile coral polyps develop into oval or oblong adults. This process has been documented for the mushroom corals *Ctenactis echinata* (Hoeksema 1991b; Claereboudt 1993; Goffredo 1995; present paper), *F. paumotensis* (Bablet 1985), and *F. scutaria* (present paper). Allometric growth is a product of less active skeletal secretion along the width than along the length axis of the oral disc, and results in (lengths being equal) a smaller oral disc surface area than in individuals with isometric growth. The relatively small surface area of oval or elongate corals may favor the removal of sediments and the acquisition of food in unstable habitats (Foster et al. 1988; Hoeksema 1991b).

Growth curves

Among the most common mushroom coral taxa at Eilat (Goffredo and Chadwick-Furman 2000), individuals of *C. echinata* grow to become the largest ($L_m = 428$ mm; Fig. 2A). In contrast, individuals of *F. granulosa* have a growth constant (K) double that of the other fungiids examined here, indicating that they reach maximum adult size most rapidly (compare our Fig. 2 with Chadwick-Furman et al. 2000). Estimates of L_m calculated here appear to be correct, as they are similar to those obtained from direct measurements of polyps in worldwide collections of these taxa (Hoeksema 1989).

Mushroom corals in the northern Red Sea have growth constants ($K = 0.049$–0.109) less than half of those of mushroom corals living near the equator ($K = 0.215$–0.404, reviewed in Chadwick-Furman et al. 2000). Within species, this pattern also occurs in *F. fungites*, the only mushroom coral for which growth data have been collected along a latitudinal gradient: Eilat (29°N) with $K = 0.049$ (present paper), Sharm el Sheikh (27°N) with $K = 0.088$ (Goffredo 1995), and Low Isles on the Australian Great Barrier Reef (17°S) with $K = 0.215$ (Stephenson and Stephenson 1933). Together, these data indicate that the growth rates of mushroom corals vary widely with latitude. A negative relationship between growth rate and latitude also has been demonstrated for corals of the genus *Porites* at sites along the Great Barrier Reef of Australia (Isdale 1983; Lough and Barnes 2000) and in the Hawaiian archipelago (Grigg 1981, 1997).

Survivorship

The population age structures of mushroom corals at Eilat are characterized by an exponential decrease in the frequency of individuals with age, with the rate of this decrease varying among the taxa (Chadwick-Furman et al. 2000; Fig. 2B). This type of pattern indicates that these populations may be numerically stable over time (Grigg 1977, 1984; Ross 1984; Yablokov 1986; Santangelo et al. 1993). Eilat's location at the northern tip of an enclosed sea appears to offer a relatively stable environment for most of these corals (Kramarsky-Winter and Loya 1998; Goffredo and Chadwick-Furman 2000), and could explain the steady state of the populations observed.

Variation in survivorship among fungiid taxa at Eilat appears related in part to differences in suitability between the reef habitats examined (Grigg 1975). Polyps of *F. fungit*es, *F. granulosa*, and *F.* (*Danafungia*) spp. occur mainly on the reef slope at wide depth ranges of 2–55 m (Goffredo and Chadwick-Furman 2000), and have similar population dynamics (our Fig. 2; Chadwick-Furman et al. 2000). Polyps of all three taxa have intermediate turnover times (4–6 years, calculated as the inverse of mortality rate Z, and also equal to mean coral age) and lifespans (24–33 years). Individuals of the two grouped species, *F.* (*Danafungia*) spp., may differ slightly in their population biology, but they are known to be closely related and ecologically similar species of fungiids (Hoeksema 1989, 1990). In contrast, individuals of *C. echinata* have a limited depth range on the reef slope of 2–8 m, and a longer turnover time (9 years) and lifespan (46 years) (Fig. 2). Polyps of *F. scutaria* occur almost exclusively on the reef flat at 1 m deep, and have a more rapid population turnover (2 years) and shorter polyp lifespan (13 years) than those of the fungiids on the reef slope (Fig. 2). Many small polyps of *F. scutaria* were attached to large, adult polyps, and were probably generated through asexual reproduction (Kramarsky-Winter and Loya 1998; Gilmour 2002). This reproductive strategy is observed in mushroom coral populations subjected to disturbance, and results in high mortality rates to the asexually produced young (Gilmour 2002). In contrast, mushroom corals on the reef slope likely reproduce mainly via sexual reproduction of dispersive propagules (Kramarsky-Winter and Loya 1998; Chadwick-Furman et al. 2000), which have lower rates of mortality (Gilmour 2002). We observed relatively few 1- to 2-year-old individuals of mushroom corals in the

field, except for those of *F. scutaria* (Fig. 2B). This variation appears to result from differences in reproductive patterns among these coral species (see discussion in Chadwick-Furman et al. 2000).

Population yield

We propose that the Beverton and Holt population dynamic model, which expresses a cohort's biomass curve in relation to age, be applied more widely to the management of exploited populations of certain stony corals. This model has been used to manage a handful of commercially important species of precious and hermatypic corals in both tropical and temperate ecosystems (Grigg 1984; Ross 1984; Caddy 1993). By arriving at estimates of the minimum size at which individuals may be removed sustainably from populations, wider use of this model could contribute to techniques for the transplantation of corals from "pristine" reef habitats to damaged areas in need of restoration (Rinkevich 1995; Edwards and Clark 1998; Epstein et al. 1999). Rinkevich (1995) asserts that transplantation practices aimed at the recovery of depleted coral reefs are best done by harvesting and transplanting artificially raised organisms from local mariculture instead of exporting individuals from natural populations. He terms this renewal strategy "coral reef gardening", and suggests the transplantation of individuals belonging to relatively fast-growing coral species. Among the most common mushroom corals at Eilat, the best candidate for contribution to reef restoration would be *F. granulosa*, whose growth rate constant (K) is substantially higher than those of other local fungiids (Chadwick-Furman et al. 2000; Fig. 2A). Some mushroom corals may make a unique contribution to reef restoration, because for years following initial transplantation, the stalked polyp base continues to produce multiple free-living polyps that detach and migrate downslope onto sandy areas. After the polyps die, their skeletons provide hard substrata onto which other corals may settle, thus facilitating the natural extension of reef areas onto the surrounding sand (Chadwick-Furman and Loya 1992).

The minimum size for removal of individuals from field populations of corals must be larger than the size at first reproduction, in order to allow a buffer period for the production of sexual recruits. Among the fungiids examined here, the size at first reproduction in Eilat is known only for *F. scutaria* (Kramarsky-Winter and Loya 1998). Polyps of this species begin to release sperm at 25 mm polyp length (~1.5 years old) and eggs at 50 mm length (~3.5 years old) (Kramarsky-Winter and Loya 1998), which results in a 2–4 year buffer period for sexual reproduction before these polyps reach size at maximum yield (Fig. 2). According to the Beverton and Holt model, the size at maximum yield represents the minimum size of individuals that can be removed from the population in a sustainable manner, without decimating it.

The population dynamic models employed here may be useful tools for comparative analyses of demographic traits in certain types of stony corals. Due to the increasing exploitation of corals for the jewelry and handicraft industries, and for live displays in aquariums, sustainable management programs are urgently needed for the commercial harvest of coral populations (Rinkevich 1995; Bentley 1998; Hatcher 1999). Broader application of the Beverton and Holt model to suitable coral species could help to reduce the rapid depletion of natural coral populations, as well as contribute to planning the recovery of damaged and degraded coral reefs.

Acknowledgements We thank the staff of the Interuniversity Institute for Marine Science at Eilat for technical and administrative assistance, especially K. Tarnaruder for preparation of the graphics. Prof. F. Zaccanti of the University of Bologna contributed advice on data elaboration and models. We also thank A. Balderman, S. Bensur, T. Feldstein, O. Langmead, E. Snider, and D. Torovetsky for assistance during the fieldwork. This study was partially supported by a grant from Scuba Schools International (Italy) to S. Goffredo.

References

Abe N (1940) Growth of *Fungia actiniformis* var. *palawensis* Doederlein and its environmental conditions. Palao Trop Biol Stn Stud 2:105–145

Babcock RC (1988) Age-structure, survivorship and fecundity in populations of massive corals, vol 2. In: Choat JH, et al (eds) Proc 6th Int Coral Reef Symp. Symposium Executive Committee, Townsville, pp 625–633

Babcock RC (1991) Comparative demography of three species of scleractinian corals using age- and size-dependent classifications. Ecol Monogr 6:225–244

Bablet JP (1985) Report on the growth of a scleractinia (*Fungia paumotensis*), vol 4. In: Gabrié C, et al (eds) Proc 5th Int Coral Reef Congr. Antenne Museum – EPHE, Moorea, French Polynesia, pp 361–365

Bak RPM, Meesters EH (1998) Coral population structure: the hidden information of colony size-frequency distributions. Mar Ecol Prog Ser 162:301–306

Bentley N (1998) An overview of the exploitation, trade and management of corals in Indonesia. Traffic Bull 17:67–78

Beverton RJH, Holt SV (1957) On the dynamics of exploited fish populations. Fish Investig Minist Agric Fish Food (GB) Ser II 19:1–553

Buddemeier RW, Maragos JE (1974) Radiographic studies of reef coral exoskeletons: rates and patterns of coral growth. J Exp Mar Biol Ecol 14:179–200

Caddy JF (1993) Background concepts for a rotating harvesting strategy with particular reference to the Mediterranean red coral, *Corallium rubrum*. Mar Fish Rev 55:10–18

Chadwick-Furman N, Loya Y (1992) Migration, habitat use, and competition among mobile corals (Scleractinia: Fungiidae) in the Gulf of Eilat, Red Sea. Mar Biol 114:617–623

Chadwick-Furman NE, Goffredo S, Loya Y (2000) Growth and population dynamic model of the reef coral *Fungia granulosa* Kluzinger, 1879 at Eilat, northern Red Sea. J Exp Mar Biol Ecol 249:199–218

Claereboudt MR (1993) Distinction of three species of *Ctenactis* (Scleractinia, Fungiidae) by multivariate analysis. Bull Inst R Sci Nat Belg Biol 63:5–11

Connell JH (1973) Population ecology of reef building corals. In: Jones OA, Endean R (eds) Biology and geology of coral reefs, vol II. Biology 1. Academic, New York, pp 271–324

Edwards AJ, Clark S (1998) Coral transplantation: a useful management tool or misguided meddling? Mar Pollut Bull 37:474–487

Epstein N, Bak RPM, Rinkevich B (1999) Implementation of small-scale "no-use zone" policy in a reef ecosystem: Eilat's reef-lagoon six years later. Coral Reefs 18:327–332

Fadlallah YH (1983) Population dynamics and life history of a solitary coral, *Balanophyllia elegans*, from Central California. Oecologia 58:200–207

Foster AB, Johnson KG, Schultz LL (1988) Allometric shape change and heterochrony in the free-living coral *Trachyphyllia bilobata* (Duncan). Coral Reefs 7:37–44

Gerrodette T (1979) Ecological studies of two temperate solitary corals. PhD thesis, University of California, San Diego

Gilmour JP (2002) Substantial asexual recruitment of mushroom corals contributes little to the population genetics of adults in conditions of chronic sedimentation. Mar Ecol Prog Ser 235:81–91

Goffredo S (1995) Growth study of *Ctenactis echinata* (Pallas, 1766) and *Fungia fungites* (Linnaeus, 1758) (Madreporaria, Fungiidae) in a fringing reef at Sharm el Sheikh, southern Sinai, Egypt. MSc thesis, University of Bologna, Bologna

Goffredo S (1999) Population dynamics and reproductive biology of the solitary coral *Balanophyllia europaea* (Anthozoa, Scleractinia) in the northern Tyrrhenian Sea. PhD thesis, University of Bologna, Bologna

Goffredo S, Chadwick-Furman NE (2000) Abundance and distribution of mushroom corals (Scleractinia: Fungiidae) on a coral reef at Eilat, northern Red Sea. Bull Mar Sci 66:241–254

Grigg RW (1974) Growth rings: annual periodicity in two gorgonian corals. Ecology 55:876–881

Grigg RW (1975) Age structure of a longevous coral: a relative index of habitat suitability and stability. Am Nat 109:647–657

Grigg RW (1977) Population dynamics of two gorgonian corals. Ecology 58:278–290

Grigg RW (1981) Coral reef development at high latitudes in Hawaii. In: Gomerz ED, et al (eds) Proc 4th Int Coral Reef Symp, vol 1. University of the Phillipines, Manila, pp 687–693

Grigg RW (1984) Resource management of precious corals: a review and application to shallow water reef building corals. Mar Ecol 5:57–74

Grigg RW (1997) Paleoceanography of coral reefs in the Hawaiian-Emperor Chain – Revisited. Coral Reefs 16:33–38

Hatcher BG (1999) Varieties of science for coral reef management. Coral Reefs 18:305–306

Hoeksema BW (1989) Taxonomy, phylogeny and biogeography of mushroom corals (Scleractinia: Fungiidae). Zool Verh (Leiden) 254:1–295

Hoeksema BW (1990) Systematics and ecology of mushroom corals (Scleractinia: Fungiidae). PhD thesis, University of Leiden, Leiden

Hoeksema BW (1991a) Control of bleaching in mushroom coral populations (Scleractinia: Fungiidae) in the Java Sea: stress tolerance and interference by life history strategy. Mar Ecol Prog Ser 74:225–237

Hoeksema BW (1991b) Evolution of body size in mushroom coral (Scleractinia, Fungiidae) and its ecomorphological consequences. Neth J Zool 41:112–129

Hughes RN (1989) A functional biology of clonal animals. Chapman and Hall, New York

Hughes TP, Connell JH (1987) Population dynamics based on size or age? A reef-coral analysis. Am Nat 129:818–829

Hughes TP, Jackson JBC (1985) Population dynamics and life histories of foliaceous corals. Ecol Monogr 55:141–166

Hughes TP, Ayre D, Connell JH (1992) The evolutionary ecology of corals. Trends Ecol Evol 7:292–295

Isdale PJ (1983) Geographical patterns in coral growth rates on the Great Barrier Reef. In: Baker JT, Carter RM, Sammarco PW, Stark KP (eds) Proc Great Barrier Reef Conference, Townsville. James Cook University Press, Townsville, pp 327–330

Johnson KG (1992) Population dynamics of a free-living coral: recruitment, growth and survivorship of *Manicina areolata* (Linnaeus) on the Caribbean coast of Panama. J Exp Mar Biol Ecol 164:171–191

Knuston DW, Buddemeir RW, Smith SV (1972) Coral chronometers: seasonal growth bands in reef corals. Science 177:270–272

Kramarsky-Winter E, Loya Y (1998) Reproductive strategies of two fungiid corals from the northern Red Sea: environmental constraints? Mar Ecol Prog Ser 174:175–182

Littler MM, Littler DS, Brooks BL, Koven JF (1997) A unique coral reef formation discovered on the Great Astrolabe Reef, Fiji. Coral Reefs 16:51–54

Logan A, Anderson IH (1991) Skeletal extension growth rate assessment in corals, using CT scan imagery. Bull Mar Sci 49:847–850

Lough JM, Barnes DJ (2000) Environmental controls on growth of the massive coral *Porites*. J Exp Mar Biol Ecol 245:225–243

Loya Y (1976a) Settlement, mortality and recruitment of a Red Sea scleractinian coral population. In: Mackie GO (ed) Coelenterate ecology and behavior. Plenum, New York, pp 89–100

Loya Y (1976b) The Red Sea coral *Stylophora pistillata* is an r-strategist. Nature 259:478–480

Loya Y (1990) Changes in a Red Sea coral community structure: a long-term case history study. In: Woodwell GM (ed) The Earth in transition: patterns and processes of biotic impoverishment. Cambridge University Press, Cambridge, pp 369–384

Loya Y, Slobodkin LB (1971) The coral reefs of Eilat (Gulf of Eilat, Red Sea). Symp Zool Soc Lond 28:117–139

Meesters WH, Hilterman M, Kardinaal E, Keetman M, de Vries M, Bak RPM (2001) Colony size-frequency distributions of scleractinian coral populations: spatial and interspecific variation. Mar Ecol Prog Ser 209:43–54

Mistri M, Ceccherelli VU (1993) Growth of the Mediterranean gorgonian *Lophogorgia ceratophyta* (L., 1758). Mar Ecol 14:329–340

Mitchell ND, Dardeau MR, Schroeder WW (1993) Colony morphology, age structure, and relative growth of two gorgonian corals, *Leptogorgia hebes* (Verrill) and *Leptogorgia virgulata* (Lamarck), from the northern Gulf of Mexico. Coral Reefs 12:65–70

Nisbet RM, Gurney WS (1982) Modeling fluctuating populations. Wiley, New York

Pauly D (1984) Fish population dynamics in tropical waters: a manual for use with programmable calculators. International Center for Living Aquatic Resources Management, Manila

Prager MH, Saila SB, Recksiek CW (1989) Fishparm: a microcomputer program for parameter estimation on nonlinear models in fishery science, 2nd edn. Oceanography technical report, Old Dominion University, Norfold, Va., pp 87–10

Rinkevich B (1995) Restoration strategies for coral reefs damaged by recreational activities – The use of sexual and asexual recruits. Restor Ecol 3:241–251

Ross MA (1984) A quantitative study of the stony coral fishery in Cebu, Philippines. Mar Ecol 5:75–91

Santangelo G, Abbiati M, Caforio G (1993) Age structure and population dynamics in *Corallium rubrum* (L). In: Cicogna F, Cattaneo-Vietti R (eds) Red coral in the Mediterranean Sea: art, history and science. Min Ris Agr Al For, Rome, pp 131–157

Sparre P, Ursin E, Venema SC (1989) Introduction to tropical fish stock assessment. FAO Fish Tech Pap 306.1:1–337

Stephenson TA, Stephenson A (1933) Growth and sexual reproduction in corals. Sci Rep Gt Barrier Reef Exped 3:167–217

von Bertalanffy L (1938) A quantitative theory of organic growth. Inquiries on growth laws. II. Hum Biol 10:181–213

Wells JW (1956) Scleractinia. In: Moore RC (ed) Treatise on invertebrate paleontology. Coelenterata. Geol Soc Amer/Univ Kansas Press, Lawrence, pp 328–444

Wilkinson CR (1993) Coral reefs of the world are facing widespread devastation: can we prevent this through sustainable management practices? In: Richmond RH (ed) Proc 7th Int Coral Reef Symp, vol 1. University of Guam, Mangilao, pp 11–21

Yablokov H (1986) Population biology. MIR Publisher, Moscow

Coral Reefs (2004) 23: 433–443
DOI 10.1007/s00338-004-0395-9

REPORT

S. Goffredo · G. Mattioli · F. Zaccanti

Growth and population dynamics model of the Mediterranean solitary coral *Balanophyllia europaea* (Scleractinia, Dendrophylliidae)

Received: 3 April 2003 / Accepted: 5 November 2003 / Published online: 17 August 2004

Abstract Complex life history processes of corals, such as fission, fusion, and partial mortality of colonies, that decouple coral age from size, are rare or clearly detectable in corals that produce distinct colonial or solitary forms. In some of these corals, individual age may be determined from size, and standard age-based growth and population dynamics models may be applied. We determined population size and structure and measured growth rates of *Balanophyllia europaea* individuals at Calafuria in the eastern Ligurian Sea. We then applied demographic models to these data. Growth rate decreased with increasing coral size. The age–size curve derived from field measurements of growth rates fits that obtained from the computerized tomography analysis of skeletal growth bands. The frequency of individuals in each age class decreased exponentially with age, indicating a population in a steady state. The survival curve showed a turnover time of 3.6 years and a maximum life span of 20 years. This is nearly three times the turnover time and maximum life span recorded for *Balanophyllia elegans* living off the western coasts of North America, the only congeneric species whose population dynamics has been studied. The Beverton and Holt population model may be useful for comparative analyses of demographic traits and for resource management of solitary or compact, upright growth forms that rarely fragment. This paper completes the description of the main life-strategy characteristics of the Mediterranean endemic coral *B. europaea*, together with our previous studies on the reproductive biology of this species. This constitutes a major advance in the understanding of the biology and ecology of Mediterranean scleractinian corals, and represents the most complete description of a coral from this geographic area to date that we are aware of.

Keywords Dendrophylliidae · Solitary coral · Growth model · Population ecology · Mediterranean Sea · Reef management

Communicated by Biological Editor H.R. Lasker

S. Goffredo (✉) · F. Zaccanti
Department of Evolutionary and Experimental Biology,
University of Bologna, via F. Selmi 3, 40126 Bologna, Italy
E-mail: sgoff@tin.it
Tel.: +39-339-5991481
Fax: +39-051-251208

G. Mattioli
Operative Unit of Radiology and Diagnostics by Images,
Hospital of Porretta Terme,
Local Health Enterprise of South Bologna,
via Roma 7, 40046 Porretta Terme, Italy

Introduction

Demographic parameters reveal relationships between organisms and their environment, and contribute to the assessment of habitat stability (Grigg 1975; Bak and Meesters1998; Meesters et al. 2001). In addition, information on population turnover may contribute to techniques for the restoration of damaged or degraded coastal areas (Connell1973; Rinkevich1995; Chadwick-Furman et al. 2000; Goffredo and Chadwick-Furman 2003).

Scattered information is available on the population dynamics of scleractinian corals. Connell (1973) reviewed the modest amount of data that had been collected in the previous 30 years, and described parameters such as growth and survivorship. Since then, demographic processes have been described for some coral species in the Red Sea (Loya 1976a, 1976b; Goffredo 1995; Chadwick-Furman et al. 2000; Goffredo and Chadwick-Furman 2003), northeastern Pacific (Gerrodette 1979a; Fadlallah 1983), Caribbean Sea (Hughes and Jackson 1985; Johnson 1992; Meesters et al. 2001), Great Barrier Reef, Australia (Babcock 1988, 1991), and in the Mediterranean Sea (Goffredo 1999). The paucity of information on population dynamics in most species of scleractinian corals may be attributed in part to a distortion of age–size relationships in this group,

resulting from processes of fragmentation, fusion, and partial colony mortality (Hughes and Jackson 1985; Hughes and Connell 1987; Babcock 1991; Hughes et al. 1992). These phenomena, characteristic of clonal modular organisms (Hughes 1989), prevent the application of traditional growth and population dynamics models based on organism age and create highly complex demographic patterns (Hughes and Jackson 1985). Due to these complexities, a recent analysis of 13 Caribbean coral species used a size-based, rather than age-based, assessment of population structure (Meesters et al. 2001). However, in species in which individuals rarely fragment or fuse, and partial mortality is discernable by anomalies in the regular growth pattern, it is possible to determine coral age (Chadwick-Furman et al. 2000). Corals that form discrete, upright branching colonies that rarely fragment in certain environments, such as *Pocillopora* and *Stylophora*, are suitable for this analysis (Grigg 1984). In addition, in some solitary corals, age estimates may be easily obtained from growth bands that are visible externally (Abe 1940; Chadwick-Furman et al. 2000; Goffredo and Chadwick-Furman 2003). Growth-band analysis has been used more widely to determine the age of colonial scleractinian and gorgonian corals (Knuston et al. 1972; Buddemeir and Maragos 1974; Grigg 1974; Logan and Anderson 1991; Mistri and Ceccherelli 1993; Mitchell et al. 1993). Thus growth and population dynamics models based on age can be applied to certain growth forms of scleractinian corals to describe demographic characteristics (Nisbet and Gurney 1982; Grigg 1984; Ross 1984; Bak and Meesters 1998; Chadwick-Furman et al. 2000; Goffredo and Chadwick-Furman 2003).

Balanophyllia europaea is a solitary, ahermatypic, zooxanthellate scleractinian coral that lives on rocky substratum and is endemic to the Mediterranean Sea (Zibrowius 1980,1983; Schumacher and Zibrowius 1985; Aleem and Aleem 1992; Veron 2000). Owing to its symbiosis with zooxanthellae, depth distribution appears restricted in this species; it is found between 0 m and a maximum of 50 m depth (Zibrowius 1980), though congeneric azooxanthellate corals have been reported at depths of up to 1,100 m (Cairns 1977). The reproductive biology of this species is characterized by simultaneous hermaphroditism and brooding (Goffredo and Telò 1998). *B. europaea* is the only species in the genus *Balanophyllia* and one of the few in the family Dendrophylliidae that exhibit hermaphroditism (Harrison 1985; Goffredo et al. 2000). During the annual cycle of sexual reproduction, fertilization takes place from March to June and planulation in August and September (Goffredo et al. 2002).

We describe the population dynamics of *B. europaea* in the eastern Ligurian Sea, applying Beverton and Holt's population dynamics model based on age (Beverton and Holt 1957; Chadwick-Furman et al. 2000; Goffredo and Chadwick-Furman 2003). This paper completes the description of the life strategy of this Mediterranean endemic coral together with previous studies on the reproductive biology of this species (Goffredo and Telò1998; Goffredo et al. 2000, 2002; Goffredo and Zaccanti in press).

Materials and methods

The studied population of *Balanophyllia europaea* was located off the coast of Calafuria (10 km south of Leghorn city, Tuscany region, Italy, eastern Ligurian Sea (NW Mediterranean), 43°28.4′N, 10°20′E). From April to October 1997, five transects were surveyed to collect data on population structure and bathymetric distribution of *B. europaea* (after Gerrodette 1979a; Mistri and Ceccherelli 1994; Goffredo and Chadwick-Furman 2000). Using an underwater compass, we set transects perpendicular to the coastline towards the open sea. Transect length was determined using a metered rope. Along each transect starting at a depth of 13 m, we monitored a series of 23 quadrats, each 1 m^2. Distance between quadrats was 2 m. Within each quadrat, we recorded the depth and the size of all *B. europaea* polyps. We measured polyp length (*L*: oral disc axis parallel to stomodaeum) and width (*W*: oral disc axis perpendicular to stomodaeum) (after Chadwick-Furman et al. 2000; Goffredo and Chadwick-Furman 2003). Regular spacing of quadrats and transects may be biased if laid over a population with a natural regular spacing. However, this should not have occurred in this case since the distributional pattern of *B. europaea* individuals is disaggregated (random) (Goffredo and Zaccanti in press).

During each dive, a mercury thermometer was used to measure water temperature in the field at a depth of 6 m. We also placed two digital thermometers (DS 1921L.F5, Dallas Semiconductors) at the same depth in the center of our research area to record water temperature readings every 4 h during the period under study. Photoperiod was calculated from astronomical almanacs.

In April 1998, we collected 75 polyps at a depth of 6 m (depth of maximum population density) and performed biometric analyses on them. Polyps were dried at 400 °C for 24 h and then height (*h*) (oral–aboral axis), dry skeletal mass (*M*), length, and width were measured (after Goffredo and Telò1998; Chadwick-Furman et al. 2000; Goffredo and Chadwick-Furman 2003; Goffredo et al. 2002).

Furthermore, we recorded the growth rates of 62 individuals of *B. europaea*, marked in situ by a numbered plastic tag nailed to the rock, at a depth of 6 m from December 1999 to April 2002. Length and width were measured in situ every 3 months for 0.3–2.3 years. The period of measurement varied between individuals, because corals that died were replaced by others of similar size during the study. The choice of the depth of maximum abundance for the determination of growth rates may bias the growth rate towards fast growth. This could underestimate the age of a coral of a given size,

but the bias should not affect most individuals, since most of the population biomass (62%) is concentrated at 5–7 m (Goffredo 1999).

To obtain an objective relationship between polyp size and age, for comparison with that obtained by field measurement of growth rates, we counted the number of annual growth bands by means of computerized tomography (CT) technology (after Dodge1980; Kenter 1989; Logan and Anderson 1991; Bosscher 1993). Specimens used in the CT measurements were collected at Calafuria, at a depth of 6 m near the marked individuals. Age was determined from the growth-band counts based on the observation that temperate zooxanthellate corals deposit two bands per year, a high density band in winter and a low density band in summer (Peirano et al. 1999). Growth bands were counted on corals up to 15 mm in length (75% of the maximum coral size in this population). Individuals larger than this had growth bands too close to be distinguished by CT scans.

Growth was fit to the von Bertalanffy function (von Bertalanffy 1938):

$$L_t = L_\infty\left(1 - e^{-Kt}\right)$$

where L_t is individual length at age t, L_∞ is asymptotic length (maximum expected length), K is a growth constant, and t is individual age. The parameters L_∞ and K were determined via application of "Gulland and Holt plot" and "Ford-Walford plot" traditional methods (Ford1933; Walford1946; Gulland and Holt 1959 and see the manuals of Pauly 1984 and Sparre et al. 1989, and for the exact procedure Sebens1983 and Mitchell et al. 1993 and Chadwick-Furman et al. 2000 for examples of application to corals).

Population size structure was derived from surveying the transects, and population age structure was then determined using the above length-age function. The instantaneous rate of mortality (Z) was determined by an analysis of the age frequency distribution (after Grigg 1984; Ross 1984; Pauly 1984; Sparre et al. 1989; Babcock 1991; Chadwick-Furman et al. 2000; Goffredo and Chadwick-Furman 2003). The method consists of a plot of the natural logarithm of the numbers (frequency) in each age class (N_t) against their corresponding age (t), or

$$\ln N_t = at + b,$$

Z being estimated from the slope a, with sign changed; the intercept b is equal to the natural logarithm of the number of individuals at age zero (N_0). The most important limitation of this method to estimate mortality rate is the assumption of the steady state of the population. The instantaneous rate of mortality was then used to express the numeric reduction of the corals over time (i.e., survivorship curve):

$$N_t = N_0 e^{-Zt}$$

Maximum individual lifespan was calculated as the age at which $<0.5\%$ of the population was still surviving, based on survival curves (after Sparre et al. 1989).

According to the Beverton and Holt (1957) model, an age-specific curve expressing cohort yield in skeletal mass was generated using the growth curve of skeletal mass and the survival curve of the individuals (i.e., cohort yield = individual mass at age t×percent survival at age t; after Grigg 1984; Ross 1984; Chadwick-Furman et al. 2000; Goffredo and Chadwick-Furman 2003). Based on the rates of growth and mortality for a population, the model predicts that a cohort of organisms will gain weight until a point (i.e., age/size) is reached where growth gains are overtaken by mortality losses. Maximum production by the cohort occurs at the point where losses due to mortality equal gains from growth. As the cohort ages and reaches a point of maximum longevity, production declines to zero.

Results

Description of habitat and population distribution

The seabed at Calafuria is initially rocky and drops rapidly from the coastline to a depth of 15 m, at which point it becomes sandy and slopes slightly but steadily until it hits a rocky vertical wall approximately 200–250 m from the coastline. The rocky wall starts at a depth of 16 m and ends at 45 m in a flat sand and mud bottom.

Balanophyllia europaea occurred on rocky substrata from 2 to 12 m deep with an average density of 16 individuals m^{-2} (SE = 3). Population density reached a peak of 113 individuals m^{-2} (SE = 33) at a depth of 6 m (Fig. 1).

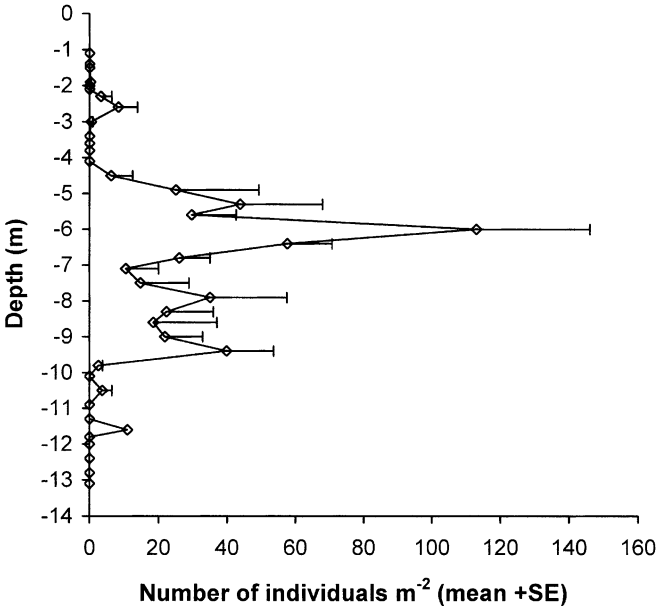

Fig. 1 Variation in the abundance of *Balanophyllia europaea* individuals according to depth on a rocky reef at Calafuria, eastern Ligurian Sea

The water temperature at 6-m depth varied seasonally by approximately 10 °C; the lowest temperatures occurred between January and March with an average of 13.7 °C (range = 13.0–15.5 °C), and the highest temperatures were in August with an average of 23.3 °C (range = 19.5–27 °C). The average annual temperature was 18.1 °C. Summer and winter photoperiods had a 6-h difference, with the longest daylength being 15 h, and the shortest, 9 h.

Individual growth patterns

The length of *B. europaea* was chosen as the primary biometrical measurement because it provided the best fit to dry skeletal mass. The mass-length plot produced the equation $M\ (\mathrm{g}) = 0.0018L(\mathrm{mm})^{2.537}$ ($r = 0.930$; $p < 0.01$). *B. europaea* growth was characterized by an inverse exponential relationship between individual length and width:length ratio, this ratio changing with coral growth (Fig. 2A). This changing proportion indicated allometric growth, with oral disc length increasing more rapidly than width, resulting in an oval body shape. Individual height and length had a linear relationship, with a constant ratio as the coral grew, indicating isometric growth (Fig. 2B).

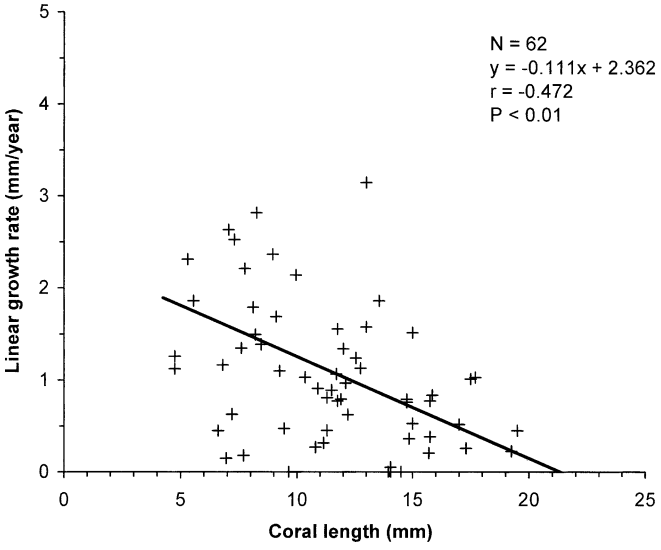

Fig. 3 Variation in linear growth rate among individuals of *Balanophyllia europaea*. From in situ field measurements of individual corals during 0.3–2.3 years on a rocky reef at Calafuria, eastern Ligurian Sea. This plot corresponds to the Gulland and Holt plot for the estimation of von Bertalanffy Growth function parameters K and L_∞. The observations are independent of one another; i.e., a single coral contributes one point. The ordinate is size increment per unit time $[(L_2-L_1)/(t_2-t_1)]$, and the abscissa are mean size for the increments in question $[(L_1+L_2)/2]$

Growth rate and lifetime growth curve

The growth rate of individuals of *B. europaea* decreased linearly with increasing coral size (Fig. 3). According to the Gulland and Holt plot method for the estimation of von Bertalanffy growth function parameters, the rate of this decrease is the growth constant K, which is the slope of the linear regression, with sign reversed. The population of *B. europaea* had $K = 0.111$ (0.058–0.163, 95% confidence interval (CI); Fig. 3). The maximum expected coral length (L_∞) corresponds to the coral length where the growth regression intercepts the x-axis (Fig. 3), which for *B. europaea* at Calafuria $L_\infty = 2.362$ (intercept)/0.111 (−slope) = 21.279 mm (16.365–26.505, 95% CI).

For corals < 10–11 years in age (< 14–15 mm in length), the von Bertalanffy growth curve derived from field measurements of growth rates produced a similar age–size relationship as that obtained from the CT analysis of skeletal growth bands; after this 10–11 year age, coral growth was so slow that bands became indistinguishable and hence the CT analysis unusable (Fig. 4, Fig. 5). Using the Ford-Walford plot method for parameter estimation, we also calculated a von Bertalanffy growth curve from the CT data (Fig. 4). A Ford-Walford plot factors out differences in growth that are age-dependent by plotting size (coral length, L) at age $t+1$ on the ordinate versus size at age t on the abscissa. The linear regression of this plot produced the equation $L_{t+1}(\mathrm{mm}) = 0.882L_t(\mathrm{mm}) +$

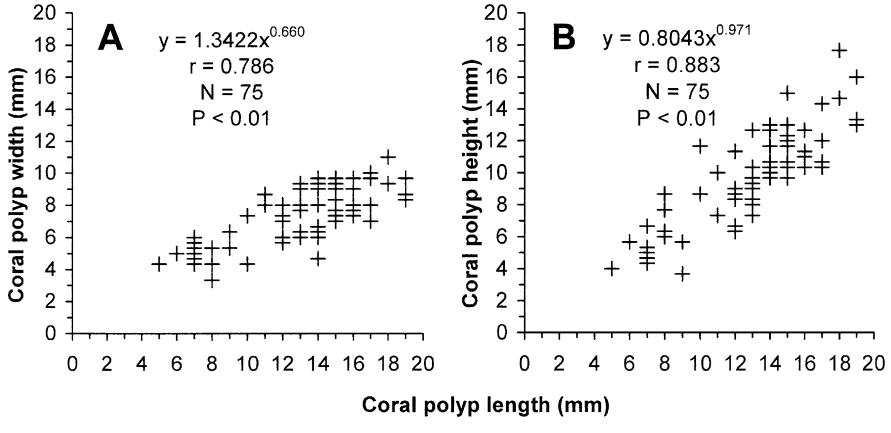

Fig. 2A, B Dependence of biometric parameters on individual length in the solitary coral *Balanophyllia europaea*. **A** Width. The confidence interval (CI) of the exponent of the nonlinear regression does not contain 1 (0.54–0.83, 95% CI), indicating allometric growth, with oral disc length increasing more rapidly than width. **B** Height. The confidence interval of the exponent of the nonlinear regression contains 1 (0.86–1.155, 95% CI), indicating coral polyp height and length have isometric growth

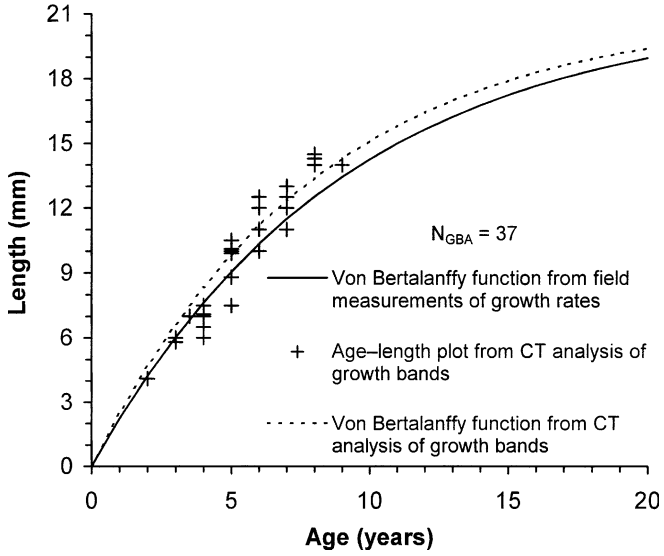

Fig. 4 Age-specific growth curves of individuals of the solitary coral *Balanophyllia europaea* at Calafuria (eastern Ligurian Sea). The age-length relationship, obtained from application of the von Bertalanffy growth model to linear extension rates measured in the field, is compared with age-length data from CT analysis of growth bands. N_{GBA} Number of corals examined for growth band analysis (37)

2.494 ($r = 0.978$; $p < 0.01$), from which L_∞ = intercept/(1−slope) = 21.136 mm (17.820–26.250, 95% CI), $K = -\ln$ (slope) = 0.126 (0.080–0.145, 95% CI). The confidence intervals of the CT function parameters fell within the confidence intervals of the function parameters from field growth rate measurements, indicating no significant differences between the two growth curves (Fig. 4).

According to the von Bertalanffy growth model, young individuals of *B. europaea* (1–2 years old) grew relatively rapidly (2.00–2.49 mm year^{-1}), but, as they aged their growth rate decreased (0.91–1.04 mm year^{-1} at 8–9 years old), and by the time they were 19–20 years old, grew at 0.23–0.30 mm year^{-1} (Fig. 4).

Population age structure and survivorship

The size-frequency of individuals observed in the field population, when converted to an age-frequency distribution using the above age–size relationship, revealed a population dominated by young individuals (Fig. 6A). Of the population sample, 50% was < 5 years old (< 9–10 mm in individual length), i.e., under or at the age of sexual maturity. The largest individuals observed were estimated to be 20 years old (= 19 mm length). The gradual diminution in number of corals in the older age categories suggests that age structure is relatively stable.

From the above age-frequency distribution, we estimated the instantaneous rate of mortality (Z). The youngest age classes (0–1 years) were excluded from the mortality-rate analysis because they are known to be under-represented in field samples (Grigg 1976, 1984; Babcock 1991; Chadwick-Furman et al. 2000; Goffredo and Chadwick-Furman 2003). In our case, the under-representation of young corals is probably a consequence of the difficulty in seeing corals of this size (< 2–3 mm in length). The plot of the natural logarithm of the numbers of individuals (frequency) in each age class (N_t) against their corresponding age (t), produced the equation $lnN_t = -0.275t(\text{years}) + 6.690$ ($r = 0.967$; $p < 0.01$). From this equation $Z = -(-0.275) = 0.275$ and $N_0 = e^{6.690} = 804.3$. The estimated survival curve for members of this population ($N_t = 804.3e^{-0.275t}$) indicated the maximum life span to be 20 years (Fig. 6B).

Population yield

The above data were used to calculate yield, in terms of skeletal mass per recruit, of *B. europaea* individuals at Calafuria (Fig. 6B). Cohort yield increased rapidly when the polyps were young, due to their rapid increases in size. Yield was maximal at 6–7 years of age, after which losses due to mortality overtook gains due to individual growth. The age at maximum yield occurred 2–4 years after the polyps reached sexual maturity (Fig. 6B).

Discussion

The population dynamics of *Balanophyllia europaea* at Calafuria revealed in this study, in combination with previous works on the species' reproductive biology (Goffredo and Telò 1998; Goffredo et al. 2000,2002; Goffredo and Zaccanti in press), have yielded a description of the main life strategy characteristics of this endemic, Mediterranean Sea, solitary coral. This constitutes a major advance in our understanding of the biology and ecology of Mediterranean scleractinian corals, and is the most complete description of a coral of this geographic area to date.

Depth distribution

The depth distribution of *B. europaea* at Calafuria was strictly limited; corals were not found below a depth of 12 m. This contrasts with previous studies, where the maximum known depth was 50 m (Ziborwius1980). Because *B. europaea* is zooxanthellate (Zibrowius1980, 1983), its bathymetric distribution is limited by light availability, while azooxanthellate congeners can live at depths of more than 1,000 m (Cairns1977). The very shallow depth distribution found in this study may be attributed to turbidity in this area that reduces light penetration (personal observations). In the nearby islands of the Tuscan archipelago (Elba and Capraia, for example), which are characterized by more transparent water because of the absence of continental terrigenous contributions, individuals of *B. europaea* have been found at depths of up to 30 m (personal observations).

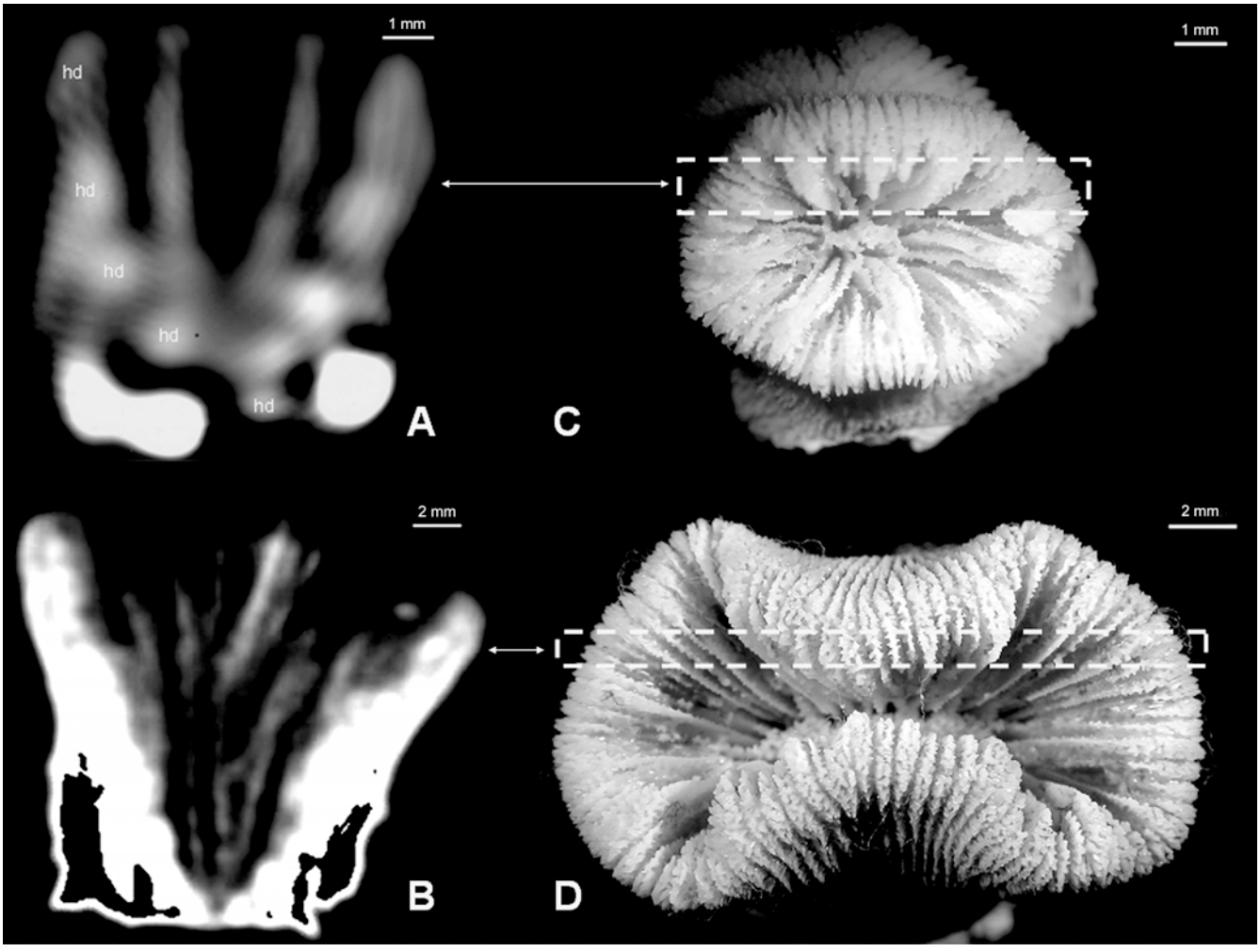

Fig. 5A–D Computerized tomography (CT) scans of *Balanophyllia europaea* corallites collected at Calafuria. Saggital CT scan sections are shown in **A** and **B** (the oral pole is at the *top*). *hd* High density band. Multiple CT views facilitated the identification of hd bands. The slab thickness of the tomography scan was 1 mm. **A** Age determination by counting the skeletal growth bands was possible in corallites up to 15 mm in length. In this sample (8 mm in length), five high-density bands, corresponding to 5 years of growth, are visible. **B** Age determination in individuals larger than 15 mm in length was not obtained by counting the skeletal growth bands because the growth bands are too close and no longer distinguishable by CT scans. In this sample (19 mm in length), determining age on the basis of an accurate band count is clearly not possible. **C, D** The original corallite is shown, in which is indicated where the saggital CT scan section was taken

Biometry

B. europaea oral disc length and width follow an allometric growth pattern leading to a change in polyp shape during its lifetime. Sexually immature polyps are round (with a width: length ratio = 1 at 1 year of age). Polyps gradually acquire a more oval shape, which becomes increasingly pronounced with age (width: length ratios of 0.75 at 3 years of age and 0.50 at 15–18 years of age). This allometric growth is the product of less active skeletal secretion along the width than along the length axis of the oral disc, and results in (lengths being equal) a smaller oral disc surface area than in individuals with isometric growth. The relatively small surface area of oval or elongate corals may favor the removal of sediments and the acquisition of food in unstable habitats (Foster et al. 1988; Hoeksema 1991).

Growth rate and models

Many scleractinian corals are known to grow indeterminately, and thus theoretically to have unlimited body size (reviewed in Hughes and Jackson 1985; Bak and Meesters 1998). However, some corals reduce their growth rate as they age. Scleractinian corals with size-dependent growth include species with branching colonies (*Pocillopora* spp.; Stephenson and Stephenson 1933; Grigg and Maragos1974), massive colonies (*Goniastrea* spp.; Motoda 1940; Sakai 1998), free-living colonies (*Manicina areolata*; Johnson 1992), free living solitary polyps (many species of mushroom corals; Stephenson and Stephenson 1933; Goffredo 1995; Yamashiro and Nishihira 1998; Chadwick-Furman et al. 2000; Goffredo and Chadwick-Furman 2003), and attached solitary polyps such as *B. europaea* (this study), *B. elegans,* and

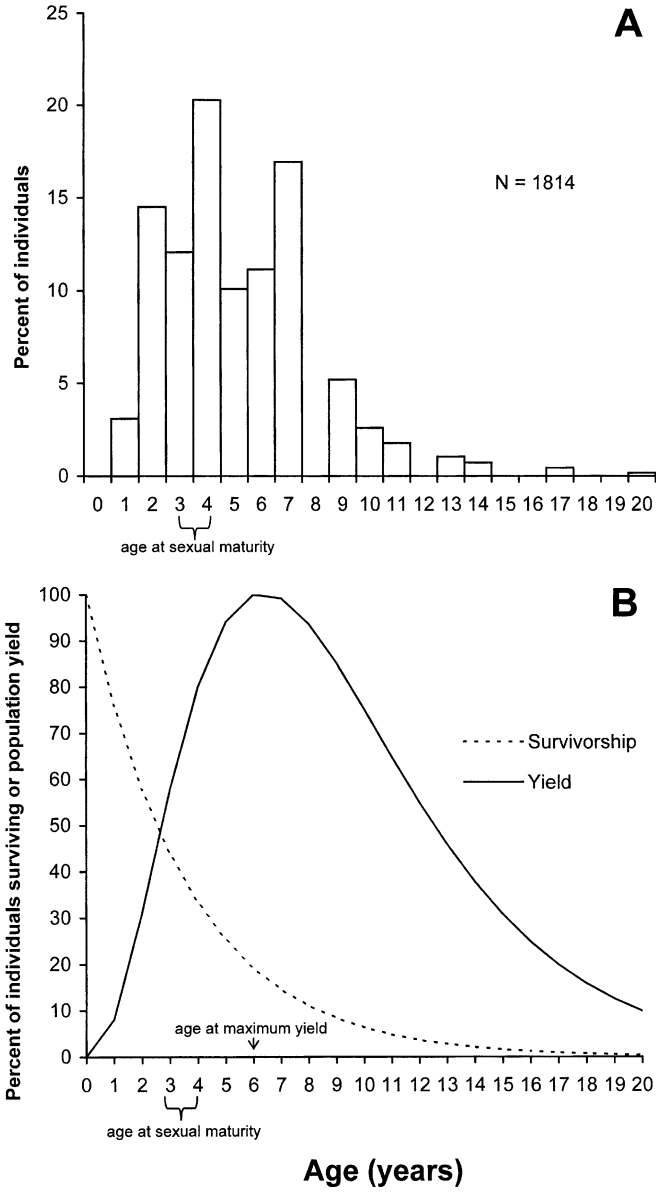

Fig. 6A, B Population age structure (**A**), and (B) survivorship curve and population yield (**B**) in dry skeletal mass of the solitary coral *Balanophyllia europaea* at Calafuria (eastern Ligurian Sea). Age at sexual maturity is from Goffredo et al. (2002). *N* Sample size

Paracyathus stearnsii (Gerrodette 1979a). In free-living corals, which often colonize soft substrata, a genetic limitation on maximum size may represent an adaptation to avoid sinking (Chadwick-Furman and Loya 1992). Among attached corals, other constraints may influence maximal size, such as the biomechanics of a skeleton with highly branched architecture, or the physiology of a solitary polyp with a single mouth.

The maximum individual length predicted by the von Bertalanffy model ($L_\infty = 21$ mm) is similar to that observed in the field population sampled at Calafuria (maximum observed length is 19 mm). Zibrowius (1980) gave 24 mm as the maximum length for *B. europaea* individuals, although larger individuals, up to 28 mm in length, are common in depths ranging from 0 to 30 m in the Straits of Messina about 625 km south of Calafuria (G. Neto, personal communication). The smaller size of the Calafuria individuals compared to those found at Messina and observations by Zibrowius (1980) could be attributed both to latitudinal characteristics of the annual daylength cycle and water temperature, and to mechanical limitations of the colonized environment (see Denny et al. 1985). A negative relationship between growth rate and latitude was shown for scleractinians in the genus *Porites* (Isdale1983; Lough and Barnes 2000; Grigg 1981, 1997) and in the family Fungiidae (Goffredo and Chadwick-Furman 2003). Alternatively, the Calafuria coast is often hit by storms, which expose the coral population to intense wave action. Organisms growing in strong wave action environments are generally smaller than organisms living in deeper or calmer waters (Harger 1970, 1972; Paine 1976; Adey 1978; Smith and Harrison 1977; Vosburgh 1977).

Population dynamics

The age structure of the examined population showed an exponential decrease in the frequency of individuals with age. This structure indicates a population in steady state, in that no age cohorts were missing or over-represented, as would be the case if a major disturbance event had recently altered recruitment patterns (Coe1956; Grigg 1977, 1984; Santangelo et al. 1993; Chadwick-Furman et al. 2000; Goffredo and Chadwick-Furman 2003). Other coral populations reported to occur in a steady state are those of the scleractinian *Pocillopora verrucosa* (Grigg 1984; Ross 1984), of scleractinian mushroom corals (Chadwick-Furman et al. 2000; Goffredo and Chadwick-Furman 2003), the gorgonians *Muricea californica* (Grigg 1977) and *Lophogorgia ceratophyta* (Mistri 1995), and the commercially important *Corallium rubrum* (Santangelo et al. 1993), *C. secundum* and *Anthipathes dichotoma* (Grigg 1984).

In a theoretical population in steady state, the coefficient of correlation of the semi-log regression from which the instantaneous rate of mortality (Z) is estimated has a value $r = -1.000$ (see Beverton and Holt 1956; Robson and Chapman 1961; Pauly 1984 for reviews on this method). In *B. europaea*, this coefficient of correlation was $r = -0.967$. This value is close to the best value of those calculated for other coral populations reported to occur in a steady state (r values reported for other coral populations with a stationary age distribution range from -0.851 to -0.993; Grigg 1984; Ross 1984; Chadwick-Furman et al. 2000; Goffredo and Chadwick-Furman 2003). This indicates that the steady-state assumption that we made in order to calculate the instantaneous rate of mortality is not unreasonable. According to population dynamics models, the instantaneous rate of mortality equals the inverse of the mean lifespan of the individuals in a population (turnover time), and hence is equal to their turnover rate, or

annual production:biomass ratio (P/B) (Pauly 1984; Clasing et al. 1994; Chadwick-Furman et al. 2000; Goffredo and Chadwick-Furman 2003). The turnover time for *B. europaea* at Calafuria was 3.6 years (calculated as the reciprocal of *Z*). Our estimates of the mortality rate and maximum life span for *B. europaea* appear to be reasonable, in that values derived from the survival curve closely reflect field observations.

We did not observe any 0-year-old and relatively few 1-year-old individuals of *B. europaea* at Calafuria. Probably, newly settled individuals are under-represented because of the difficulty in locating them, due to their small size (< 2–3 mm in individual length). Young of other coral species are known to be under-represented in field samples (as mentioned in Results), and the youngest age classes of corals are usually excluded from population dynamic analyses to overcome this difficulty (Grigg 1984; Babcock 1991).

Life strategies in the genus *Balanophyllia*

The average population density of *B. europaea* in Calafuria (16 individuals m^{-2}) is markedly lower than the only other *Balanophyllia* species for which population dynamics and reproductive biology are reported, namely *Balanophyllia elegans* off western North America (Table 1). *B. elegans* occurs from the Island of Vancouver (50°N) to Baja California (29°N) (Gerrodette 1979b). At the center of its geographic range, between a depth 6 and 13 m, the average population density is 563 individuals m^{-2} (Fadlallah1983), while at its northern limit, at a depth of 15 m the average population density is 136 individuals m^{-2} (Bruno and Witman1996). The higher population density of *B. elegans* is most likely due to the low dispersion capability of the azooxanthellate benthic larvae which attach to the bottom less than 0.5 m from the parent polyp (Gerrodette1981; Fadlallah and Pearse1982; Fadalallah1983). On the other hand, the low population density of *B. europaea* may be caused by the high dispersion capability of the larvae, which are zooxanthellate and have neutral buoyancy, with a prevalently swimming and pelagic behavior (Goffredo and Zaccanti in press). Symbiont zooxanthellae contribute to the energy requirement of larvae during dispersion and this may increases the dispersion capability (Richmond 1987, 1989; Ben-David-Zaslow and Benayahu 1998; Goffredo and Zaccanti in press).

Pianka (1970) visualized an *r–K* continuum, with any particular organism occupying a position along it. The *r*-endpoint represents the quantitative strategy, while the *K*-endpoint represents the qualitative strategy (see Table 1 in Pianka 1970 for a summary of the correlates of the *r*- and *K*-selected extremes). The comparison of the biological characteristics of the two congeneric species *B. europaea* and *B. elegans*, which is presented in Table 1 of this paper, reveals that the two species have evolved opposite life strategies, which are not identifiable with the endpoints of the *r–K* continuum. Rather, the two strategies appear mixed; *B. europaea* shows *K* characteristics for demography and *r* characteristics for reproduction, while on the contrary, *B. elegans* has a demography with *r* characteristics and a reproduction with *K* characteristics.

Application to the management of exploited populations

We propose that the Beverton and Holt population dynamics model, which expresses a cohort's biomass curve in relation to age, could be applied more widely to the management of exploited populations of certain scleractinian corals. This model has been previously applied to the study and/or management of populations of precious corals in Hawaii (Grigg 1976, 1984) and in the Mediterranean (Caddy 1993), as well as to populations of reef-building stony corals in the Philippines (Ross 1984) and in the Red Sea (Chadwick-Furman et al. 2000, Goffredo and Chadwick-Furman 2003). By estimating the minimum size at which individuals may

Table 1 Life-history characteristics of two species of the genus *Balanophyllia*. Data for *B. europaea* are from Goffredo and Telò (1998), Goffredo (1999), Goffredo et al. (2000, 2002), Goffredo and Zaccanti (in press), and this paper. Data for *B. elegans* are from Gerrodette (1979a, 1979b, 1981), Fadlallah and Pearse (1982), Fadlallah (1983), and Beauchamp (1993)

	Balanophyllia europaea	*Balanophyllia elegans*
Trophic strategy	Zooxanthellate coral	Azooxanthellate coral
Demography	Large coral size (maximum length = 21 mm)	Small coral size (maximum length < 10 mm)
	Long time of turnover (3.6 years)	Short time of turnover (1.3 years)
	Long longevity (maximum = 20 years)	Short longevity (maximum = 7 years)
	Low population density (mean = 16 individuals/m^2)	High population density (mean = 563 individuals/m^2)
Reproductive biology	Hermaphroditism	Gonochorism
	High fecundity (14 mature oocytes/100 mm^3polyp volume)	Low fecundity (6 mature oocytes/100 mm^3polyp volume)
	Short period of embryo incubation (4–5 months)	Long period of embryo incubation (14–15 months)
	Small planulae size (mean oral-aboral diameter = 2,150 μm)	Large planulae size (mean oral-aboral diameter = 4,000 μm)
	Pelagic dispersion of planulae	Benthic dispersion of planulae

be removed sustainably from populations (i.e., the size at maximum yield), a wider use of this model could contribute to techniques for the transplantation of corals from "pristine" reef habitats to damaged areas in need of restoration (Rinkevich 1995; Edwards and Clark 1998; Epstein et al. 1999).

The approach used in this study, the Beverton Holt model, to examine the population dynamics of a solitary temperate coral may have wider applications to other scleractinians. Due to the increasing exploitation of corals on a global scale for the jewelry and handicraft industries and for live displays in aquariums, sustainable management programs are urgently needed for the commercial harvesting of coral populations (Rinkevich 1995; Bentley1998; Hatcher1999). Broader application of the Beverton and Holt model to suitable coral species would reduce over-harvesting and rapid depletion of stony coral populations in economies that depend upon this natural resource, and may contribute to the recovery of damaged and degraded reefs.

Acknowledgements This study was supported by grants from the Italian Ministry for University, Scientific, and Technological Research; the Scuba Schools International Italia; and sponsored by the Underwater Life Project. We wish to thank Barbara Mantovani (University of Bologna, Italy), Olivia Langmead (Marine Biological Association, United Kingdom), Jason Hall-Spencer (University of Plymouth, United Kingdom), Howard R. Lasker (The State University of New York, USA), and two anonymous reviewers for their valuable revision of the text; Elettra Pignotti (Statistical Analysis, Rizzoli Orthopaedic Institute of Bologna, Italy) for her valuable advice on statistical treatment of data; the Bologna Scuba Team for its logistical support for the dives; the divers Elena Manzardo, Mario Pasquini, and Marco Longagnani for their assistance in the field; and the Marine Science Group for organizing and supervising the underwater scientific work.

References

Abe N (1940) Growth of *Fungia actiniformis* var. *palawensis* Doederlein and its environmental conditions. Palao Trop Biol Station Stud 2:105–145

Adey WH (1978) Coral reef morphogenesis: a multidimensional model. Science 202:831–837

Aleem AA, Aleem EAA (1992) *Balanophyllia europaea* (Risso, 1826). A scleractinian solitary coral in the southeastern Mediterranean. J Egypt Gen Soc Zool 8:227–233

Babcock RC (1988) Age-structure, survivorship and fecundity in populations of massive corals. Proc 6th Int Coral Reef Symp 2:625–633

Babcock RC (1991) Comparative demography of three species of scleractinian corals using age- and size-dependent classifications. Ecol Monogr 6:225–244

Bak RPM, Meesters EH (1998) Coral population structure: the hidden information of colony size-frequency distributions. Mar Ecol Prog Ser 162:301–306

Beauchamp KA (1993) Gametogenesis, brooding and planulation in laboratory populations of a temperate scleractinian coral *Balanophyllia elegans* maintained under contrasting photoperiod regimes. Invert Repr Dev 23:171–182

Ben-David-Zaslow R, Benayahu Y (1998) Competence and longevity in planulae of several species of soft corals. Mar Ecol Prog Ser 163:235–243

Bentley N (1998) An overview of the exploitation, trade and management of corals in Indonesia. Traffic Bull 17:67–78

Beverton RJH, Holt SV (1956) A review of methods for estimating mortality rates in fish populations, with special reference to sources of bias in catch sampling. Rapp P V Réun Cons Int Explor Mer 140:67–83

Beverton RJH, Holt SV (1957) On the dynamics of exploited fish populations. Fish Invest Minist Agric Fish Food (G B) Ser II 19:1–553

Bosscher H (1993) Computerized tomography and skeletal density of coral skeletons. Coral Reefs 12:97–103

Bruno JF, Witman JD (1996) Defense mechanisms of scleractinian cup corals against overgrowth by colonial invertebrates. J Exp Mar Biol Ecol 207:229–241

Buddemeier RW, Maragos JE (1974) Radiographic studies of reef coral exoskeletons: rates and patterns of coral growth. J Exp Mar Biol Ecol 14:179–200

Caddy JF (1993) Background concepts for a rotating harvesting strategy with particular reference to the Mediterranean red coral, *Corallium rubrum*. Mar Fish Rev 55:10–18

Cairns DS (1977) Biological results of the University of Miami deep-sea expedition. 121. A review of the recent species of *Balanophyllia* (Anthozoa: Scleractinia) in the western Atlantic, with descriptions of four new species. Proc Biol Soc Wash 90:132–148

Chadwick-Furman N, Loya Y (1992) Migration, habitat use, and competition among mobile corals (Scleractinia: Fungiidae) in the Gulf of Eilat, Red Sea. Mar Biol 114:617–623

Chadwick-Furman NE, Goffredo S, Loya Y (2000) Growth and population dynamic model of the reef coral *Fungia granulosa* Kluzinger, 1879 at Eilat, northern Red Sea. J Exp Mar Biol Ecol 249:199–218

Clasing E, Brey T, Stead R, Navarro J, Asencio G (1994) Population dynamics of *Venus antiqua* (Bivalvia: Veneracea) in the Bahia de Yaldad, Isla de Chiloe, Southern Chile. J Exp Mar Biol Ecol 177:171–186

Coe WR (1956) Fluctuations in populations of littoral marine invertebrates. J Mar Res 15:212–232

Connell JH (1973) Population ecology of reef building corals. In: Jones OA, Endean R (eds) Biology and geology of coral reefs, vol. II: biology 1. Academic, New York, pp 271–324

Denny MW, Daniel TL., Koehl MAR (1985) Mechanical limits to size in wave-swept organisms. Ecol Monogr 55:69–102

Dodge RE (1980) Preparation of coral skeletons for growth studies. In: Rhoads DC, Lutz RA (eds) Skeletal growth of aquatic organism. Plenum, New York, pp 615–618

Edwards AJ, Clarks S (1998) Coral transplantation: a useful management tool or misguided meddling? Mar Pollut Bull 37:474–487

Epstein N, Bak RPM, Rinkevich B (1999) Implementation of small-scale "no-use zone" policy in a reef ecosystem: Eilat's reef-lagoon six years later. Coral Reefs 18:327–332

Fadlallah YH (1983) Population dynamics and life history of a solitary coral, *Balanophyllia elegans*, from Central California. Oecologia 58:200–207

Fadlallah YH, Pearse JS (1982) Sexual reproduction in solitary corals: overlapping oogenic and brooding cycles, and benthic planulas in *Balanophyllia elegans*. Mar Biol 71:223–231

Foster AB, Johnson KG, Schultz LL (1988) Allometric shape change and heterochrony in the free-living coral *Trachyphyllia bilobata* (Duncan). Coral Reefs 7:37–44

Ford E (1933) An account of the herring investigations conducted at Plymouth during the years from 1924–1933. J Mar Biol Assoc U K 19:305–384

Gerrodette T (1979a) Ecological studies of two temperate solitary corals. PhD thesis, University of California, San Diego

Gerrodette T (1979b) Equatorial submergence in solitary coral, *Balanophyllia elegans*, and the critical life stage excluding the species from the shallow water in the south. Mar Ecol Prog Ser 1:227–235

Gerrodette T (1981) Dispersal of the solitary coral *Balanophyllia elegans* by demersal planular larvae. Ecology 62:611–619

Goffredo S (1995) Growth study of *Ctenactis echinata* (Pallas, 1766) and *Fungia fungites* (Linnaeus, 1758) (Madreporaria, Fungiidae)

in a fringing reef at Sharm el Sheikh, southern Sinai, Egypt. M Sc Thesis, University of Bologna, Bologna
Goffredo S (1999) Population dynamics and reproductive biology of the solitary coral *Balanophyllia europaea* (Anthozoa, Scleractinia) in the Northern Tyrrhenian Sea. PhD Thesis, University of Bologna, Bologna
Goffredo S, Arnone S, Zaccanti F (2002) Sexual reproduction in the Mediterranean solitary coral *Balanophyllia europaea* (Scleractinia, Dendrophylliidae). Mar Ecol Prog Ser 229:83–94
Goffredo S, Chadwick-Furman NE (2000) Abundance and distribution of mushroom corals (Scleractinia: Fungiidae) on a coral reef at Eilat, northern Red Sea. Bull Mar Sci 66:241–254
Goffredo S, Chadwick-Furman NE (2003) Comparative demography of mushroom corals (Scleractinia, Fungiidae) at Eilat, northern Red Sea. Mar Biol 142:411–418
Goffredo S, Telò T (1998) Hermaphroditism and brooding in the solitary coral *Balanophyllia europaea* (Cnidaria, Anthozoa, Scleractinia). Ital J Zool 65:159–165
Goffredo S, Telò T, Scanabissi F (2000) Ultrastructural observations of the spermatogenesis of the hermaphroditic solitary coral *Balanophyllia europaea* (Anthozoa, Scleractinia). Zoomorphology 119:231–240
Goffredo S, Zaccanti F (in press) Laboratory observations on larval behavior and metamorphosis in the Mediterranean solitary coral *Balanophyllia europaea* (Scleractinia, Dendrophylliidae). Bull Mar Sci
Grigg RW (1974) Growth rings: annual periodicity in two gorgonian corals. Ecology 55:876–881
Grigg RW (1975) Age structure of a longevous coral: a relative index of habitat suitability and stability. Am Nat 109:647–657
Grigg RW (1976) Fishery management of precious and stony corals in Hawaii. UNIHI-SEAGRANT-TR-77–03:1–48
Grigg RW (1977) Population dynamics of two gorgonian corals. Ecology 58:278–290
Grigg RW (1981) Coral reef development at high latitudes in Hawaii. Proc 4th Int Coral Reef Symp 1:687–693
Grigg RW (1984) Resource management of precious corals: a review and application to shallow water reef building corals. Mar Ecol PSZNI 5:57–74
Grigg RW (1997) Paleoceanography of coral reefs in the Hawaiian-Emperor Chain—revisited. Coral Reefs 16:33–38
Grigg RW, Maragos JE (1974) Recolonization of hermatypic corals on submerged lava flows in Hawaii. Ecology 55:387–395
Gulland JA, Holt SJ (1959) Estimation of growth parameters for data at unequal time intervals. J Cons Int Explor Mer 25:47–49
Harger JRE (1970) The effect of wave impact on some aspects of the biology of sea mussels. Veliger 12:401–414
Harger JRE (1972) Competitive co-existence: maintenance of interacting associations of the sea mussels *Mytilus edulis* and *Mytilus californianus*. Veliger 14:195–201
Harrison PL (1985) Sexual characteristics of scleractinian corals: systematic and evolutionary implications. Proc 5th Int Coral Reef Symp 4:337–342
Hatcher BG (1999) Varieties of science for coral reef management. Coral Reefs 18:305–306
Hoeksema BW (1991) Evolution of body size in mushroom coral (Scleractinia, Fungiidae) and its ecomorphological consequences. Neth J Zool 41:112–129
Hughes RN (1989) A functional biology of clonal animals. Chapman, New York
Hughes TP, Ayre D, Connell JH (1992) The evolutionary ecology of corals. Trends Ecol Evol 7:292–295
Hughes TP, Connell JH (1987) Population dynamics based on size or age? A reef-coral analysis. Am Nat 129:818–829
Hughes TP, Jackson JBC (1985) Population dynamics and life histories of foliaceous corals. Ecol Monogr 55:141–166
Isdale PJ (1983) Geographical patterns in coral growth rates on the Great Barrier Reef. In: Baker JT, Carter RM, Sammarco PW, Stark KP (eds) Proceedings Great Barrier Reef conference, Townsville. James Cook University Press, Townsville, pp 327–330
Johnson KG (1992) Population dynamics of a free-living coral: recruitment, growth and survivorship of *Manicina areolata* (Linnaeus) on the Caribbean coast of Panama. J Exp Mar Biol Ecol 164:171–191
Kenter JAM (1989) Applications of computerized tomography in sedimentology. Mar Geotechnol 8:201–211
Knuston DW, Buddemeir RW, Smith SV (1972) Coral chronometers: seasonal growth bands in reef corals. Science 177:270–272
Logan A, Anderson IH (1991) Skeletal extension growth rate assessment in corals, using CT scan imagery. Bull Mar Sci 49:847–850
Lough JM, Barnes DJ (2000) Environmental controls on growth of the massive coral *Porites*. J Exp Mar Biol Ecol 245:225–243
Loya Y (1976a) Settlement, mortality and recruitment of a Red Sea scleractinian coral population. In: Mackie GO (ed) Coelenterate ecology and behavior. Plenum, New York, pp 89–100
Loya Y (1976b) The Red Sea coral *Stylophora pistillata* is an r-strategist. Nature 259:478–480
Meesters WH, Hilterman M, Kardinaal E, Keetman M, de Vries M, Bak RPM (2001) Colony size–frequency distributions of scleractinian coral populations: spatial and interspecific variation. Mar Ecol Prog Ser 209:43–54
Mistri M (1995) Population structure and secondary production of the Mediterranean octocoral *Lophogorgia ceratophyta* (L. 1758). PSZNI Mar Ecol 16:181–188
Mistri M, Ceccherelli VU (1993) Growth of the Mediterranean gorgonian *Lophogorgia ceratophyta* (L., 1758). Mar Ecol PSZNI 14:329–340
Mistri M, Ceccherelli VU (1994) Growth and secondary production of the Mediterranean gorgonian *Paramuricea clavata*. Mar Ecol Prog Ser 103:291–296
Mitchell ND, Dardeau MR, Schroeder WW (1993) Colony morphology, age structure, and relative growth of two gorgonian corals, *Leptogorgia hebes* (Verrill) and *Leptogorgia virgulata* (Lamark), from the northern Gulf of Mexico. Coral Reefs 12:65–70
Motoda S (1940) The environment and the life of massive reef coral, *Goniastrea aspera* Verrill, inhabiting the reef flat in Palao. Palao Trop Biol Station Stud 2:41–80
Nisbet RM, Gurney WS (1982) Modeling fluctuating populations. Wiley, New York
Paine RT (1976) Biological observations on a subtidal *Mytilus californianus*. Veliger 19:125–130
Pauly D (1984) Fish population dynamics in tropical waters: a manual for use with programmable calculators. International Center for Living Aquatic Resources Management, Manila
Peirano A, Morri C, Bianchi CN (1999) Skeleton growth and density pattern of the temperate, zooxanthellate scleractinian *Cladocora caespitosa* from the Ligurian Sea (NW Mediterranean). Mar Ecol Prog Ser 185:195–201
Pianka ER (1970) On r- and K-selection. Am Nat 104:592–597
Richmond RH (1987) Energetics, competency, and long-distance dispersal of planula larvae of the coral *Pocillopora damicornis*. Mar Biol 93:527–533
Richmond RH (1989) Competency and dispersal potential of planula larvae of a spawning versus a brooding coral. Proc 6th Int Coral Reef Symp 2:827–831
Rinkevich B (1995) Restoration strategies for coral reefs damaged by recreational activities—the use of sexual and asexual recruits. Restor Ecol 3:241–251
Robson DS, Chapman DG (1961) Catch curves and mortality rates. Trans Am Fish Soc 90:181–189
Ross MA (1984) A quantitative study of the stony coral fishery in Cebu, Philippines. Mar Ecol PSZNI 5:75–91
Sakai K (1998) Delayed maturation in the colonial coral *Goniastrea aspera* (Scleractinia): whole-colony mortality, colony growth and polyp egg production. Res Popul Ecol (Kyoto) 40:287–292
Sebens KP (1983) Size structure and growth rates in populations of colonial and solitary invertebrates. In: Reaka ML (ed) The ecology of deep and shallow coral reefs. NOAA's Undersea Research Prog, pp 9–15

Santangelo G, Abbiati M, Caforio G (1993) Age structure and population dynamics in *Corallium rubrum* (L). In: Cicogna F, Cattaneo-Vietti R (eds) Red Coral in the Mediterranean Sea: art, history and science. Min Ris Agr Al For, Rome, pp 131–157

Schumacher H, Zibrowius H (1985) What is hermatypic? A redefinition of ecological groups in corals and other organisms. Coral Reefs 4:1–9

Smith SV, Harrison JT (1977) Calcium carbonate production of the mare incognitum, the upper windward reef slope, at Enewetak Atoll. Science 197:556–559

Sparre P, Ursin E, Venema SC (1989) Introduction to tropical fish stock assessment. FAO Fisheries Technical Paper, Rome

Stephenson TA, Stephenson A (1933) Growth and sexual reproduction in corals. Great Barrier reef Expedition 1928–1929. Scientific Reports 3:167–217

Veron J (2000) Corals of the world. Australian Institute of Marine Science, Townsville

von Bertalanffy L (1938) A quantitative theory of organic growth (inquiries on growth laws II). Hum Biol 10:181–213

Vosburgh F (1977) The response to drag of the reef coral *Acropora reticulata*. Proc 3rd Int Coral Reef Symp 1:477–482

Walford LA (1946) A new graphic method of describing the growth of animals. Biol Bull 90:141–147

Yamashiro H, Nishihira M (1998) Experimental study of growth and asexual reproduction in *Diaseris distorta* (Michelin, 1843), a free-living fungiid coral. J Exp Mar Biol Ecol 225:253–267

Zibrowius H (1980) Les scléractiniaires de la Méditerraée et de l'Atlantique nord-oriental. Mém Inst Océanogr Monaco 11:1–284

Zibrowius H (1983) Nouvelles données sur la distribution de quelques scléractiniaires "méditerranéens" à l'est et à l'ouest du détroit de Gibraltar. Rapp Comm Int Mer Médit 28:307–309

Mar Biol (2007) 152:351–361
DOI 10.1007/s00227-007-0695-z

RESEARCH ARTICLE

Variation in biometry and population density of solitary corals with solar radiation and sea surface temperature in the Mediterranean Sea

Stefano Goffredo · Erik Caroselli · Elettra Pignotti · Guido Mattioli · Francesco Zaccanti

Received: 28 November 2006 / Accepted: 28 March 2007 / Published online: 19 April 2007

Abstract The correlation between two environmental factors (solar radiation and sea surface temperature), biometry, and population density was assessed along a latitudinal gradient in the zooxanthellate coral *Balanophyllia europaea* and in the azooxanthellate coral *Leptopsammia pruvoti*. With increasing polyp size, the oral disc of *B. europaea* assumed an oval shape, while that of *L. pruvoti* retained a circular shape. In both species, biometric parameters varied more with temperature than with solar radiation. In the zooxanthellate species, temperature explained a higher percentage of biometric parameter variance than in the azooxanthellate species. While environmental factors did not co-vary with demographic characteristics in *L. pruvoti*, temperature was negatively related to the population density of *B. europaea.* It is hypothesized that the negative effect of temperature on biometry and population density of *B. europaea* depends on photosynthesis inhibition of symbiotic zooxanthellae at high temperatures, which would lower the calcification rate and availability of energetic resources.

Communicated by R. Cattaneo-Vietti.

S. Goffredo (✉) · E. Caroselli · F. Zaccanti
Department of Evolutionary and Experimental Biology,
Alma Mater Studiorum—University of Bologna,
Via F. Selmi 3, 40126 Bologna, Italy
e-mail: stefano.goffredo@marinesciencegroup.org

E. Pignotti
Taskforce for Statistical Analysis,
Marine and Freshwater Science Group Association,
Via F. Selmi 3, 40126 Bologna, Italy

G. Mattioli
Operative Unit of Radiology and Diagnostics by Images,
Hospital of Porretta Terme, Local Health Enterprise of Bologna,
Via Roma 16, 40046 Porretta Terme, Bologna, Italy

Introduction

The variation of environmental parameters due to latitude is a substantial causal factor of the global distribution of corals (Kleypas et al. 1999). The distribution of atolls and main coral reefs of the world, confined between 30°N and 30°S latitude (Kinsey and Davies 1979), suggests that coral growth actually decreases at high latitudes to a point where coral reef development no longer occurs (Grigg 1982). Coral ''growth'' is a composite of the three related characters of annual calcification, skeletal density, and linear extension rate (calcification = skeletal density × linear extension; Lough and Barnes 2000; Carricart-Ganivet 2004), and their measurement is essential when assessing the effects of environmental parameters on coral growth (Dodge and Brass 1984). These three variables have been studied along a latitudinal gradient in the genera *Porites* (Grigg 1982; Lough and Barnes 2000) and *Montastraea* (Carricart-Ganivet 2004) and variation in the three parameters has been related to variation in temperature and light associated with latitude. In colonies of the genus *Porites* in the Hawaiian archipelago, Australian Great Barrier Reef, and Thailand, negative correlations with latitude were found for the linear extension, leading to an increase in skeletal density of the colonies (Grigg 1982; Lough and Barnes 2000). In colonies of the genus *Montastraea* in the Gulf of Mexico and Caribbean Sea, negative correlations with latitude were found for calcification and skeletal density, leading to an increase in linear extension rate (Carricart-Ganivet 2004). Rates of linear extension in

the colonial corals of the genera *Pocillopora* and *Acropora* and in a number of species of the Faviidae family in subtropical Australia (Crossland 1981; Stimson 1996; Harriott 1999) were considerably slower than those at low latitude. Also in the solitary corals of the Fungiidae family, a negative relationship was found between growth rate and latitude (Goffredo and Chadwick-Furman 2003). In contrast, there seem to be cases where rates of coral growth do not vary with increasing latitude. For instance, *Acropora yongei*, *Acropora formosa*, *Turbinaria frondens*, and *Porites heronensis* from subtropical Australia have linear extension rates similar to those of closely related taxa in the tropics, confounding any causal link between latitude and growth rates of coral colonies or coral reefs (Harriott 1999).

For temperate areas, studies on the relationship between environmental parameters and coral growth are scarce. In *Astrangia danae* (Jacques et al. 1983) and *Plesiastrea versipora* (Howe and Marshall 2002), calcification rate increases with temperature, similar to the trend in tropical corals, albeit at lower temperatures. This study presents the relationship between latitudinal variation of environmental factors [solar radiation and sea surface temperature (SST)] and biometry and population density of two Mediterranean Sea corals, *Balanophyllia europaea* (Risso 1826) and *Leptopsammia pruvoti* (Lacaze-Duthiers 1897).

Balanophyllia europaea is a solitary, ahermatypic, zooxanthellate, and scleractinian coral, which is endemic to the Mediterranean Sea (Zibrowius 1980). Due to its symbiosis with zooxanthellae, the distribution of this coral is restricted to 0-50 m depth (Zibrowius 1980), where its population density can reach dozens of individuals per square meter (Goffredo et al. 2004). Its reproductive biology is characterized by simultaneous hermaphroditism and brooding (Goffredo et al. 2002). *L. pruvoti* is an ahermatypic, azooxanthellate, solitary, and scleractinian coral, which is distributed in the Mediterranean basin and along the European Atlantic coast from Portugal to southern England. It is one of the most common organisms under overhangs, in caverns, and crevices at 0–70 m depth, reaching densities of thousands of individuals per square meter (Zibrowius 1980; Goffredo et al. 2006). Its reproductive biology is characterized by gonochorism and brooding (Goffredo et al. 2006).

The aim of this study is to assess the variation in the biometric parameters and population density of the zooxanthellate *B. europaea* and of the azooxanthellate *L. pruvoti* along a solar radiation and SST gradient.

Materials and methods

From November 9, 2003 to September 30, 2005, specimens of *B. europaea* and *L. pruvoti* were collected from six sites along a latitudinal gradient, from 44°20′N to 36°45′N (Fig. 1). Latitude is the main factor influencing the variation of temperature and light (Kain 1989), which are the two environmental parameters considered in this study since they are strongly linked to coral biometry, physiology, and demography (Kleypas et al. 1999; Lough and Barnes 2000; Harriott and Banks 2002; Al-Horani 2005). At each site, a transect was sampled for both species. For *B. europaea*, the transect consisted of three patches of 1 m^2 each, arranged in a line, 5 m apart and situated along a reef exposed south at a depth of 5–7 m. For *L. pruvoti*, the transect consisted of at least three patches of 0.00425 m^2 each, situated on the vault of crevices 3 m apart, at a depth of 15–17 m (site and number of patches for *B. europaea*: Genova $n = 8$, Calafuria $n = 18$, Elba $n = 3$, Palinuro $n = 3$, Scilla $n = 8$, and Pantelleria $n = 3$; site and number of patches for *L. pruvoti*: Genova $n = 3$, Calafuria $n = 3$, Elba $n = 4$, Palinuro $n = 3$, Scilla $n = 3$, and Pantelleria $n = 3$). Regular spacing of quadrats and transects may be biased if laid over a population with a natural regular spacing. However, this should not have occurred in these cases since the distributional pattern of the two species is disaggregated (random) (personal observation; Goffredo and Zaccanti 2004; Goffredo et al. 2004). All of the coral polyps present were collected from each patch. The sampling was performed at depths known to have high population densities and where the reproductive biology of the two species had been studied previously (Goffredo and Zaccanti 2004; Goffredo et al. 2002, 2004, 2006). The area of each patch was smaller for *L. pruvoti* than for *B. europaea* because of the very high density of the former species and the difficulty of sampling on the vaults, inside narrow caves.

Collected corals were dried at 50°C for 4 days, and then observed under a binocular microscope to remove fragments of substratum and calcareous deposits produced by other organisms. A low drying temperature was chosen to avoid phase transitions in the skeletal aragonite/calcite composition (Vongsavat et al. 2006), as this problematic will be investigated using these samples in a diffractometric analysis in preparation. Polyp length (*L*: maximum axis of the oral disc), width (*W*: minimum axis of the oral disc), and height (*h*: oral-aboral axis) were measured using a pair of calipers, and dry skeletal mass (*M*) was measured using a precision balance (Goffredo and Chadwick-Furman 2003; Goffredo et al. 2002). Polyp volume (*V*) was determined by applying the formula $V = \frac{L}{2} \times \frac{W}{2} \times h\pi$ (Goffredo et al. 2002, 2006). Skeletal density (*D*) was calculated by dividing *M* by *V*. The population density was obtained as: (1) *NI*, number of individuals per area unit (N m^{-2}), (2) *G*, grams per unit area (g m^{-2}), and (3) *P*, percent coverage.

All data relating to the Calafuria site of *B. europaea* were taken from the dataset of Goffredo et al. (2004),

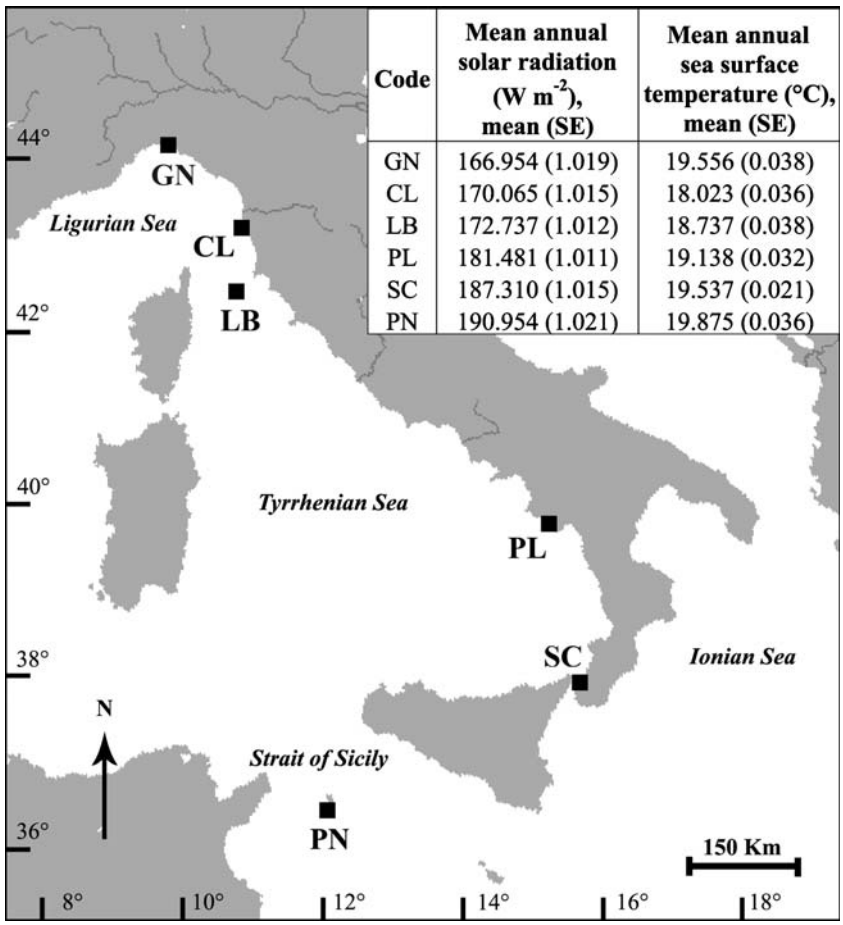

Fig. 1 Map of the Italian coastline indicating the sites where the corals were collected. Abbreviations and coordinates of the sites in decreasing order of latitude: *GN* Genova–Portofino, 44°20′N, and 9°08′E; *CL* Calafuria, 43°27′N, and 10°21′E; *LB* Elba Isle, 42°45′N, and 10°24′E; *PL* Palinuro, 40°02′N, and 15°16′E; *SC* Scilla, 38°01′N, and 15°38′E; *PN* Pantelleria Isle, 36°45′N, and 11°57′E. For each site, solar radiation and sea surface temperature values are indicated. Solar radiation and SST both varied among the sites (Kruskal–Wallis test and $P < 0.001$)

where the biometric analysis was performed on 75 polyps collected randomly at 6 m, and several patches were sampled between 0 and 13 m to examine the bathymetric distribution. For the biometric analysis, the same 75 polyps were used in this work, while for the correlation analysis between biometry, population density, and environmental parameters, only the patches sampled between 5 and 7 m were considered.

As done by a number of authors (e.g., Harriott 1999; Lough and Barnes 2000; Carricart-Ganivet 2004; Peirano et al. 2005a, b) in their studies on the influence of environmental parameters on coral growth, the physical measurement data in our study also (SST and solar radiation) have been obtained from data banks. During 2003–2005, SST data were obtained for each site from the National Mareographic Network of the Agency for the Protection of the Environment and Technical Services (APAT, available at http://www.apat.gov.it). These data are measured by mareographic stations SM3810, manufactured by the Italian Society for Precision Apparatuses (SIAP), placed close to the sampling sites. Mean annual SST was obtained from hourly values measured from January 2001 to January 2005 (number of hourly values = 35,064 for each site). Monthly values of solar radiation (W m^{-2}) were obtained from the International Cloud Climatology Project (ISCCP; available at http://www.ingrid.ldgo.columbia.edu/). These estimates are derived from satellite measurements of cloud and atmospheric optical properties. Mean annual solar radiation of each site was obtained for the 2.5°-latitude-by-longitude square associated with each of the six sites (number of monthly values = 48 for each site).

Statistical analyses

Spearman's rank correlation coefficient is an alternative to Pearson's correlation coefficient (Altman 1991). It is useful when data are non-normally distributed, and thus the assumptions of Pearson's correlation coefficient are not met. Spearman's rank correlation coefficient was used to calculate the significance of the correlations between biometric parameters and environmental variables, and between population density and environmental variables.

Kruskal–Wallis test is a non-parametric alternative to the analysis of variance (ANOVA), and it is used to compare groups of means. The advantage of this test is that the assumption of normality of data is not required, as the

test is based on the ranks of data. This distribution-free test proved to be more robust than its parametric counterpart in the case of non-normal distribution of sample data, and it is a viable alternative to parametric statistics (Potvin and Roff 1993). Kruskal–Wallis test was used to compare mean solar radiation, SST, polyp length, and population density among study sites.

Covariance analysis (ANCOVA) is a combination of linear regression and variance analysis (Altman 1991). It can be used to compare the regression equations between different groups. For example, given the linear regression equations between the same two variables of three groups of treatments, the analysis compares the slopes and intercepts of the three equations. ANCOVA was used to compare the relationships between biometric parameters and polyp length among study sites.

The Monte Carlo method (Gabriel and Lachenbruch 1969) solves problems in the non-parametric test for small samples. In fact, it estimates the *P*-value by taking a random sample from the reference set and studies its permutations (Senchaudhuri et al. 1995). Our Monte Carlo estimate for *P* used 100,000 random permutations. This method was used to estimate the significance of the Kruskal–Wallis test when comparing the mean population densities among study sites for both species.

Kruskal–Wallis tests, Spearman's correlation coefficients, and Monte Carlo corrections for small sample size were calculated with SPSS 12.0 (Apache Computer Software Foundation, Forest Hill, MD).

Results

Solar radiation and SST both varied among the sites (Kruskal–Wallis test, degrees of freedom = 5, and $P < 0.001$; Fig. 1). While solar radiation correlated negatively with latitude, SST correlated significantly after exclusion of Genova–Portofino (GN) site from analysis (Fig. 2). The GN site is characterized by particular local conditions (xeroterm site because of local currents and rock composition; APAT, available at http://www.apat.gov.it) and typically has higher SSTs than expected at that latitude (annual SST of Ligurian Sea = 18°C and Genova–Portofino (GN) = 19.6°C); (Fig. 1).

Polyp length (Fig. 3) was selected as the main biometric parameter since it is a good indicator of skeletal mass and has been used as the measure of size in biometric, reproductive biology, and population dynamic studies of *B. europaea*, *L. pruvoti*, and other solitary corals (Hoeksema 1991; Bell and Turner 2000; Goffredo and Chadwick-Furman 2003; Goffredo et al. 2002, 2004, 2006). Polyp width, height, volume, and skeletal mass all correlated positively with polyp length in both the coral species examined (Figs. 4, 5). Skeletal density correlated positively with polyp length in *B. europaea* at only two sites (Palinuro and Pantelleria). In contrast, skeletal density correlated negatively with polyp length in *L. pruvoti* at all sites (Figs. 4, 5). In both the coral species, the relationships between biometric parameters and polyp length varied significantly among the study sites (ANCOVA, degrees of freedom between exponents = 5, and $P < 0.05$). Each relationship between the biometric parameters and polyp length was linearized and the obtained slopes (representing the original equation exponent) were compared among study sites. None of the slopes was homogeneous among study sites.

The increase in polyp width in comparison with that of polyp length differed in the two species (Figs. 4, 5). In *B. europaea*, an allometric relationship was found; length increased more rapidly than did width, which resulted in an oval oral disc as polyp size increased (at all sites, the confidence interval CI of the regression equation exponent was <1, 0.52–0.90, CI 95%, and degrees of freedom = 37–94; Fig. 4). *L. pruvoti* had either isometric growth (at Scilla and Pantelleria, the confidence interval of the regression equation exponent contained 1, 0.96–1.01, CI 95%, and degrees of freedom = 114–143) or allometric growth, with the polyp length increasing less quickly than the width did (at Genova–Portofino, Calafuria, Elba, and Pantelleria, the confidence interval of the regression equation exponent >1, 1.00–1.10, CI 95%, and degrees of freedom = 75–209; Fig. 5), which resulted in a circular oral disc as polyp size increased.

In both species, the lengths of the sampled individuals differed significantly among the sites (Kruskal–Wallis test, degrees of freedom = 5, and $P < 0.001$). For this reason, analyses of correlations between environmental variables and biometric parameters were performed after applying to the data the method of the adjusted values in relation to length (Steel 1980). In *B. europaea*, whereas polyp length, width, height, and volume positively correlated with solar radiation and SST, skeletal mass and skeletal density were negatively correlated (Fig. 6). In all cases, SST explained 2.5–7.4 times more of the variance than did solar radiation (the percentage of biometric parameter variance explained by SST ranged from 3.9% for length to 63.8% for skeletal mass; Fig. 6). In *L. pruvoti*, solar radiation did not correlate with any biometric parameter. Polyp length, height, volume, and skeletal density were correlated with SST, which explained from 0.5% of the variance for volume to 1.2% for length (Fig. 6). SST was more highly correlated with biometric parameters in *B. europaea* than in *L. pruvoti* (r^2 of the relationship between biometric parameters and SST was three times higher for length to 638 times higher for skeletal mass).

In *B. europaea*, population density varied significantly among the sites (Kruskal–Wallis test, Monte Carlo

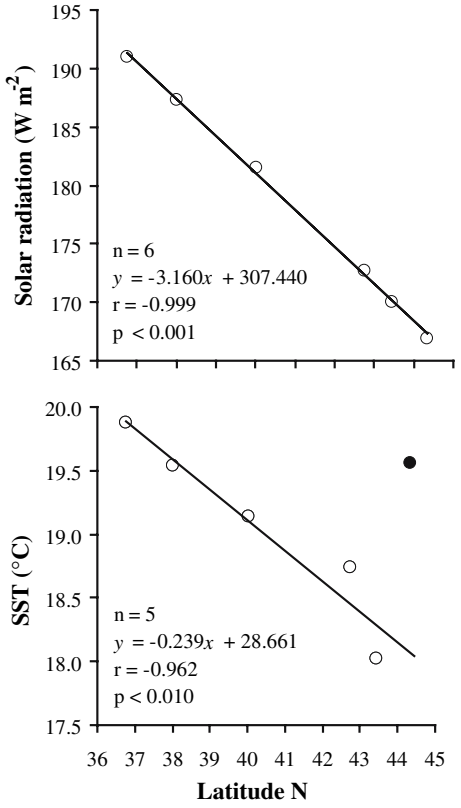

Fig. 2 Relationship between environmental parameters (mean annual solar radiation and SST) and the latitude of study sites along the coast of Italy. The *black dot* indicates the site of Genova–Portofino, which was characterized by special local conditions that cause a temperature deviation from the norm at that latitude, and thus was excluded from the correlation coefficient calculation. *n* number of stations; *r* Pearson correlation coefficient

correction for small sample size, degrees of freedom = 5, and $P < 0.001$) and was negatively correlated with SST (Fig. 7). In *L. pruvoti*, population density did not vary among the sites (Kruskal–Wallis test, Monte Carlo correction for small sample size, degrees of freedom = 5, and $P > 0.05$). Mean population density for *L. pruvoti* was 10.155 individuals m^{-2} (SE 1.317), 2,030 g m^{-2} (SE 232), and 15.4% cover (SE 1.4).

Discussion

The difference between the two species in the relationship between skeletal density and polyp size can be interpreted in terms of relationship between calcification and linear extension. As polyp size of *B. europaea* increases, there is a progressive decrease in linear extension rate (Goffredo et al. 2004). A parallel diminution of the calcification rate could explain the maintenance of skeletal density among mean values of 0.001–0.002 g mm^{-3} regardless of polyp size, at four of the six sites studied (Genova–Portofino, Calafuria, Elba, and Scilla). At the Palinuro and Pantelleria sites, calcification rate could decrease less quickly than did linear extension rate, causing a positive correlation between skeletal density and polyp size. In *L. pruvoti*, as known for several other solitary corals (Bablet 1985; Yamashiro and Nishihira 1998; Goffredo and Chadwick-Furman 2003; Goffredo et al. 2004), the linear extension rate should decrease with increasing polyp size. The diminution of skeletal density with increasing polyp size may have been due to a greater decrease in calcification than in

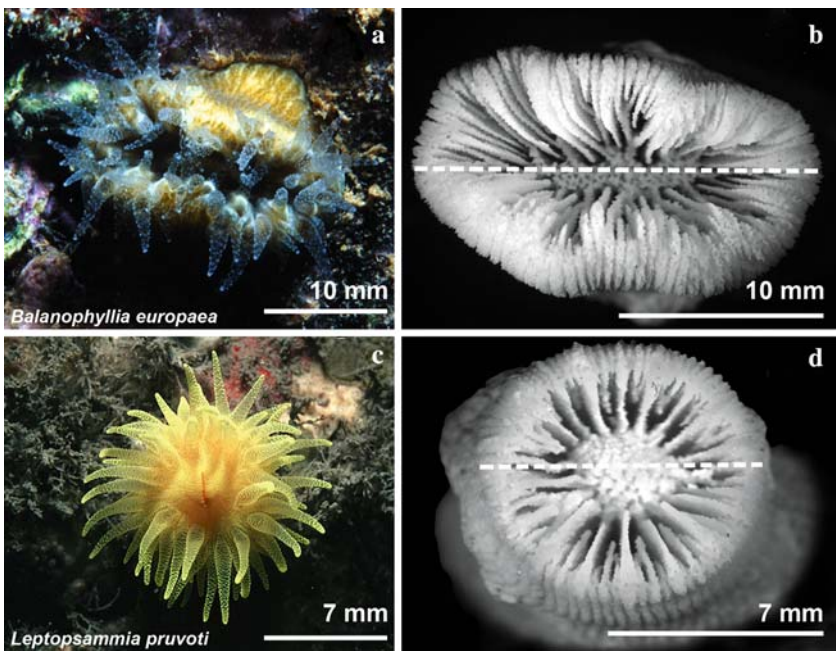

Fig. 3 *Balanophyllia europaea* (**a** living polyp**; b** corallite) and *Leptopsammia pruvoti* (**c** living polyp; **d** corallite) specimens from Genova–Portofino. *Dotted line* indicates polyp length (*L*: maximum axis of the oral disc)

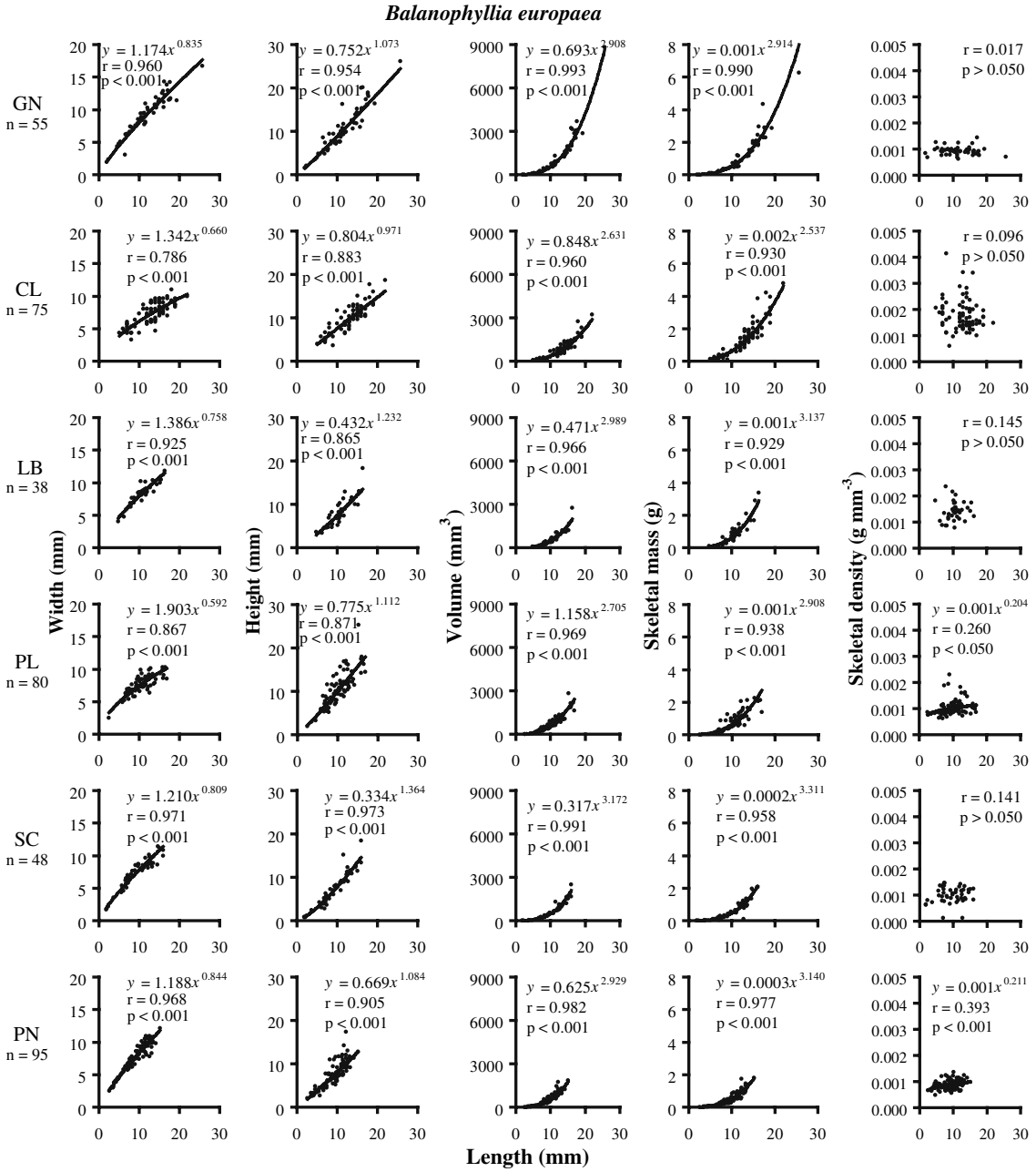

Fig. 4 *Balanophyllia europaea*. Dependence of biometric parameters on polyp length at six sites along the western coast of Italy (*GN* Genova–Portofino, *CL* Calafuria, *LB* Elba, *PL* Palinuro, *SC* Scilla, and *PN* Pantelleria). *n* number of individuals; *r* Pearson correlation coefficient. The sites are arranged in order of decreasing latitude

linear extension rate. The radiological analyses underway on both species are expected to provide an understanding of the relationship between calcification and linear extension rates.

The difference in the biometric relationship between the oral disc axes between the two species may relate to sedimentation stress. Sedimentation has many negative effects on corals, including prevention of growth and calcification, interference with respiration, nourishment and photosynthesis, increase in energy dissipation, damaging polyp tissues, lowering the fecundity, and interfering with substratum colonization process (Rosenfeld et al. 1999, and references therein). Corals can adopt different strategies to prevent these negative effects, i.e., sediment rejection behavior or resistant growth forms (Stafford-Smith and Ormond 1992; Bell and Turner 2000). The oval form of the oral disc is one of these resistant forms, since it decreases the area affected by sedimentation and favors the removal

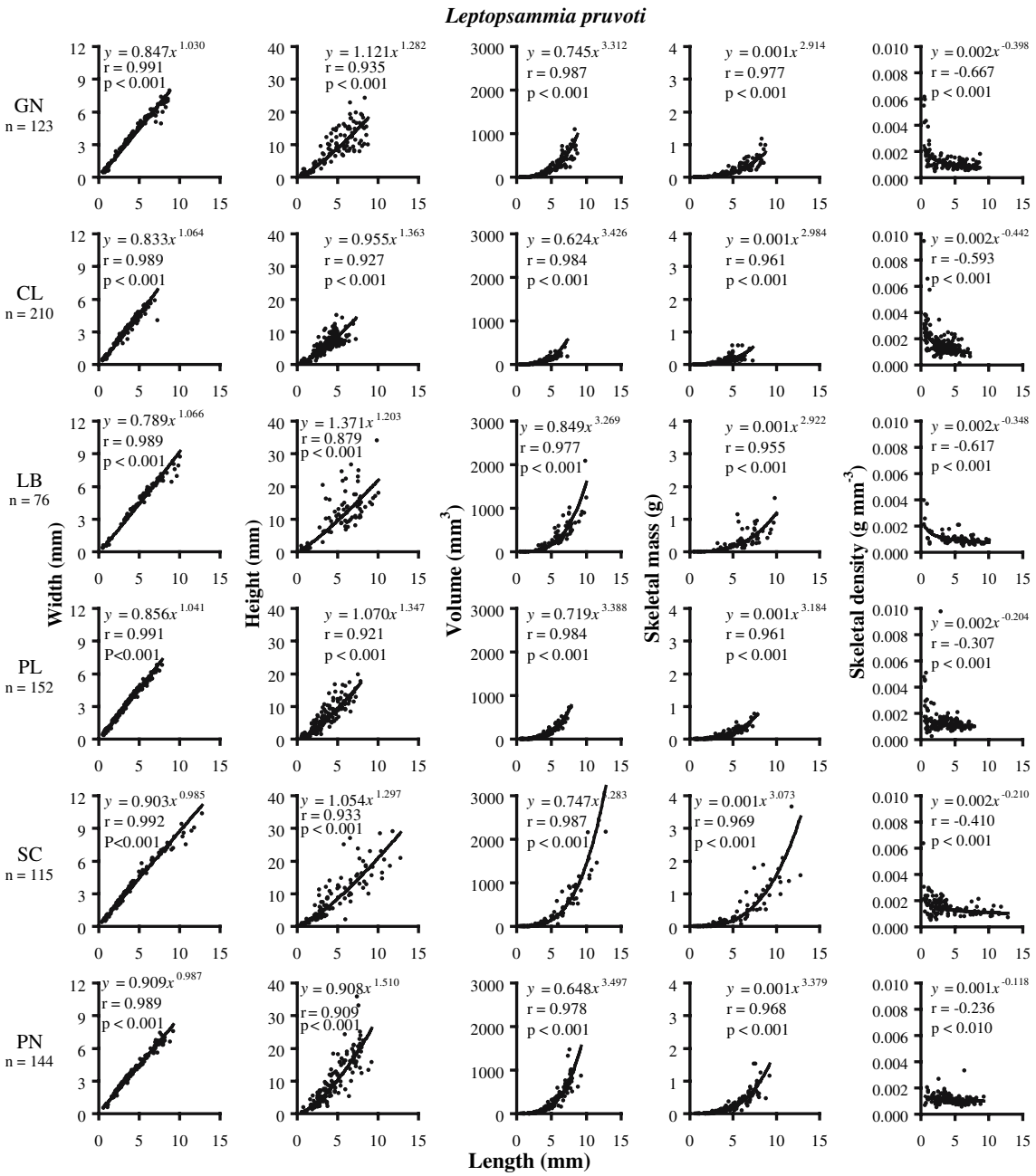

Fig. 5 *Leptopsammia pruvoti*. Dependence of biometric parameters on polyp length at six sites along the western coast of Italy (*GN* Genova–Portofino, *CL* Calafuria, *LB* Elba, *PL* Palinuro, *SC* Scilla, and *PN* Pantelleria). *n* number of individuals; *r* Pearson correlation coefficient. The sites are arranged in order of decreasing latitude

of sediment from the polyp surface (Hoeksema 1991). The allometric relationship between polyp width and length in *B. europaea*, which produces a progressively oval-shaped oral disc, may prevent damage from sedimentation that might otherwise occur as the polyp becomes larger (Goffredo et al. 2004). In corals living on the vertical walls, the removal of sediment is carried out by gravity, rather than by active mechanisms (Stafford-Smith and Ormond 1992). Moreover, in shallow water overhangs of the Ligurian Sea, a thin coat of sediment covers the vertical surfaces, while it is absent on the down-facing surfaces (Virgilio et al. 2006). *L. pruvoti* polyps, characterized by circular oral discs, do not need growth forms resistant to damage from sedimentation, since they colonize the vaults of caves and crevices with their oral pole directed downward.

The SST environmental variable correlated with biometric parameters more strongly than did solar radiation in

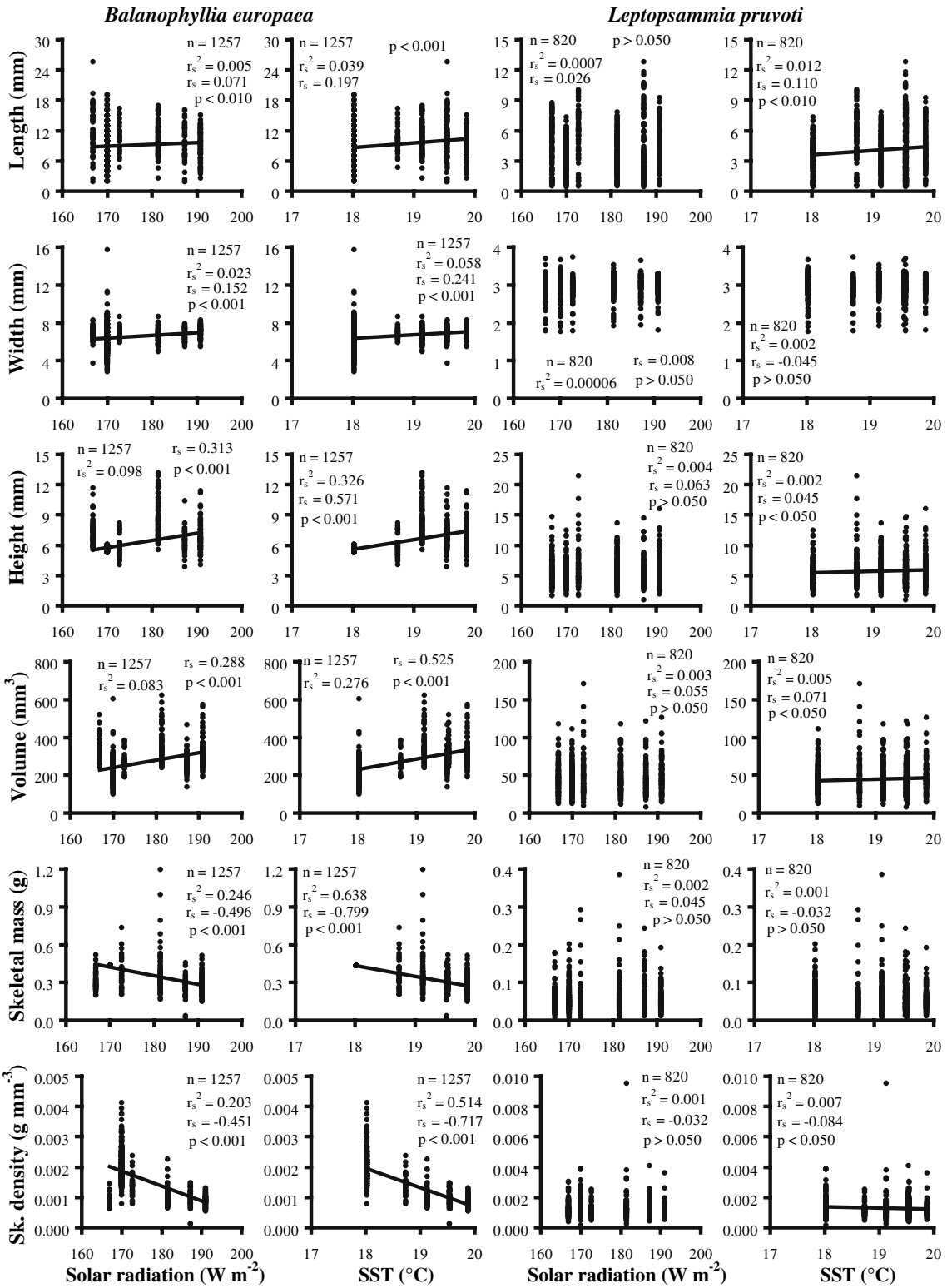

Fig. 6 Variation in the biometric parameters of two corals, *Balanophyllia europaea* and *Leptopsammia pruvoti* with environmental variables (annual mean solar radiation and SST). r_s^2 Spearman's determination coefficient; *n* number of individuals. Note that scale of the ordinate axes differs between species

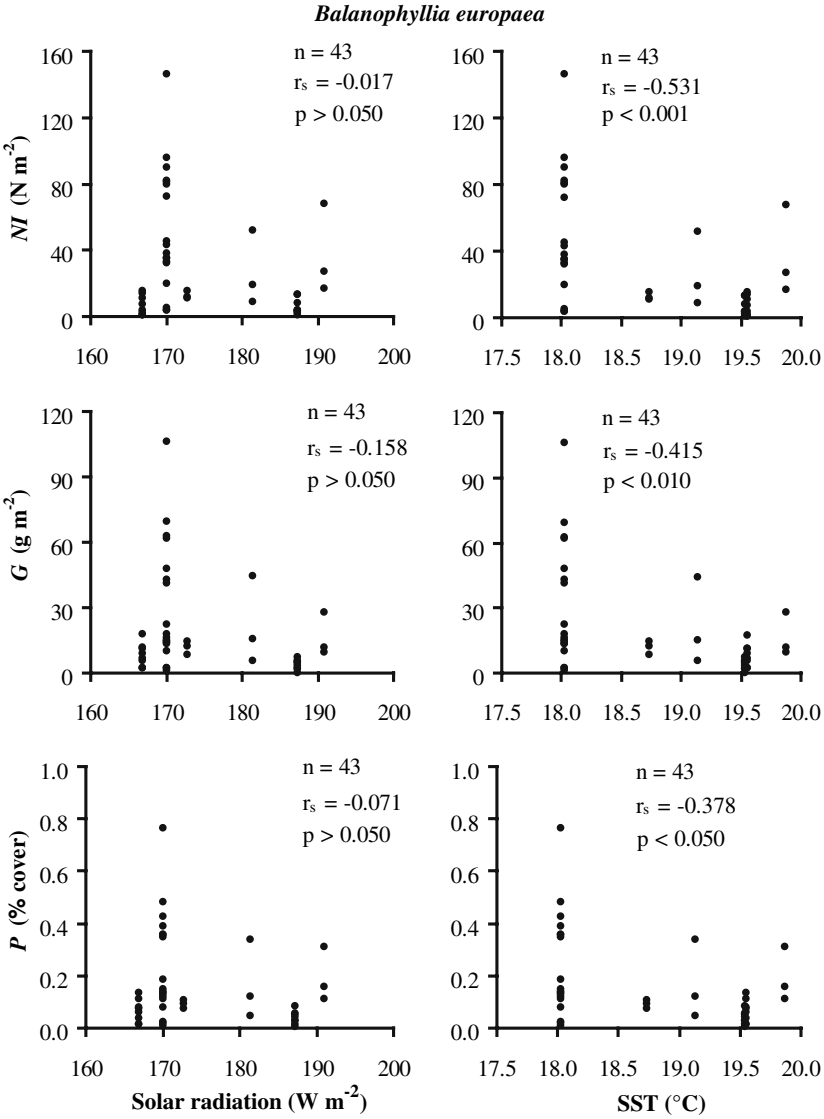

Fig. 7 *Balanophyllia europaea*. Variation in population density parameters with environmental variables (mean annual solar radiation and SST). *NI* number of individuals per square meter, *G* grams per square meter, *P* percent cover. r_s Spearman's correlation coefficient; *n* number of quadrats examined. Correlations for *Leptopsammia pruvoti* are not shown because population density was homogeneous among the sites examined

both species. This relationship is more marked in *B. europaea*, which is zooxanthellate, suggesting the possible effect of temperature on photosynthesis in the algal symbionts. In zooxanthellate corals, photosynthesis enhances calcification (Gattuso et al. 1999; Al-Horani et al. 2005), and both processes have temperature optima (Howe and Marshall 2002; Al-Horani 2005). In *B. europaea*, the decrease in skeletal density with increasing SST could depend on an attenuation of calcification due to an inhibition of the photosynthetic process at higher temperatures. In *L. pruvoti*, the weak relationship between temperature and skeletal density could be due to the absence of zooxanthellae, and thus lack of a physiological dependence of calcification on photosynthesis.

The spatial distribution of adult corals is influenced by the number of offspring produced per reproductive event and their dispersal capability (Hughes et al. 2000). Theoretically, low fecundity combined with wide larval dispersal results in a low density of local populations. In contrast, high fecundity combined with limited larval dispersal produces high local population density (Gerrodette 1981; Carlon 2002; Goffredo and Zaccanti 2004; Goffredo et al. 2004). In symbiotic corals, a large portion of the energy needed for gametogenesis and larval development is supplied by photosynthate from the zooxanthellae (Rinkevich 1989). The low population density of *B. europaea* relative to that of *L. pruvoti* could be due to lower polyp fecundity and the greater dispersion capability of its larvae (Goffredo and Zaccanti 2004; Goffredo et al. 2002, 2004, 2006). However, population density also depends on recruitment and mortality due to various factors, including predation, so this hypothesis requires further testing. The decrease in population density of *B. europaea* with increasing SST might depend on a polyp's reduced fecundity, consequent to a decrement of the photosynthetic efficiency of the symbiont zooxanthellae at higher than

optimal temperatures (Al-Horani 2005), resulting in lower energy resources for gametogenesis (Rinkevich 1989; Carlon 2002). Without utilizing photosynthesis, *L. pruvoti* would maintain its population density around the mean value regardless of the SST. Further studies on the reproductive biology of these two species at different sites situated along a latitudinal gradient might clarify the relationship between polyp fecundity and SST.

In conclusion, it is hypothesized that high temperature is a negative factor for the zooxanthellate *B. europaea*, since it would lower the photosynthetic efficiency of its symbionts, causing negative effects on both polyp growth and colonization process, while it would not significantly influence the azooxanthellate *L. pruvoti*. An alternative explanation for the decrease of skeletal and population density of *B. europaea* with increasing temperature could be related to suspension feeding. In the Mediterranean Sea, nutrient levels and zooplankton availability are typically lower in summer–fall (i.e., high temperature) than in winter–spring (i.e., low temperature; Coma et al. 2000; Coma and Ribes 2003). Low nutrients and zooplankton availability cause stress and starvation in *Cladocora caespitosa* (Peirano et al. 2005a) and a summer dormancy in the metabolism of several benthic suspension feeding taxa (Coma et al. 2000; Coma and Ribes 2003). Moreover, in *Stylophora pistillata* colonies, starved corals present significantly lower levels of calcification and photosynthesis than fed corals (Houlbrèque et al. 2004). Low energetic resources could be the causes of low skeletal and population density in *B. europaea* at high temperatures. However, if this was the case, the inhibition would be stronger in *L. pruvoti*, which is a full heterotrophic, than in *B. europaea*, which can rely on the symbiont. In contrast, we found that the skeletal and population densities of *L. pruvoti* are almost the same in low and high temperature study sites; thus the hypothesis of a photosynthetic inhibition at high temperatures seems to be more appropriate. Anyway, other factors such as pollution could influence the spatial distributions of populations. During the sampling period of this study, the Italian Ministry of the Environment and Land and Sea Protection conducted sea water quality surveys along the Italian coasts, based on basic oceanographic data (NO_3^-, NO_2^-, NH_4^+, PO_4^{3-}, SiO_4^{4-}, salinity, chlorophyll, and transparency, which are parameters included in the Sea Water Classification; Seawater Monitoring Program, available at www2.minambiente.it/sito/settori_azione/sdm/pubblicazioni/pubblicazioni.asp; www.sidimar.ipzs.it). Ministry data exhibited negative correlations between latitude and environmental quality along the western coasts of Italy, but this is hardly linkable to our data since we found that the population density of both species does not co-vary with latitude.

Future work to test the hypothesis of an inhibition of photosynthetic efficiency of *B. europaea* at high temperatures will involve experimental measurements of photosynthesis at different temperatures and stable isotopes analyses on *B. europaea* skeletons to reconstruct the photosynthetic efficiency of the polyps.

Acknowledgments We wish to thank L. Bortolazzi, M. Ghelia, G. Neto, and L. Tomesani for their underwater assistance in collecting the samples. The diving centers Centro Immersioni Pantelleria, Il Pesciolino, Polo Sub, and Sub Maldive supplied logistic assistance in the field. The Bologna Scuba Team collaborated in the underwater activities. The Marine Science Group (http://www.marinescience-group.org) supplied scientific, technical, and logistical support. H. R. Lasker, J. Bilewitch, and N. Kirk (State University of New York at Buffalo), N. E. Chadwick-Furman (Auburn University), and two anonymous reviewers gave comments that improved the manuscript. This research was financed by the Associazione dei Tour Operator Italiani (ASTOI), the Marine and Freshwater Science Group Association (http://www.msgassociation.net), the Canziani foundation of the Department of Evolutionary and Experimental Biology of the Alma Mater Studiorum—University of Bologna, and the Ministry of Education, University and Research (MIUR). The experiments complied with current Italian law.

References

Al-Horani FA (2005) Effects of changing seawater temperature on photosynthesis and calcification in the scleractinian coral *Galaxea fascicularis*, measured with O_2, Ca^{2+} and pH microsensors. Sci Mar 69:347–354

Al-Horani FA, Ferdelman T, Al-Moghrabi SM, de Beer D (2005) Spatial distribution of calcification and photosynthesis in the scleractinian coral *Galaxea fascicularis*. Coral Reefs 24:173–180

Altman DG (1991) Practical statistics for medical research. Chapman & Hall, London

Bablet JP (1985) Report on the growth of a scleractinia (*Fungia paumotensis*). In: Proceedings of the 5th International Coral Reef Symposium 4:361–365

Bell JJ, Turner JR (2000) Factors influencing the density and morphometrics of the cup coral *Caryophyllia smithii* in Lough Hyne. J Mar Biol Assoc UK 80:437–441

Carlon DB (2002) Production and supply of larvae as determinants of zonation in a brooding tropical coral. J Exp Mar Biol Ecol 268:33–46

Carricart-Ganivet JP (2004) Sea surface temperature and the growth of the West Atlantic reef-building coral *Montastraea annularis*. J Exp Mar Biol Ecol 302:249–260

Coma R, Ribes M (2003) Seasonal energetic constraints in Mediterranean benthic suspension feeders: effects at different levels of ecological organization. Oikos 101:205–215

Coma R, Ribes M, Gili JM, Zabala M (2000) Seasonality in coastal ecosystems. Trends Ecol Evol 12:448–453

Crossland CJ (1981) Seasonal growth of *Acropora* cf. *formosa* and *Pocillopora damicornis* on a high latitude reef (Houtman Abrolhos, Western Australia). In: Proceedings of the 4th International Coral Reef Symposium 1:663–667

Dodge RE, Brass GW (1984) Skeletal extension, density and calcification of the reef coral *Montastrea annularis*: St Croix, US Virgin Islands. Bull Mar Sci 34:288–307

Gabriel KR, Lachenbruch PA (1969) Non-parametric ANOVA in small samples: a Monte Carlo study of the adequacy of the asymptotic approximation. Biometrics 25:593–596

Gattuso JP, Allemand D, Frankignoulle M (1999) Photosynthesis and calcification at cellular, organismal and community levels in coral reefs: a review on interaction and control by carbonate chemistry. Am Zool 39:160–183

Gerrodette T (1981) Dispersal of the solitary coral *Balanophyllia elegans* by demersal planular larvae. Ecology 62:611–619

Goffredo S, Arnone S, Zaccanti F (2002) Sexual reproduction in the Mediterranean solitary coral *Balanophyllia europaea* (Scleractinia, Dendrophylliidae). Mar Ecol Prog Ser 229:83–94

Goffredo S, Chadwick-Furman NE (2003) Comparative demography of mushroom corals (Scleractinia, Fungiidae) at Eilat, northern Red Sea. Mar Biol 142:411–418

Goffredo S, Zaccanti F (2004) Laboratory observations of larval behavior and metamorphosis in the Mediterranean solitary coral *Balanophyllia europaea* (Scleractinia, Dendrophylliidae). Bull Mar Sci 74:449–458

Goffredo S, Mattioli G, Zaccanti F (2004) Growth and population dynamics model of the Mediterranean solitary coral *Balanophyllia europaea* (Scleractinia, Dendrophylliidae). Coral Reefs 23:433–443

Goffredo S, Airi V, Radetić J, Zaccanti F (2006) Sexual reproduction of the solitary sunset cup coral *Leptopsammia pruvoti* (Scleractinia: Dendrophylliidae) in the Mediterranean. 2. Quantitative aspects of the annual reproductive cycle. Mar Biol 148:923–932

Grigg RW (1982) Darwin point: a threshold for atoll formation. Coral Reefs 1:29–34

Harriott VJ (1999) Coral growth in subtropical eastern Australia. Coral Reefs 15:281–291

Harriott VJ, Banks SA (2002) Latitudinal variation in coral communities in eastern Australia: a qualitative biophysical model of factors regulating coral reefs. Coral Reefs 21:83–94

Hoeksema BW (1991) Evolution of body size in mushroom corals (Scleractinia: Fungiidae) and its ecomorphological consequences. Neth J Zool 41:112–129

Houlbrèque F, Tambuttè E, Allemand D, Ferrier-Pagès C (2004) Interactions between zooplankton feeding, photosynthesis and skeletal growth in the scleractinian coral *Stylophora pistillata*. J Exp Biol 207:1461–1469

Howe SA, Marshall AT (2002) Temperature effects on calcification rate and skeletal deposition in the temperate coral, *Plesiastrea versipora* (Lamarck). J Exp Mar Biol Ecol 275:63–81

Hughes TP, Baird AH, Dinsdale EA, Moltschaniwskyj NA, Pratchett MS, Tanner JE, Willis BL (2000) Supply-side ecology works both ways: the link between benthic adults, fecundity, and larval recruits. Ecology 81:2241–2249

Jacques TG, Marshall N, Pilson MEQ (1983) Experimental ecology of the temperate scleractinian coral *Astrangia danae*: II. Effect of temperature, light intensity and symbiosis with zooxanthellae on metabolic rate and calcification. Mar Biol 76:135–148

Kain JM (1989) The seasons in the subtidal. Br Phycol J 24:203–215

Kinsey DW, Davies PJ (1979) Carbon turnover calcification and growth in coral reefs. In: Trudinger PA, Swaine DJ (eds) Biogeochemical cycling of mineral forming elements. Elsevier, Amsterdam, pp 131–162

Kleypas JA, McManus JW, Menez LAB (1999) Environmental limits to coral reef development: where do we draw the line? Am Zool 39:146–159

Lough JM, Barnes DJ (2000) Environmental controls on growth of the massive coral *Porites*. J Exp Mar Biol Ecol 245:225–243

Peirano A, Abbate M, Cerrati G, Difesca V, Peroni C, Rodolfo-Metalpa R (2005a) Monthly variations in calyx growth, polyp tissue, and density banding of the Mediterranean scleractinian *Cladocora caespitosa* (L.). Coral Reefs 24:404–409

Peirano A, Damasso V, Montefalcone M, Morri C, Bianchi CN (2005b) Effects of climate, invasive species and anthropogenic impacts on the growth of the seagrass *Posidonia oceanica* (L.) Delile in Liguria (NW Mediterranean Sea). Mar Pollut Bull 50:817–822

Potvin C, Roff DA (1993) Distribution-free and robust statistical methods: viable alternatives to parametric statistics? Ecology 74:1617–1628

Rinkevich B (1989) The contribution of photosynthetic products to coral reproduction. Mar Biol 101:259–263

Rosenfeld M, Bresler V, Abelson A (1999) Sediment as a possible source of food for corals. Ecol Lett 2:345–348

Senchaudhuri P, Mehta CR, Patel NR (1995) Estimating exact p-values by the method of control variates, or Monte Carlo rescue. J Am Stat Assoc 90:640–648

Stafford-Smith MG, Ormond RFG (1992) Sediment-rejection mechanisms of 42 species of Australian Scleractinian. Aust J Mar Freshw Res 43:683–705

Steel RGD (1980) Principles and procedures of statistics: a biometrical approach, 2nd edn. McGraw-Hill College, New York

Stimson J (1996) Wave-like outward growth of some table- and plate-forming corals, and a hypothetical mechanism. Bull Mar Sci 58:301–313

Virgilio M, Airoldi L, Abbiati M (2006) Spatial and temporal variations of assemblages in a Mediterranean coralligenous reef and relationships with surface orientation. Coral Reefs 25:265–272

Vongsavat V, Winotai P, Meejoo S (2006) Phase transitions of natural corals monitored by ESR spectroscopy. Nucl Instr Meth B 243:167–173

Yamashiro H, Nishihira M (1998) Experimental study of growth and asexual reproduction in *Diaseris distorta* (Michelin, 1843), a free-living fungiid coral. J Exp Mar Biol Ecol 225:253–267

Zibrowius H (1980) Les scléractiniaires de la Méditerranée et de l'Atlantique nord-oriental. Mem Inst Oceanogr (Monaco) 11:1–284

Coral Reefs (2008) 27:623–632
DOI 10.1007/s00338-008-0362-y

REPORT

Relationships between growth, population structure and sea surface temperature in the temperate solitary coral *Balanophyllia europaea* (Scleractinia, Dendrophylliidae)

S. Goffredo · E. Caroselli · G. Mattioli · E. Pignotti · F. Zaccanti

Received: 25 October 2007 / Accepted: 8 February 2008 / Published online: 22 February 2008

Abstract The demographic characteristics of the solitary zooxanthellate scleractinian *Balanophyllia europaea*, endemic to the Mediterranean, were determined in six populations, on a latitudinal gradient along the Italian coast, and compared with the mean annual sea surface temperature (SST). Growth rate correlated negatively, and asymptotic length of the individuals positively with SST. With increasing SST, the distributions of age frequencies moved away from a typical steady state structure (i.e., exponential decrease in the frequency of individuals with age), indicating less stable populations and showed a deficiency of individuals in the younger-age classes. These observations suggest that high temperatures are an adverse factor to the *B. europaea* symbiosis. Using projected increases in seawater temperature, most of the *B. europaea* populations in the Mediterranean are expected to be close to their thermal limits by 2100 and the populations at that time may support few young individuals.

Communicated by Environment Editor Prof. van Woesik.

S. Goffredo (✉) · E. Caroselli · F. Zaccanti
Department of Evolutionary and Experimental Biology, Alma Mater Studiorum, University of Bologna, Via F. Selmi 3, 40126 Bologna, Italy
e-mail: stefano.goffredo@marinesciencegroup.org

G. Mattioli
Operative Unit of Radiology and Diagnostics by Images, Hospital of Porretta Terme, Local Health Enterprise of Bologna, Via Roma 16, 40046 Porretta Terme, Bologna, Italy

E. Pignotti
Taskforce for Statistical Analysis, Marine & Freshwater Science Group Association, Via Andrea Costa 174, 40134 Bologna, Italy

Keywords Demography · Environmental parameters · Growth rate · Latitudinal gradient · Mediterranean Sea · Population stability

Introduction

Latitude differences in temperature and irradiance are an important influence on global coral distribution patterns (Kleypas et al. 1999). In general, coral growth decreases with increasing latitude, to a point beyond 30°N and 30°S where coral-reef development no longer occurs (Kinsey and Davies 1979; Grigg 1982). For temperate regions, studies on the relationship between environmental parameters and coral growth are scarce. For *Astrangia danae* (Jacques et al. 1983) and *Plesiastrea versipora* (Howe and Marshall 2002), calcification rate has been shown to increase with temperature, similar to the trend observed in tropical corals (Lough and Barnes 2000; Carricart-Ganivet 2004; McNeil et al. 2004), but for the zooxanthellate coral *Balanophyllia europaea*, Goffredo et al. (2007) reported a negative correlation between sea surface temperature (SST) and skeletal and population density.

There is limited information available on population dynamics of scleractinian corals. In 1973 the modest amount of data collected over the previous 30 years was reviewed and parameters such as growth and survivorship were described (Connell 1973). Since then, demographic processes have been described for some species in the Red Sea (Loya 1976; Chadwick-Furman et al. 2000; Goffredo and Chadwick-Furman 2003; Glassom and Chadwick 2006; Guzner et al. 2007), Northeastern Pacific (Fadlallah 1983), Caribbean (Hughes and Jackson 1985; Johnson 1992; Meesters et al. 2001; Vermeij 2006), Great Barrier Reef (Babcock 1991), and the Mediterranean (Goffredo

et al. 2004; Shenkar et al. 2005). The paucity of information on population dynamics of most scleractinian corals can be attributed, partly, to a distortion of the age–size relationships in this group, resulting from processes of fragmentation, fusion, and partial colony mortality (Hughes and Jackson 1985; Babcock 1991; Hughes et al. 1992). These phenomena prevent the application of traditional growth and population dynamic models based on organism age, and create very complex demographic patterns (Hughes and Jackson 1985). However, in species where the individuals rarely fragment or fuse and partial mortality is discernable by anomalies in the regular growth pattern, it is possible to determine coral age (Chadwick-Furman et al. 2000).

Growth band analysis is a technique that can be used to determine the age of certain forms of gorgonian and scleractinian, solitary and colonial corals, and to describe their demographic characteristics by applying age-based growth and population dynamics models (Knuston et al. 1972; Buddemeier et al. 1974; Grigg 1974; Mistri and Ceccherelli 1994; Peirano et al. 1999; Chadwick-Furman et al. 2000; Goffredo and Chadwick-Furman 2003; Goffredo et al. 2004; Goffredo and Lasker 2006). Demographic parameters reveal relationships between organisms and their environment, contributing to habitat stability assessment (Grigg 1975; Meesters et al. 2001). The demographic analysis of coral populations can reveal the level of stress to which they are subjected (Bak and Meesters 1999; Guzner et al. 2007). In addition, information on population turnover aids in the development of techniques for the restoration of damaged or degraded coastal areas (Chadwick-Furman et al. 2000; Epstein et al. 2001; Goffredo and Chadwick-Furman 2003).

Balanophyllia europaea (Risso 1826) is a solitary, ahermatypic, zooxanthellate scleractinian coral, which is endemic to the Mediterranean (Zibrowius 1980). Because of its symbiosis with zooxanthellae, it is restricted to depths of 0–50 m (Zibrowius 1980), where the population density can reach dozens of individuals per square meter (Goffredo et al. 2004). Its reproductive biology is characterized by simultaneous hermaphroditism and brooding (Goffredo et al. 2002). Goffredo et al. (2007) examined the correlations between SST, biometry, and population density of this species and a closely related one, the azooxanthellate *Leptopsammia pruvoti*, along the Italian coasts. They found a negative correlation between mean annual SST and skeletal and population density in *B. europaea*, but no correlation in *L. pruvoti*. To explain these results, they hypothesized that the negative effects on *B. europaea* skeletal and population density could be related to an inhibition of the photosynthesis of *B. europaea* symbiotic zooxanthellae at high temperatures.

This present study aimed to assess growth rates and population structure variation of *B. europaea* along a latitudinal gradient of mean annual SST. Considering the negative effects of temperature on the *B. europaea* symbiosis (Goffredo et al. 2007), it was expected that the same negative trend, shown by biometry and population density, would also apply to growth and population structure. Consequently, this study tested the hypothesis that high temperature has a negative effect on growth rates and population structure of *B. europaea*.

Materials and methods

Sample collection

Between 9th November 2003 to 30th September 2005, specimens of *B. europaea* were collected from six populations along a latitudinal gradient, from 44°20′N to 36°45′N (Fig. 1). Latitude is the main factor influencing the variation in SST (Kain 1989), which is the environmental parameter considered in this study because it has been shown to be strongly linked to coral growth, physiology, and demography (Kleypas et al. 1999; Lough and Barnes 2000; Al-Horani 2005). With the exception of the Calafuria population, for which data were obtained from a previous study (Goffredo et al. 2004), samples were

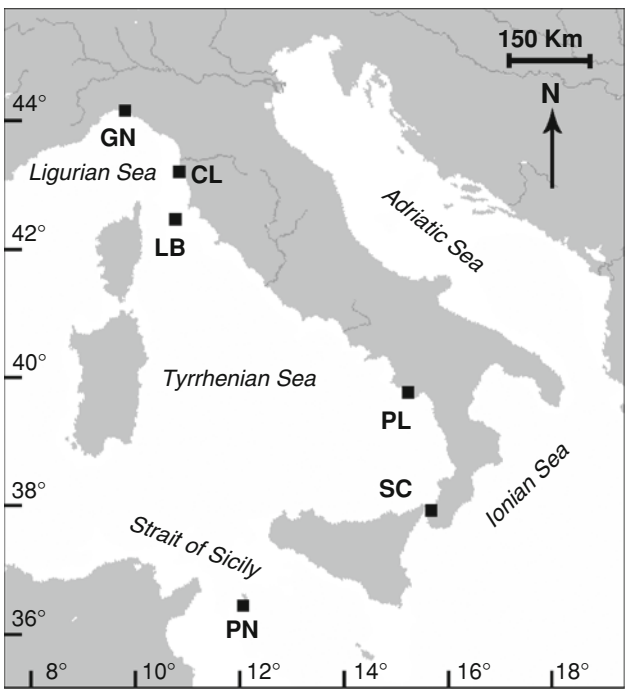

Fig. 1 Map of the Italian coastline indicating sites where corals were collected. Abbreviations and coordinates of the sites in decreasing order of latitude: GN Genova, 44°20′N, 9°08′E; CL Calafuria, 43°27′N, 10°21′E; LB Elba Isle, 42°45′N, 10°24′E; PL Palinuro, 40°02′N, 15°16′E; SC Scilla, 38°01′N, 15°38′E; PN Pantelleria Isle, 36°45′N, 11°57′E

collected for each population using transects that consisted of at least 3 patches of 1 m^2 each, arranged in a line 5 m apart along the southern side of each reef at a depth of 5–7 m. Because the distribution pattern of *B. europaea* is random, the problems associated with regularly spaced quadrats and transects do not apply to this study (Goffredo and Zaccanti 2004; Goffredo et al. 2004). All of the polyps present were collected from each patch. The sampling was at depths known to have high population densities and where the reproductive biology, biometry, and population density of this species had been studied previously (Goffredo et al. 2002, 2004, 2007; Goffredo and Zaccanti 2004). Choosing the sampling depth based on maximum abundance may bias growth toward a higher rate, and in turn underestimate age, but by sampling in the depth range of 5–7 m where 62% of this species are found (Goffredo et al. 2004) this maximum-abundance bias is reduced.

Sample analysis

Corals were dried at 50°C for 4 days and observed under a binocular microscope to remove fragments of substratum and calcareous deposits produced by other organisms. Corallite length was selected as the main biometric parameter, since it is a good indicator of skeletal mass and has been used as the primary measure of size in other biometric, reproductive biology, and population dynamics studies of this species and other solitary corals (Lasker 1981; Foster et al. 1988; Goffredo et al. 2002, 2004, 2007; Goffredo and Chadwick-Furman 2003; Vermeij 2006). Corallite length (*L*: maximum axis of the oral disc) was measured using a caliper, and corallite mass was measured with a precision balance (after Lasker 1981; Goffredo et al. 2002; Goffredo and Chadwick-Furman 2003).

Data modeling

To obtain an objective relationship between corallite size and age, the number of annual growth bands was counted by means of computerized tomography (CT). This technique is commonly applied to scleractinian corals (Bosscher 1993; Helmle et al. 2000) and has been successfully used for *B. europaea* (Goffredo et al. 2004). For each population, CT measurements were taken from about 40 skeletons randomly selected from the collected samples. The age of each skeleton was determined from the growth-band counts, based on one high-density band in winter and a low-density band in summer (Peirano et al. 1999; Goffredo et al. 2004; Fig. 2).

The von Bertalanffy growth model (von Bertalanffy 1938) predicts decreasing growth rate with age, with growth rate that tends to zero approaching an asymptotic size/age, and has been validated by Goffredo et al. (2004)

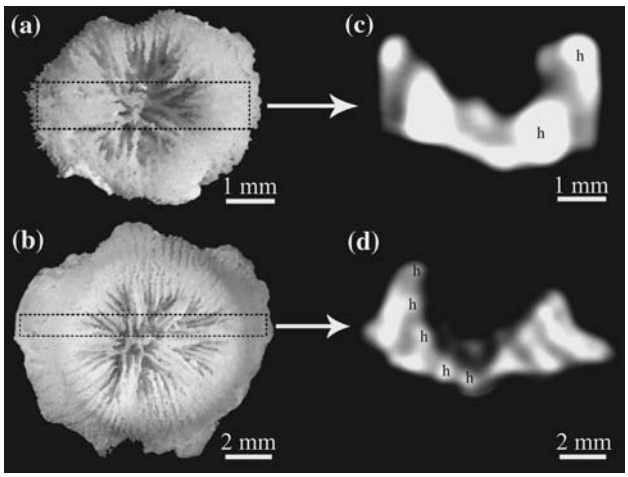

Fig. 2 *Balanophyllia europaea*. Computerized tomography scans (CT) of two corallites from the Elba island population (LB). (**a**, **b**) view of the skeleton from the oral pole. The dotted line shows the section, 1-mm wide, of the CT scan. The Multiple CT views facilitated the recognition of high-density bands (h). (**c**, **d**) sagittal CT scan (the oral pole is turned upward). Age was determined by counting the growth bands of the skeleton. (**c**) In this sample, 4.75-mm long, two high-density bands can be seen, corresponding to 2 years' growth. (**d**) In this sample, 9.95-mm long, five high-density bands can be seen, corresponding to 5 years' growth

for the Calafuria (CL) population of *B. europaea* using CT density bands. To test if the von Bertalanffy function could be used for all populations sampled in this study, the decreasing growth rate of *B. europaea* with age was checked at each location (Fabens 1965). For each sample dated by CT scans, a mean growth rate was obtained by dividing length by age, and the mean growth rate was plotted against individual age (Fig. 3). All the populations showed a marked decrease of mean growth rate with age, the best fit being a negative exponential curve (Fig. 3), from which growth was fitted to the von Bertalanffy function (von Bertalanffy 1938):

$$L_t = L_\infty(1 - e^{-Kt}) \quad (1)$$

where L_t is individual length at age t, L_∞ is asymptotic length (maximum expected length in the population), K is a growth constant (higher for a fast growth up to the asymptotic length, smaller for a slow one), and t is the age of the individual. The parameters L_∞ and K were determined by applying the "von Bertalanffy plot" method (see Pauly 1984; Sparre et al. 1989 for the exact procedure, and Goffredo and Chadwick-Furman 2003 for examples of applications to corals).

The population size structure was obtained from the survey transects, and age structure was determined using Eq. 1. In a theoretical population in steady state, 100% of the variance of the frequency of age classes is explained by age. To estimate population structure stability, the age-frequency distribution was analyzed using a regression

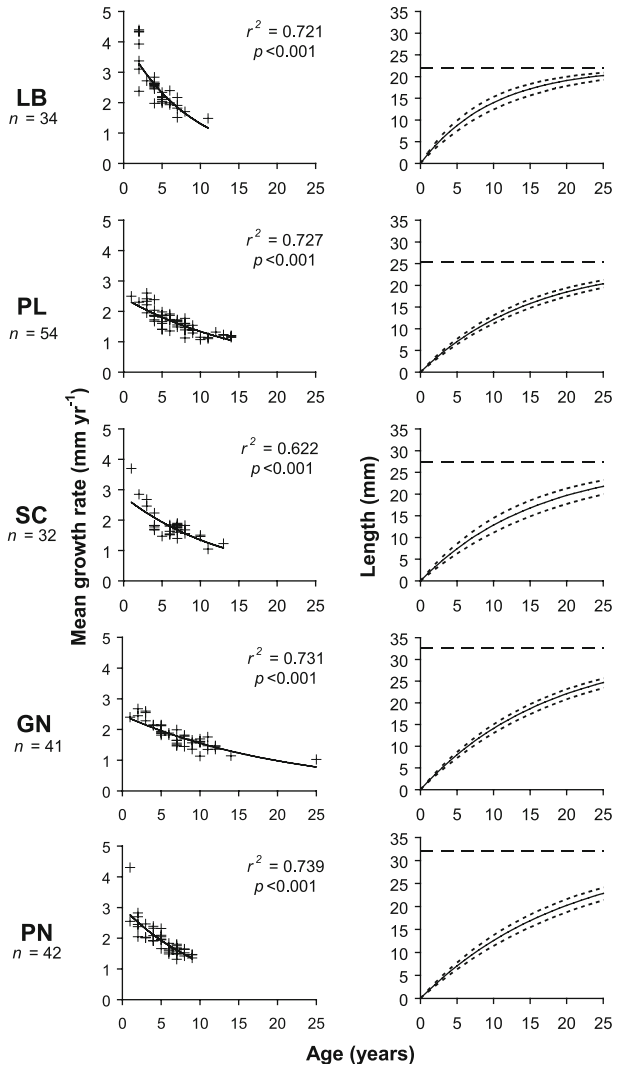

Fig. 3 *Balanophyllia europaea*. Relationships between mean growth rate and age (left hand graphs) and age–length von Bertalanffy growth curves (right hand graphs; see Eq. 1) of each population with 95% confidence interval (dotted lines). The dotted horizontal line represents L_∞ value. n = number of individuals dated by computerized tomography scans (CT)

analysis of the natural logarithm of the numbers of individuals (frequency) in each age class (N_t) against their corresponding age (t), or

$$\ln N_t = at + b \tag{2}$$

the slope a can be used to estimate the theoretical numeric reduction of individuals over time, the intercept b is equal to the natural logarithm of the number of individuals at age zero (N_0) (Pauly 1984; Sparre et al. 1989; Babcock 1991; Chadwick-Furman et al. 2000; Goffredo and Chadwick-Furman 2003; Goffredo et al. 2004). In a theoretical population in a steady state (rate of recruitment equal to rate of mortality; Grigg 1984) the coefficient of determination (r^2) is equal to unity (Beverton and Holt 1956; Pauly 1984). As natural populations deviate from the steady state, r^2 decreases to zero. In applying this method, the age classes corresponding to lengths <5 mm were ignored, since polyps this small are difficult to see during field surveys, resulting in an underestimate of these age classes (Pauly 1984; Babcock 1991; Chadwick-Furman et al. 2000; Goffredo and Chadwick-Furman 2003; Goffredo et al. 2004). This method for estimating population stability has previously been used for colonial and solitary corals (Grigg 1984; Ross 1984; Babcock 1991; Chadwick-Furman et al. 2000; Goffredo and Chadwick-Furman 2003; Tsounis et al. 2007), including *B. europaea* (Goffredo et al. 2004).

The slope a was used to express the theoretical numerical reduction of the corals over time (survivorship curve):

$$N_t = N_0 e^{at} \tag{3}$$

N_t is the number of individuals in each age class, N_0 is the number of individuals at age 0, a is the slope of Eq. 2, t is the age.

The mean age of the individuals in each population was computed from the mean age of samples from the growth curves (Eq. 1). The observed percentage of individuals below sexual maturity was obtained by summing the frequencies of the age classes below sexual maturity, which is 3–4 years (Goffredo et al. 2002, 2004). The theoretical mean age was estimated as the mean age of the theoretical number of individuals in each population. The theoretical percentage of individuals below sexual maturity was obtained by summing the frequencies of the theoretical number of individuals of the age classes below sexual maturity in each population.

The observed biomass distribution per age class was obtained by adding the mass of each corallite in each age class. A theoretical age–mass growth curve was obtained for each population using the age–length growth curve (Eq. 1) and the length–mass relationship from Goffredo et al. (2007). The theoretical biomass distribution per age class was then obtained by multiplying the theoretical number of individuals in each age class (according to the survivorship curve, Eq. 3) for the expected mass at that age. The theoretical age at maximum percentage biomass was estimated as the age class representing the highest percentage biomass. The observed age at maximum percentage biomass was determined in the same way using the observed biomass distribution. The observed mean age of biomass in the population was calculated as the sum of the products of the observed biomass in each age class multiplied by its age, then divided by the total observed biomass. This parameter estimates how old the biomass is in each population; populations with most of the biomass accumulated in younger corals will have a lower mean age of biomass than populations in which most of the biomass is represented by older individuals. The theoretical mean age

Table 1 Sea surface temperature, L_∞, K, and r^2 (coefficient of determination of the semi-log regression used to estimate population structure stability in Eq. 2) values of the sampled populations

Population	Code	SST (°C), Annual mean (SD)	L_∞ (mm)	K	r^2
Calafuria	CL	18.023 (4.770)	21.3	0.111	0.935
Elba	LB	18.737 (5.057)	22.0	0.101	0.605
Palinuro	PL	19.138 (4.170)	25.5	0.065	0.550
Scilla	SC	19.537 (2.783)	27.4	0.063	0.503
Genova	GN	19.556 (4.723)	32.5	0.057	0.505
Pantelleria	PN	19.875 (4.766)	32.0	0.050	0.423

Growth data of the CL population from Goffredo et al. (2004). The populations are arranged in increasing order of sea temperature

of biomass in the population was calculated in the same way, but using the theoretical biomass in each age class and the total theoretical biomass.

SST data

SST data for the years 2003–2005 were obtained for each location from the National Mareographic Network of the Agency for the Protection of the Environment and Technical Services (APAT, available at http://www.apat.gov.it). The data were from stations close to the sampling sites (<1 km) at a depth of 1 m below minimum low tide level. Mean annual SST was computed from hourly measurements from January 2001 to January 2005 (Table 1).

Statistical analyses

Analysis of covariance (ANCOVA) was used to examine differences in regression slopes and intercepts. Because of the heteroscedastic data sets, non-parametric Kruskal-Wallis was used to compare mean SST among the sites. Pearson correlation coefficients were calculated for estimating population structure stability in each population (coefficient of determination of Eq. 2), and for the relationships between SST and L_∞, K, population structure stability, observed and theoretical % of individuals below sexual maturity, observed and theoretical mean age, observed and theoretical age at maximum % biomass, observed and theoretical mean age of biomass. Because of the low n value ($n = 6$) and the assumptions of the Pearson method, correlation coefficients were also estimated with bootstrapping (Efron 1981), with 100,000 resamples. The non-parametric Kolmogorov–Smirnov test was used to compare the age-frequency distributions among the populations. All analyses were computed using SPSS 12.0, except bootstrapping (S-PLUS 6.0 Professional).

Results

Mean annual SST was significantly different between sites (Kruskal-Wallis, $P < 0.001$; Table 1). Mean growth rate was negatively related to age in all populations, with age explaining between 62 and 74% of growth rate variance (Fig. 3). Growth rates decreased from 2–5 mm year^{-1} at ages <5 year to 1–2 mm year^{-1} at ages >10 year (Fig. 3).

L_∞ and K values (Table 1) differed between the populations (ANCOVA for slope of the "von Bertalanffy plot" used to estimate L_∞ and K, $P < 0.05$). These values were therefore used to model the age–length growth curve (Eq. 1) for each population (Fig. 3). L_∞ and K values were significantly correlated with SST (Table 2). SST explained more than 80% of the variance of L_∞ and more than 90% of the variance of K (Table 2).

Table 2 Linear regression and correlation analyses between sea surface temperature (Independent variable) and growth and demographic parameters (Dependent variable) in the sampled populations

Dependent variable	n	Slope (SE)	Intercept (SE)	r^2	R	r^2_{BS}	r_{BS}
L_∞	6	6.373 (1.567)	−95.224 (30.018)	0.805	0.897*	0.826	0.909*
K	6	−0.036 (0.005)	0.757 (0.105)	0.913	−0.956**	0.906	−0.952**
Population structure stability	6	−0.256 (0.039)	5.486 (0.751)	0.914	−0.956**	0.941	−0.970**
Observed % of individuals below sexual maturity	6	−17.826 (7.266)	360.875 (139.179)	0.601	−0.775	0.310	−0.557
Theoretical % of individuals below sexual maturity	6	−12.951 (2.508)	289.102 (48.042)	0.870	−0.932**	0.799	−0.894*
Observed mean age	6	1.639 (0.499)	−24.062 (9.560)	0.729	0.854*	0.548	0.740
Theoretical mean age	6	1.939 (0.488)	−31.851 (9.352)	0.798	0.893*	0.755	0.869*
Observed age at maximum % biomass	6	2.550 (1.046)	−39.652 (20.043)	0.598	0.773	0.588	0.767
Theoretical age at maximum % biomass	6	5.194 (0.922)	−87.777 (17.663)	0.888	0.942**	0.846	0.920**
Observed mean age of biomass	6	2.096 (0.775)	−30.255 (14.852)	0.646	0.804	0.605	0.778
Theoretical mean age of biomass	6	4.780 (0.566)	−77.188 (10.840)	0.947	0.973**	0.889	0.943**

n number of populations. r^2 Pearson's coefficient of determination, r Pearson's correlation coefficient, r^2_{BS} and r_{BS} Pearson's coefficients calculated with bootstrapping, * $P < 0.05$, ** $P < 0.01$. SE = standard error

The age of all collected individuals in the various populations was estimated using the age–length growth curves (Eq. 1). The oldest individual came from the Genova (GN) population with an estimated age of 27 year (25.65 mm length). The age-frequency distributions for each population are shown in Fig. 4. The distributions were significantly different between populations (Kolmogorov–Smirnov, $P < 0.001$), and regressions of the natural logarithm of the numbers of individuals (frequency) in each age class (N_t) were computed (Eq. 2; Table 1, r^2 values). These r^2 values were negatively correlated with SST (Table 2), varying from $r^2 = 0.935$ in the coldest population (CL), to $r^2 = 0.423$ in the warmest population (PN; Table 1), indicating a progressive deviation from the steady state of the populations as temperature increased (Table 2).

The theoretical percentage of individuals under sexual maturity was negatively related to SST, while the theoretical mean age, the theoretical age at maximum percentage biomass, and the theoretical mean age of biomass were all positively related to SST (Table 2).

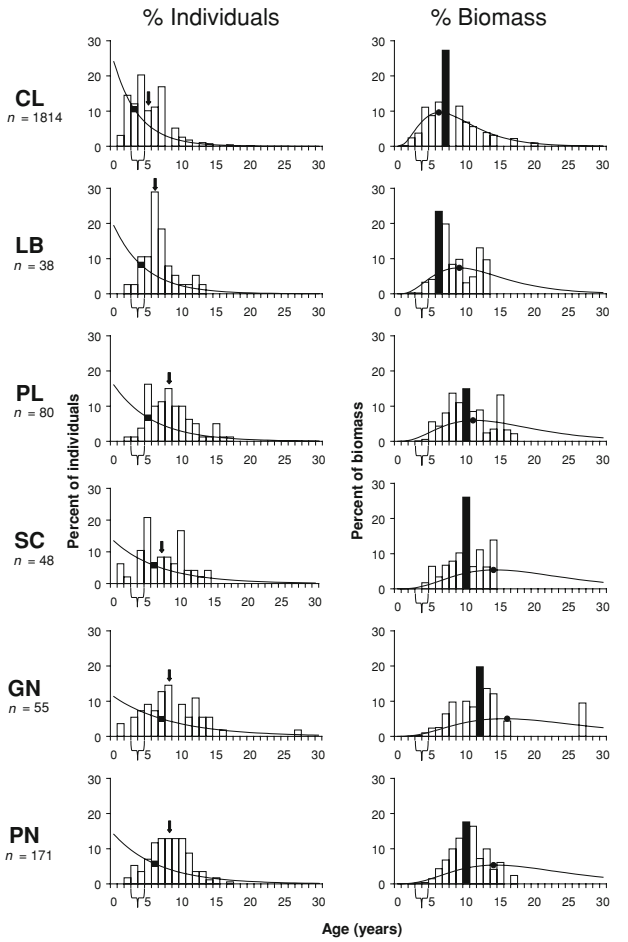

Fig. 4 *Balanophyllia europaea*. Age-class structures of each population. The lines indicate the theoretical distributions. The observed (arrow) and theoretical (black square) age class containing the mean observed age of the individuals of sampled population are indicated. The observed (black column) and theoretical (black circle) age at maximum percentage biomass are indicated. Bracketed ranges indicate the age at sexual maturity. Data for the Calafuria population (CL) are from Goffredo et al. (2004). n = number of individuals dated by growth curves

Discussion

In zooxanthellate corals, photosynthesis enhances calcification, and both processes have temperature optima (Al-Horani 2005). It was previously hypothesized that for *B. europaea*, inhibition of photosynthesis occurs at high temperatures, leading to a reduction in the calcification rate and skeletal density (Goffredo et al. 2007). Also, the reduction in growth rate (K) with increasing temperature, highlighted in this study, might be because of a reduced energy input available for skeletal deposition, caused by the inhibition of photosynthesis in zooxanthellae.

A reduced growth rate at high temperatures has been found in the genus *Montastraea* (Carricart-Ganivet 2004), but the opposite has been reported for species of the genera *Porites* (Lough and Barnes 2000), *Acropora* and *Pocillopora* (Crossland 1981) and in mushroom corals (Goffredo and Chadwick-Furman 2003). In a study of the genera *Pocillopora*, *Acropora*, *Turbinaria,* and *Porites*, both increases and decreases in calcification with increases in temperature were reported, suggesting that the influence of temperature on growth may be species-specific (Harriott 1999). These differences might in part be due to the clade of zooxanthellae hosted by the polyp, and it has been proposed that different clades of zooxanthellae associated with corals have different environmental tolerances (e.g., light, temperature, sedimentation; Knowlton and Rohwer 2003). Under experimental conditions, zooxanthellae belonging to clade A (the clade which is hosted by most Mediterranean scleractinian corals; Visram et al. 2006), have proven to be resistant to short-term increases in temperature (Rodolfo-Metalpa et al. 2006). However, severe bleaching episodes have been observed in situ in *O. patagonica* which also hosts clade A, in response to high temperatures (Fine et al. 2001).

In the present study the K growth constant was negatively correlated with SST and in an earlier study also the skeletal density was negatively correlated with SST (Goffredo et al. 2007). On this basis, calcification would also be expected to decrease at high temperatures (calcification = extension × skeletal density; Lough and Barnes 2000; Carricart-Ganivet 2004). This is in contrast to other studies on latitudinal variations of calcification in tropical and temperate corals, where the trend was an increase in calcification with decreasing latitude (Jacques et al. 1983; Lough and Barnes 2000; Howe and Marshall 2002;

Carricart-Ganivet 2004; McNeil et al. 2004). However, a recent study showed a decline of coral calcification in massive *Porites* from the Great Barrier Reef over a 16-year period (Cooper et al. 2007), and suggested that this reduction is linked to the interactive effects of increasing seawater temperatures and $pCO2$ (Reynaud et al. 2003). Calcification has an optimum temperature, and temperatures above optimum will lead to reduced calcification (Al-Horani 2005). The optimum calcification temperature for *B. europaea* may be equal to or lower than the lowest-recorded temperature in this study (18.023°C), which could explain the observed decrease in calcification with increasing SST.

Despite the theoretical nature of L_∞, in growth models, it is used as a measure of maximum size of individuals in the populations, and this seems to work well in *B. europaea*, fungiids, and gorgonian corals (Grigg 1974; Chadwick-Furman et al. 2000; Goffredo and Chadwick-Furman 2003; Goffredo et al. 2004; Goffredo and Lasker 2006). The increase in maximum corallite size of populations (asymptotic length) with mean SST is in agreement with previous observations, suggesting a positive correlation between biometric parameters (corallite length, width, height, and volume) and temperature in *B. europaea* (Goffredo et al. 2007). Although biologists have been interested in latitudinal variations of organism size for a long time, few studies have been conducted on marine invertebrates, and have often led to contrasting results (Lonsdale and Levinton 1985; Roy and Martien 2001; Olabarria and Thurston 2003). One of the hypotheses relating (terrestrial) body size with latitude is based on latitudinal changes of energy availability (see Wright 1983), and predicts smaller body size at high latitudes where available energy is reduced relative to equatorial regions (Turner and Lennon 1989; Cushman et al. 1993). This theory also seems to explain the present (marine) results, since the populations characterized by higher sea temperature (i.e., higher energy) had higher individual corallite lengths. Nevertheless, the increased length is accompanied by a marked reduction in skeletal density (Goffredo et al. 2007) and growth rate (K; present work). These reductions suggest that the increase in available energy, because of higher temperatures, cannot be exploited by the polyps, because of the reduced photosynthetic efficiency hypothesis (Goffredo et al. 2007). Moreover, the increase in individual size with temperature is accompanied by a reduction in population density (Goffredo et al. 2007), and this is in line with the hypothesis of energetic equivalence (Marquet et al. 1990), which states that, if an animal needs a certain area of space to satisfy its metabolic needs, its abundance will be inversely proportional to body size.

In a theoretical population, in a steady state, the age frequencies follow a negative exponential curve and the coefficient of determination of the semi-logarithmic regression from which a is estimated (Eq. 2) has a value of unity (Beverton and Holt 1956; Pauly 1984). In the populations considered in this study, r^2 was negatively correlated with temperature (i.e., it deviated from the theoretical steady state value as temperature increased) reducing from 0.9 in the coldest population to 0.4 in the warmest one (Tables 1 and 2) indicating that populations characterized by high temperatures were less stable than those from lower temperatures. While some populations only had few individuals, the theoretical growth curves and the parameters derived from them were comparable with those derived from the populations with many individuals, and the derived parameters can be considered good estimates of their population characteristics. Decreasing population stability with increasing temperature is further emphasized in Table 2, where SST was correlated with almost all dependent variables. As temperature increased, the theoretical percentage of immature individuals decreased, while the theoretical mean age of individuals, the theoretical age at maximum percentage biomass, and the theoretical mean age of biomass increased, all indicating a progressive reduction in young individuals. Reduced growth and increased mortality of juvenile tropical corals as temperature increases have been reported in a case study in the US Virgin Islands (Edmunds 2004). The deficiency of younger age classes as the temperature increased might be related to recent local perturbations (e.g., excessively high temperatures) such as the 2°C increase in the maximum SST in the northwest Mediterranean recorded in the year 2003, relative to the previous 50 years, and the short-term increase in SST of 3–4°C relative to the mean values in the year 2003 (Rodolfo-Metalpa et al. 2006; Diaz-Almela et al. 2007). *Balanophyllia europaea* larvae are zooxanthellate and rely on the energy derived from photosynthesis (Goffredo and Zaccanti 2004), and in zooxanthellate corals most of the energetic resources needed for gametogenesis come from photosynthesis (Rinkevich 1989). Reduced photosynthetic efficiency of zooxanthellae at high temperatures, besides limiting energetic resources for polyp gametogenesis (Rinkevich 1989; Goffredo et al. 2007), might decrease the energy available for larvae. Together, high mortality and reduced energy might explain both the low population density (Goffredo et al. 2007), and the reduction in numbers of young individuals with increasing temperature.

An alternative explanation for the negative effects on growth and population structure stability of *B. europaea* with increasing temperature could be related to suspension feeding. In the Mediterranean, nutrient levels and zooplankton availability are typically lower in summer-fall (i.e., high temperature) than in winter-spring (i.e., low temperature; Coma et al. 2000; Coma and Ribes 2003). Low nutrients and zooplankton availability proved to be a

stress factor for corals and several benthic suspension feeding taxa (Coma et al. 2000, Coma and Ribes 2003, Peirano et al. 2005). Moreover, in *Stylophora pistillata* colonies, starved corals present significantly lower levels of calcification and photosynthesis than fed corals (Houlbrèque et al. 2004). At high temperatures, low availability of resources would cause slow growth and low population stability in *B. europaea.* However, if this was the case, the inhibition would also be found in *L. pruvoti*, a closely related species which is totally heterotrophic but it is not. Goffredo et al. (2007) found that skeletal and population density of *L. pruvoti* were almost the same at low- and high-temperature study sites, compared to *B. europaea* where they decrease at high temperature. Thus the hypothesis of photosynthetic inhibition at high temperatures seems more likely.

Global increase in sea temperature is one of the greatest threats for reef corals (Hughes et al. 2003). Rising temperatures may pose the greatest threat to populations of *B. europaea* in the warmest areas of its distribution, which could reduce the abundance of recruits. The regression between SST and theoretical percentage of individuals below sexual maturity predicts that at a mean annual SST of 22.3°C, a population will be characterized by no immature individuals, and then will be condemned to a progressive decrease in abundance until extinction. The Intergovernmental Panel on Climate Change (IPCC) projected an increase of global SST of 1–3°C by 2100 (Solomon et al. 2007). Assuming an intermediate and rather conservative increase (2°C), it is expected that most of the populations of *B. europaea* would be near their thermal limit (expected temperature in 2100 in the population of CL = 20.0°C; LB = 20.7°C; PL = 21.1°C; SC = 21.5°C; GN = 21.6°C; PN = 21.9°C). This would result in a large decrease in the input of new individuals to the population. A decrease of population density of this species with increasing SST has already been reported (Goffredo et al. 2007).

Present evidence suggests that corals and their symbiotic zooxanthellae may be unable to acclimate or adapt fast enough to cope with the present rapid rate of water warming (Hoegh-Guldberg 1999; Hoegh-Guldberg et al. 2007). Moreover, being endemic to the Mediterranean, *B. europaea* has very limited possibilities to react to seawater warming by moving northwards toward lower temperatures, since the northern limit of the Mediterranean basin is only 1° of latitude north of the northernmost population considered in this work. The future for *B. europaea* would therefore appear to be bleak.

Acknowledgments We wish to thank L. Bortolazzi, A. Comini, M. Ghelia, G. Neto, L. Tomesani, Centro Immersioni Pantelleria, Il Pesciolino, Polo Sub, and Sub Maldive, Bologna Scuba Team, Scientific Diving School, Marine Science Group, J. Bilewitch (State University of New York at Buffalo), and M. Mukherjee (University of Georgia) for help and assistance, and two anonymous reviewers for their comments on the manuscript. This research was financed by the Associazione dei Tour Operator Italiani, the Marine & Freshwater Science Group Association, the Canziani foundation of the Department of Evolutionary and Experimental Biology of the Alma Mater Studiorum, University of Bologna, and the Ministry of Education, University and Research. This study is dedicated to the memory of U. Pepoli. The experiments complied with current Italian law.

References

Al-Horani FA (2005) Effects of changing seawater temperature on photosynthesis and calcification in the scleractinian coral *Galaxea fascicularis*, measured with O_2, Ca^{2+} and pH microsensors. Sci Mar 69:347–354

Babcock RC (1991) Comparative demography of three species of scleractinian corals using age- and size-dependent classifications. Ecol Monogr 6:225–244

Bak RPM, Meesters EH (1999) Population structure as a response of coral communities to global change. Am Zool 39:56–65

Beverton RJH, Holt SV (1956) A review of methods for estimating mortality rates in fish populations, with special reference to sources of bias in catch sampling. Rapports et Proces-Verbaux des Reunions - Conseil International pour l'Exploration de la Mer 140:67–83

Bosscher H (1993) Computerized tomography and skeletal density of coral skeletons. Coral Reefs 12:97–103

Buddemeier RW, Maragos JE, Knutson DW (1974) Radiographic studies of reef coral exoskeletons: rates and patterns of coral growth. J Exp Mar Biol Ecol 14:179–200

Carricart-Ganivet JP (2004) Sea surface temperature and the growth of the West Atlantic reef-building coral *Montastraea annularis*. J Exp Mar Biol Ecol 302:249–260

Chadwick-Furman NE, Goffredo S, Loya Y (2000) Growth and population dynamic model of the reef coral *Fungia granulosa* Kluzinger, 1879 at Eilat, northern Red Sea. J Exp Mar Biol Ecol 249:199–218

Coma R, Ribes M (2003) Seasonal energetic constraints in Mediterranean benthic suspension feeders: effects at different levels of ecological organization. Oikos 101:205–215

Coma R, Ribes M, Gili JM, Zabala M (2000) Seasonality in coastal ecosystems. Trends Ecol Evol 12:448–453

Connell JH (1973) Population ecology of reef building corals. In: Jones OA, Endean R (eds) Biology and geology of coral reefs, vol. II: biology 1. Academic, New York, pp 271–324

Cooper TF, De'ath G, Fabricius KE, Lough JM (2007) Declining coral calcification in massive Porites in two nearshore regions of the northern Great Barrier Reef. Global Change Biol 14:529–538

Crossland CJ (1981) Seasonal growth of *Acropora* cf. *formosa* and *Pocillopora damicornis* on a high latitude reef (Houtman Abrolhos, Western Australia). Proc 4th Int Coral Reef Symp 1:663–667

Cushman JH, Lawton JH, Manly BFJ (1993) Latitudinal patterns in European ant assemblages: variation in species richness and body size. Oecologia 95:30–37

Diaz-Almela E, Marbà N, Duarte CM (2007) Consequences of Mediterranean warming events in seagrass (*Posidonia oceanica*) flowering records. Global Change Biol 13:224–235

Edmunds PJ (2004) Juvenile coral population dynamics track rising seawater temperature on a Caribbean reef. Mar Ecol Prog Ser 269:111–119

Efron B (1981) Nonparametric estimates of standard error: the jackknife, the bootstrap and other methods. Biometrika 68:589–599

Epstein N, Bak RPM, Rinkevich B (2001) Strategies for gardening denuded coral reef areas: the applicability of using different types of coral material for reef restoration. Restor Ecol 9:432–442

Fabens AJ (1965) Properties and fitting of the von Bertalanffy growth curve. Growth 29:265–289

Fadlallah YH (1983) Population dynamics and life history of a solitary coral, *Balanophyllia elegans*, from Central California. Oecologia 58:200–207

Fine M, Zibrowius H, Loya Y (2001) *Oculina patagonica*: a non-lessepsian scleractinian coral invading the Mediterranean Sea. Mar Biol 138:1195–1203

Foster AB, Johnson KG, Schultz LL (1988) Allometric shape change and heterocrony in the freeliving coral *Trachyphyllia bilobata* (Duncan). Coral Reefs 7:37–44

Glassom D, Chadwick NE (2006) Recruitment, growth and mortality of juvenile corals at Eilat, northern Red Sea. Mar Ecol Prog Ser 318:111–122

Goffredo S, Chadwick-Furman NE (2003) Comparative demography of mushroom corals (Scleractinia, Fungiidae) at Eilat, northern Red Sea. Mar Biol 142:411–418

Goffredo S, Lasker HR (2006) Modular growth of a gorgonian coral can generate predictable patterns of colony growth. J Exp Mar Biol Ecol 336:221–229

Goffredo S, Zaccanti F (2004) Laboratory observations of larval behavior and metamorphosis in the Mediterranean solitary coral *Balanophyllia europaea* (Scleractinia, Dendrophylliidae). Bull Mar Sci 74:449–458

Goffredo S, Arnone S, Zaccanti F (2002) Sexual reproduction in the Mediterranean solitary coral *Balanophyllia europaea* (Scleractinia, Dendrophylliidae). Mar Ecol Prog Ser 229:83–94

Goffredo S, Mattioli G, Zaccanti F (2004) Growth and population dynamics model of the Mediterranean solitary coral *Balanophyllia europaea* (Scleractinia, Dendrophylliidae). Coral Reefs 23:433–443

Goffredo S, Caroselli E, Pignotti E, Mattioli G, Zaccanti F (2007) Variation in biometry and demography of solitary corals with environmental factors in the Mediterranean Sea. Mar Biol 152:351–361

Grigg RW (1974) Growth rings: annual periodicity in two gorgonian corals. Ecology 55:876–881

Grigg RW (1975) Age structure of a longevous coral: a relative index of habitat suitability and stability. Am Nat 109:647–657

Grigg RW (1982) Darwin point: a threshold for atoll formation. Coral Reefs 1:29–34

Grigg RW (1984) Resource management of precious corals: a review and application to shallow water reef building corals. PSZNI Mar Ecol 5:57–74

Guzner B, Novoplansky A, Chadwick NE (2007) Population dynamics of the reef-building coral *Acropora hemprichii* as an indicator of reef condition. Mar Ecol Prog Ser 333:143–150

Harriott VJ (1999) Coral growth in subtropical eastern Australia. Coral Reefs 18:281–291

Helmle KP, Dodge RE, Ketcham RA (2000) Skeletal architecture and density banding in *Diploria strigosa* by X-ray computed tomography. Proc 9th Int Coral Reef Symp 1:365–371

Hoegh-Guldberg O (1999) Climate change, coral bleaching and the future of the world's coral reefs. Mar Freshw Res 50:839–866

Hoegh-Guldberg O, Mumby PJ, Hooten AJ, Steneck RS, Greenfield P, Gomez E, Harvell CD, Sale PF, Edwards AJ, Caldeira K, Knowlton N, Eakin CM, Iglesias-Prieto R, Muthiga N, Bradbury RH, Dubi A, Hatziolos ME (2007) Coral reefs under rapid climate change and ocean acidification. Science 318:1737–1742

Houlbrèque F, Tambuttè E, Allemand D, Ferrier-Pagès C (2004) Interactions between zooplankton feeding, photosynthesis and skeletal growth in the scleractinian coral *Stylophora pistillata*. J Exp Biol 207:1461–1469

Howe SA, Marshall AT (2002) Temperature effects on calcification rate and skeletal deposition in the temperate coral, *Plesiastrea versipora* (Lamarck). J Exp Mar Biol Ecol 275:63–81

Hughes TP, Jackson JBC (1985) Population dynamics and life histories of foliaceous corals. Ecol Monogr 55:141–166

Hughes TP, Ayre D, Connell JH (1992) The evolutionary ecology of corals. Trends Ecol Evol 7:292–295

Hughes TP, Baird AH, Bellwood DR, Card M, Connolly SR, Folke C, Grosberg R, Hoegh-Guldberg O, Jackson JBC, Kleypas J, Lough JM, Marshall P, Nyström M, Palumbi SR, Pandolfi JM, Rosen B, Roughgarden J (2003) Climate change, human impacts, and the resilience of coral reefs. Nature 301:929–933

Jacques TG, Marshall N, Pilson MEQ (1983) Experimental ecology of the temperate scleractinian coral *Astrangia danae*: II. Effect of temperature, light intensity and symbiosis with zooxanthellae on metabolic rate and calcification. Mar Biol 76:135–148

Johnson KG (1992) Population dynamics of a free-living coral: recruitment, growth and survivorship of *Manicina areolata* (Linnaeus) on the Caribbean coast of Panama. J Exp Mar Biol Ecol 164:171–191

Kain JM (1989) The seasons in the subtidal. Br Phycol J 24:203–215

Kinsey DW, Davies PJ (1979) Carbon turnover calcification and growth in coral reefs. In: Trudinger PA, Swaine DJ (eds) Biogeochemical cycling of mineral forming elements. Elsevier, Amsterdam, pp 131–162

Kleypas JA, McManus JW, Menez LAB (1999) Environmental limits to coral reef development: where do we draw the line? Am Zool 39:146–159

Knowlton N, Rohwer F (2003) Multispecies microbial mutualism on coral reefs: the host as a habitat. Am Nat 162:S51–S62

Knuston DW, Buddemeir RW, Smith SV (1972) Coral chronometers: seasonal growth bands in reef corals. Science 177:270–272

Lasker HR (1981) Phenotypic variation in the coral *Montastrea cavernosa* and its effects on colony energetics. Biol Bull 160:292–302

Lonsdale DJ, Levinton JS (1985) Latitudinal differentiation in copepod growth: an adaptation to temperature. Ecology 66:1397–1407

Lough JM, Barnes DJ (2000) Environmental controls on growth of the massive coral *Porites*. J Exp Mar Biol Ecol 245:225–243

Loya Y (1976) The Red Sea coral *Stylophora pistillata* is an r-strategist. Nature 259:478–480

Marquet PA, Navarrete SA, Castilla JC (1990) Scaling population density to body size in rocky intertidal communities. Science 250:1125–1127

Mc Neil BI, Matear RJ, Barnes DJ (2004) Coral reef calcification and climate change: the effect of ocean warming. Geophys Res Lett 31:L22309

Meesters EH, Hilterman M, Kardinaal E, Keetman M, deVries M, Bak RPM (2001) Colony size-frequency distributions of scleractinian coral populations: spatial and interspecific variation. Mar Ecol Prog Ser 209:43–54

Mistri M, Ceccherelli VU (1994) Growth and secondary production of the Mediterranean gorgonian *Paramuricea clavata*. Mar Ecol Prog Ser 103:291–296

Olabarria C, Thurston MH (2003) Latitudinal and bathymetric trends in body size of the deep-sea gastropod *Troschelia berniciensis* (King). Mar Biol 143:723–730

Pauly D (1984) Fish population dynamics in tropical waters: a manual for use with programmable calculators. International Center for Living Aquatic Resources Management, Manila

Peirano A, Morri C, Bianchi CN (1999) Skeleton growth and density pattern of the temperate, zooxanthellate scleractinian *Cladocora caespitosa* from the Ligurian Sea (NW Mediterranean). Mar Ecol Prog Ser 185:195–201

Peirano A, Abbate M, Cerrati G, Difesca V, Peroni C, Rodolfo-Metalpa R (2005) Monthly variations in calyx growth, polyp tissue, and density banding of the Mediterranean scleractinian *Cladocora caespitosa* (L.). Coral Reefs 24:404–409

Reynaud S, Leclercq N, Romaine-Lioud S, Ferrier-Pages C, Jaubert J, Gattuso JP (2003) Interacting effects of CO_2 partial pressure and temperature on photosynthesis and calcification in a scleractinian coral. Global Change Biol 9:1660–1668

Rinkevich B (1989) The contribution of photosynthetic products to coral reproduction. Mar Biol 101:259–263

Rodolfo-Metalpa R, Richard C, Allemand D, Bianchi CN, Morri C, Ferrier-Pagès C (2006) Response of zooxanthellae in symbiosis with the Mediterranean corals *Cladocora caespitosa* and *Oculina patagonica* to elevated temperatures. Mar Biol 150:45–55

Ross MA (1984) A quantitative study of the stony coral fishery in Cebu, Philippines. PSZNI Mar Ecol 5:75–91

Roy K, Martien KK (2001) Latitudinal distribution of body size in north-eastern Pacific marine bivalves. J Biogeogr 28:485–493

Shenkar N, Fine M, Loya Y (2005) Size matters: bleaching dynamics of the coral *Oculina patagonica*. Mar Ecol Prog Ser 294:181–188

Solomon S, Qin D, Manning M, Chen Z, Marquis M, Averyt K, Tignor MMB, Miller HL (2007) Climate change 2007: the physical science basis. Cambridge University Press, Cambridge

Sparre P, Ursin E, Venema SC (1989) Introduction to tropical fish stock assessment. FAO Fisheries Technical Paper, Rome

Tsounis G, Rossi S, Gili JM, Arntz WE (2007) Red coral fishery at the Costa Brava (NW Mediterranean): case study of an overharvested precious coral. Ecosystems 10:975–986

Turner JRG, Lennon JJ (1989) Species richness and energy theory. Nature 340:351

Vermeij MJA (2006) Early life-history dynamics of Caribbean coral species on artificial substratum: the importance of competition, growth and variation in life-history strategy. Coral Reefs 25:59–71

Visram S, Wiedenmann J, Douglas AE (2006) Molecular diversity of symbiotic algae of the genus *Symbiodinium* (Zooxanthellae) in cnidarians of the Mediterranean Sea. J Mar Biol Assoc UK 86:1281–1283

von Bertalanffy L (1938) A quantitative theory of organic growth (inquiries on growth laws II). Hum Biol 10:181–213

Wright DH (1983) Species-energy theory: an extension of species-area theory. Oikos 41:496–506

Zibrowius H (1980) Les scléractiniaires de la Méditeranée et de l'Atlantique nord-oriental. Mem Inst Oceanogr (Monaco) 11:1–284

Limnol. Oceanogr., 54(3), 2009, 930–937

Inferred level of calcification decreases along an increasing temperature gradient in a Mediterranean endemic coral

Stefano Goffredo,[a,*] Erik Caroselli,[a] Guido Mattioli,[b] Elettra Pignotti,[c] Zvy Dubinsky,[d] and Francesco Zaccanti[a]

[a] Marine Science Group, Department of Evolutionary and Experimental Biology, Alma Mater Studiorum–University of Bologna, Bologna, Italy
[b] Operative Unit of Radiology and Diagnostics by Images, Hospital of Porretta Terme, Local Health Enterprise of Bologna, Bologna, Italy
[c] Taskforce for Statistical Analysis, Marine & Freshwater Science Group Association, Bologna, Italy
[d] The Mina and Everard Goodman Faculty of Life Sciences, Bar-Ilan University, Ramat-Gan, Israel

Abstract

The correlation between solar radiation and sea surface temperature (SST) and growth was assessed along a latitudinal gradient. Extension rate and skeletal density were both correlated with calcification rate, indicating that calcium carbonate deposition was allocated evenly between skeletal density and linear extension. Unlike most studies on other tropical and temperate corals, in which calcification was positively correlated with solar radiation and SST, in the present study calcification was not correlated with solar radiation, whereas it was negatively correlated with SST. We hypothesize that photosynthesis of the symbiotic algae of *Balanophyllia europaea* is inhibited at high temperatures, consequently causing an inhibition of calcification. The regressions between calcification and SST predicted that the calcification of *B. europaea* would be depressed at 20.5–21.0°C mean annual SST. The scenarios of the Intergovernmental Panel on Climate Change conclude that by 2100, SST will exceed this physiological threshold for most of the populations considered in this study. This study comprises the first field investigation of the relationships between environmental parameters and calcification of a Mediterranean coral and highlights the risks of losing Mediterranean marine biodiversity over the course of future decades.

Temperature and irradiance variations associated with latitude have an important influence on global coral distribution patterns (Kleypas et al. 1999). Latitude is the main factor influencing the variation of light and temperature (Kain 1989), which are the two environmental parameters considered in this study because they have been shown to be strongly linked to coral growth, physiology, and demography (Kleypas et al. 1999; Lough and Barnes 2000). In general, coral growth decreases with increasing latitude, to a boundary beyond 30°N and 30°S, where coral reef development no longer occurs (Kinsey and Davies 1979). Coral growth is a composite of three related parameters (calcification = linear extension × skeletal density; Lough and Barnes 2000; Carricart-Ganivet 2004), and their measurement is essential when assessing the effects of environmental parameters on coral growth, because none of the three is a perfect predictor of the other two (Dodge and Brass 1984). Analyzing these variables also allows for prediction of the possible effect that climatic changes can have on coral ecosystems (Cooper et al. 2008). These three variables have been studied along a latitudinal gradient in the genera *Montastraea* (Carricart-Ganivet 2004) and *Porites* (Lough and Barnes 2000; Cooper et al. 2008), and variation of the three parameters has been linked to changes in temperature and light associated with latitude. In colonies of *Montastraea annularis* in the Gulf of Mexico and the Caribbean Sea, sea surface temperature (SST) is positively correlated with calcification rate and skeletal density, while it is negatively correlated with linear extension rate (Carricart-Ganivet 2004). In colonies of *Porites* of the Hawaiian archipelago, Thailand, and the Great Barrier Reef (Australia), solar radiation and SST were found to be positively correlated with calcification and linear extension rates and negatively correlated with skeletal density (Lough and Barnes 2000). In contrast, a recent monitoring of 16 yr of calcification in *Porites* colonies from the Great Barrier Reef shows that calcification declined over time and indicates that the response may be due to the interactive effects of elevated seawater temperatures and pCO_2 increase (Cooper et al. 2008), as previously reported for colonies of *Stylophora pistillata* grown in aquaria (Reynaud et al. 2003).

Although there are numerous studies of the relationships between environmental parameters and coral growth in the tropics (Lough and Barnes 2000; Carricart-Ganivet 2004; Cooper et al. 2008), such studies are scarce for temperate zones. In *Astrangia danae* and *Plesiastrea versipora*, calcification rate increases with temperature, as is the trend for some tropical corals, albeit over a lower temperature range (Howe and Marshall 2002). Laboratory observations on calcification rates in *Cladocora caespitosa* and *Oculina patagonica* indicate that prolonged periods of high temperatures (corresponding to or higher than the maximum summer temperature in the field) lead to a decrease in calcification (Rodolfo-Metalpa et al. 2006*b*).

This study aimed to investigate the relationships between environmental parameters (solar radiation and SST) and the three growth components (calcification, skeletal density, and linear extension) in the Mediterranean coral

* Corresponding author: stefano.goffredo@marinesciencegroup.org

Balanophyllia europaea (Risso 1826). *B. europaea* is a solitary, zooxanthellate scleractinian coral, which is endemic to the Mediterranean Sea (Zibrowius 1980). Being zooxanthellate, its distribution is limited to 0–50 m in depth (Zibrowius 1980), with abundances of more than 100 individuals m^{-2} (Goffredo et al. 2004*a*). It is a simultaneous hermaphrodite and brooder (Goffredo et al. 2002). Along the Italian coasts, skeletal density and population abundance are negatively correlated with SST (Goffredo et al. 2007). In addition, the population structures of this species become less stable and deviate from the steady state with increasing SST as the result of a progressive deficiency of young individuals (Goffredo et al. 2008). In the azooxanthellate coral *Leptopsammia pruvoti*, closely related to *B. europaea* and studied in the same sites sampled in this study, no significant variation was found in the skeletal and population density with solar radiation and SST (Goffredo et al. 2007). It has been hypothesized that temperature negatively influences the photosynthesis of the symbiotic algae of *B. europaea*, leading to negative effects on its growth and reproductive activity (Goffredo et al. 2007, 2008). Suggested by Goreau (1959) as the 'light enhanced calcification' hypothesis, in zooxanthellate corals photosynthesis stimulates calcification, as has been confirmed in several studies (Al-Horani et al. 2005; Mass et al. 2007), and both processes have an optimal temperature (Howe and Marshall 2002). Rinkevich (1989) demonstrated the energetic contribution of photosynthetic products to coral reproduction in zooxanthellate corals.

This is the first study on the variation of the three growth components in a temperate scleractinian coral, and the study aims to assess the variations in calcification rate, linear extension rate, and skeletal density in populations arranged along a temperature and solar radiation gradient. The results are also considered in light of the most recent scenarios on climate changes for the near future.

Methods

Specimens of *B. europaea* were collected from six sites along a latitudinal gradient, from 44°20′N to 36°45′N, between 09 November 2003 and 30 September 2005 (Fig. 1). With the exception of the Calafuria population, for which data were obtained from a previous study (Goffredo et al. 2004*a*), samples were collected at each site using transects of at least three patches of 1 m^2 each, arranged in a line 5 m apart along the southern side of each reef at a depth of 5–7 m. Given the random distribution pattern of *B. europaea*, this study is not affected by the problems associated with regularly spaced quadrats and transects (Goffredo et al. 2004*a*). All of the polyps included were collected from each patch. Sampling was performed at depths known to have high population densities and where the reproductive biology, biometry, population density, growth, population dynamics, and genetics of the species had previously been studied (Goffredo et al. 2002, 2004*a*,*b*). Sampling at the depth of maximum abundance may bias growth estimates toward a higher rate and in turn underestimate age, but by sampling in the chosen depth range, where 62% of the biomass of this species is found (Goffredo et al. 2004*a*), this bias is reduced.

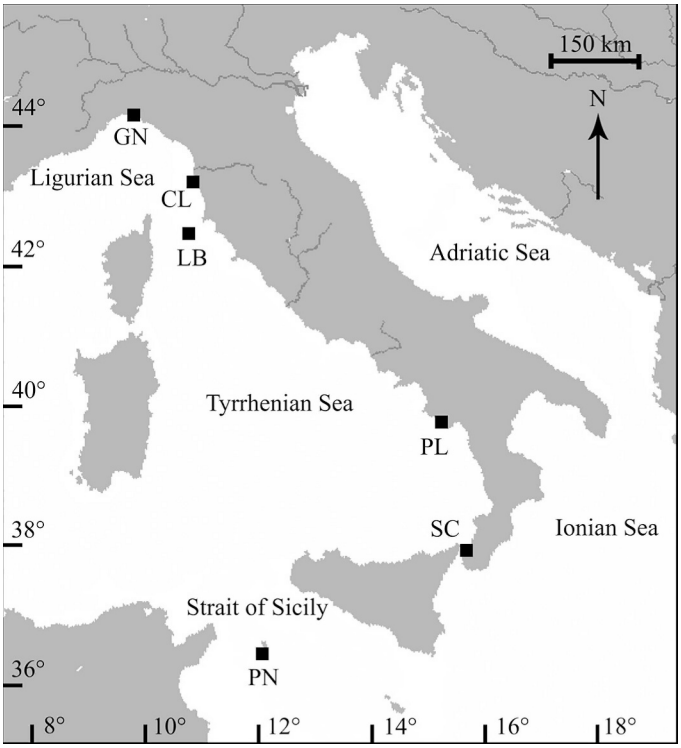

Fig. 1. Map of the Italian coastline indicating sites at which corals were collected. Abbreviations and coordinates of the sites, in decreasing order of latitude, are as follows: GN, Genova: 44°20′N, 9°08′E; CL, Calafuria: 43°27′N, 10°21′E; LB, Elba Isle: 42°45′N, 10°24′E; PL, Palinuro: 40°02′N, 15°16′E; SC, Scilla: 38°01′N, 15°38′E; and PN, Pantelleria Isle: 36°45′N, 11°57′E.

Corals were dried at 50°C for 4 d and were observed under a binocular microscope to remove fragments of substratum and calcareous deposits produced by other organisms. Corallite length (L: maximum axis of the oral disc), width (W: minimum axis of the oral disc), and height (h: oral–aboral axis) were measured with calipers, and the dry skeletal mass (M) was measured with a precision balance. Corallite volume (V) was determined by applying the following formula: $V = (L/2) \times (W/2) \times h\pi$ (Goffredo et al. 2007). Skeletal density (D) was calculated by dividing M by V.

The age of each sample was estimated using the von Bertalanffy length–age growth functions, previously obtained for each population based on growth bands analysis by means of computerized tomography (von Bertalanffy 1938; Goffredo et al. 2008). According to the age of the polyp, the annual linear extension rate was obtained for each sample using the von Bertalanffy length–age growth functions (von Bertalanffy 1938; Goffredo et al. 2008). The mean annual calcification rate (mass of $CaCO_3$ deposited per year per area unit) was calculated for each sample by the following formula: calcification (mg mm^{-2} yr^{-1}) = skeletal density (mg mm^{-3}) × linear extension (mm yr^{-1}) (Lough and Barnes 2000; Carricart-Ganivet 2004). Thus, for each population the mean values of skeletal density, linear extension, and calcification rates of the corallites were

Table 1. Average annual solar radiation and SST values of the sample sites. The sites are arranged in order of increasing SST.*

		Solar radiation (W m^{-2})	SST (°C)
Population	Code	Annual mean (SE)	Annual mean (SE)
Calafuria	CL	170.07 (1.02)	18.02 (0.04)
Elba	LB	172.74 (1.02)	18.74 (0.04)
Palinuro	PL	181.48 (1.01)	19.14 (0.03)
Scilla	SC	187.31 (1.02)	19.54 (0.02)
Genova	GN	166.95 (1.02)	19.56 (0.04)
Pantelleria	PN	190.95 (1.02)	19.88 (0.04)

* SE, standard error.

obtained. Samples were also divided into three age classes: immature (0–4 yr, after Goffredo et al. 2004*a*); mature (4–8 yr, double the age at sexual maturity); and old (>8 yr).

Correlation and regression analyses between environmental and growth parameters were performed both for the full data set and for the three age classes to check for differences due to the different mean age of the samples in the populations (Goffredo et al. 2008). Relationships between environmental and growth parameters were performed using two models: a linear model and a power function model. The linear model was used to compare the results with other studies on environmental controls of coral growth, in which linear functions are used (Lough and Barnes 2000; Carricart-Ganivet 2004). We used the power function model as it produced the best fit with the data and to compare the results obtained by the linear model. The power function model,

$$y = ax^b \quad (1)$$

was linearized with a log-transformation of both the independent and dependent variables, producing the equation

$$\ln(y) = b\ln(x) + \ln(a) \quad (2)$$

SST data for 2003–2005 were obtained for each location from the National Mareographic Network of the Agency for the Protection of the Environment and Technical Services (available at http://www.apat.gov.it). These data are measured by mareographic stations SM3810, built by the Italian Society for Precision Apparatuses. Mean annual SST was obtained from hourly values measured from January 2001 to January 2005 (Table 1). Monthly values of solar radiation (W m^{-2}) were obtained from the International Cloud Climatology Project (available at http://ingrid.ldgo.columbia.edu/). These estimates are derived from satellite measurements of cloud and atmospheric optical properties. Mean annual solar radiation was obtained for the 2.5°–latitude-by-longitude square associated with each of the six sites (Table 1).

Because of the heteroskedastic nature of the data, the nonparametric Kruskal–Wallis test was used to compare mean solar radiation, SST, skeletal density, linear extension, and calcification rates among the populations. Pearson correlation coefficients were calculated for the relationships among growth parameters and between environmental and growth parameters. Because of the low n value ($n = 6$) and the assumptions of the Pearson method, correlation coefficients were also estimated with bootstrapping (Efron 1981), with 100,000 resamples. All analyses were computed using SPSS 12.0, except for the bootstrapping analyses (S-PLUS 6.0 Professional).

Results

Both mean annual solar radiation and SST varied significantly among the sites (Kruskal–Wallis test, $p < 0.001$; Table 1). Mean skeletal density, linear extension, and calcification rates were significantly different among the populations (Kruskal–Wallis test, $p < 0.001$; Table 2). Mean calcification rate of the corallites in the populations was positively correlated with mean linear extension rate and mean skeletal density (Table 3). Based on the bootstrapping coefficients, calcification rate explained 66% of the variance in linear extension rate and 84% of the variance in skeletal density (Table 3).

Considering the full data set (all ages), both the linear and power function models showed that mean skeletal density of the populations was not correlated with solar radiation, whereas it was negatively correlated with SST, which explained 92–94% of its variance (Tables 4, 5). Mean linear extension rate of the populations was not significantly correlated with either solar radiation or SST (Tables 4, 5). Mean calcification rate of the populations was not correlated with solar radiation, but it was significantly negatively correlated with SST, which explained 74–75% of its variance (Tables 4, 5). The linear model indicated that a 1°C rise in SST lowered the mean skeletal density of the populations by 0.58 mg mm^{-3} and lowered the mean calcification rate of the populations by 1.00 mg mm^{-2} yr^{-1}. The trends from the whole data set

Table 2. *Balanophyllia europaea*. Mean skeletal density, linear extension, and calcification rate values of the populations. The sites are arranged in order of increasing SST.*

Population	Code	n	Average skeletal density (mg mm^{-3})	SE	Average linear extension rate (mm yr^{-1})	SE	Average calcification rate (mg mm^{-2} yr^{-1})	SE
Calafuria	CL	941	1.95	0.01	1.49	0.01	2.86	0.03
Elba	LB	38	1.41	0.06	1.15	0.04	1.62	0.09
Palinuro	PL	80	1.05	0.03	0.96	0.02	1.02	0.04
Scilla	SC	48	1.01	0.04	1.12	0.03	1.12	0.06
Genova	GN	55	0.93	0.02	1.17	0.04	1.09	0.04
Pantelleria	PN	171	0.91	0.02	1.08	0.01	0.97	0.02

* n, number of individuals; SE, standard error.

Table 3. *Balanophyllia europaea*. Linear regression and correlation analysis between mean skeletal density, linear extension rate, and calcification rate in the six sites ($n = 6$).†

Dependent variable	Independent variable	Slope (SE)	Intercept (SE)	r^2	r	r^2_{BS}	r_{BS}
Skeletal density	Linear extension	1.931 (0.612)	−1.034 (0.718)	0.713	0.845*	0.392	0.626
Calcification	Linear extension	3.805 (0.795)	−2.973 (0.932)	0.851	0.923**	0.661	0.813*
Calcification	Skeletal density	1.773 (0.163)	−0.699 (0.206)	0.967	0.984***	0.841	0.917*

† r^2, Pearson's coefficient of determination; r, Pearson's correlation coefficient; r^2_{BS} and r_{BS}, Pearson's coefficients calculated with bootstrapping; SE, standard error.
* $p<0.050$.
** $p<0.010$.
*** $p<0.001$.

were confirmed by the age-stratified analyses on the subsets of immature and mature samples (Tables 4, 5). The old-samples subset showed a similar trend, except that the mean linear extension rate of the populations was positively correlated with SST and the mean calcification rate was not significantly correlated with SST when considering the bootstrapping r value (Tables 4, 5).

Based on the two significant regressions from the whole data set, the linear model predicted that calcification would have ceased at a mean annual SST of 20.5°C and the skeletal density would fall to zero values at a mean annual SST of 21.2°C (Table 4). The power function model predicted that calcification would have approached zero values at 21.0°C and the skeletal density would have approached zero values at a mean annual SST of 21.3°C (Table 5).

Discussion

The 'stretching modulation of skeletal growth' is a mechanism that corals can adopt for preferentially

Table 4. *Balanophyllia europaea*. Linear model. Linear regression and correlation analysis between environmental and growth parameters in the six sites ($n = 6$). Regression parameters are shown only where the relationship is significant.†

Dependent variable	Independent variable	Slope (SE)	Intercept (SE)	r^2	r	r^2_{BS}	r_{BS}
			All samples				
Skeletal density	Solar radiation	—	—	0.260	−0.510	0.244	−0.494
Linear extension	Solar radiation	—	—	0.304	−0.551	0.343	−0.586
Calcification	Solar radiation	—	—	0.278	−0.527	0.314	−0.560
Skeletal density	SST	−0.580 (0.077)	12.313 (1.475)	0.934	−0.967**	0.920	−0.959**
Linear extension	SST	—	—	0.527	−0.726	0.296	−0.544
Calcification	SST	−0.997 (0.209)	20.542 (4.012)	0.850	−0.922**	0.740	−0.860*
			Immature samples (0–4 yr)				
Skeletal density	Solar radiation	—	—	0.372	−0.610	0.389	−0.624
Linear extension	Solar radiation	—	—	0.493	−0.702	0.530	−0.728
Calcification	Solar radiation	—	—	0.379	−0.615	0.416	−0.645
Skeletal density	SST	−0.572 (0.121)	12.049 (2.320)	0.848	−0.921**	0.674	−0.821*
Linear extension	SST	—	—	0.615	−0.784	0.415	−0.644
Calcification	SST	−1.226 (0.277)	25.192 (5.300)	0.831	−0.911*	0.667	−0.817*
			Mature samples (5–8 yr)				
Skeletal density	Solar radiation	—	—	0.263	−0.513	0.329	0.574
Linear extension	Solar radiation	—	—	0.314	−0.561	0.245	−0.495
Calcification	Solar radiation	—	—	0.314	−0.561	0.318	−0.564
Skeletal density	SST	−0.643 (0.089)	13.527 (1.711)	0.928	−0.964**	0.899	−0.948**
Linear extension	SST	—	—	<0.001	−0.005	<0.001	−0.004
Calcification	SST	−0.766 (0.135)	16.109 (2.587)	0.890	−0.943**	0.792	−0.890*
			Old samples (>8 yr)				
Skeletal density	Solar radiation	—	—	0.206	−0.454	0.175	−0.418
Linear extension	Solar radiation	—	—	0.255	0.505	0.233	0.483
Calcification	Solar radiation	—	—	0.166	−0.408	0.105	−0.324
Skeletal density	SST	−0.704 (0.125)	14.778 (2.396)	0.888	−0.942*	0.841	−0.917*
Linear extension	SST	0.170 (0.012)	−2.436 (0.224)	0.981	0.991***	0.974	0.987**
Calcification	SST	—	—	0.800	0.895*	0.571	−0.756

† r^2, Pearson's coefficient of determination; r, Pearson's correlation coefficient; r^2_{BS} and r_{BS}, Pearson's coefficients calculated with bootstrapping; SST, sea surface temperature; SE, standard error.
* $p<0.050$.
** $p<0.010$.
*** $p<0.001$.

Table 5. *Balanophyllia europaea*. Power function model (Eq. 2). Linear regression and correlation analysis between environmental and growth parameters in the six sites ($n = 6$) calculated on log-transformed data. Regression parameters are shown only where the relationship is significant.†

Dependent variable	Independent variable	Slope (SE)	Intercept (SE)	r^2	r	r^2_{BS}	r_{BS}
			All samples				
Skeletal density	Solar radiation	—	—	0.252	−0.502	0.230	−0.480
Linear extension	Solar radiation	—	—	0.318	−0.564	0.352	−0.593
Calcification	Solar radiation	—	—	0.316	−0.562	0.333	−0.577
Skeletal density	SST	−8.162 (0.876)	24.241 (2.586)	0.956	−0.978***	0.935	−0.967**
Linear extension	SST	—	—	0.488	−0.698	0.289	−0.538
Calcification	SST	−10.932 (1.981)	32.551 (5.848)	0.884	−0.940**	0.752	−0.867*
			Immature samples (0–4 yr)				
Skeletal density	Solar radiation	—	—	0.407	−0.638	0.408	−0.639
Linear extension	Solar radiation	—	—	0.516	−0.718	0.540	−0.735
Calcification	Solar radiation	—	—	0.452	−0.672	0.460	−0.678
Skeletal density	SST	−8.829 (2.073)	26.095 (6.120)	0.819	−0.905*	0.661	−0.813*
Linear extension	SST	—	—	0.050	−0.224	0.411	−0.641
Calcification	SST	−11.503 (2.943)	34.396 (8.687)	0.792	−0.890*	0.659	−0.812*
			Mature samples (5–8 yr)				
Skeletal density	Solar radiation	—	—	0.274	−0.523	0.248	−0.498
Linear extension	Solar radiation	—	—	0.314	−0.560	0.324	−0.569
Calcification	Solar radiation	—	—	0.353	−0.594	0.347	−0.589
Skeletal density	SST	−9.007 (0.918)	26.730 (2.710)	0.960	−0.980***	0.922	−0.960**
Linear extension	SST	—	—	<0.001	−0.015	<0.001	−0.016
Calcification	SST	−8.936 (1.431)	26.685 (4.224)	0.907	−0.952**	0.799	−0.894*
			Old samples (>8 yr)				
Skeletal density	Solar radiation	—	—	0.191	−0.437	0.167	−0.403
Linear extension	Solar radiation	—	—	0.246	0.496	0.229	0.479
Calcification	Solar radiation	—	—	0.152	−0.390	0.097	−0.311
Skeletal density	SST	−8.980 (1.316)	26.713 (3.885)	0.921	−0.960**	0.857	−0.926**
Linear extension	SST	4.127 (0.268)	−12.382 (0.792)	0.983	0.992***	0.974	0.987***
Calcification	SST	—	—	0.798	−0.893*	0.570	−0.755

† r^2, Pearson's coefficient of determination; r, Pearson's correlation coefficient; r^2_{BS} and r_{BS}, Pearson's coefficients calculated with bootstrapping; SST, sea surface temperature; SE, standard error.
* $p<0.050$.
** $p<0.010$.
*** $p<0.001$.

investing calcification in skeletal density or linear extension (Carricart-Ganivet and Merino 2001; Carricart-Ganivet 2004). *Porites*, for example, invests increased calcification at higher temperatures into linear extension, allowing the coral to occupy space as rapidly as possible (Lough and Barnes 2000). In contrast, *M. annularis* invests increased calcification at higher temperatures to construct more dense skeletons (Carricart-Ganivet and Merino 2001; Carricart-Ganivet 2004). In *B. europaea*, linear extension rate and skeletal density were both positively correlated with calcification rate, indicating that the capacity to colonize the substratum quickly and the mechanical strength of the skeleton are both important for this species and that calcification is allocated evenly between increasing skeletal density and linear extension, in comparison with *Porites* and *M. annularis*. For each 1 mg mm^{-2} yr^{-1} of calcification rate reduction, linear extension rate decreased by ~0.3 mm yr^{-1}, and skeletal density decreased by ~0.6 mg mm^{-3}.

Calculated density values were reasonable with respect to other studies on tropical species (Bucher et al. 1998; Lough and Barnes 2000; Carricart-Ganivet 2004). The geometrically computed skeletal density used in this and previous studies (Goffredo et al. 2007) is analogous to the bulk density (Bucher et al. 1998), which is equal to the skeletal mass divided by the total volume (skeletal matrix volume + pores volume; Bucher et al. 1998). Skeletal matrix volume is further composed by the $CaCO_3$ and by the intracrystalline organic framework regulating the crystallization process (Cohen and McConnaughey 2003). Analyses to quantify the organic framework content and porosity in the same samples are currently underway to verify if the variation in bulk skeletal density depends on the porosity or on the specific gravity of $CaCO_3$ crystals or on the content of organic framework. Estimates of micro-density may be obtained by a water displacement technique, but we chose not to use this method because the procedure involves the use of acetone (Bucher et al. 1998) and could have affected the above-mentioned fine studies on organic framework quantification.

The fact that calcification rate and skeletal density were not correlated with solar radiation, while they were negatively correlated with SST, confirms previous studies on the biometry, growth, and population structure stability

of this species, in which the coral parameters show stronger and more significant relationships with temperature than with light (Goffredo et al. 2007, 2008). For both the linear and power function models, trends of the analyses performed on the full data set were confirmed by most of the analyses on the three age-based subsets, indicating that differences in the mean age of the samples in the populations (Goffredo et al. 2008) did not bias the results. The positive correlation between linear extension rate and SST in the older samples is expected, since corallite asymptotic length in the populations is positively correlated with SST. Given the reduced growth rate of this species as corallite size approaches the asymptotic one, old samples in cooler waters are close to their asymptotic length and extend their size very slowly, while old samples in warmer waters are far from the asymptote and still significantly increase their size (Goffredo et al. 2008). This is very likely the cause of the lowered r value in the negative correlation between calcification and SST for the old samples subset (i.e., linear extension in the old samples subset does not decrease with SST, as in the other subsets, and the decrease in calcification with SST is less steep).

The decrease in calcification rate with increasing temperature for *B. europaea* is in contrast with the findings of other studies on latitudinal variations of calcification in tropical and temperate corals, in which the trend was the opposite (Lough and Barnes 2000; Howe and Marshall 2002; Carricart-Ganivet 2004). In addition to being an opposite trend, the response of *B. europaea* calcification rate to temperature (-1.00 mg mm^{-2} yr^{-1} °C^{-1}; present work, Table 4) was three times lower than that of *Porites* ($+3.30$ mg mm^{-2} yr^{-1} °C^{-1}; Lough and Barnes 2000) and five times lower in comparison with *M. annularis* ($+5.70$ mg mm^{-2} yr^{-1} °C^{-1}; Carricart-Ganivet 2004). However, a recent study shows a decline in coral calcification in massive *Porites* from the Great Barrier Reef over a 16-yr period (Cooper et al. 2008) and indicates that this reduction is linked to the interactive effects of increasing seawater temperatures and pCO_2-associated acidification (Reynaud et al. 2003).

The reduction of *B. europaea* calcification with increasing temperature might depend on the response of zooxanthellae photosynthesis to temperature, since in zooxanthellate corals calcification is enhanced by photosynthesis (Al-Horani et al. 2005), and both processes have temperature optima (Howe and Marshall 2002). In the closely related nonphotosynthetic coral *Leptopsammia pruvoti* the skeletal density measured in the same localities of this study is not affected by temperature (Goffredo et al. 2007). Moreover, linear extension rate and calcification are not significantly different between two populations of *L. pruvoti* situated 850 km apart, despite the different thermal regimes (S. Goffredo et al. unpubl.). Preliminary studies of various populations of *B. europaea* have found zooxanthellae belonging exclusively to clade A (M. A. Coffroth pers. comm.), as previously reported for one population in Spain (Visram et al. 2006). Under experimental conditions, zooxanthellae belonging to this clade hosted by *Cladocora caespitosa* have proved to be resistant to short-term temperature increases, even above those recorded in nature (Rodolfo-Metalpa et al. 2006*a*). However, exposure to the same temperature range for prolonged periods has been lethal for 100% of the colonies of *C. caespitosa* studied (Rodolfo-Metalpa et al. 2006*b*). In situ, several mass mortality events have been reported for *B. europaea* and *C. caespitosa*, linked to periods of elevated temperatures and zooxanthellae bleaching (Rodolfo-Metalpa et al. 2000). The optimal temperature for the photosynthesis of the *B. europaea* symbiotic system might be equal to or lower than the lowest ever recorded in nature in the populations sampled in this study (18.0°C). Testing the hypothesis that a rise in temperature causes a significant reduction in the photosynthetic efficiency of clade A zooxanthellae in *B. europaea* requires further investigations using experimental approaches (Karako-Lampert et al. 2005; Rodolfo-Metalpa et al. 2006*a*,*b*).

Energetic constraints related to suspension feeding may provide an alternative explanation for the negative effects of increasing temperature on calcification of *B. europaea*. In the Mediterranean, the warm summer–fall season is characterized by lower nutrient levels and zooplankton availability than the cool winter–spring season (Coma et al. 2000). Corals and several benthic suspension feeding taxa have proved to be stressed by low nutrients and limited zooplankton availability (Coma et al. 2000). In *Stylophora pistillata* colonies, starved corals show significantly lower levels of calcification and photosynthesis than fed corals (Houlbrèque et al. 2004). Low availability of resources at high temperatures may slow calcification in *B. europaea*. However, if this was the case, the inhibition would also be found in the azooxanthellate, nonphotosynthetic species *L. pruvoti*. Instead, *L. pruvoti* demography seems to be unaffected by temperature (Goffredo et al. 2007). Although the hypothesis of photosynthetic inhibition at high temperatures is intriguing, other environmental parameters may influence coral growth (pH, total alkalinity, wave exposition, flow rate, etc.) and contribute to producing the observed trends. Further investigations are needed to better constrain the environmental controls on the growth of this species.

Our results encourage speculation regarding the possible effect of global climate change on this species. Global increase in sea temperature is one of the greatest threats for reef corals (Hughes et al. 2003). The linear regression between calcification rate and SST predicted that calcification of *B. europaea* would cease at a mean annual SST of 20.5°C (zero values of skeletal density would occur at 21.2°C). When considering the power function model, calcification is expected to approach zero values at 21.0°C (21.3°C for the skeletal density), values very close to the ones obtained by the linear model. Extrapolating the regressions between calcification and SST has the limitation of assuming that the linear (or power function) relationship will be maintained. This may not necessarily be true, in fact, from 18.0°C (CL) to 19.1°C (PL) calcification drops by 64% (2.86–1.02 mg mm^{-2} yr^{-1}) and from 19.1°C (PL) to 19.9°C (PN) it drops only by 5% (1.02–0.97 mg mm^{-2} yr^{-1}), indicating the existence of a possible plateau (Table 2). Using a power function model partially addresses this problem, but the limits of extrapolating beyond the warmest temperature recorded remain.

The conclusions must be taken with caution, but the concern for the possible negative fate of this endemic species with continued global warming remains. While adaptive changes such as acclimation (modifying cell metabolism to perform better at the new temperatures) or adaptation (the selection of organisms that respond better to the new temperatures; Clarke 1983) cannot be excluded as SST rises, evidence that corals and their symbionts can adapt to rapid climate change is equivocal or nonexistent (Hoegh-Guldberg et al. 2007). Global SSTs are projected to increase by 1–3°C by 2100, with a higher increase in temperate areas of the northern hemisphere than in tropical areas (Solomon et al. 2007).

Assuming an intermediate and rather conservative increase (2°C), SST is expected to approach the zero calcification point for most of the populations considered in this study (projected temperature in 2100 in the population of Calafuria = 20.0°C; Elba = 20.7°C; Palinuro = 21.1°C; Scilla = 21.5°C; Genova = 21.6°C; and Pantelleria = 21.9°C). This scenario would indicate a possible reduction in the distribution area of this species, with irrecoverable losses in terms of genetic variability, considering the fragmented genetic structure that characterizes the species (Goffredo et al. 2004*b*). At the same time, the fragmented genetic structure indicates that changes from one latitude to another may involve genetic differences between locally adapted corals, and corals used in our study may have had an untold number of years to adapt to the average annual temperature at their site (Kleypas et al. 2005). This may have biased our approach of using a spatial relationship to infer how populations will respond to future temperatures. Studies have shown that corals can adapt if given thousands of years, but the Intergovernmental Panel on Climate Change (IPCC) scenarios we considered are on a timescale of one order of magnitude shorter, and this could give no chances for adaptation. To produce a more accurate projection of future calcification rates in response to increased temperature, physiological experimental studies of the calcification–temperature relationship in corals from the various populations under current-seasonal and future-expected temperatures are needed. Even then, we cannot be sure that corals could not adapt if given 50–100 yr, since little is known about rates of adaptation.

This study is the first field investigation of the relationship between environmental parameters and estimated growth parameters of a Mediterranean coral. Being endemic to the Mediterranean, *B. europaea* has very limited possibilities to respond to seawater warming by moving northward toward lower temperatures, since the latitudinal range considered covers almost the entire northern distribution of this species. Even with the limits of curve extrapolation, this study highlights the risk of losing Mediterranean marine biodiversity over the course of future decades, adding a voice to the choir of scientists who for years have been asking for worldwide political intervention to slow down global warming.

Acknowledgments

We thank L. Bortolazzi, A. Comini, M. Ghelia, G. Neto, and L. Tomesani for their underwater assistance in collecting the samples. The diving centres Centro Immersioni Pantelleria, Il Pesciolino, Polo Sub, and Sub Maldive supplied logistical assistance in the field. The Bologna Scuba Team and the Scientific Diving School collaborated in the underwater activities. The Marine Science Group (http://www.marinesciencegroup.org) supplied scientific, technical, and logistical support. Two anonymous reviewers gave valuable comments that improved the manuscript.

This research was financed by the Ministry of Education, University and Research, the Ministry of Tourism of the Arab Republic of Egypt, the Associazione dei Tour Operator Italiani, the Project AWARE Foundation, the Scuba Nitrox Safety International, the Scuba Schools International, the Underwater Life Project, the Marine & Freshwater Science Group Association, and the Canziani Foundation of the Department of Evolutionary and Experimental Biology of the Alma Mater Studiorum–University of Bologna. The experiments complied with current Italian law.

References

Al-Horani, F. A., T. Ferdelman, S. M. Al-Moghrabi, and D. de Beer. 2005. Spatial distribution of calcification and photosynthesis in the scleractinian coral *Galaxea fascicularis*. Coral Reefs **24:** 173–180.

Bucher, D. J., V. J. Harriott, and L. G. Roberts. 1998. Skeletal micro-density, porosity and bulk density of acroporid corals. J. Exp. Mar. Biol. Ecol. **228:** 117–136.

Carricart-Ganivet, J. P. 2004. Sea surface temperature and the growth of the West Atlantic reef-building coral *Montastraea annularis*. J. Exp. Mar. Biol. Ecol. **302:** 249–260.

———, and M. Merino. 2001. Growth responses of the reef-building coral *Montastraea annularis* along a gradient of continental influence in the southern Gulf of Mexico. Bull. Mar. Sci. **68:** 133–146.

Clarke, A. 1983. Life in cold water: The physiological ecology of polar marine ectotherms. Oceanogr. Mar. Biol. Annu. Rev. **21:** 341–453.

Cohen, A. L., and T. A. McConnaughey. 2003. Geochemical perspectives on coral mineralization. Rev. Miner. Geochem. **54:** 151–187.

Coma, R., M. Ribes, J. M. Gili, and M. Zabala. 2000. Seasonality in coastal ecosystems. Trends Ecol. Evol. **12:** 448–453.

Cooper, T. F., G. De'ath, K. E. Fabricius, and J. M. Lough. 2008. Declining coral calcification in massive *Porites* in two nearshore regions of the northern Great Barrier Reef. Glob. Change Biol. **14:** 529–538.

Dodge, R. E., and G. W. Brass. 1984. Skeletal extension, density and calcification of the reef coral, *Montastrea annularis*: St. Croix, U.S. Virgin Islands. Bull. Mar. Sci. **34:** 288–307.

Efron, B. 1981. Nonparametric estimates of standard error: The jackknife, the bootstrap and other methods. Biometrika **68:** 589–599.

Goffredo, S., S. Arnone, and F. Zaccanti. 2002. Sexual reproduction in the Mediterranean solitary coral *Balanophyllia europaea* (Scleractinia, Dendrophylliidae). Mar. Ecol. Prog. Ser. **229:** 83–94.

———, E. Caroselli, G. Mattioli, E. Pignotti, and F. Zaccanti. 2008. Relationships between growth, population structure and sea surface temperature in the temperate solitary coral *Balanophyllia europaea* (Scleractinia, Dendrophylliidae). Coral Reefs **27:** 623–632.

———, ———, E. Pignotti, G. Mattioli, and F. Zaccanti. 2007. Variation in biometry and demography of solitary corals with environmental factors in the Mediterranean Sea. Mar. Biol. **152:** 351–361.

———, G. Mattioli, and F. Zaccanti. 2004*a*. Growth and population dynamics model of the Mediterranean solitary coral *Balanophyllia europaea* (Scleractinia, Dendrophylliidae). Coral Reefs **23:** 433–443.

———, L. Mezzomonaco, and F. Zaccanti. 2004*b*. Genetic differentiation among populations of the Mediterranean hermaphroditic brooding coral *Balanophyllia europaea* (Scleractinia, Dendrophylliidae). Mar. Biol. **145:** 1075–1083.

Goreau, T. F. 1959. The physiology of skeleton formation in corals. I. A method for measuring the rate of calcium deposition by corals under different conditions. Biol. Bull. **116:** 59–75.

Hoegh-Guldberg, O., and others. 2007. Coral reefs under rapid climate change and ocean acidification. Science **318:** 1737–1742.

Houlbrèque, F., E. Tambutté, D. Allemand, and C. Ferrier-Pagès. 2004. Interactions between zooplankton feeding, photosynthesis and skeletal growth in the scleractinian coral *Stylophora pistillata*. J. Exp. Biol. **207:** 1461–1469.

Howe, S. A., and A. T. Marshall. 2002. Temperature effects on calcification rate and skeletal deposition in the temperate coral, *Plesiastrea versipora* (Lamarck). J. Exp. Mar. Biol. Ecol. **275:** 63–81.

Hughes, T. P., and others. 2003. Climate change, human impacts, and the resilience of coral reefs. Nature **301:** 929–933.

Kain, J. M. 1989. The seasons in the subtidal. Br. Phycol. J. **24:** 203–215.

Karako-Lampert, S., D. J. Katcoff, Y. Achituv, Z. Dubinsky, and N. Stambler. 2005. Responses of *Symbiodinium microadriaticum* clade B to different environmental conditions. J. Exp. Mar. Biol. Ecol. **318:** 11–20.

Kinsey, D. W., and P. J. Davies. 1979. Carbon turnover, calcification and growth in coral reefs, p. 131–162. *In* P. A. Trudinger and D. J. Swaine [eds.], Biogeochemical cycling of mineral forming elements. Elsevier.

Kleypas, J. A., J. W. McManus, and L. A. B. Menez. 1999. Environmental limits to coral reef development: Where do we draw the line? Am. Zool. **39:** 146–159.

———, and others. 2005. Comment on "Coral reef calcification and climate change: The effect of ocean warming." Geophys. Res. Lett. **32:** L08601, doi:10.1029/2004GL022329.

Lough, J. M., and D. J. Barnes. 2000. Environmental controls on growth of the massive coral *Porites*. J. Exp. Mar. Biol. Ecol. **245:** 225–243.

Mass, T., S. Einbinder, E. Brokovich, N. Shashar, R. Vago, J. Erez, and Z. Dubinsky. 2007. Photoacclimation of *Stylophora pistillata* to light extremes: Metabolism and calcification. Mar. Ecol. Prog. Ser. **334:** 93–102.

Reynaud, S., N. Leclercq, S. Romaine-Lioud, C. Ferrier-Pages, J. Jaubert, and J. P. Gattuso. 2003. Interactive effects of CO_2 partial pressure and temperature on photosynthesis and calcification in a scleractinian coral. Glob. Change Biol. **9:** 1660–1668.

Rinkevich, B. 1989. The contribution of photosynthetic products to coral reproduction. Mar. Biol. **101:** 259–263.

Rodolfo-Metalpa, R., C. N. Bianchi, A. Peirano, and C. Morri. 2000. Coral mortality in NW Mediterranean. Coral Reefs **19:** 24.

———, C. Richard, D. Allemand, C. N. Bianchi, C. Morri, and C. Ferrier-Pagès. 2006*a*. Response of zooxanthellae in symbiosis with the Mediterranean corals *Cladocora caespitosa* and *Oculina patagonica* to elevated temperatures. Mar. Biol. **150:** 45–55.

———, ———, ———, and C. Ferrier-Pagès. 2006*b*. Growth and photosynthesis of two Mediterranean corals, *Cladocora caespitosa* and *Oculina patagonica*, under normal and elevated temperatures. J. Exp. Biol. **209:** 4546–4556.

Solomon, S., and others. 2007. Climate change 2007: The physical science basis. Cambridge Univ. Press.

Visram, S., J. Wiedenmann, and A. E. Douglas. 2006. Molecular diversity of symbiotic algae of the genus *Symbiodinium* (Zooxanthellae) in cnidarians of the Mediterranean Sea. J. Mar. Biol. Assoc. UK **86:** 1281–1283.

von Bertalanffy, L. 1938. A quantitative theory of organic growth (inquiries on growth laws II). Hum. Biol. **10:** 181–213.

Zibrowius, H. 1980. The scleractinians of the Mediterranean and of the North-Eastern Atlantic. Mem. Inst. Oceanogr. (Monaco) **11:** 1–284. [In French.]

Associate editor: Anthony Larkum

Received: 04 September 2008
Accepted: 19 January 2009
Amended: 08 February 2009

OPEN ACCESS Freely available online

PLoS one

Growth and Demography of the Solitary Scleractinian Coral *Leptopsammia pruvoti* along a Sea Surface Temperature Gradient in the Mediterranean Sea

Erik Caroselli[1], Francesco Zaccanti[1], Guido Mattioli[2], Giuseppe Falini[3], Oren Levy[4], Zvy Dubinsky[4], Stefano Goffredo[1]*

1 Marine Science Group, Department of Evolutionary and Experimental Biology, Alma Mater Studiorum - University of Bologna, Bologna, Italy, European Union, **2** Operative Unit of Radiology and Diagnostics by Images, Hospital of Porretta Terme, Local Health Enterprise of Bologna, Porretta Terme, Italy, European Union, **3** Department of Chemistry, University of Bologna, Bologna, Italy, European Union, **4** The Mina and Everard Goodman Faculty of Life Sciences, Bar-Ilan University, Ramat-Gan, Israel

Abstract

The demographic traits of the solitary azooxanthellate scleractinian *Leptopsammia pruvoti* were determined in six populations on a sea surface temperature (SST) gradient along the western Italian coasts. This is the first investigation of the growth and demography characteristics of an azooxanthellate scleractinian along a natural SST gradient. Growth rate was homogeneous across all populations, which spanned 7 degrees of latitude. Population age structures differed between populations, but none of the considered demographic parameters correlated with SST, indicating possible effects of local environmental conditions. Compared to another Mediterranean solitary scleractinian, *Balanophyllia europaea*, zooxanthellate and whose growth, demography and calcification have been studied in the same sites, *L. pruvoti* seems more tolerant to temperature increase. The higher tolerance of *L. pruvoti*, relative to *B. europaea*, may rely on the absence of symbionts, and thus the lack of an inhibition of host physiological processes by the heat-stressed zooxanthellae. However, the comparison between the two species must be taken cautiously, due to the likely temperature differences between the two sampling depths. Increasing research effort on determining the effects of temperature on the poorly studied azooxanthellate scleractinians may shed light on the possible species assemblage shifts that are likely to occur during the current century as a consequence of global climatic change.

Citation: Caroselli E, Zaccanti F, Mattioli G, Falini G, Levy O, et al. (2012) Growth and Demography of the Solitary Scleractinian Coral *Leptopsammia pruvoti* along a Sea Surface Temperature Gradient in the Mediterranean Sea. PLoS ONE 7(6): e37848. doi:10.1371/journal.pone.0037848

Editor: Sebastian C. A. Ferse, Leibniz Center for Tropical Marine Ecology, Germany

Received January 3, 2012; **Accepted** April 29, 2012; **Published** June 1, 2012

Funding: The research leading to these results has received funding from the European Research Council under the European Union's Seventh Framework Programme (FP7/2007-2013)/ERC grant agreement n° [249930 – CoralWarm: Corals and global warming: the Mediterranean versus the Red Sea]. This research was financed by the Associazione dei Tour Operator Italiani (ASTOI), the Marine and Freshwater Science Group Association, and the Ministry of Education, University and Research (MIUR). The funders had no role in study design, data collection and analysis, decision to publish, or preparation of the manuscript.

Competing Interests: The authors have declared that no competing interests exist.

* E-mail: stefano.goffredo@marinesciencegroup.org

Introduction

Climate change is the defining environmental, economic, and social issue of our time, and it is now certain that the rapid increase in CO_2 concentration in the atmosphere since the 19th century industrial revolution is driving significant changes in the physical and chemical environment of Earth [1]. The rate of global climatic changes is accelerating, and the average surface temperature of the Earth is likely to increase by 1.1–6.4°C by the end of the 21st century [2]. Growing evidence suggests that climate change is having more substantial and rapid effects on marine communities than on terrestrial ones [3]. Synergy among increased seawater temperature, enhanced ultraviolet-B (UVB) radiation, surface ocean acidification, and human anthropogenic stress is affecting all levels of ecological hierarchies in a broad array of marine ecosystems [4]. The magnitude of temperature warming is expected to be greater in temperate areas than in tropical ones [2]. The Mediterranean basin is likely to be one of the regions most affected by the ongoing warming trend and by an increase in extreme events [5], thus representing a natural focus of interest for research. The Mediterranean is already one of the most impacted seas in the world, due to its central position as the cradle of civilization in antiquity, and as a contemporary hub of oil and commodities shipping [6]. The enhancement of interactions between climate change and many other disturbances such as eutrophication caused by fertilizer runoff and the damming of rivers [7] all increase the stresses to which Mediterranean biota are exposed.

Since the first investigations, the characteristics of scleractinian population structure and dynamics have been related to environmental conditions and their effects on these corals' symbiosis with unicellular algae [8–12]. It is now commonly accepted that the demographic traits of coral populations may reveal relationships between the organisms and their environment, and can be used to assess habitat stability and suitability [8,13–16]. Moreover, information such as population turnover can be used to design strategies for reef restoration and bioremediation of degraded or damaged coastal areas [17–20].

Notwithstanding their importance, few studies have quantified life-history parameters of scleractinian corals, partly because of the

processes of fragmentation, fusion and partial colony mortality, which cause corals of similar size to be of widely different ages, thus distorting the age-size relationships [12,21]. The scarce studies on population dynamics of scleractinian corals were reviewed in the '70 s, describing their growth and survivorship [17]. Since then, demography has been studied for some species in the Southwestern Atlantic [22], Pacific [23], Red Sea, Caribbean, Great Barrier Reef, and the Mediterranean [16]. Replication, growth and death of the modules can be used to model the growth of modular individuals [24], and studies of modular growth have often focused on plasticity of form and the complexity of both individual colony growth and population dynamics of these organisms [12,21,25].

Coral age can be reliably determined in species whose individuals rarely fragment or fuse, and where partial mortality can be recognized by anomalies in the regular growth pattern [19,21]. The growth and dynamics of modular organisms that fulfill these prerequisites can be analyzed using age-based models applied to colony morphology [8,26,27]. In some solitary corals, age estimates can be obtained from externally visible growth bands [19,20]. Growth band analysis has been used to determine the age of colonial scleractinian and gorgonian corals [27–29], and in solitary forms [15,16,19,20,30]. Hence, for some species growth and population dynamic models based on age can be applied to describe demographic characteristics [15,16,19,20,26,30,31]. Recently, an age-based Beverton-Holt model provided an adaptive management approach for regulating an octocoral fishery for bioactive compounds in the Bahamas, avoiding long-term characterization of population dynamics which is rarely feasible [32].

Leptopsammia pruvoti Lacaze-Duthiers, 1897 is an ahermatypic, non-zooxanthellate, and solitary scleractinian coral, widely distributed in the Mediterranean basin and along the European Atlantic coast from Portugal through Southern England and Ireland [33]. It is one of the most common organisms in semi-enclosed rocky habitats, under overhangs, in caverns, and small crevices at 0–70 m depth [33]. Sea surface temperature (SST) and solar radiation along an 850-km latitudinal gradient in Western Italian coasts have been reported not to significantly influence neither its population abundance, nor skeletal architecture features such as corallite length, width, height [34]. However, the density of the calcium carbonate crystals of its skeleton (micro-density) [35] is positively correlated with SST [36]. It is a gonochoric internal brooder [37], with a genetic structure characterized by heterozygote deficits at all scales, from patch to populations, without correlations between genetic differentiation and geographic distance and with most genetic differentiation occurring between patches of the same study site, rather than between sites [38]. Its bright yellow colour and abundance makes this species attractive to recreational divers, who represent an important income for coastal tourist resorts in the Mediterranean [39] (Fig. 1).

The aim of this study was to determine the growth and population dynamics traits of *L. pruvoti* in sites along a latitudinal gradient spanning 850 Km along the Italian west coast and a 2°C range of average SST. Considering the detrimental population conditions reported in sites with higher SSTs for the Mediterranean solitary dendrophylliid coral *Balanophyllia europaea* studied in the same sites, during the same time interval, and using the same methods as the present study [16,34,36,40], we tested the hypothesis of a negative correlation with SST for the growth and population dynamics traits of *L. pruvoti*. Ours is the first investigation of the growth and demography characteristics of an azooxanthellate scleractinian along a natural SST gradient. The counterintuitive results we obtained are considered in relation to the possible different sensitivity to global warming between corals hosting algal symbionts and those devoid of such mutualistic symbioses.

Figure 1. Living specimens of *Leptopsammia pruvoti* in an overhang on the Italian coasts.
doi:10.1371/journal.pone.0037848.g001

Methods

Sample collection

From 9th November 2003 to 30th September 2005, specimens of *L. pruvoti* were collected from six sites along a latitudinal gradient, from 44°20′N to 36°45′N (Fig. 2). Latitude is the main factor influencing the variation in SST [41], which is the environmental parameter considered in this study and that has already shown correlations with biologic parameters of *L. pruvoti* in previous studies [34,36]. Samples were collected for each site using transects that consisted of at least 3 triangular patches of basis*height equal to 12 cm * 7.1 cm (single patch area = 42.6 cm^2; transect area per each site = at least 42.6*3 = at least 128 cm^2; Table 1). A triangular shape of the patch was chosen because it was more easily placed in the narrow crevices colonized by the species, with respect to traditional square patches. Such a small patch area was chosen because of the high population density of the species (about 10000 individuals m^{-1}) which makes the sampling of all individuals present in larger areas (such as 1 m^2) unfeasible [34]. Moreover, such sampling area is considered representative of the studied site in previous studies of the biometry and growth of this species, where significant differences among sites and correlations with SST have been found [30,34]. Patches were collected on the

vault of crevices 3 m apart, at a depth of 15–17 m, during a single dive per site. Patches were located in crevices clearly separated one from each other, without a continuous presence of polyps from one patch to each other. The analysis of genetic differentiation between *L. pruvoti* populations living in different sites [38] shows that most genetic differentiation occurs between patches of the same study site, rather than between sites. Since the goal of the present manuscript was to check differences in growth and population dynamics and their relations with SST in coral populations subject to different SST regimes, to have a meaningful picture of the growth and population dynamics conditions at each site it was necessary to sample different patches at each site and treat them as replicates. Using replicates from different patches to characterize the conditions at each site, considers a wider proportion of the genotypes living in that site than by treating each patch as a separate population. Because of the random distribution pattern of the species, the problems associated with regularly spaced quadrats and transects do not apply to this study [34]. All of the polyps present in each patch were collected (See Table 1 for the number of samples collected in each site). The sampling took place at depths known to have high population densities and where the reproductive biology, biometry, population genetics and dynamics of this species had been studied previously [30,34,37,38,42].

Sample analysis

All collected corals were dried at 50°C for four days and observed under a stereoscope to remove fragments of substratum and calcareous deposits produced by other organisms. Corallite length was selected as the main biometric parameter, since it is a good indicator of skeletal mass and has been used as the primary measure of size in other biometric, reproductive biology and population dynamics studies of this species and other solitary corals [15,16,20,30,34,37,43–45]. Corallite length (*L*: maximum axis of the oral disc) of all corals (see table 1 for number of corals in each site) was measured using a caliper, and corallite mass was weighed with an analytical balance [20,44,46].

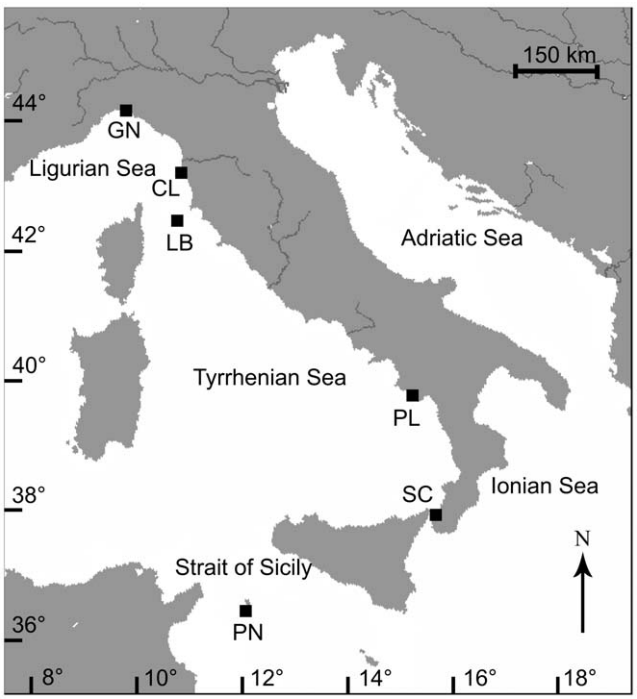

Figure 2. Map of the Italian coastline indicating sites where corals were collected. Abbreviations and coordinates of the sites in decreasing order of latitude: GN Genova, 44°20′N, 9°08′E; CL Calafuria, 43°27′N, 10°21′E; LB Elba Isle, 42°45′N, 10°24′E; PL Palinuro, 40°02′N, 15°16′E; SC Scilla, 38°01′N, 15°38′E; PN Pantelleria Isle, 36°45′N, 11°57′E.
doi:10.1371/journal.pone.0037848.g002

Growth and population demography modeling

By means of computerized tomography (CT), the number of annual growth bands was counted on about 30 skeletons randomly selected from the collected samples aimed at obtaining an objective relationship between corallite size and age. This technique is commonly applied to scleractinian corals [47,48] and has been successfully used for *L. pruvoti* [30]. The age of each skeleton was determined from the growth-band counts, based on one high-density band in winter and a low density band in summer [30,49].

The von Bertalanffy growth model [50] predicts decreasing growth rate with age, approaching zero asymptotically, and has been validated for the Calafuria (CL) population of *L. pruvoti* using CT density bands and field measurements [30]. To test if the von Bertalanffy function could be used for all populations sampled in this study, the decreasing growth rate of *L. pruvoti* with age was checked at each location [51]. For each sample dated by CT scans, a mean growth rate was obtained by dividing length by age, and the mean growth rate was plotted against individual age (Fig. 3). All the populations showed a marked decrease of mean growth rate with age, and fitted a negative exponential curve (Fig. 3), from which growth was modeled with the von Bertalanffy function [50]:

$$L_t = L_\infty(1-e^{-Kt}) \quad (1)$$

where L_t is individual length at age t, L_∞ is asymptotic length (maximum expected length in the population), K is a growth constant (higher for a fast growth up to the asymptotic length, smaller for a slow one), and t is the age of the individual. The parameters L_∞ and K were determined by applying the "Ford-Walford plot" method [15,30,52–55].

The population size structures were obtained from the survey transects, and age structure was determined using Equation 1. In a theoretical steady state population, 100% of the variance of the frequency of age classes is explained by age. To estimate population structure stability, the age frequency distribution was analyzed using a regression analysis of the natural logarithm of the numbers of individuals (frequency) in each age class (N_t) against their corresponding age (t), or

$$\ln N_t = at + b \quad (2)$$

The slope a with sign changed is usually indicated as Z (instantaneous rate of mortality), and can be used to estimate the theoretical numeric reduction of individuals over time, the intercept b is equal to the natural logarithm of the number of individuals at age zero (N_0) [15,16,19–21,30,54,55]. In a theoretical population in a steady state (rate of recruitment equal to rate of mortality) [26] the coefficient of determination (r^2) is equal to unity [54,56]. As natural populations deviate from the steady state, r^2 decreases to zero. This method for estimating population stability has previously been used for colonial and solitary corals [15,16,19–21,26,31,57], including *L. pruvoti* [30].

The instantaneous rate of mortality Z was used to express the theoretical reduction of the corals over time (survivorship curve):

Table 1. Sea surface temperature, number of patches and collected samples, L_∞, K, r^2 (coefficient of determination of the semi-log regression of Eq. 2, which is an estimator of population structure stability) and demographic parameter values of each sampled populations.

Population	Genova	Calafuria	Elba	Palinuro	Scilla	Pantelleria	General
Code	GN	CL	LB	PL	SC	PN	
SST (°C), Annual Mean (SE)	19.556 (0.038)	18.023 (0.036)	18.737 (0.038)	19.138 (0.032)	19.537 (0.021)	19.875 (0.036)	
Number of patches	3	3	4	3	3	3	
Number of samples collected	123	210	76	152	115	144	
L_∞ (mm)	9.2	8.6	10.2	9.3	15.9	10.0	15.4
K	0.218	0.185	0.114	0.136	0.107	0.120	0.062
R^2	0.410	0.839	0.421	0.675	0.719	0.796	-
Instantaneous rate of mortality (Z)	0.073	0.427	0.123	0.211	0.115	0.249	-
Observed % of immature individuals	30.9	28.6	13.2	36.8	35.7	22.9	-
Theoretical % of immature individuals	21.9	57.5	31.5	46.9	52.6	29.9	-
Observed mean age (years)	5.9	3.0	7.7	4.3	6.1	5.7	-
Theoretical mean age (years)	9.6	1.9	7.0	4.2	7.3	3.5	-
Observed age at max % biomass (years)	8	4	11	8	12	11	-
Theoretical age at max % biomass (years)	20	5	15	11	16	10	-
Observed mean age of biomass (years)	9.2	4.0	10.2	6.9	13.8	8.8	-
Theoretical mean age of biomass (years)	19.1	6.2	16.9	13.7	17.5	12.7	-

Growth data of the CL population were taken by [30]. The populations are arranged in decreasing order of latitude. SE = standard error.
doi:10.1371/journal.pone.0037848.t001

$$N_t = N_0 e^{-Zt} \quad (3)$$

N_t is the number of individuals in each age class, N_0 is the number of individuals at age 0, Z is the instantaneous rate of mortality (slope of Equation 2 with sign changed), t is the age.

The mean age of the individuals at each site was computed from that of samples dated with the growth curve (Equation 1). The observed percentage of individuals below sexual maturity was obtained by summing the frequencies of the age classes below sexual maturity, which is 2–3 years (3 mm length) [30,37]. The theoretical mean age was estimated as that of the theoretical number of individuals at each site. The theoretical percentage of individuals below sexual maturity was estimated by summing the frequencies of the theoretical number of individuals of the age classes below sexual maturity at each site.

The observed biomass distribution per age class was obtained by adding the mass of each corallite in each age class. A theoretical age-mass growth curve was obtained for each site using the age-length growth curve (Equation 1) and the length-mass relationship from [34]. The theoretical biomass distribution per age class was then obtained by multiplying the theoretical number of individuals in each age class (according to the survivorship curve, Equation 3) for the expected mass at that age. The theoretical age at maximum percentage biomass was estimated as the age class representing the highest percentage biomass. The observed age at maximum percentage biomass was determined in the same way, using the observed biomass distribution. The observed mean age of biomass in the population was calculated as the sum of the products of the observed biomass in each age class multiplied by its age, then divided by the total observed biomass. This parameter estimates how old the biomass is at each site; populations with most of the biomass accumulated in younger corals will have a lower mean age of biomass than populations in which most of the biomass is represented by older individuals [16]. The theoretical mean age of biomass in each site was calculated in the same way, but using the theoretical biomass in each age class and the total theoretical biomass.

SST data

SST data for the years 2003–2005 were obtained for each location from the National Mareographic Network of the Agency for the Protection of the Environment and Technical Services (APAT, now renamed to Superior Institute for Environmental Research and Protection, ISPRA, data available at http://www.isprambiente.gov.it). The data were from stations close to the sampling sites (<1 km) at a depth of 1 m below minimum low tide level. Mean annual SST values were computed from hourly measurements from January 2001 through January 2005 (Table 1). Three digital thermometers (i-Button, DS1921G-F5#, Maxim Integrated Products, Dallas Semiconductors) were placed close to the experimental sites of Genova, Calafuria, Scilla and Pantelleria at 16 m, to record seawater temperature every 2–3 hours during a time interval depending on the site (Figure S1). Thermometers were replaced every 3 months to avoid problems of encrustation and overgrowth by marine organisms. Thermometer data were used to check if SST data are representative of the temperature at the depth of coral sampling.

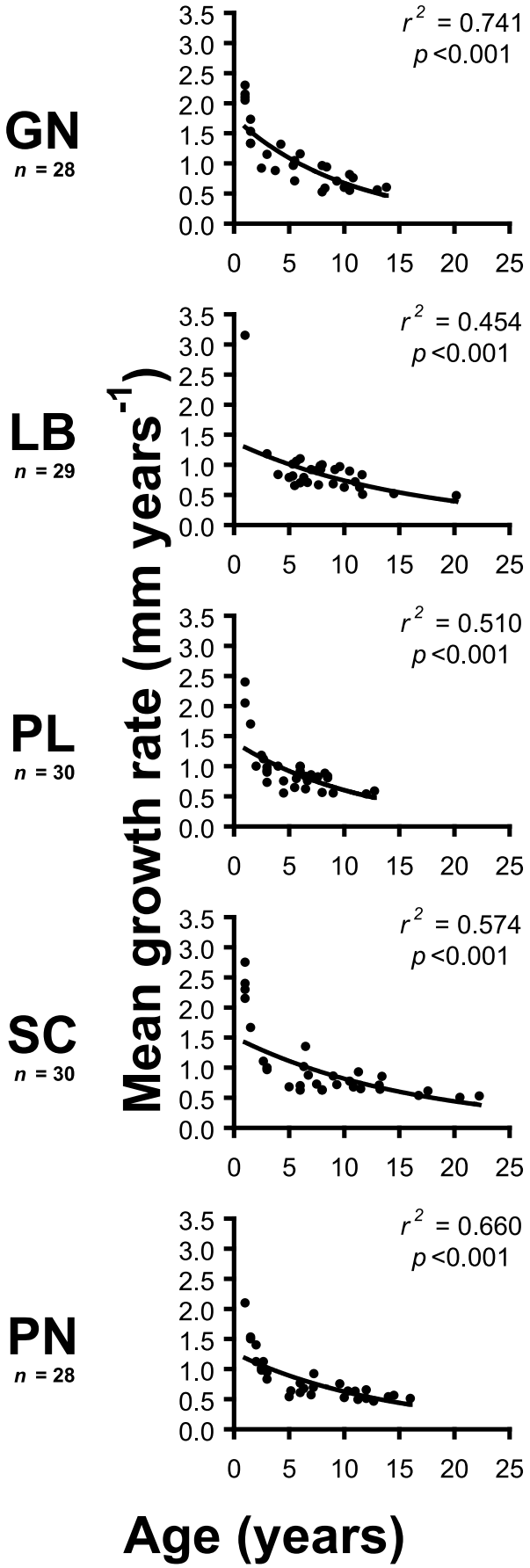

Figure 3. Relationships between mean growth rate and age of each population. Data were fitted with exponential curves to verify the exponential decrease of growth rate with age assumed by the von Bertalanffy growth model. n = number of individuals dated by computerized tomography scans (CT).
doi:10.1371/journal.pone.0037848.g003

Statistical analyses

Because of the heteroskedastic data sets, non-parametric Kruskal-Wallis was used to compare mean SST among the sites. Analysis of covariance (ANCOVA) was used to compare the slopes and intercepts of the equation of the Ford-Walford plots from which K and L_∞ values were obtained. Pearson correlation coefficients were calculated for estimating population structure stability at each site (coefficient of determination of Equation 2), and for the relationships between SST and L_∞, K, population structure stability, observed and theoretical % of individuals below sexual maturity, observed and theoretical mean age, observed and theoretical age at maximum % biomass, observed and theoretical mean age of biomass. Because of the low n value ($n = 6$) and the assumptions of the Pearson method, correlation coefficients were also estimated with bootstrapping [58], with 100,000 resamples. The non-parametric Kolmogorov-Smirnov test was used to compare the age frequency distributions among sites. All analyses were computed using PASW Statistics 18.0.

Results

The correlation between average daily SST data from data banks and average daily temperature data collected by the digital thermometers at 16 m produced r^2 values ranging from 0.784 to 0.935, indicating that 78–94% of the variance of seawater temperature at 16 m is explained by SST variations (Fig. S1). At Calafuria, the mean difference between SST and temperature at 16 m on an annual basis was 2.18°C (SD = 1.98°C; SE = 0.04°C). Sampling sites were characterized by significantly different mean annual SST values (Kruskal-Wallis, $p<0.001$; Table 1).

All sites were characterized by a negative exponential relationship between mean growth rate and age, with age explaining 45–74% of growth rate variance (Fig. 3). Growth rates decreased from 1–1.5 mm year^{-1} at age <5 years to 0.4–0.8 mm year^{-1} at age >10 years (Fig. 3).

L_∞ and K values (Table 1) were not significantly different among sites (ANCOVA for the slope and intercept of the "Ford-Walford" plot used to estimate L_∞ and K, $p>0.05$). Age-length data obtained by growth band counts in all the sites were thus merged together, obtaining a general "Ford-Walford" plot to estimate general L_∞ and K values (Table 1). These parameters produced a general age/length von Bertalanffy growth curve describing growth across all the sampling latitudinal range (Fig. 4).

All collected individuals in all sites were dated using the general age-length growth curve. The oldest individual came from the Scilla population (SC) with an estimated age of 28 years (12.8 mm length). The age-frequency distributions (Fig. 5) were significantly different among sites (Kolmogorov-Smirnov, $p<0.001$). For each site, a regression of the natural logarithm of the number of individuals (frequency) in each age class (N_t) was computed (Eq. 2). The r^2 values of these regressions varied between 0.410–0.838 and were not correlated with SST (Table 1). No observed or theoretical demographic parameter obtained by the analysis of the age-frequency structures was significantly correlated with SST (Table 1 and 2; Fig. 5).

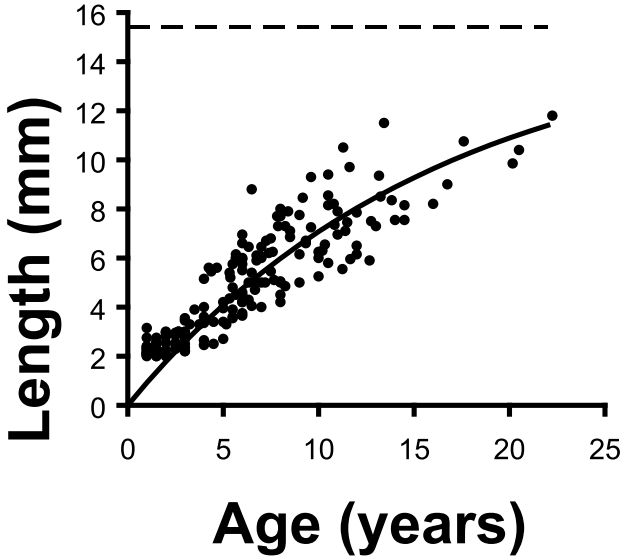

Figure 4. General age-length von Bertalanffy growth curve (see Eq. 1) describing the growth in all populations. Dotted line indicates the maximum expected length of corals in all populations ($L_\infty = 15.4$ mm). Points indicate the age/size of all samples in all populations dated by CT scans ($n = 175$) from which the general growth curve was obtained.
doi:10.1371/journal.pone.0037848.g004

Discussion

The 78–94% of the variance of seawater temperature at the depth of coral sampling (16 m) was explained by variations in SST, indicating that SST generally follows the actual temperature trend present at the sampling depth, as shown by the temperature trends at both depths (Fig. S1). At the Calafuria site, were a full year (November 2001–November 2002) of measurements were available, 84% of SST variance was explained by variations of temperature at 16 m (Fig. S1). This trend was maintained across the 4 analyzed populations, which include the northern (Genova), coldest (Calafuria) and southern-warmest (Pantelleria) sites were corals were collected, and is likely to be maintained also in Elba and Palinuro, which are in between the other sites. Thus, SST has been used as variable to discriminate thermal differences among sites to allow meaningful comparisons between this study and previous investigations on other Mediterranean scleractinian, all of which correlated biological parameters with SST [16,34,36,40].

Polyps of *L. pruvoti* in all of the studied populations were found to reduce their growth rate with increasing age (determinate growth). Within the mechanical constraints of organism design, the environment plays a key role in determining the maximum size an organism can attain [59]. Growth can also be limited by energetic costs, and when an individual decreases its growth rate and has an upper size limit, the excess energy no longer allocated to growth as the individual gets older can be allocated to other processes such as sediment removal, locomotion, maintenance, and reproduction [60–62]. Coral species known to have a determinate growth include colonial octocorals [27,32,63,64] and scleractinians such as the branching *Pocillopora spp.* [65], the massive *Goniastrea aspera* [66], and the free-living *Manicina areolata* [67]. Most species for which a determined growth has been observed are solitary forms, such as many free-living fungiids [19,20,68,69], the free-living deep coral *Flabellum alabastrum* [70], and attached polyps such as *B. elegans*, *Paracyathus stearnsii* [71], *B. europaea* [15,16], and *L. pruvoti* [30]. In these species, the determinate growth could be due to ageing or to a preferential energetic allocation towards processes other than growth, such as reproduction.

Most analyses of coral growth in natural populations are focused on zooxanthellate species, and growth variations are usually related to the varying environmental conditions, such as light intensity, temperature, nutrients and zooplankton [72]. In contrast, knowledge about the growth rates of azooxanthellate corals is very sparse [73]. Measurements of growth in natural populations of azooxanthellate scleractinians are available only for the deep coral *Lophelia pertusa* [74], and for the shallow water *L. pruvoti* at Calafuria [30]. In *L. pruvoti*, the age-length relationships were not significantly different among sites, based on which a general growth curve was obtained (Fig. 4) which describes the growth of individuals across the whole latitudinal range of the present study. Instead, in the Mediterranean endemic solitary zooxanthellate coral *B. europaea*, sampled in the same sites of the present study, during the same time interval, and analyzed using the same methods, the growth constant K of the age-length growth curve and the calcification rate are negatively related with SST [16,40]. The most likely hypothesis to explain the decreasing growth of *B. europaea* with increasing temperature states that the photosynthesis of its symbionts or its calcification machinery would be depressed at temperatures higher than the optimal one for this species, consequently causing an inhibition of calcification [16,40]. Alternatively, a role may be played by the much steeper response of respiration to subtle temperature increases (Q_{10}) than that of photosynthesis, resulting in significant decrease of the residual net photosynthesis and of the energy surplus needed for calcification, growth and reproduction [75]. Besides local factors, the apparent insensitivity of *L. pruvoti* growth to the range of SSTs experienced in the present study may be due either to 1) the lack of zooxanthellate, and thus a lack of inhibition of calcification by the depressed net photosynthesis, or 2) to a higher optimal temperature for the calcification of this species, or 3) a coupling between the above two factors, or 4) a sampling area not representative of the species conditions at the collection sites. However, *L. pruvoti* lives also outside the Mediterranean Sea, up to the southern coasts of Ireland and UK, where seawater temperature is considerably lower [33]. It is then unlikely that this species has a higher optimal temperature for calcification than the Mediterranean endemic *B. europaea*, since *L. pruvoti* lives in much colder seas and deeper waters (up to 70 m depth). The lack of inhibition of calcification by the photosynthetic process seems then the most likely hypothesis to justify the homogeneous growth across the 7 degrees of latitude of the sampling range of the present study. However, any comparison between *L. pruvoti* and *B. europaea* must be taken cautiously, since the two species were sampled at different depths (16 m and 6 m, respectively), which may be subject to different thermal regimes throughout the year.

In theoretical populations with constant mortality across age classes and with a number of recruits equal to the total number of deaths in all age classes (steady state) [76], the coefficient of determination (r^2) of the semi-log regression (Eq. 2) used to estimate the instantaneous rate of mortality (Z) is equal to unity [57,59]. In the sites considered in the present study, r^2 varied from 0.8 to 0.4, without a latitudinal trend. This is further emphasized in Table 2, where none of the demographic parameters derived from the age class distributions (which were significantly different among sites) correlated with SST. This indicates that while the growth characteristics are homogeneous across sites, their population dynamics differ, but not according to the SST gradient existing along the sampling latitudinal range. This is quite different to what is reported for the zooxanthellate dendrophylliid *B.*

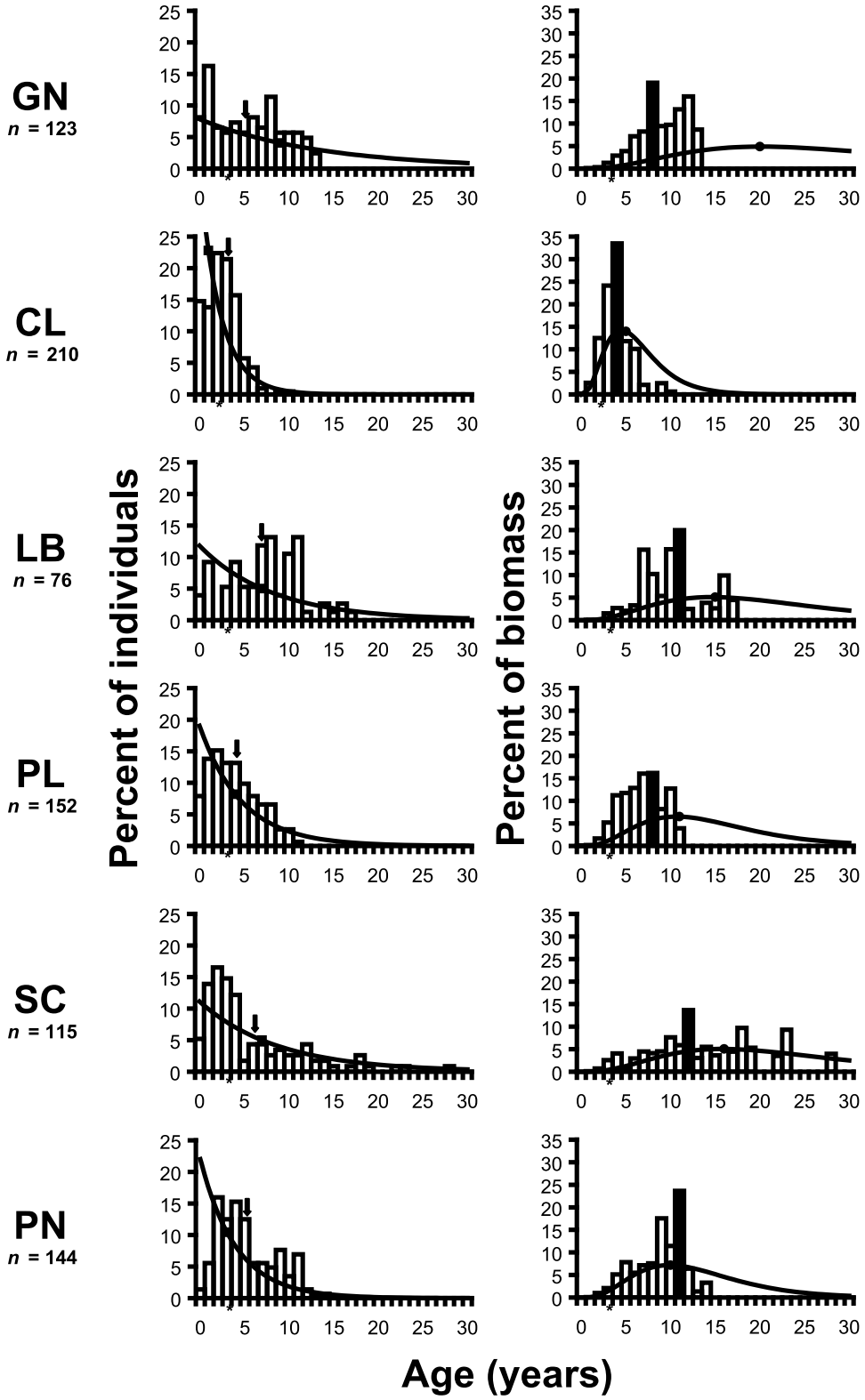

Figure 5. Age class structures of each population. The lines indicate the theoretical distributions. The observed (arrow) and theoretical (black square) age class containing the mean age of the individuals of sampled population are indicated. The observed (black column) and theoretical (black circle) age at maximum percentage biomass are indicated. Asterisks indicate the age at sexual maturity. Data for the Calafuria population (CL) are from [30]. *n* number of individuals dated by growth curves.
doi:10.1371/journal.pone.0037848.g005

Table 2. Correlation analyses between sea surface temperature (independent variable) and demographic parameters (dependent variables) in the sampled populations.

Dependent variable	*n*	r^2	*r*	r^2_{BS}	r_{BS}
Instantaneous rate of mortality (*Z*)	6	0.393	−0.627	0.193	−0.439
Population structure stability	6	0.018	−0.134	0.002	−0.046
Observed % of individuals below sexual maturity	6	0.038	0.195	0.027	0.163
Theoretical % of individuals below sexual maturity	6	0.295	−0.543	0.242	−0.492
Observed mean age	6	0.209	0.457	0.132	0.363
Theoretical mean age	6	0.211	0.459	0.149	0.386
Observed age at maximum % biomass	6	0.492	0.701	0.307	0.554
Theoretical mean age at maximum % biomass	6	0.318	0.564	0.199	0.446
Observed mean age of biomass	6	0.397	0.630	0.264	0.514
Theoretical mean age of biomass	6	0.411	0.641	0.214	0.463

No correlation resulted significant. *n* number of populations. r^2Pearson's coefficient of determination, *r* Pearson's correlation coefficient, r^2_{BS} and r_{BS} Pearson's coefficient calculated with bootstrapping.
doi:10.1371/journal.pone.0037848.t002

europaea sampled in the same sites of the present study, during the same time interval, and analyzed using the same methods, [16]. *B. europaea* in fact, lives in populations that deviate from the steady state and exhibit a progressive reduction of young individuals with increasing temperature [16]. Even if comparisons between the two species may be biased by the different sampling depths, the variation of population dynamics characteristics among sites, found for *L. pruvoti*, could thus be related to particular local conditions unrelated to temperature. Since the present study focused on the influence of SST, we selected sites with similar environmental traits other than SST, but we did not thoroughly analyzed all the site characteristics such as nutrients and zooplankton availability or competitive interactions with other organisms, which could all contribute to the observed differences in population dynamics traits. However, these local differences, while contributing to the variability of population dynamic characteristics, are not strong enough to determine significant variations in population abundance, which is homogeneous across all sites with about 10,000 individuals per square meter [34]. It may be argued that no correlation with SST has been found because the selected sampling area for this study was too small and unrepresentative of the population. However, the same sampling area adequately represents the sites in previous studies on the biometry and growth of the species, where trends in the biometric parameters (such as polyp length) with temperature have been found [30,34]. The number of coral specimens collected in the sampling area of the present study (76–210 polyps per site; table 1) is even higher than the one observed in other studies on growth and demography of Mediterranean solitary corals (38–95 polyps per site) where larger sampling areas (1 m^2) were used because of the lower population density of the species [30,34,40]. Moreover, significant differences in the demographic traits among sites have actually been found in the present study, but they do not correlate to temperature, and are likely due to local differences in parameters other than temperature. An alternative explanation of the difference in demographic parameters among sites may be related to suspension feeding. In the Mediterranean, the warm summer–fall season is characterized by lower nutrient levels and zooplankton availability than the cool winter–spring season [77]. Corals and several benthic suspension feeding taxa have proved to be stressed by low nutrients and limited zooplankton availability [77]. Different availability of resources among sites may produce the different demographic traits in *L. pruvoti*. However, if this was the case, negative effects on demographic traits would be expected in the warmest sites (where the warm season is longer and the zooplankton availability lower, on average). Instead, *L. pruvoti* demography seems to be unrelated to SST ([34] and this study). Other environmental parameters not considered in this study may influence coral population dynamics (pH, total alkalinity, wave exposition, flow rate, etc.) and contribute to producing the observed trends. Further investigations are needed to better constrain the environmental controls on the population dynamics of this species, possibly with a higher number of patches per site to better characterize the population dynamics traits at each location.

Global temperature increase is one of the greatest threats for coral and coral reefs survival [78]. The speeds of many negative changes to the oceans are near or are tracking the worst-case scenarios from the IPCC and other predictions [79]. Recently, the coralligenous community, one of the most diverse in the Mediterranean Sea (~1,666 species) [80] where suspension feeders are dominant, has been strongly affected by several mass mortality events related to high temperatures [81–85]. The zooxanthellate dendrophylliid *B. europaea* is a Mediterranean endemic species which is likely to be negatively affected by seawater warming, since increasing temperature lowers its population abundance, its skeletal density [34], by increasing its skeletal porosity [36], and lowers its calcification rate [40]. Moreover, warmer populations are less stable and show a progressive deficiency of young individuals, so that there is concern for the future of this species [16]. All these effects of temperature increase seem to be related to the symbiosis with zooxanthellae, whose photosynthesis could be depressed at high temperatures causing cascading negative effects on the growth and reproductive traits of this species, although this hypothesis is yet to be tested [16,34,36,40]. *L. pruvoti*, instead, seems to be quite tolerant to the same temperature range experienced by *B. europaea*, since none of its biological traits studied until now in the same sites, time interval and using the same methods, results negatively correlated with SST ([34,36] and present study). It even seems that *L. pruvoti* may benefit from increasing temperature, since corals living in sites with higher SSTs have a higher density of the crystals of calcium carbonate (micro-density) [35] composing their skeleton [36]. However, the limit of temperature increase that will still be tolerable by this species is unknown, and it must be kept in mind that the sampling depth of the two species is different, thus the in situ temperature may be different at the same SST value. These findings indicate that two species belonging to the same family and sharing a wide part of their distribution area may have very different temperature tolerance and consequent response to seawater warming. The higher tolerance of *L. pruvoti*, relative to *B. europaea*, may indeed rely on the absence of symbionts, and thus the lack of an inhibition of host physiological processes by the heat-stressed zooxanthellae. Increasing research effort on determining the effects of temperature on the poorly studied azooxanthellate scleractinians may thus shed light on the possible species assemblage shifts that are likely to occur during the current century as a consequence of global climatic change.

Supporting Information

Figure S1 Comparison between SST and temperature at 16 m depth during the indicated time interval. The left

column shows correlation analyses between average daily SST and temperature at 16 m (left column) in the sampling sites for the indicated time interval. The right column shows SST (red line) and temperature at 16 m depth (black line) trends. *n* number of samples (days)
(EPS)

Acknowledgments

We wish to thank L. Bortolazzi, A. Comini, M. Ghelia, L. Tomesani, Centro Immersioni Pantelleria, Il Pesciolino, Polo Sub, and Submaldive, Bologna Scuba Team, Scientific Diving School and Marine Science Group for help and assistance. G. Neto for the picture of *L. pruvoti* living specimens. The experiments complied with current Italian law.

Author Contributions

Conceived and designed the experiments: SG. Performed the experiments: EC GM. Analyzed the data: EC. Wrote the paper: EC FZ GM GF OL ZD SG.

References

1. Hoegh-Guldberg O (2011) The impact of climate change on coral reef ecosystems. In: Dubinsky Z, Stambler N, eds. Coral reefs: an ecosystem in transition. Dordrecht: Springer Science+Business Media BV. pp 391–403.
2. Solomon S, Qin D, Manning M, Chen Z, Marquis M, et al. (2007) Climate change 2007: the physical science basis. Cambridge: Cambridge University Press. 996 p.
3. Richardson AJ, Poloczanska ES (2008) Under-resourced, under threat. Science 320: 1294–1295.
4. Walther GR, Post E, Convey P, Menzel A, Parmesan C, et al. (2002) Ecological responses to recent climate change. Nature 416: 389–395.
5. Lejeusne C, Chevaldonné P, Pergent-Martini C, Boudouresque CF, Pérez T (2010) Climate change effects on a miniature ocean: the highly diverse, highly impacted Mediterranean Sea. Trends Ecol Evol 25: 250–260.
6. Queguiner J (1978) The Mediterranean as a maritime trade route. Ocean Manage 3: 179–189.
7. Tsimplis MN, Zervakis V, Josey S, Peeneva E, Struglia MV, et al. (2006) Changes in the oceanography of the Mediterranean Sea and their link to climate variability. In: Lionello P, Malanotte-Rizzoli P, Boscolo R, eds. Mediterranean climate variability. Amsterdam: Elsevier. pp 227–282.
8. Grigg RW (1975) Age structure of a longevous coral: a relative index of habitat suitability and stability. Am Nat 109: 647–657.
9. Loya Y (1976) The red sea coral *Stylophora pistillata* is an r strategist. Nature 259: 478–480.
10. Buddemeier RW, Kinzie RA (1976) Coral growth. Oceanogr Mar Biol Annu Rev 14: 183–225.
11. Bablet JP (1985) Report on the growth of a scleractinian. Proc 5th Int Coral Reef Symp 4: 361–365.
12. Hughes TP, Jackson JBC (1985) Population dynamics and life histories of foliaceous corals. Ecol Monogr 55: 141–166.
13. Bak RPM, Meesters EH (1998) Coral population structure: the hidden information of colony size-frequency distributions. Mar Ecol Prog Ser 162: 301–306.
14. Meesters WH, Hilterman M, Kardinaal E, Keetman M, de Vries M, et al. (2001) Colony size–frequency distributions of scleractinian coral populations: spatial and interspecific variation. Mar Ecol Prog Ser 209: 43–54.
15. Goffredo S, Mattioli G, Zaccanti F (2004) Growth and population dynamics model of the Mediterranean solitary coral *Balanophyllia europaea* (Scleractinia, Dendrophylliidae). Coral Reefs 23: 433–443.
16. Goffredo S, Caroselli E, Mattioli G, Pignotti E, Zaccanti F (2008) Relationships between growth, population structure and sea surface temperature in the temperate solitary coral *Balanophyllia europaea* (Scleractinia, Dendrophylliidae). Coral Reefs 27: 623–632.
17. Connell JH (1973) Population ecology of reef building corals. In: Jones OA, Endean R, eds. Biology and geology of coral reefs, vol. II: biology 1. New York: Academic. pp 271–324.
18. Rinkevich B (1995) Restoration strategies for coral reefs damaged by recreational activities—the use of sexual and asexual recruits. Restor Ecol 3: 241–251.
19. Chadwick-Furman NE, Goffredo S, Loya Y (2000) Growth and population dynamic model of the reef coral *Fungia granulosa* Kluzinger, 1879 at Eilat, northern Red Sea. J Exp Mar Biol Ecol 249: 199–218.
20. Goffredo S, Chadwick-Furman NE (2003) Comparative demography of mushroom corals (Scleractinia, Fungiidae) at Eilat, northern Red Sea. Mar Biol 142: 411–418.
21. Babcock RC (1991) Comparative demography of three species of scleractinian corals using age- and size-dependent classifications. Ecol Monogr 6: 225–244.
22. Lins de Barros MM, Pires DO (2006) Colony size-frequency distributions among different populations of the scleractinian coral *Siderastrea stellata* in Southwestern Atlantic: implications for life history patterns. Braz J Oceanogr 54: 213–223.
23. Nozawa Y, Tokeshi M, Nojima S (2008) Structure and dynamics of a high-latitude scleractinian coral community in Amakusa, southwestern Japan. Mar Ecol Prog Ser 358: 151–160.
24. Harper JL (1977) Population biology of plants. London: Academic Press. 892 p.
25. Hughes RN (1989) A functional biology of clonal animals. New York: Chapman and Hall. 331 p.
26. Grigg RW (1984) Resource management of precious corals: a review and application to shallow water reef building corals. P S Z N I Mar Ecol 5: 57–74.
27. Goffredo S, Lasker HR (2006) Modular growth of a gorgonian coral can generate predictable patterns of colony growth. J Exp Mar Biol Ecol 336: 221–229.
28. Knuston DW, Buddemeier RW, Smith SV (1972) Coral chronometers: seasonal growth bands in reef corals. Science 177: 270–272.
29. Logan A, Anderson IH (1991) Skeletal extension growth rate assessment in corals, using CT scan imagery. Bull Mar Sci 49: 847–850.
30. Goffredo S, Caroselli E, Mattioli G, Zaccanti F (2010) Growth and population dynamic model for the non-zooxanthellate temperate solitary coral *Leptopsammia pruvoti* (Scleractinia, Dendrophylliidae). Mar Biol 157: 2603–2612.
31. Ross MA (1984) A quantitative study of the stony coral fishery in Cebu, Philippines. P S Z N I Mar Ecol 5: 75–91.
32. Goffredo S, Lasker HR (2008) An adaptive management approach to an octocoral fishery based on the Beverton-Holt model. Coral Reefs 27: 751–761.
33. Zibrowius H (1980) Les scléractiniaires de la Méditeranée et de l'Atlantique nord-oriental. Mem Inst Oceanogr (Monaco) 11: 1–284.
34. Goffredo S, Caroselli E, Pignotti E, Mattioli G, Zaccanti F (2007) Variation in biometry and population density of solitary corals with solar radiation and sea surface temperature in the Mediterranean Sea. Mar Biol 152: 351–361.
35. Barnes DJ, Devereux MJ (1988) Variations in skeletal architecture associated with density banding in the hard corals *Porites*. J Exp Mar Biol Ecol 121: 37–54.
36. Caroselli E, Prada F, Pasquini L, Nonnis Marzano F, Zaccanti F, et al. (2011) Environmental implications of skeletal micro-density and porosity variation in two scleractinian corals. Zoology 114: 255–264.
37. Goffredo S, Airi V, Radetić J, Zaccanti F (2006) Sexual reproduction of the solitary sunset cup coral *Leptopsammia pruvoti* (Scleractinia, Dendrophylliidae) in the Mediterranean. 2. Quantitative aspects of the annual reproductive cycle. Mar Biol 148: 923–932.
38. Goffredo S, Di Ceglie S, Zaccanti F (2009) Genetic differentiation of the temperate-subtropical stony coral *Leptopsammia pruvoti* in the Mediterranean Sea. Isr J Ecol Evol 55: 99–115.
39. Mundet L, Ribera L (2001) Characteristics of divers at a Spanish resort. Tour Manag 22: 201–510.
40. Goffredo S, Caroselli E, Mattioli G, Pignotti E, Dubinsky Z, et al. (2009) Inferred level of calcification decreases along an increasing temperature gradient in a Mediterranean endemic coral. Limnol Oceanogr 54: 930–937.
41. Kain JM (1989) The seasons in the subtidal. Br Phycol J 24: 203–215.
42. Goffredo S, Radetić J, Airi V, Zaccanti F (2005) Sexual reproduction of the solitary sunset cup coral *Leptopsammia pruvoti* (Scleractinia, Dendrophylliidae) in the Mediterranean. 1. Morphological aspects of gametogenesis and ontogenesis. Mar Biol 147: 485–495.
43. Foster AB, Johnson KG, Schultz LL (1988) Allometric shape change and heterocrony in the freeliving coral *Trachyphyllia bilobata* (Duncan). Coral Reefs 7: 37–44.
44. Goffredo S, Arnone S, Zaccanti F (2002) Sexual reproduction in the Mediterranean solitary coral *Balanophyllia europaea* (Scleractinia, Dendrophylliidae). Mar Ecol Prog Ser 229: 83–94.
45. Vermeij MJA (2006) Early life-history dynamics of Caribbean coral species on artificial substratum: the importance of competition, growth and variation in life-history strategy. Coral Reefs 25: 59–71.
46. Lasker HR (1981) Phenotypic variation in the coral *Montastrea cavernosa* and its effects on colony energetics. Biol Bull 160: 292–302.
47. Bosscher H (1993) Computerized tomography and skeletal density of coral skeletons. Coral Reefs 12: 97–103.
48. Helmle KP, Dodge RE, Ketcham RA (2000) Skeletal architecture and density banding in *Diploria strigosa* by X-ray computed tomography. Proc 9th Int Coral Reef Symp 1: 365–371.
49. Peirano A, Morri C, Bianchi CN (1999) Skeleton growth and density pattern of the temperate, zooxanthellate scleractinian *Cladocora caespitosa* from the Ligurian Sea (NW Mediterranean). Mar Ecol Prog Ser 185: 195–201.
50. von Bertalanffy L (1938) A quantitative theory of organic growth (inquiries on growth laws II). Hum Biol 10: 181–213.
51. Fabens AJ (1965) Properties and fitting of the Von Bertalanffy growth curve. Growth 29: 265–289.
52. Ford E (1933) An account of the herring investigations conducted at Plymouth during the years from 1924–1933. J Mar Biol Assoc U K 19: 305–384.

53. Walford LA (1946) A new graphic method of describing the growth of animals. Biol Bull 90: 141–147.
54. Pauly D (1984) Fish population dynamics in tropical waters: a manual for use with programmable calculators. Manila: International Center for Living Aquatic Resources Management. 325 p.
55. Sparre P, Ursin E, Venema SC (1989) Introduction to tropical fish stock assessment. Rome: FAO Fisheries Technical Paper. 422 p.
56. Beverton RJH, Holt SV (1956) A review of methods for estimating mortality rates in fish populations, with special reference to sources of bias in catch sampling. Rapports et Proces-Verbaux des Reunions - Conseil International pour l'Exploration de la Mer 140: 67–83.
57. Tsounis G, Rossi S, Gili JM, Arntz WE (2007) Red coral fishery at the Costa Brava (NW Mediterranean): case study of an overharvested precious coral. Ecosystems 10: 975–986.
58. Efron B (1981) Nonparametric estimates of standard error: the jackknife, the bootstrap and other methods. Biometrika 68: 589–599.
59. Sebens KP (1987) The ecology of indeterminate growth in animals. Ann Rev Ecol Syst 18: 371–407.
60. Hall VR, Hughes TP (1996) Reproductive strategies of modular organisms: comparative studies of reef- building corals. Ecology 77: 950–963.
61. Elahi R, Edmunds P (2007) Determinate growth and the scaling of photosynthetic energy intake in the solitary coral *Fungia concinna* (Verril). J Exp Mar Biol Ecol 349: 183–193.
62. Goffredo S, Caroselli E, Gasparini G, Marconi G, Putignano MT, et al. (2011) Colony and polyp biometry and size structure in the orange coral *Astroides calycularis* (Scleractinia: Dendrophylliidae). Mar Biol Res 7: 272–280.
63. Cordes EE, Nybakken JW, VanDykhuizen G (2001) Reproduction and growth of *Anthomastus ritteri* (Octocorallia: Alcyonacea) from Monterey Bay, California, USA. Mar Biol 138: 491–501.
64. Bastidas C, Fabricius KE, Willis BL (2004) Demographic aspects of the soft coral *Sinularia flexibilis* leading to local dominance on coral reefs. Hydrobiologia 530/ 531: 433–441.
65. Grigg RW, Maragos JE (1974) Recolonization of hermatypic corals on submerged lava flows in Hawaii. Ecology 55: 387–395.
66. Sakai K (1998) Effect of colony size, polyp size, and budding mode on egg production in a colonial coral. Biol Bull 195: 319–325.
67. Johnson KG (1992) Population dynamics of a free-living coral: recruitment, growth and survivorship of *Manicina areolata* (Linnaeus) on the Caribbean coast of Panama. J Exp Mar Biol Ecol 164: 171–191.
68. Yamashiro H, Nishihira M (1998) Experimental study of growth and asexual reproduction in *Diaseris distorta* (Michelin, 1843), a free-living fungiid coral. J Exp Mar Biol Ecol 225: 253–267.
69. Knittweis L, Jompa J, Richter C, Wolff M (2009) Population dynamics of the mushroom coral *Heliofungia actiniformis* in the Spermonde Archipelago, South Sulawesi, Indonesia. Coral Reefs 28: 793–804.
70. Hamel JF, Sun Z, Mercier A (2010) Influence of size and seasonal factors on the growth of the deep-sea coral *Flabellum alabastrum* in mesocosm. Coral Reefs 29: 521–525.
71. Gerrodette T (1979) Ecological studies of two temperate solitary corals. PhD thesis. San Diego: University of California. 112 p.
72. Tambutte S, Holcomb M, Ferrier-Pages C, Reynaud S, Tambutte E, et al. (2011) Coral biomineralization: from the gene to the environment. J Exp Mar Biol Ecol DOI:10.1016/j.jembe.2011.07.026.
73. Brahmi C, Meibom A, Smith DC, Stolarski J, Auzoux-Bordenave S, et al. (2010) Skeletal growth, ultrastructure and composition of the azooxanthellate scleractinian coral *Balanophyllia regia*. Coral Reefs 29: 175–189.
74. Gass SE, Roberts JM (2006) The occurrence of the cold-water coral *Lophelia pertusa* (Scleractinia) on oil and gas platforms in the North Sea: Colony growth, recruitment and environmental controls on distribution. Mar Poll Bull 52: 549–559.
75. Al-Horani FA (2005) Effects of changing seawater temperature on photosynthesis and calcification in the scleractinian coral *Galaxea fascicularis*, measured with O_2, Ca^{2+} and pH microsensors. Sci Mar 69: 347–354.
76. Wetherall JA, Polovina JJ, Ralston S (1987) Estimating growth and mortality in steady-state fish stocks from length-frequency data. In: Pauly D, Morgan GR, eds. Length-based methods in fisheries research. ICLARM conference proceedings. Manila and Safat: International Center for Living Aquatic Resources Management and Kuwait Institute for Scientific Research. pp 53–74.
77. Coma RM, Ribes M, Gili JM, Zabala M (2000) Seasonality in coastal ecosystems. Trends Ecol Evol 12: 448–453.
78. Hughes TP, Baird AH, Bellwood DR, Card M, Connolly SR, et al. (2003) Climate change, human impacts, and the resilience of coral reefs. Nature 301: 929–933.
79. Rogers AD, Laffoley Dd'A (2011) International Earth system expert workshop on ocean stresses and impacts. Summary report. Oxford: IPSO. 21 p.
80. Ballesteros E (2006) Mediterranean coralligenous assemblages: A synthesis of the present knowledge. Oceanogr Mar Biol Annu Rev 44: 123–195.
81. Cerrano C, Bavestrello G, Bianchi CN, Cattaneo-Vietti R, Bava S, et al. (2000) A catastrophic mass-mortality episode of gorgonians and other organisms in the Ligurian Sea (NW Mediterranean), summer 1999. Ecol Lett 3: 284–293.
82. Perez T, Garrabou J, Sartoretto S, Harmelin JG, Francour P, et al. (2000) Mass mortality of marine invertebrates: an unprecedented event in the Northwestern Mediterranean. C R Acad Sci Paris, Ser III 323: 853–865.
83. Rodolfo-Metalpa R, Bianchi CN, Peirano A, Morri C (2000) Coral mortality in NW Mediterranean. Coral Reefs 19: 24.
84. Coma R, Ribes M, Serrano E, Jimenez E, Salat J, et al. (2009) Global warming-enhanced stratification and mass mortality events in the Mediterranean. Proc Natl Acad Sci U S A 106: 6176–6181.
85. Garrabou J, Coma R, Bensoussan N, Bally M, Chevaldonne P, et al. (2009) Mass mortality in the NW Mediterranean rocky benthic communities: Effects of the 2003 heat wave. Glob Change Biol 15: 1090–1103.

FRONTIERS IN ZOOLOGY

RESEARCH Open Access

Inferred calcification rate of a Mediterranean azooxanthellate coral is uncoupled with sea surface temperature along an 8° latitudinal gradient

Erik Caroselli[1], Guido Mattioli[2], Oren Levy[3], Giuseppe Falini[4], Zvy Dubinsky[3] and Stefano Goffredo[1*]

Abstract

Introduction: Correlations between sea surface temperature (SST) and growth parameters of the solitary azooxanthellate Dendrophylliid *Leptopsammia pruvoti* were assessed along an 8° latitudinal gradient on western Italian coasts (Mediterranean Sea), to check for possible negative effects of increasing temperature as the ones reported for a closely related, sympatric but zooxanthellate species.

Results: Calcification rate was correlated with skeletal density but not with linear extension rate, indicating that calcium carbonate deposition was preferentially allocated to keep a constant skeletal density. Unlike most studies on both temperate and tropical zooxanthellate corals, where calcification rate is strongly related to environmental parameters such as SST, in the present study calcification rate was not correlated with SST.

Conclusions: The lower sensitivity of *L. pruvoti* to SST with respect to other sympatric zooxanthellate corals, such as *Balanophyllia europaea*, may rely on the absence of a temperature induced inhibition of photosynthesis, and thus the absence of an inhibition of the calcification process. This study is the first field investigation of the relationship between SST and the three growth parameters of an azooxanthellate coral. Increasing research effort on determining the effects of temperature on biological traits of the poorly studied azooxanthellate scleractinians may help to predict the possible species assemblage shifts that are likely to occur in the immediate future as a consequence of global climatic change.

Keywords: Asymbiotic coral, Coral growth, Dendrophylliidae, Global warming, Scleractinia, Temperate coral

Introduction

Latitude is the main factor influencing the variation of light and temperature [1], two environmental parameters strongly linked to coral growth, physiology, demography and distribution pattern [2,3]. As a general trend, coral growth decreases with increasing latitude until a limit is reached where coral reef development no longer occurs, beyond 30°N and 30°S [4]. Coral growth can be defined by three related parameters (calcification = linear extension x skeletal density; [3,5]) whose measurement is essential when assessing the environmental effects on coral growth, because none of the three can perfectly predict the other two [6]. Analyzing these variables also allows predicting the possible effect of climatic changes on coral ecosystems [7,8]. These three variables have been studied in the field in the tropical genera *Montastraea* [5], *Diploastrea* [9], and *Porites* [3,7,8,10], and their variation has been linked to changes in sea surface temperature (SST) and light associated with time and latitude. In colonies of *M. annularis* of the Gulf of Mexico and the Caribbean Sea, SST is positively correlated with calcification rate and skeletal density, while it is negatively correlated with linear extension rate [5]. In colonies of *Porites* of the Hawaiian archipelago, Thailand, and the Great Barrier Reef (Australia) SST is positively correlated with calcification and linear extension rates, and negatively correlated with skeletal density [5]. In

* Correspondence: s.goffredo@unibo.it
[1]Marine Science Group, Department of Biological, Geological and Environmental Sciences, Alma Mater Studiorum, University of Bologna, Via F. Selmi 3, Bologna, EU 40126, Italy
Full list of author information is available at the end of the article

contrast, monitoring efforts of 16 years of calcification in *Porites* colonies from the Great Barrier Reef [7] and 21 years of calcification in *Porites* colonies from Thailand [8] show that calcification declined over time, and suggests that the response may be due to the interactive effects of elevated seawater temperatures and pCO_2 increase, as previously reported for colonies of *Stylophora pistillata* grown in aquaria [11]. However, a recent analysis of calcification of *Porites* colonies along an 11° latitudinal gradient along Western Australia coasts has found no widespread patterns of decreasing calcification since 1900, and concludes that the main driver of change in coral calcification is the rate of change in the thermal environment of coral reefs [10].

In contrast with the large number of studies about the relationships between environmental parameters and coral growth in the tropics [3,5,7,8,10], such studies are scarce for temperate zones. In *Astrangia danae* and *Plesiastrea versipora*, calcification rate increases with temperature, similarly to some tropical corals, albeit over a lower temperature range [12]. Laboratory observations on calcification rates in *Cladocora caespitosa* and *Oculina patagonica* show that long periods of elevated temperatures, corresponding to or higher than the maximum summer temperature in the field, lead to a decrease of calcification [13].

This study investigated the relationships between SST and the three growth components (calcification, skeletal density, and linear extension) in the temperate/subtropical coral *Leptopsammia pruvoti* Lacaze-Duthiers, 1897. *Leptopsammia pruvoti* is an ahermatypic, non-zooxanthellate and solitary scleractinian coral, widely distributed in the Mediterranean basin and along the European Atlantic coast from Portugal through Southern England and Ireland [14]. It is one of the most common organisms in semi-enclosed rocky habitats, under overhangs, in caverns and small crevices at 0–70 m depth [14]. SST and solar radiation along an 850-km latitudinal gradient on Western Italian coasts do not significantly influence its population abundance or skeletal architecture features such as corallite length, width, height [15], or its population structure stability and demographic traits [16]. However, the density of calcium carbonate crystals composing its skeleton (micro-density; [17]) is positively correlated with SST [18]. It is a gonochoric internal brooder [19], with a genetic structure characterized by heterozygote deficits at all scales, from patch to populations, without correlations between genetic differentiation and geographic distance, and with most genetic differentiation occurring between patches of the same study site, rather than between sites [20]. Its bright yellow colour and abundance makes this species attractive to recreational divers, who represent an important income for coastal tourist resorts in the Mediterranean Sea [21].

This is the first study on the variation of the three growth components in an azooxanthellate coral, and it aims to assess the variations of calcification rate, linear extension rate, and skeletal density in populations arranged along a latitudinal SST gradient. The results are also considered in the light of the most recent climate change scenarios and compared to the findings on the zooxanthellate Mediterranean endemic Dendrophylliiid coral *Balanophyllia europaea*.

Results

Mean annual SST varied significantly among the sites (Kruskal-Wallis test, $p < 0.001$; Table 1). Mean skeletal density, linear extension and calcification rates were significantly different among the populations of *Leptopsammia pruvoti* (Kruskal-Wallis test, $p < 0.001$; Table 2). To facilitate comparisons with published studies, the dependent and independent variables for the linear regression analyses between growth parameters (Table 3) were chosen according to literature data [3,5,22]. Mean skeletal density and calcification rate of the corallites in the populations were not correlated with mean linear extension rate (Table 3). Mean calcification rate of the corallites in the populations was positively correlated with mean skeletal density (Table 3). Based on the bootstrapping coefficients, calcification rate explained 67% of the variance in skeletal density (Table 3).

Considering the whole dataset (all ages), both the linear and power function models showed that none of the mean growth parameters of the populations were correlated with SST (Tables 4, 5). The lack of trends from the whole dataset was confirmed by the age-stratified analyses on the subsets of immature, mature, and old samples (Tables 4, 5). Thus, the mean growth parameters significantly differed among study sites, but their variation was not related to SST.

Discussion

The 'stretching modulation of skeletal growth' is a mechanism allowing corals to preferentially invest calcification resources in thickening the skeleton, thus increasing skeletal density, or accelerating linear extension [5,23].

Table 1 Average annual solar radiation and SST values of the sample sites

Population	Code	SST (°C) annual mean (SE)
Calafuria	CL	18.02 (0.04)
Elba	LB	18.74 (0.04)
Palinuro	PL	19.14 (0.03)
Scilla	SC	19.54 (0.02)
Genova	GN	19.56 (0.04)
Pantelleria	PN	19.88 (0.04)

The sites are arranged in order of increasing SST.

Table 2 *Leptopsammia pruvoti*. Mean skeletal density, linear extension, and calcification rates values of the populations

Population	Code	*n*	Average skeletal density (mg mm^{-3})	SE	Average linear extension rate (mm yr^{-1})	SE	Average calcification rate (mg mm^{-2} yr^{-1})	SE
Calafuria	CL	210	1.56	0.07	0.79	0.01	1.26	0.06
Elba	LB	76	1.07	0.07	0.61	0.02	0.76	0.06
Palinuro	PL	152	1.38	0.08	0.74	0.01	1.14	0.06
Scilla	SC	115	1.50	0.07	0.69	0.02	1.00	0.05
Genova	GN	123	1.31	0.09	0.61	0.01	1.08	0.07
Pantelleria	PN	144	1.14	0.03	0.68	0.01	0.71	0.01

The sites are arranged in order of increasing SST. *n* number of individuals, SE standard error.

The tropical *Porites*, for example, invests increased calcification at higher temperatures into linear extension [3,8]. In contrast, the tropical *Montastraea annularis* invests increased calcification at higher temperatures to construct denser skeletons [5,23]. In the Mediterranean endemic *Balanophyllia europaea*, calcification is allocated evenly between increasing skeletal density and linear extension, indicating that the ability to colonize the substratum quickly and the mechanical strength of the skeleton are both important for this species [22]. The temperate *L. pruvoti* exhibited a response which was similar to the one of *M. annularis*, in that calcification was positively correlated with skeletal density but not with linear extension. For each 1 mg mm^{-2} yr^{-1} of calcification rate variation, skeletal density varied by ~ 1 mg mm^{-3}.

Geometrically calculated skeletal density values in the present work were reasonable with respect to other studies on tropical and temperate species [3,5,17,22]. The computed skeletal density used in this and in previous studies [15,22] is analogous to the bulk density [17], which is defined as the skeletal mass divided by the total volume (skeletal matrix volume plus pores volume; [17]). Skeletal matrix volume is further composed by the crystals of $CaCO_3$ and by the intracrystalline organic matrix regulating the crystallization process [24]. Analyses to quantify the porosity in the same samples of the present study show that the variation of bulk density depends on variations of porosity, while the variation in the density of the skeletal framework (micro-density, [17]) is not strong enough to significantly affect bulk density [18].

The lack of correlations with SST exhibited by the calcification rate and skeletal density in the present study on *Leptopsammia pruvoti* confirms previous studies on the population density, growth and population structure stability of this species, where the coral parameters were always shown to be unrelated to environmental variables such as solar radiation or SST [15,16]. For both the linear and power function models, trends of the analyses performed on the full dataset were confirmed by the analyses on the three age-based subsets, indicating that differences in the mean age of the samples in the populations [16] did not bias the results.

The lack of correlation between calcification rate of the azooxanthellate *L. pruvoti* and SST along the latitudinal gradient is a different response with respect to the similar studies on temperate and tropical zooxanthellate species. For example, calcification rate of the Mediterranean endemic *B. europaea* is negatively related to SST [22], while in the tropical *Porites* and *M. annularis* it is positively related to SST [3,5]. However, mid-term studies on *Porites* highlight a reduction of its calcification rate as SST increases [7,8], even if a recent long-term analysis of *Porites* calcification along Australian coasts show no evidence of widespread patterns of decline in calcification rate since 1900 [10]. In that analysis, calcification rates at high-latitude reefs were found to be more sensitive to temperature increase than more tropical reefs [10]. Another recent analysis of *Porites* spp. and *Montastraea* spp. in the Great Barrier Reef and Mexican Caribbean highlighted a negative response of calcification to increasing SST for both genera, but a higher sensitivity to temperature increase for the former genus, rather than the latter one [25]. This has fundamental consequences in light of future global warming scenarios, since differential reduction of calcification between

Table 3 *Leptopsammia pruvoti*

Dependent variable	Independent variable	Slope (SE)	Intercept (SE)	r^2	r	r^2_{BS}	r_{BS}
Skeletal density	Linear extension	-	-	0.518	0.720	0.457	0.676
Calcification	Linear extension	-	-	0.396	0.629	0.347	0.589
Calcification	Skeletal density	0.969	−0.294	0.753	0.868*	0.666	0.816*

Linear regression and correlation analysis between mean skeletal density, linear extension rate, and calcification rate in the six sites ($n = 6$). r^2 Pearson's coefficient of determination, r Pearson's correlation coefficient, r^2_{BS} and r_{BS} Pearson's coefficients calculated with bootstrapping, * $p < 0.05$. SE standard error.

Table 4 *Leptopsammia pruvoti*

Dependent variable	r^2	r	r^2_{BS}	r_{BS}
All samples				
Skeletal density	0.126	−0.355	0.073	−0.271
Linear extension	0.250	−0.500	0.143	−0.378
Calcification	0.261	−0.510	0.181	−0.426
Immature samples (0–4 years)				
Skeletal density	0.018	−0.133	0.0003	−0.018
Linear extension	0.013	−0.115	0.017	−0.129
Calcification	0.178	−0.422	0.129	−0.359
Mature samples (5–8 years)				
Skeletal density	0.049	−0.221	0.030	−0.174
Linear extension	0.077	−0.278	0.014	−0.118
Calcification	0.016	−0.126	0.008	−0.090
Old samples (>8 years)				
Skeletal density	0.301	0.548	0.274	0.523
Linear extension	0.148	−0.384	0.122	−0.349
Calcification	0.181	0.425	0.091	0.302

Linear model. Correlation analysis between SST and growth parameters in the six sites ($n = 6$). No correlation resulted significant. r^2 Pearson's coefficient of determination, r Pearson's correlation coefficient, r^2_{BS} and r_{BS} Pearson's coefficients calculated with bootstrapping.

coral genera could profoundly affect community structure [25]. Our results suggest a higher sensitivity of zooxanthellate species to the variations of temperature, while asymbiotic corals may be more tolerant to temperature variations. The higher sensitivity of symbiotic species may be due to the decrease of photosynthetic performance at higher temperatures, since in zooxanthellate corals calcification is enhanced by photosynthesis [26], and both processes have temperature optima [12]. Alternatively, a role may be played by the much steeper response of respiration to subtle temperature increases (Q_{10}) than that of photosynthesis, resulting in significant decrease of the residual net photosynthesis and of the energy surplus needed for calcification and other physiological processes [27]. Although the hypothesis of photosynthetic inhibition at high temperatures is intriguing, other environmental parameters may influence coral calcification (pH, total alkalinity, wave exposition, flow rate, etc.). Besides local factors, the apparent insensitivity of *L. pruvoti* growth to the SST range experienced in the present study may be due either to 1) the lack of zooxanthellate, and thus a lack of inhibition of calcification by the depressed net photosynthesis, or 2) a higher optimal temperature for the calcification of this species with respect to *B. europaea*, or 3) a coupling between the above two factors, or 4) a sampling area not representative of the species conditions at the collection sites. *L. pruvoti* distribution area includes also regions outside the Mediterranean Sea, up to the southern coasts of Ireland and UK, where seawater temperature is considerably lower [14]. It is then unlikely that this species has a higher optimal temperature for calcification than the Mediterranean endemic *B. europaea*, since *L. pruvoti* lives in much colder seas and deeper waters (up to 70 m depth). Even if any comparison between *L. pruvoti* and *B. europaea* must be taken cautiously, since the two species were sampled at different depths (16 m and 6 m, respectively), which may be subject to different thermal regimes throughout the year, the variation of calcification rate among sites, found in *L. pruvoti*, could be related to particular local conditions unrelated to temperature. Since the present study focused on the influence of SST, we selected sites with similar environmental traits other than SST, but we did not thoroughly analyze all the site characteristics such as nutrients and zooplankton availability or competitive interactions with other organisms, which could all contribute to the observed differences in calcification rate. However, these local differences, while contributing to the variability of calcification rate (this study) and of population dynamics traits [16], are not strong enough to determine significant variations in population abundance, which is homogeneous across all sites with about 10,000 individuals per square meter [15]. It may be argued that no correlation with SST has been found because the selected sampling area for this study was too small and unrepresentative of the population. However, the same sampling area adequately represents the sites in previous studies on the biometry, growth and population dynamics

Table 5 *Leptopsammia pruvoti*

Dependent variable	r^2	r	r^2_{BS}	r_{BS}
All samples				
Skeletal density	0.105	−0.324	0.067	−0.258
Linear extension	0.225	−0.474	0.133	−0.365
Calcification	0.223	−0.472	0.165	−0.406
Immature samples (0–4 years)				
Skeletal density	0.032	−0.178	0.0004	−0.022
Linear extension	0.013	−0.114	0.012	−0.111
Calcification	0.204	−0.451	0.123	−0.351
Mature samples (5–8 years)				
Skeletal density	0.051	−0.225	0.021	−0.146
Linear extension	0.077	−0.277	0.013	−0.112
Calcification	0.014	−0.119	0.004	−0.065
Old samples (>8 years)				
Skeletal density	0.299	0.546	0.299	0.546
Linear extension	0.143	−0.378	0.113	−0.336
Calcification	0.268	0.518	0.144	−0.380

Power function model (eqn 2). Linear regression and correlation analysis between SST and growth parameters in the six sites ($n = 6$) calculated on log-transformed data. No correlation resulted significant. r^2 Pearson's coefficient of determination, r Pearson's correlation coefficient, r^2_{BS} and r_{BS} Pearson's coefficients calculated with bootstrapping.

of the species [15,16,22], where trends in the biometric parameters (such as polyp length) with temperature have been found [15]. Moreover, significant differences in calcification rate among sites have actually been found in the present study, but they do not correlate to temperature, and are likely due to local differences in parameters other than temperature. An alternative explanation of the difference in demographic parameters among sites may be related to suspension feeding. In the Mediterranean, the warm summer–fall season is characterized by lower nutrient levels and zooplankton availability than the cool winter–spring season [28]. Corals and several benthic suspension feeding taxa have proved to be stressed by low nutrients and limited zooplankton availability [28]. Different availability of resources among sites may affect calcification rate in *L. pruvoti*. However, if this was the case, negative effects on calcification rate would be expected in the warmest sites (where the warm season is longer and the zooplankton availability lower, on average). Instead, *L. pruvoti* calcification seems to be unrelated to SST. The differences in calcification rates and population dynamics traits among sites may be related to other environmental parameters not considered in this study (pH, total alkalinity, wave exposition, flow rate, etc.). Further investigations are thus needed to better constrain the environmental controls on the population dynamics of this species. Moreover, further investigation on the poorly studied azooxanthellate species are needed to differentiate the environmental controls on the growth of symbiotic and asymbiotic corals.

One of the main threats for coral and coral reefs survival is global temperature increase [29]. The speeds of many negative changes to the oceans are near or are tracking the worst-case scenarios from the IPCC and other predictions [30]. Recently, one of the most diverse communities in the Mediterranean Sea, the coralligenous (~1,666 species; [31]), where suspension feeders are dominant, has been strongly affected by several mass mortality events related to high temperatures [32-36]. The zooxanthellate dendrophylliid *B. europaea* is a Mediterranean endemic species which will likely be negatively affected by seawater warming, since increasing temperature lowers its population abundance, its skeletal density [15], by increasing its skeletal porosity [18], and lowers its calcification rate [22]. Moreover, warmer populations are less stable and show a progressive deficiency of young individuals, so that there is concern for the future of this species [37]. These detrimental effects of increasing temperature seem to be related to the symbiosis with zooxanthellae, whose photosynthesis could be depressed at high temperatures causing cascading negative effects on the growth and reproductive traits of *B. europaea*, although this hypothesis is yet to be tested [15,18,22,37]. *L. pruvoti*, instead, seems to be tolerant to the same temperature range experienced by *B. europaea*. In fact, biological traits of the former species have been studied in the same sites and time interval, but none of them is negatively correlated with SST ([15,16,18] and present study). Increasing temperature may even favour *L. pruvoti*, since the corals living in populations characterized by higher SSTs have a higher micro-density, even if this increase in micro-density is not strong enough to cause significant variations of bulk density [18]. However, the limit of temperature increase that will still be tolerable by this species is unknown. Moreover, it should be noted that the results derived from analyses based on latitudinal variations of calcification are not necessarily the same as those derived from time-based analyses. In fact, while calcification may have a positive correlation with SST along a latitudinal gradient, such as in *Porites* [3], it may be negatively correlated with the increasing SST recorded in recent years [7,8], and may fluctuate during the yearly cycle of temperature variation [38]. Thus, any extrapolations of spatial derived data to time resolved predictions has to be taken cautiously.

Conclusions

Unlike the zooxanthellate *B. europaea*, the differences in growth and population dynamics traits of the azooxanthellate *L. pruvoti* seem unrelated to SST along a wide latitudinal gradient in the Mediterranean Sea. These findings confirm previous observations that two species belonging to the same family and sharing a wide part of their distribution area may have very different temperature tolerance and consequent response to seawater warming [16]. The higher tolerance of *L. pruvoti*, relative to *B. europaea*, may indeed rely on the absence of symbionts, and thus the lack of an inhibition of host physiological processes by the heat-stressed zooxanthellae.

This study is the first field investigation of the relationship between SST and the three growth parameters of an azooxanthellate coral. Increasing research effort on determining the effects of temperature on biological traits of the poorly studied azooxanthellate scleractinians may help to predict the possible species assemblage shifts that are likely to occur in the immediate future as a consequence of global climatic change.

Materials and methods

Specimens of *Leptopsammia pruvoti* were collected from six sites along a latitudinal gradient, from 44°20'N to 36° 45'N, between 9 November 2003 and 30 September 2005 (Figure 1). Sampling sites were selected along the gradient to be characterized by different SST, which is the environmental parameter considered in this study and that has already shown correlations with biologic parameters of *L. pruvoti* in previous studies [15,18]. Samples were collected in each site using transects of three triangular patches of base × height equal to

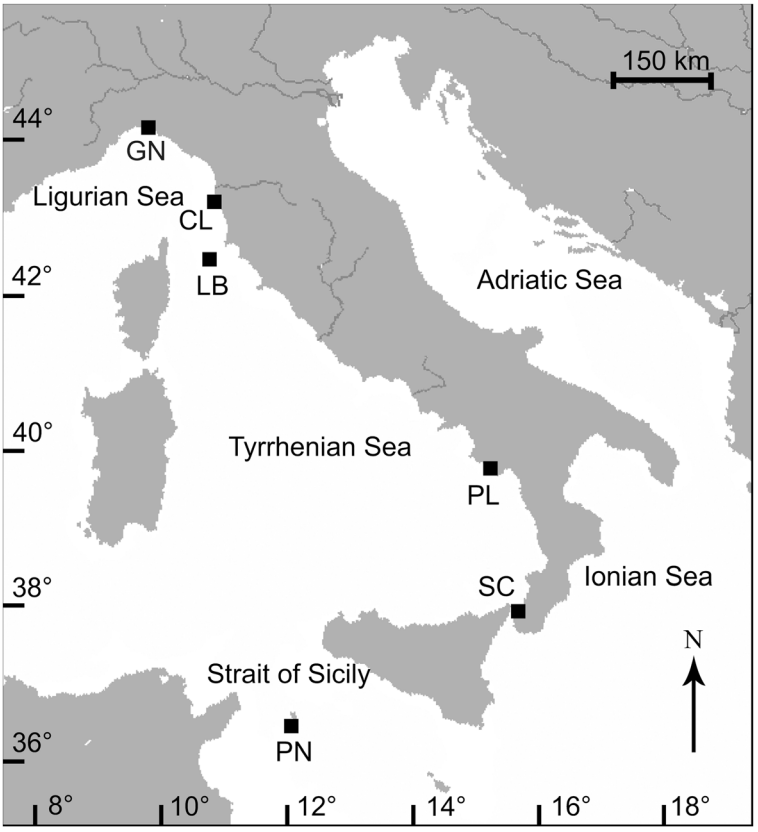

Figure 1 Map of the Italian coastline indicating sites where corals were collected. Abbreviations and coordinates of the sites in decreasing order of latitude: GN Genova, 44°20'N, 9°08'E; CL Calafuria, 43°27'N, 10°21'E; LB Elba Isle, 42°45'N, 10°24'E; PL Palinuro, 40°02'N, 15°16'E; SC Scilla, 38°01'N, 15°38'E; PN Pantelleria Isle, 36°45'N, 11°57'E.

12 cm × 7.1 cm (single patch area = 42.6 cm^2; transect area per each site = at least 42.6 × 3 = at least 128 cm^2; [16]). Triangular patches were more easily placed in the narrow crevices colonized by the species, with respect to traditional square patches. Such a small patch area was chosen because of the high population density of the species (about 10,000 individuals m^{-1}) which makes the sampling of all individuals present in larger areas (such as 1 m^2) unfeasible [15]. Moreover, such sampling area is considered representative of the studied site in previous studies of the biometry, growth and population dynamics of this species, where significant differences among sites and correlations with SST have been found [15,16,39]. Sampling was performed at depths known to have high population densities and where the reproductive biology, biometry, population density, growth, population dynamics, and genetics of the species had previously been studied [15,16,19,20,39]. Patches were collected on the vault of crevices 3 m apart, at a depth of 15–17 m. All crevices were clearly separated one from each other, without a continuous presence of polyps from one patch to each other. In order to account for the high within-site genetic variation characterizing the species [20], it was necessary to sample different patches at each site and treat them as replicates, to have a meaningful picture of the growth parameters at each site. Because of the random distribution pattern of the species, the problems associated with regularly spaced quadrats and transects do not apply to this study [15]. All of the polyps present in each patch were collected.

Corals were dried at 50°C for four days and observed under a binocular microscope to remove fragments of substratum and calcareous deposits produced by other organisms. Corallite length (L: maximum axis of the oral disc), width (W: minimum axis of the oral disc) and height (h: oral-aboral axis) were measured with calipers and the dry skeletal mass (M) was measured with a precision balance. Corallite volume (V) was determined by applying the formula: $V=L^2 \times W^2 \times h\pi$ [15]. Skeletal density (D) was calculated by dividing M by V.

The age of each sample was estimated using the von Bertalanffy length-age growth function previously obtained and based on growth bands analysis by means of computerized tomography [37,40]. According to the age of the polyp, the annual linear extension rate was obtained for each sample using the von Bertalanffy

length-age growth function [16,40]. The mean annual calcification rate (mass of $CaCO_3$ deposited per year per area unit) was calculated for each sample by the formula: calcification (mg mm^{-2} yr^{-1}) = skeletal density (mg mm^{-3}) x linear extension (mm yr^{-1}) [3,5,22]. Thus, for each population the mean values of skeletal density, linear extension and calcification rates of the corallites were obtained. Samples were divided into three age classes: immature (0–4 years, after [16]); mature (4–8 years, double the age at sexual maturity); old (>8 years).

Correlation and regression analyses between environmental and growth parameters were performed both for the full dataset and for the three age classes, to check for differences due to the different mean age of the samples in the populations [12]. Relationships between environmental and growth parameters were performed using two models: a linear model and a power function model. The linear model was used to compare the results with other studies on environmental controls of coral growth, where linear functions are used [3,5]. Also the power function model was used as it produced the best fit with the data, and to compare the results obtained by the linear model. The power function model:

$$y = \mathrm{a}x^{\mathrm{b}} \quad (1)$$

was linearized with a log-transformation of both the independent and dependent variables, producing the equation:

$$\ln(y) = \mathrm{b}\ln(x) + \ln(\mathrm{a}) \quad (2)$$

SST data for 2003–2005 were obtained for each location from the National Mareographic Network of the Agency for the Protection of the Environment and Technical Services (APAT, now renamed to Superior Institute for Environmental Research Protection, ISPRA, [41]). The data are measured by mareographic stations SM3810, built by the Italian Society for Precision Apparatuses (SIAP). Mean annual SST was obtained from hourly values measured from January 2001 to January 2005 (Table 1).

Because of the heteroskedastic nature of the data, the non-parametric Kruskal-Wallis test was used to compare mean SST, skeletal density, linear extension and calcification rates among the populations. Pearson correlation coefficients were calculated for the relationships among growth parameters and between environmental and growth parameters. Because of the low n value (n = 6) and the assumptions of the Pearson method, correlation coefficients were also estimated with bootstrapping [42], with 100,000 resamples. All analyses were computed using PASW 18.0.

Competing interests
The authors declare that they have no competing interests.

Authors' contributions
SG conceived and designed the experiments. EC and GM performed the experiments. EC analyzed the data. EC, GM, OL, GF, ZD and SG wrote the paper. All authors read and approved the final manuscript.

Acknowledgements
The research leading to these results has received funding from the European Research Council under the European Union's Seventh Framework Programme (FP7/2007-2013) / ERC grant agreement n° 249930 – CoralWarm: Corals and global warming: the Mediterranean versus the Red Sea. This research was also financed by the Associazione dei Tour Operator Italiani (ASTOI), the Marine & Freshwater Science Group Association, and the Ministry of Education, University and Research (MIUR). We wish to thank L. Bortolazzi, A. Comini, M. Ghelia, L. Tomesani, Centro Immersioni Pantelleria, Il Pesciolino, Polo Sub, and Submaldive, Bologna Scuba Team, Scientific Diving School and Marine Science Group for help and assistance. Two anonymous reviewers gave comments which improved manuscript quality. The experiments complied with current Italian law.

Author details
[1]Marine Science Group, Department of Biological, Geological and Environmental Sciences, Alma Mater Studiorum, University of Bologna, Via F. Selmi 3, Bologna, EU 40126, Italy. [2]Operative Unit of Radiology and Diagnostics by Images, Hospital of Porretta Terme, Local Health Enterprise of Bologna, Via Roma 16 Porretta Terme, Bologna, EU 40046, Italy. [3]The Mina and Everard Goodman Faculty of Life Sciences, Bar-Ilan University, Ramat-Gan 52900, Israel. [4]Department of Chemistry "G. Ciamician", Alma Mater Studiorum, University of Bologna, Via F. Selmi 2, Bologna, EU 40126, Italy.

Received: 4 October 2012 Accepted: 6 November 2012
Published: 19 November 2012

References
1. Kain JM: **The seasons in the subtidal.** *Br Phycol J* 1989, **24:**203–215.
2. Kleypas JA, McManus JW, Menez LAB: **Environmental limits to coral reef development: where do we draw the line?** *Am Zool* 1999, **39:**146–159.
3. Lough JM, Barnes DJ: **Environmental controls on growth of the massive coral *Porites*.** *J Exp Mar Biol Ecol* 2000, **245:**225–243.
4. Kinsey DW, Davies PJ: **Carbon turnover, calcification and growth in coral reefs**. In *Biogeochemical cycling of mineral forming elements*. Edited by Trudinger PA, Swaine DJ. Amsterdam: Elsevier; 1979:131–162.
5. Carricart-Ganivet JP: **Sea surface temperature and the growth of the West Atlantic reef-building coral *Montastraea annularis*.** *J Exp Mar Biol Ecol* 2004, **302:**249–260.
6. Dodge RE, Brass GW: **Skeletal extension, density and calcification of the reef coral, *Montastrea annularis*: St. Croix, U.S. Virgin Islands.** *Bull Mar Sci* 1984, **34:**288–307.
7. Cooper TF, De'ath G, Fabricius KE, Lough JM: **Declining coral calcification in massive *Porites* in two nearshore regions of the northern Great Barrier Reef.** *Glob Change Biol* 2008, **14:**529–538.
8. Tanzil JTI, Brown BE, Tudhope AW, Dunne RP: **Decline in skeletal growth of the coral *Porites lutea* from the Andaman Sea, South Thailand between 1984 and 2005.** *Coral Reefs* 2009, **28:**519–528.
9. Cantin NE, Cohen AL, Karnauskas KB, Tarrant AM, McCorkle DC: **Ocean warming slows coral growth in the Central Red Sea.** *Science* 2010, **329:**322–325.
10. Cooper TF, O'Leary RA, Lough JM: **Growth of Western Australian corals in the Anthropocene.** *Science* 2012, **335:**593–596.
11. Reynaud S, Leclercq N, Romaine-Lioud S, Ferrier-Pages C, Jaubert J, Gattuso JP: **Interactive effects of CO_2 partial pressure and temperature on photosynthesis and calcification in a scleractinian coral.** *Glob Change Biol* 2003, **9:**1660–1668.
12. Howe SA, Marshall AT: **Temperature effects on calcification rate and skeletal deposition in the temperate coral, *Plesiastrea versipora* (Lamarck).** *J Exp Mar Biol Ecol* 2002, **275:**63–81.
13. Rodolfo-Metalpa R, Richard C, Allemand D, Ferrier-Pagès C: **Growth and photosynthesis of two Mediterranean corals, *Cladocora caespitosa* and**

Oculina patagonica, under normal and elevated temperatures. *J Exp Biol* 2006, **209:**4546–4556.
14. Zibrowius H: **Les scléractiniaires de la Méditeranée et de l'Atlantique nord-oriental.** *Mèm Inst Ocèanogr (Monaco)* 1980, **11:**1–284.
15. Goffredo S, Caroselli E, Pignotti E, Mattioli G, Zaccanti F: **Variation in biometry and population density of solitary corals with solar radiation and sea surface temperature in the Mediterranean Sea.** *Mar Biol* 2007, **152:**351–361.
16. Caroselli E, Zaccanti F, Mattioli G, Falini G, Levy O, Dubinsky Z, Goffredo S: **Growth and demography of the solitary scleractinian coral *Leptopsammia pruvoti* along a sea surface temperature gradient in the Mediterranean Sea.** *PLoS ONE* 2012, **7:**e37848.
17. Bucher DJ, Harriott VJ, Roberts LG: **Skeletal micro-density, porosity and bulk density of acroporid corals.** *J Exp Mar Biol Ecol* 1998, **228:**117–136.
18. Caroselli E, Prada F, Pasquini L, Nonnis Marzano F, Zaccanti F, Falini G, Levy O, Dubinsky Z, Goffredo S: **Environmental implications of skeletal micro-density and porosity variation in two scleractinian corals.** *Zoology* 2011, **114:**255–264.
19. Goffredo S, Airi V, Radetić J, Zaccanti F: **Sexual reproduction of the solitary sunset cup coral Leptopsammia pruvoti (Scleractinia, Dendrophylliidae) in the Mediterranean. 2. Quantitative aspects of the annual reproductive cycle.** *Mar Biol* 2006, **148:**923–932.
20. Goffredo S, Di Ceglie S, Zaccanti F: **Genetic differentiation of the temperate-subtropical stony coral *Leptopsammia pruvoti* in the Mediterranean Sea.** *Isr J Ecol Evol* 2009, **55:**99–115.
21. Mundet L, Ribera L: **Characteristics of divers at a Spanish resort.** *Tourism Manage* 2001, **22:**201–510.
22. Goffredo S, Caroselli E, Mattioli G, Pignotti E, Dubinsky Z, Zaccanti F: **Inferred level of calcification decreases along an increasing temperature gradient in a Mediterranean endemic coral.** *Limnol Oceanogr* 2009, **54:**930–937.
23. Carricart-Ganivet JP, Merino M: **Growth responses of the reef-building coral *Montastraea annularis* along a gradient of continental influence in the southern Gulf of Mexico.** *Bull Mar Sci* 2001, **68:**133–146.
24. Cohen AL, McConnaughey TA: **Geochemical perspectives on coral mineralization.** *Rev Mineral Geochem* 2003, **54:**151–187.
25. Carricart-Ganivet JP, Cabanillas-Teran N, Cruz-Ortega I, Blanchon P: **Sensitivity of calcification to thermal stress varies among genera of massive reef-building corals.** *PLoS ONE* 2012, **7:**e32859.
26. Al-Horani FA, Ferdelman T, Al-Moghrabi SM, de Beer D: **Spatial distribution of calcification and photosynthesis in the scleractinian coral *Galaxea fascicularis*.** *Coral Reefs* 2005, **24:**173–180.
27. Al-Horani FA: **Effects of changing seawater temperature on photosynthesis and calcification in the scleractinian coral *Galaxea fascicularis*, measured with O_2, Ca^{2+} and pH microsensors.** *Sci Mar* 2005, **69:**347–354.
28. Coma RM, Ribes M, Gili JM, Zabala M: **Seasonality in coastal ecosystems.** *Trends Ecol Evol* 2000, **12:**448–453.
29. Hughes TP, Baird AH, Bellwood DR, Card M, Connolly SR, Folke C, Grosberg R, Hoegh-Guldberg O, Jackson JBC, Kleypas J, Lough JM, Marshall P, Nyström M, Palumbi SR, Pandolfi JM, Rosen B, Roughgarden J: **Climate change, human impacts, and the resilience of coral reefs.** *Nature* 2003, **301:**929–933.
30. Rogers AD, Laffoley D'A: *International Earth system expert workshop on ocean stresses and impacts. Summary report*. Oxford: IPSO; 2011.
31. Ballesteros E: **Mediterranean coralligenous assemblages: A synthesis of the present knowledge.** *Oceanogr Mar Biol Annu Rev* 2006, **44:**123–195.
32. Cerrano C, Bavestrello G, Bianchi CN, Cattaneo-Vietti R, Bava S, Morganti C, Morri C, Picco P, Sara G, Schiaparelli S, Siccardi A, Sponga F: **A catastrophic mass-mortality episode of gorgonians and other organisms in the Ligurian Sea (NW Mediterranean), summer 1999.** *Ecol Lett* 2000, **3:**284–293.
33. Perez T, Garrabou J, Sartoretto S, Harmelin JG, Francour P, Vacelet J: **Mass mortality of marine invertebrates: an unprecedented event in the Northwestern Mediterranean.** *CR Acad Sci III* 2000, **323:**853–865.
34. Rodolfo-Metalpa R, Bianchi CN, Peirano A, Morri C: **Coral mortality in NW Mediterranean.** *Coral Reefs* 2000, **19:**24.
35. Coma R, Ribes M, Serrano E, Jimenez E, Salat J, Pascual J: **Global warming-enhanced stratification and mass mortality events in the Mediterranean.** *Proc Natl Acad Sci U S A* 2009, **106:**6176–6181.
36. Garrabou J, Coma R, Bensoussan N, Bally M, Chevaldonne P, Cigliano M, Diaz D, Harmelin JG, Gambi MC, Kersting DK, Ledoux JB, Lejeusne C, Linares C, Marschal C, Perez T, Ribes M, Romano JC, Serrano E, Teixido N, Torrents O, Zabala M, Zuberer F, Cerrano C: **Mass mortality in the NW Mediterranean rocky benthic communities: Effects of the 2003 heat wave.** *Glob Change Biol* 2009, **15:**1090–1103.
37. Goffredo S, Caroselli E, Mattioli G, Pignotti E, Zaccanti F: **Relationships between growth, population structure and sea surface temperature in the temperate solitary coral *Balanophyllia europaea* (Scleractinia, Dendrophylliidae).** *Coral Reefs* 2008, **27:**623–632.
38. Carricart-Ganivet JP: **Coral skeletal extension rate: an environmental signal or a subject to inaccuracies?** *J Exp Mar Biol Ecol* 2011, **405:**73–79.
39. Goffredo S, Caroselli E, Mattioli G, Zaccanti F: **Growth and population dynamic model for the non-zooxanthellate temperate solitary coral *Leptopsammia pruvoti* (Scleractinia, Dendrophylliidae).** *Mar Biol* 2010, **157:**2603–2612.
40. von Bertalanffy L: **A quantitative theory of organic growth (inquiries on growth laws II).** *Hum Biol* 1938, **10:**181–213.
41. *Superior Institute for Environmental Research Protection*. http://www.isprambiente.gov.it
42. Efron B: **Nonparametric estimates of standard error: the jackknife, the bootstrap and other methods.** *Biometrika* 1981, **68:**589–599.

doi:10.1186/1742-9994-9-32
Cite this article as: Caroselli *et al.*: Inferred calcification rate of a Mediterranean azooxanthellate coral is uncoupled with sea surface temperature along an 8° latitudinal gradient. *Frontiers in Zoology* 2012 **9**:32.

OPEN ACCESS Freely available online

PLOS ONE

Reproductive Efficiency of a Mediterranean Endemic Zooxanthellate Coral Decreases with Increasing Temperature along a Wide Latitudinal Gradient

Valentina Airi[1], Francesca Gizzi[1], Giuseppe Falini[2], Oren Levy[3], Zvy Dubinsky[3], Stefano Goffredo[1]*

1 Marine Science Group, Department of Biological, Geological and Environmental Sciences, Section of Biology, Alma Mater Studiorum – University of Bologna, Bologna, Italy, European Union, **2** Department of Chemistry "G. Ciamician," Alma Mater Studiorum – University of Bologna, Bologna, Italy, European Union, **3** The Mina and Everard Goodman Faculty of Life Sciences, Bar-Ilan University, Ramat-Gan, Israel

Abstract

Investments at the organismal level towards reproduction and growth are often used as indicators of health. Understanding how such energy allocation varies with environmental conditions may, therefore, aid in predicting possible responses to global climatic change in the near future. For example, variations in seawater temperature may alter the physiological functioning, behavior, reproductive output and demographic traits (e.g., productivity) of marine organisms, leading to shifts in the structure, spatial range, and abundance of populations. This study investigated variations in reproductive output associated with local seawater temperature along a wide latitudinal gradient on the western Italian coast, in the zooxanthellate Mediterranean coral, *Balanophyllia europaea*. Reproductive potential varied significantly among sites, where *B. europaea* individuals from the warmest site experienced loss of oocytes during gametogenesis. Most of the early oocytes from warmest sites did not reach maturity, possibly due to inhibition of metabolic processes at high temperatures, causing *B. europaea* to reabsorb the oocytes and utilize them as energy for other vital functions. In a progressively warming Mediterranean, the efficiency of the energy invested in reproduction could be considerably reduced in this species, thereby affecting vital processes. Given the projected increase in seawater temperature as a consequence of global climate change, the present study adds evidence to the threats posed by high temperatures to the survival of *B. europaea* in the next decades.

Citation: Airi V, Gizzi F, Falini G, Levy O, Dubinsky Z, et al. (2014) Reproductive Efficiency of a Mediterranean Endemic Zooxanthellate Coral Decreases with Increasing Temperature along a Wide Latitudinal Gradient. PLoS ONE 9(3): e91792. doi:10.1371/journal.pone.0091792

Editor: Christina A. Kellogg, U.S. Geological Survey, United States of America

Received October 30, 2013; **Accepted** February 13, 2014; **Published** March 11, 2014

Funding: The research leading to these results has received funding from the European Research Council under the European Union's Seventh Framework Programme (FP7/2007–2013)/ERC grant agreement no. 249930 – CoralWarm: Corals and global warming: the Mediterranean versus the Red Sea. The funders had no role in study design, data collection and analysis, decision to publish, or preparation of the manuscript.

Competing Interests: The authors have declared that no competing interests exist.

* E-mail: stefano.goffredo@marinesciencegroup.org

Introduction

Coral reefs, like many other ecosystems, are currently undergoing changes in biodiversity, ecosystem function, and resilience due to rising seawater temperatures acting in synergy with additional environmental pressures [1]. A rise in global average temperature of 0.7°C since the start of the industrial revolution has caused or contributed to significant losses of global coral cover over the past few decades, and oceans are expected to experience a further warming of 1.1–6.4°C within the 21st century [2]. Climatic models [3] predict that the Mediterranean basin will be one of the most impacted regions by the ongoing warming trend [4]. The Mediterranean is already showing rates of seawater warming that exceed threefold those of the global ocean [2,4], making it a potential model for global scenarios to occur in the world's marine biota, and a natural focus of interest for research [5].

Increasing temperatures are having a strong impact on marine systems [6]. Indeed, temperature is the major environmental factor controlling invertebrate development, marine species distributions and recruitment dynamics [7,8]. Seawater temperature increases will likely affect the population biology of coral species by reducing reproductive capacity [9]. The harmful effects of increasing temperature on coral reproduction include reduced individual fecundity, egg quality, lowered fertilization success and reduced recruitment through effects on post-fertilization processes (e.g., embryonic development, larval development, survival, settlement, metamorphosis, and early post-settlement growth) [10,11]. The combined effects of fertilization failure and reduced embryonic development in some coral species are likely to exacerbate ecological impacts of climate change by reducing biodiversity [12]. Several studies assessed the immediate and delayed impacts of environmental change on Mediterranean gorgonian colonies [11–14] including sublethal impacts on reproductive effort [11,15,16,17], but few studies have examined temperate solitary corals. Research focusing on reproductive processes in regions with peculiar physical conditions is urgently needed as a baseline against which to test the effects of climate change on sexual reproduction (e.g. fecundity) [10,18] and organismal performance, that are essential to understand population dynamics of marine organisms [19].

Organismal performance under both "normal" and "stressful" conditions is mainly determined by the energetic status of the individual, which can ultimately affect its fitness (i.e. reproductive output). During prolonged periods of stress, the energy balance of

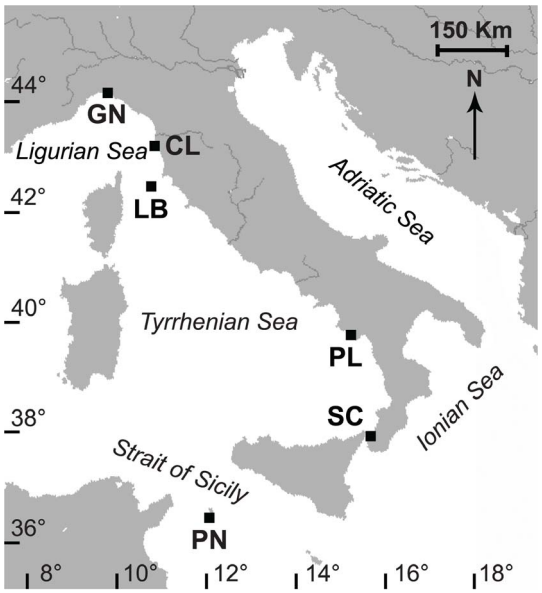

Figure 1. Map of the Italian coastline indicating the sites where corals were collected. Abbreviations and coordinates of the sites in decreasing order of latitude: GN Genova, 44°20′N, 9°08′E; CL Calafuria, 43°27′N, 10°21′E; LB Elba Isle, 42°45′N, 10°24′E; PL Palinuro, 40°02′N, 15°16′E; SC Scilla, 38°01′N, 15°38′E; PN Pantelleria Isle, 36°45′N, 11°57′E.
doi:10.1371/journal.pone.0091792.g001

a coral is negative and the organism is drawing on all biochemical pools, and thus both storage and structural components for energy could be compromised [20]. Shallow water reef corals strongly rely on energy derived from photosynthesis by its symbiotic zooxanthellae [21]. In particular, key processes like gametogenesis [22], larval longevity and settlement [23] are dependent on the availability of stored energy as lipids that are reabsorbed when resources are limited [24]. If metabolic processes involved in recovery from stress deplete lipid reservoirs in oocytes, then fewer resources are available for new egg production [25], significantly affecting gametogenesis.

This study focused on an endemic zooxanthellate Mediterranean scleractinian, *Balanophyllia europaea* (Fig. S1), a simultaneous hermaphrodite and brooding coral [26]. There is growing concern for the future of this endemic species in light of expected seawater warming, since increasing temperature negatively affects *B. europaea* skeletal density [27] (due to increased porosity [28]), population abundance [29], population structure stability [30], growth and calcification [28]. Our specific aim was to quantify the reproductive output of *B. europaea* along a latitudinal gradient of temperature. We expected to find a similar negative response of reproductive output with increasing temperature.

Materials and Methods

Ethics Statement

This study was carried out following the fundamental ethical principles. According to the European normative, there is no active conservation measure for the Mediterranean scleractinian coral studied here (*B. europaea*). The species is not protected in Italy, nor is it subject to any regulations. Thus, no permit was needed to sample specimens. For this study, sampling was limited strictly to the number necessary and performed where the species has high population density to minimize the impact of removing individuals and preserve both the demographic and genetic structure of the natural populations.

Specimens of *B. europaea* came from six sites along a latitudinal gradient, from 44°20′N to 36°45′N (Fig. 1). Coral collection began in June 2010 and ended in November 2012. During this period, 18 samples were taken monthly from five populations (Genova: April 2011-September 2012; Elba: December 2010-May 2012; Palinuro: June 2010-November 2011; Scilla: June 2011-November 2012; Pantelleria: June 2011-November 2012), with a minimum of 15 polyps collected during each excursion. Data from Calafuria population came from a previous study [26] in which samples were collected from July 1997 to October 1998.

Biometric analyses were performed by measuring length (L, maximum axis of the oral disc), width (W, minimum axis of the oral disc) and height (h, oral–aboral axis) of each sampled polyp. The volume (V) of the individual polyp was calculated using the formula [26].

Polyps were post-fixed in Bouin solution. After decalcification in EDTA and dehydration in a graded alcohol series from 80% to 100%, polyps were embedded in paraffin and serial transverse sections were cut at 7 μm intervals along the oral-aboral axis, from the oral to the aboral poles. Tissues were then stained with Mayer's haematoxylin and eosin [26].

Cytometric analyses were made with an optical microscope using the image analyzer NIKON NIS-Elements D 3.2. The maximum and minimum diameters of oocytes in nucleated sections and spermaries were measured and the presence of embryos in the coelenteric cavity was recorded. Spermaries were classified into five developmental stages in accordance with earlier studies on gametogenesis in scleractinians [19,31,32].

Reproductive output was defined through three reproductive parameters: a) *fecundity rate* and *spermary abundance*, both defined as

Table 1. Mean annual solar radiation (W/m^2) and temperature (DT; °C) values of the sampled populations.

Population	Code	DT (°C) mean ± SE	Solar radiation (W/m^2) mean ± SE
Calafuria	CL	17.73±0.16	174.1±1.9
Elba	LB	18.07±0.24	184.9±2.3
Genova	GN	18.13±0.43	156.9±3.2
Scilla	SC	18.73±0.15	205.5±1.8
Palinuro	PL	19.14±0.14	194.6±2.7
Pantelleria	PN	19.69±0.05	218.2±0.5

DT sensors (I-Button DS1921H, Maxim Integrated Products), were placed at the sampling location, at 5–7 m depth in each population. Solar radiation (W/m^2) was collected from MFG satellites. The sites are arranged in order of increasing DT; SE, standard error.
doi:10.1371/journal.pone.0091792.t001

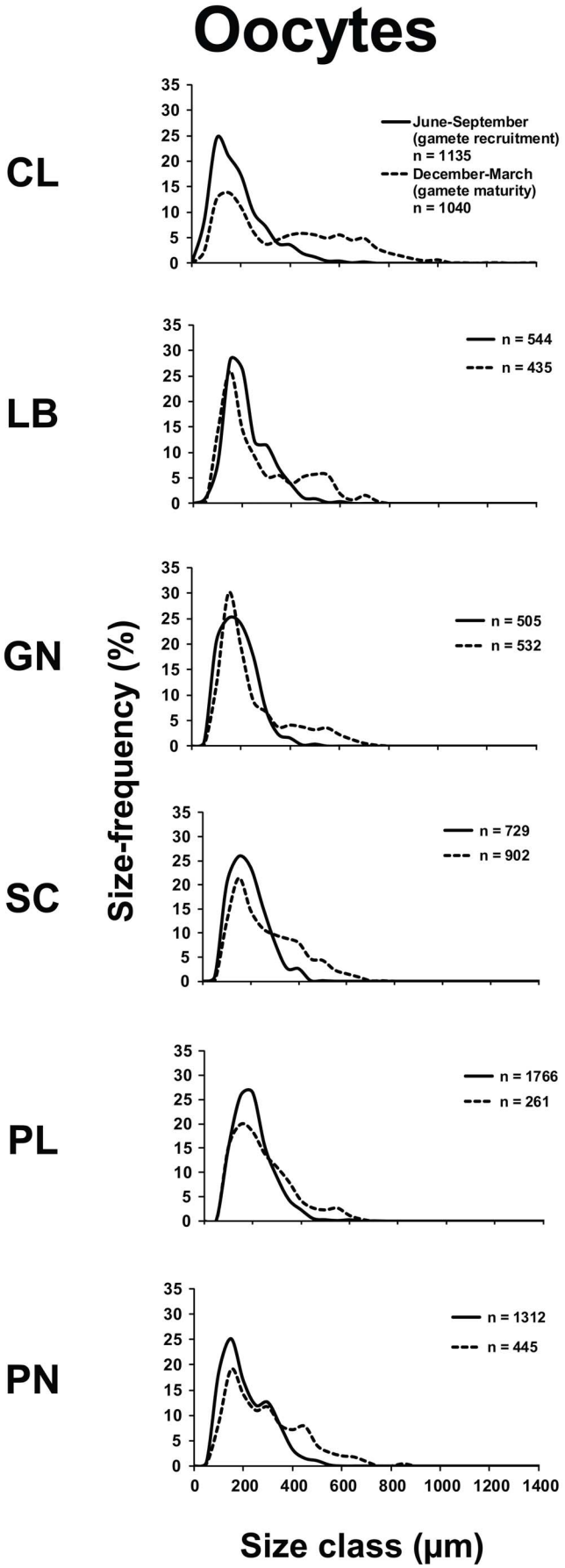

Figure 2. Oocyte size/frequency distribution in the recruitment and maturity periods. Distribution of the oocytes size during gamete recruitment period (solid line) and gamete maturity period (dashed line).
doi:10.1371/journal.pone.0091792.g002

the number of reproductive elements per body volume unit (100 mm^3); b) *"gonadal" index*, defined as the percentage of body volume occupied by germ cells [26]); and c) *reproductive element size*, defined as the average of the maximum and minimum diameter of spermaries and oocytes in nucleated section [26].

Based on the reproductive season [26], gametal development in *B. europaea* was divided in two gamete activity periods. The *gametes recruitment period* [33,34] was defined as the post-fertilization period, between June and September, generally characterized by: 1) a stock of smaller oocytes; 2) the recruitment of new oocytes; and 3) the beginning of spermary development [26]. The *gametes maturity period* [33,34] was defined as the pre-fertilization period taking place between December and March and generally characterized by the presence of larger oocytes and advanced stage of maturation of spermaries [26].

Temperature data (Depth Temperature – DT; °C) came from temperature sensors (I-Button DS1921H, Maxim Integrated Products), placed at the sampling location for each population. Sensors recorded temperatures during the entire experimental period. Sea Surface Temperature data (SST; °C) for each site were recorded hourly from the National Mareographic Network of the Institute for the Environmental Protection and Research (ISPRA, available to http://www.mareografico.it). These data are measured by mareographic stations placed close to the sampling sites using SM3810 manufactured by the Society for the Environmental and Industrial monitoring (SIAP+MICROS). A linear regression was produced between DT and SST data to estimate historical at-depth temperatures. In this study we considered the average DT temperature of the three years preceding the sampling (n = 36 monthly temperatures).

Solar radiation (W/m^2) was collected from the archives of the Satellite Application Facility on Climate Monitoring (CM-SAF/EUMETSAT, available to http://www.cmsaf.eu), using real time data sets based on intersensor calibrated radiances from MFG satellites. Mean annual solar radiation of each site was obtained for the 2.5°-latitude-by-longitude square associated with each of the six sites. As for temperature, also for solar radiation we considered the average of the three years preceding the sampling (n = 36 monthly solar radiation).

Data were checked for normality using a Kolmogorov-Smirnov's test and for variance homoskedasticity using a Levene's test. When assumptions for parametric statistics were not fulfilled, a nonparametric test was used. The Kruskal–Wallis test is a non-parametric alternative to the analysis of variance (ANOVA) and is used to compare groups of means; it is useful for data that do not meet ANOVA's assumptions. The non-parametric Kruskal–Wallis test was used to compare reproductive parameters among study sites. The non-parametric Kolmogorov-Smirnov test was used to compare the size-frequency distribution of reproductive elements between populations and between the two periods. Student's *t* test was used to compare the mean oocytes and spermaries size of populations between periods. Spearman's rank correlation coefficient was used to calculate the significance of the correlations between reproductive and environmental parameters. Spearman's rank correlation coefficient is an alternative to Pearson's correlation coefficient [35]. It is useful for data that are non-normally distributed and do not meet the assumptions of Pearson's correlation coefficient [36]. All analyses were computed using PASW Statistics 17.0.

Table 2. Mean fecundity, gonadal index and diameter of oocytes in each population.

Gametes recruitment period (June – September)					
Population	**N**	**Fecundity (#/100 mm^3) mean ± SE**	**Gonadal Index (%) mean ± SE**	**N**	**Diameter (μm) mean ± SE**
Calafuria	18	161±39	0.22±0.07	1135	166.3±3.3
Elba	6	148±37	0.65±0.17	544	193.7±3.8
Genova	8	168±47	0.27±0.12	505	166.0±3.3
Scilla	9	256±58	0.41±0.13	729	166.7±2.8
Palinuro	10	734±194	1.57±0.38	1766	178.4±1.9
Pantelleria	8	663±240	1.43±0.51	1312	188.2±2.6
Gametes maturity period (December – March)					
Population	**N**	**Fecundity (#/100 mm^3) mean ± SE**	**Gonadal Index (%) mean ± SE**	**N**	**Diameter (μm) mean ± SE**
Calafuria	19	117±38	1.04±0.30	1040	350.3±7.5
Elba	8	175±32	0.79±0.16	435	243.4±7.7
Genova	4	411±183	1.37±0.40	532	222.5±6.2
Scilla	4	602±257	2.72±1.50	902	241.1±4.5
Palinuro	7	112±30	0.39±0.15	261	217.7±7.5
Pantelleria	6	236±106	1.25±0.41	445	265.4±7.1

Mean fecundity, gonadal index and diameter of oocytes in each population for both reproductive periods. The sites are arranged in order of increasing DT; SE, standard error. N, polyp number for fecundity and gonadal index, oocyte number for diameter.

doi:10.1371/journal.pone.0091792.t002

Results

Mean annual solar radiation (W/m^2) and mean annual DT (°C) were significantly different among sites (solar radiation, ANOVA, $p<0.001$; DT, Kruskal-Wallis, $p<0.05$; Table 1; Fig S2).

All populations contained both oocytes and spermaries during both reproductive periods, while embryos were detected only between June and September (gametes recruitment period). The oocyte size/frequency distribution of June-September (gametes recruitment period) was significantly different from that of December-March (gametes maturity period), in all populations (Kolmogorov-Smirnov, $p<0.001$; Fig. 2). Within June and September (gametes recruitment period) most oocytes were smaller than 400 μm, in all populations. In the following season (December-March, gametes maturity period), two distinct oocyte stocks appeared in all populations, characterized respectively by small (immature<400 μm) and large (mature >400 μm) cells (Fig. 2). The mean oocyte size of June-September (gametes recruitment period) was significantly lower than that of December-March (gametes maturity period) in all populations (Student's *t*-test, $p<0.001$; Table 2; Fig. S3).

The distribution of spermary maturation stages in June-September (gametes recruitment period) was significantly different from that in December-March (gametes maturity period), in all populations (Kolmogorov-Smirnov, $p<0.001$; Fig. 3). Each population was characterized, from June to September (gametes recruitment period), by small spermaries, mainly belonging to the earliest maturation stages (stages I and II). In the period December-March (gametes maturity period), all populations were characterized by more advanced maturation stages (mainly stage III; Fig. 3). The mean spermary size of June-September (gametes recruitment period) was significantly lower than that of December-March (gametes maturity period) in all populations (Student's *t*-test, $p<0.001$; Table 3; Fig. 3). In all populations, June-September (gametes recruitment period) was characterized by the presence of embryos in the coelenteric cavity.

Fecundity, gonadal index and oocyte size were significantly different among populations, during June-September (gametes recruitment period) (fecundity, Kruskal–Wallis test, $p<0.01$; gonadal index and oocyte size, Kruskal–Wallis test, $p<0.001$; Tables 2 and S1). In this period, all oocyte reproductive parameters showed positive correlations with both environmental parameters (DT and solar radiation; Table S1; Fig. S4). During December-March (gametes maturity period), the fecundity and oocyte size were significantly different among populations (fecundity, Kruskal–Wallis test, $p<0.05$; diameter, Kruskal–Wallis test, $p<0.001$; Tables 2 and S1). The mean size of oocytes across all populations was negatively correlated with the DT (Table S1; Fig. S5). In the warmest population (Pantelleria island, 19.69±0.05°C; Table 1), the number of mature oocytes at fertilization was three times lower than in the recruitment period, indicating a clear reduction of fecundity during this period (Table 2). In the coldest population (Calafuria, 17.73±0.16°C; Table 1), fecundity was the same during both periods (Table 2).

In both periods, only the spermary size was significantly different among populations (Kruskal–Wallis test, $p<0.001$; Tables 3 and S2) and in both reproductive periods, spermary size was negatively correlated with both DT and solar radiation (Table S2; Fig. S6 and S7).

Discussion

Traditionally, seawater temperature cycles and solar radiation fluctuations have been related to reproductive timing of gamete development, fertilization and planulation [16,37] providing a reliable cue to reset the biological clock and trigger the physiological changes related to oocyte yolk deposition [38] and spermary development [26,39,40]. The effects of changing photoperiod and seawater temperature on gametogenic cycles of anthozoans have been largely overlooked [15,41,42]. The reproductive biology of *B. europaea*, studied at Calafuria, shows a reproductive seasonality induced by annual variation of seawater

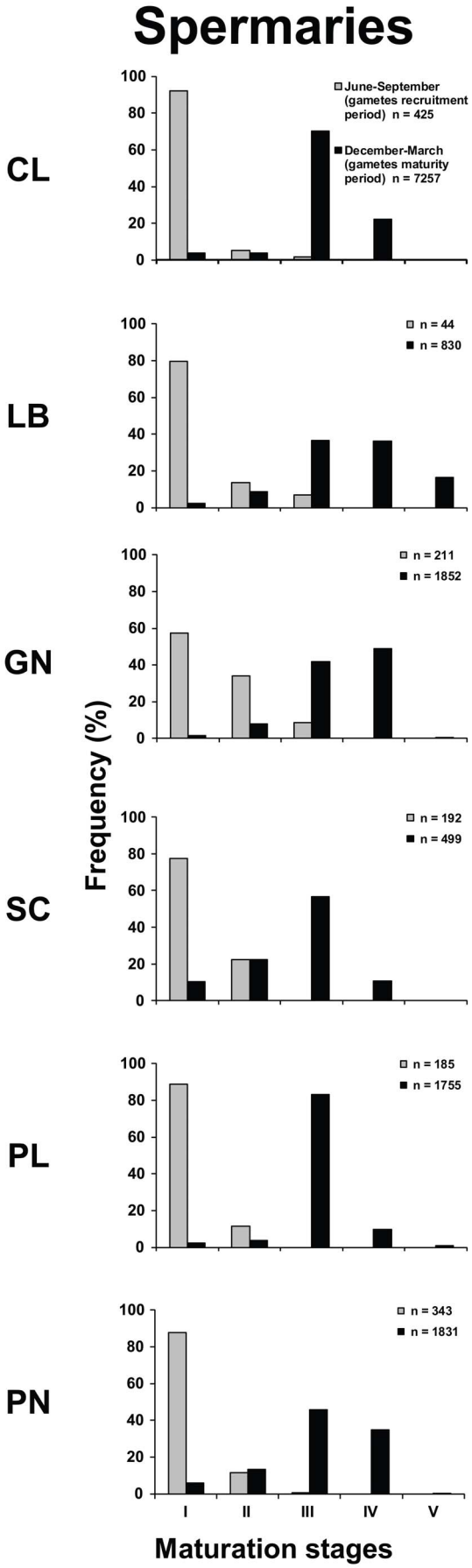

Figure 3. Spermary frequency distribution in the recruitment and maturity periods. Distribution of the maturation stages during gamete recruitment period (gray histogram bars) and gamete maturity period (black histogram bars).
doi:10.1371/journal.pone.0091792.g003

temperature and photoperiod [26]. The same pattern seems to appear in other Mediterranean dendrophylliids like *Leptopsammia pruvoti* [39] and *Astroides calycularis* [40] and in the Mediterranean endemic oculinid *Cladocora caespitosa* [43,44]. A similar periodicity for gamete development and embryonic presence during the recruitment period, suggest an overlap of reproductive seasonality in all populations along the latitudinal gradient by *B. europaea*. In broadcasting scleractinian corals, where temperature dependence leads to location-specific synchronous reproductive times [45], temporal variation in spawning events by corals from different latitudes, over two or more consecutive months, is uncommon [18]. In brooding scleractinians, reproductive cycles are protracted over several months coinciding with environmental seasonality change [46,47].

Specimens from the warmer and more irradiated populations of *B. europaea* generated a significantly greater number of oocytes during the initial stages of gametogenesis (gametes recruitment period). Before fertilization (gametes maturity period), however, individual oocyte number was not related to temperature/irradiance along the gradient, while oocyte size was smaller with increasing temperature (Tables 2 and S1). A reduction of photosynthetic efficiency is documented for several species when temperatures are above optimal [48,49], thereby limiting energetic resources for polyp gametogenesis [9,50]. The onset of gametogenesis (proliferation of germ cells and their differentiation into gametes) may require little energy investment and may, therefore, be less sensitive to selective pressures such as food availability and more reliant on environmental seasonal cycles [51]. In this scenario, warmer populations of *B. europaea* could invest in energetically inexpensive early stages of oogenesis to generate a potential energy resource that would guarantee sufficient metabolic efficiency. On the other hand, the ripening of gametes, especially of oocytes, is an energy consuming process and, therefore, extremely sensitive to selective pressures [51].

Regarding male gametogenesis, during both reproductive periods, the size of spermaries decreased with increasing temperature (Tables 3, S2), while their abundance was not significantly related to environmental parameters. The energetic investment for gametogenesis between males and females is often assumed to differ [52]. For many lower invertebrates, and especially sessile ones, mating effort and parental care are minimal and reproductive output provides a good approximation of the reproductive effort, so most of the energy involved in reproduction is stored in gonads [53]. This "cost of sex" is mainly represented by oogenesis, while the investment of spermary production minimally influences the energetic balance of the organism [52].

For all organisms, energy flow provides an important cost for physiological performance, including maintenance, growth and reproduction, all of which have implications on survival and fitness. Reproductive investment and growth are often used as indicators of health or stress at the organism level (e.g. [54]), and knowledge of how such allocation varies among species or morphological types is crucial for the interpretation of physiological response to environmental factors [53]. Essentially, organisms invest their energy in continuous trade-offs between somatic/skeletal growth and reproduction, which in many species includes the possibility of asexual reproduction [55]. In a changing environment, physiological trade-offs vary through time, reflecting variations in resource availability [56], and the 'energy allocation'

Table 3. Mean abundance, gonadal index and diameter of spermaries in each population.

Gametes recruitment period (June – September)					
Population	**N**	**Abundance (#/100 mm^3) mean ± SE**	**Gonadal Index (%) mean ± SE**	**N**	**Diameter (μm) mean ± SE**
Calafuria	17	140±52	0.010±0.003	425	51.4±1.2
Elba	2	169±106	0.010±0.001	44	54.2±2.8
Genova	1	1463	0.080	211	46.3±1.1
Scilla	6	272±80	0.010±0.004	192	40.7±0.8
Palinuro	6	393±133	0.020±0.006	185	40.0±1.0
Pantelleria	5	760±368	0.030±0.020	343	42.0±0.7
Gametes maturity period (December – March)					
Population	**N**	**Abundance (#/100 mm^3) mean ± SE**	**Gonadal Index (%) mean ± SE**	**N**	**Diameter (μm) mean ± SE**
Calafuria	19	1840±609	1.10±0.40	7257	120.5 ±0.8
Elba	8	595±235	0.47±0.23	830	126.0 ±1.8
Genova	4	2135±1122	1.95±1.51	1852	124.8 ±1.3
Scilla	4	981±561	0.16±0.09	499	81.7 ±1.6
Palinuro	6	1875±1664	0.85±0.80	1755	103.2 ±1.1
Pantelleria	5	2660±2320	0.93±0.25	1831	92.0 ±1.0

Mean abundance, gonadal index and diameter of spermaries in each population for both reproductive periods. The sites are arranged in order of increasing DT; SE, standard error. N, polyps number for abundance and gonadal index, spermaries number for diameter.

doi:10.1371/journal.pone.0091792.t003

explains this partitioning between the various investment options (e.g. growth, sexual reproduction, defense) [57]. For example, the coral *Montipora digitata* under varying light regimes shows an increase of energy allocated to reproduction versus growth at intermediate light levels. In this species the skeletal growth is less susceptible to environmental variations and during periods of resource shortage, energy is preferentially allocated for skeletal growth [57]. *B. europaea* shows a reduction of skeletal density, due to increasing porosity, and especially of pores with larger size, with increasing temperature [28,29,58]. Also its growth and calcification are negatively related to temperature [27,30]. Warmer populations are less stable, showing a progressive reduction in young individuals and reduced population density [29,30]. It has been hypothesized that the decrease in calcification rate [27] and skeletal density [29] in *B. europaea* with increasing temperature could be due to a reduction of energy input available, maybe due to photosynthetic inhibition of the symbionts [29,30]. Populations of *B. europaea* in warmer sites could potentially resorb earlier oocytes adjusting their energetic budget by reallocating the resources destined to oocyte maturity into other vital functions depleted by the negative effect of temperature. Resorption of oocytes is not fully understood, but it is thought that by breaking down the large amount of lipid vesicles in oocytes, energy can be absorbed back into the coral [59]. In the soft coral *Lobophytum compactum*, fecundity is reduced after an induced bleaching event. In this zooxanthellate coral, early oocytes are resorbed to allow development of remaining ones. Energy allocated to reproduction is apparently shifted towards maintaining fewer eggs than normal to ensure that they reach a mature size [37]. The branching coral *Acropora formosa* shows lower survival rate and a resorption of early vitellogenic oocytes after fragmentation, suggesting that there is a trade-off of energy between reproduction and survival [60].

In conclusion, *B. europaea* shows the highest ecological performance in the coldest part of its distribution, characterized by a higher growth coefficient [30], a greater population density [29,61] and a higher efficiency in partitioning the energy budget (this work; [27-30]). On the contrary, populations in warmer regions appear to invest their energy in the initial stages of gametogenesis in order to ensure a sufficient gamete number ready for fertilization in the maturity period. Nevertheless, this effort is not enough to guarantee the same reproductive performance at higher temperatures, as adult populations in warmer sites are less abundant, less stable, and contain fewer young individuals [29,30]. This suggests that increasing temperature may negatively influence post-fertilization life stages, such as larval dispersal, survival and settlement. Depressed organismal condition exhibited by the warmer population could be due to their location near the edge of the species distribution range, where species generally show a lower ecological performance with reduced adaptability to variations in climate [62]. Being endemic to the Mediterranean [63], *B. europaea* has limited potential to respond to seawater warming by migrating northward toward lower temperatures, since the latitudinal range considered covers almost the entire northern distribution of this species [27]. This scenario would indicate a possible reduction in the distribution area of this species, with irrecoverable losses in terms of genetic variability, particularly considering the fragmented genetic structure that characterizes the species [64]. The present study, therefore, confirms the concerns for the future of this endemic species [27–30]. In fact, in a progressively warming Mediterranean, the energetic efficiency of this species could be considerably reduced, affecting vital processes (e.g. growth). Thus, an effective allocation strategy will be crucial for ensuring adaptability to a changing environment.

Supporting Information

Figure S1 Living specimens of *Balanophyllia europaea* photographed at Scilla (South Italy, 38°01′N, 15°38′E). (TIF)

Figure S2 Annual fluctuation of solar radiation and temperature. Mean monthly solar radiation (W/m^2) and temperature (DT; °C) during three years preceding the sampling.

Annual fluctuation referred to January 1995 - December 1997 in the Calafuria population. For the other five populations it referred to January 2009 - December 2011.
(EPS)

Figure S3 Oocyte diameter during recruitment and maturity periods. Monthly size increase of the oocyte diameter during gamete recruitment (gray indicators) and maturity (black indicators) period.
(EPS)

Figure S4 Oocytes. Correlation analyses. Spearman's correlation between reproductive and environmental parameters during gamete recruitment period; N, polyp number for fecundity and gonadal index, oocyte number for diameter; r_s, Spearman's correlation coefficient; p, significance of the correlation test.
(EPS)

Figure S5 Oocytes. Correlation analyses. Spearman's correlation between reproductive and environmental parameters during gamete maturity period; N, polyp number for fecundity and gonadal index, oocyte number for diameter; r_s, Spearman's correlation coefficient; p, significance of the correlation test.
(EPS)

Figure S6 Spermaries. Correlation analyses. Spearman's correlation between reproductive and environmental parameters during gamete recruitment period; N, polyps number for abundance and gonadal index, spermaries number for diameter; r_s, Spearman's correlation coefficient; p, significance of the correlation test.
(EPS)

Figure S7 Spermaries. Correlation analyses. Spearman's correlation between reproductive and environmental parameters during gamete maturity period; N, polyps number for abundance and gonadal index, spermaries number for diameter; r_s, Spearman's correlation coefficient; p, significance of the correlation test.
(TIF)

Table S1 Oocytes. Kruskal-Wallis test and correlation analyses between reproductive and environmental parameters in the sampled populations, in both periods.
(DOC)

Table S2 Spermaries. Kruskal-Wallis test and correlation analyses between reproductive and environmental parameters in the sampled populations, in both periods.
(DOC)

Acknowledgments

We wish to thank M. Ghelia, M. Pisconti, A. Picariello, S. Guerrieri, F. Croci, F. Fasoli, F. Sesso, Centro Immersioni Pantelleria, Il Pesciolino, Bubble Lounge Diving and Submaldive that supplied logistic assistance in the field and collaborated in the underwater activities. We thank F. Sesso also for the picture of a living *B. europaea* specimen. The Scientific Diving School provided scientific, technical, and logistical support. We are grateful to E. Caroselli (University of Bologna), F. Prada (University of Bologna), G. Goodbody-Gringley (Bermuda Institute of Ocean Sciences) for their critical reading and valuable suggestions on the early drafts. Two anonymous reviewers gave comments which improved manuscript quality.

Author Contributions

Conceived and designed the experiments: SG. Performed the experiments: VA FG SG. Analyzed the data: VA FG SG. Contributed reagents/materials/analysis tools: SG. Wrote the paper: VA FG GF OL ZD SG. Gave conceptual advice: GF OL ZD.

References

1. Pandolfi JM, Connolly SR, Marshall DJ, Cohen AL (2011) Projecting coral reef futures under global warming and ocean acidification. Science 333: 418–422.
2. Solomon S, Qin D, Manning M, Chen Z, Marquis M, et al. (2007) Climate Change 2007: The Physical Science Basis. Contribution of Working Group I to the Fourth Assessment Report of the Intergovernmental Panel on Climate Change. Cambridge and New York: Cambridge University Press. 996 p.
3. Parry M (2000) Assessment of potential effects and adaptions for climate change in Europe: The europe acacia project (a concerted action towards a comprehensive climate impacts and adaptions assessment for the European Union). Jackson Environment Institute, University of East Anglia. 320 p.
4. Field CB, Barros V, Stocker TF, Dahe Q (2012) Managing the Risks of Extreme Events and Disasters to Advance Climate Change Adaptation: Special Report of the Intergovernmental Panel on Climate Change. Cambridge and New York: Cambridge University Press. 594 p.
5. Lejeusne C, Chevaldonné P, Pergent-Martini C, Boudouresque CF, Pérez T (2010) Climate change effects on a miniature ocean: the highly diverse, highly impacted Mediterranean Sea. Trends Ecol Evol 25: 250–260.
6. Brierley A, Kingsford M (2009) Impacts of climate change on marine organisms and ecosystems. Curr Biol 19: 602-614.
7. Hoegh-Guldberg OVE, Pearse JS (1995) Temperature, food availability, and the development of marine invertebrate larvae. Am Zool 35: 415–425.
8. Gillooly JF, Charnov EL, West GB, Savage VM, Brown JH (2002) Effects of size and temperature on developmental time. Nature 417: 70–73.
9. Baird AH, Marshall PA (2002) Mortality, growth and reproduction in scleractinian corals following bleaching on the Great Barrier Reef. Mar Ecol Prog Ser 237: 133–141.
10. Albright R, Mason B (2013) Projected near-future levels of temperature and pCO_2 reduce coral fertilization success. PloS One 8: e56468.
11. Linares C, Coma R, Zabala M (2008) Effects of a mass mortality event on gorgonian reproduction. Coral reefs 27: 27–34.
12. Negri AP, Marshall PA, Heyward AJ (2007) Differing effects of thermal stress on coral fertilization and early embryogenesis in four Indo Pacific species. Coral Reefs 26: 759–763.
13. Coma R, Ribes M, Serrano E, Jiménez E, Salat J, et al. (2009) Global warming-enhanced stratification and mass mortality events in the Mediterranean. Proc Natl Acad Sci 106: 6176–6181.
14. Cupido R, Cocito S, Manno V, Ferrando S, Peirano A, et al. (2012) Sexual structure of a highly reproductive, recovering gorgonian population: quantifying reproductive output. Mar Ecol Prog Ser 469: 25–36.
15. Gori A, Linares C, Rossi S, Coma R, Gili JM (2007) Spatial variability in reproductive cycle of the gorgonians *Paramuricea clavata* and *Eunicella singularis* (Anthozoa, Octocorallia) in the Western Mediterranean Sea. Mar Biol 151: 1571–1584.
16. Torrents O, Garrabou J (2011) Fecundity of red coral *Corallium rubrum* (L.) populations inhabiting in contrasting environmental conditions in the NW Mediterranean. Mar Biol 158: 1019–1028.
17. Kipson S, Linares C, Teixidó N, Bakran-Petricioli T, Garrabou J (2012) Effects of thermal stress on the early development stages of a gorgonian coral. Mar Ecol Prog Ser 470: 69–78.
18. Bauman AG, Baird AH, Cavalcante GH (2011) Coral reproduction in the world's warmest reefs: southern Persian Gulf (Dubai, United Arab Emirates). Coral Reefs 30: 405–413.
19. Goffredo S, Radetić J, Airi V, Zaccanti F (2005) Sexual reproduction of the solitary sunset cup coral *Leptopsammia pruvoti* (Scleractinia, Dendrophylliidae) in the Mediterranean. 1. Morphological aspects of gametogenesis and ontogenesis. Mar Biol 147: 485–495.
20. Lesser MP (2013) Using energetic budgets to assess the effects of environmental stress on corals: are we measuring the right things?. Coral Reefs 32: 25–33.
21. Muscatine L (1990) The role of symbiotic algae in carbon and energy flux in reef corals. In: Dubinsky Z, editor. Coral reefs. Ecosystems of the World. New York: Elsiever. vol. 25, pp. 75–87.
22. Henry LA, Hart M (2005) Regeneration from injury and resource allocation in sponges and corals - a review. International review of hydrobiology 90: 125–158.
23. Graham EM, Baird AH, Connolly SR (2008) Survival dynamics of scleractinian coral larvae and implications for dispersal. Coral Reefs 27: 529–539.
24. Weil E, Cróquer A, Urreiztieta I (2009) Yellow band disease compromises the reproductive output of the Caribbean reef-building coral *Montastraea faveolata* (Anthozoa, Scleractinia). Dis Aquat Org 87: 45.
25. Tamelander J (2002) Coral recruitment following a mass mortality event. Ambio 31: 551–557.
26. Goffredo S, Arnone S, Zaccanti F (2002) Sexual reproduction in the Mediterranean solitary coral *Balanophyllia europaea* (Scleractinia, Dendrophylliidae). Mar Ecol Prog Ser 229: 83–94.

27. Goffredo S, Caroselli E, Mattioli G, Pignotti E, Dubinsky Z, et al. (2009) Inferred level of calcification decreases along an increasing temperature gradient in a Mediterranean endemic coral. Limnol Oceanogr 54: 930–937.
28. Caroselli E, Prada F, Pasquini L, Nonnis Marzano F, Zaccanti F, et al. (2011) Environmental implications of skeletal micro-density and porosity variation in two scleractinian corals. Zoology 114: 255–264.
29. Goffredo S, Caroselli E, Pignotti E, Mattioli G, Zaccanti F (2007) Variation in biometry and population density of solitary corals with environmental factors in the Mediterranean Sea. Mar Biol 152: 351–361.
30. Goffredo S, Caroselli E, Mattioli G, Pignotti E, Zaccanti F (2008) Relationships between growth, population structure and sea surface temperature in the temperate solitary coral *Balanophyllia europaea* (Scleractinia, Dendrophylliidae). Coral Reefs 27: 623–632.
31. Goffredo S, Gasparini G, Marconi G, Putignano MT, Pazzini C, et al. (2010) Gonochorism and planula brooding in the Mediterranean endemic orange coral *Astroides calycularis* (Scleractinia: Dendrophylliidae). Morphological aspects of gametogenesis and ontogenesis. Mar Biol Res 6: 421–436.
32. Goffredo S, Marchini C, Rocchi M, Airi V, Caroselli E, et al. (2012) Unusual pattern of embryogenesis of *Caryophyllia inornata* (Scleractinia, Caryophylliidae) in the Mediterranean Sea: Maybe agamic reproduction?. J Morphol 273: 943–956.
33. Korta M, Murua H, Kurita Y, Kjesbu OS (2010) How are the oocytes recruited in an indeterminate fish? Applications of stereological techniques along with advanced packing density theory on European hake (*Merluccius merluccius* L.). Fish Res 104: 56–63.
34. Lowerre-Barbieri SK, Ganias K, Saborido-Rey F, Murua H, Hunter JR (2011) Reproductive timing in marine fishes: variability, temporal scales, and methods. Mar Coast Fish 3: 71–91.
35. Altman DG (1991) Practical statistics for medical research. New York: Chapman & Hall, CRC. 624 p.
36. Potvin C, Roff DA (1993) Distribution-free and robust statistical methods: viable alternatives to parametric statistics?. Ecology 74: 1617–1628.
37. Michalek-Wagner K, Willis BL (2001) Impacts of bleaching on the soft coral *Lobophytum compactum*. I. Fecundity, fertilization and offspring viability. Coral Reefs 19: 231–239.
38. McClintock JB, Watts SA (1990) The effects of photoperiod on gametogenesis in the tropical sea urchin *Eucidaris tribuloides* (Lamarck)(Echinodermata, Echinoidea). J Exp Mar Biol Ecol 139: 175–184.
39. Goffredo S, Airi V, Radetić J, Zaccanti F (2006) Sexual reproduction of the solitary sunset cup coral *Leptopsammia pruvoti* (Scleractinia, Dendrophylliidae) in the Mediterranean. 2. Quantitative aspects of the annual reproductive cycle. Mar Biol 148: 923–931.
40. Goffredo S, Gasparini G, Marconi G, Putignano MT, Pazzini C, et al. (2011) Sexual reproduction in the Mediterranean endemic orange coral *Astroides calycularis* (Scleractinia, Dendrophylliidae). Bull Mar Sci 87: 589–604.
41. Ribes M, Coma R, Rossi S, Micheli M (2007). Cycle of gonadal development in Eunicella singularis (Cnidaria: Octocorallia): trends in sexual reproduction in gorgonians. Inv Biol 126: 307–317.
42. Harrison PL (2011) Sexual reproduction of scleractinian corals. In Coral Reefs: an ecosystem in transition. Springer Netherlands. pp. 59–85.
43. Kružić P, Žuljević A, Nikolić V (2008) Spawning of the colonial coral *Cladocora caespitosa* (Anthozoa, Scleractinia) in the Southern Adriatic Sea. Coral Reefs 27: 337–341.
44. Kersting DK, Casado C, López-Legentil S, Linares C (2013) Unexpected patterns in the sexual reproduction of the Mediterranean scleractinian coral *Cladocora caespitosa*. Mar Ecol Prog Ser 486: 165–171.
45. De Putron SJ, Ryland JS (2009) Effect of seawater temperature on reproductive seasonality and fecundity of *Pseudoplexaura porosa* (Cnidaria, Octocorallia): latitudinal variation in Caribbean gorgonian reproduction. Invertebr Biol 128: 213–222.
46. Fadlallah YH (1983) Sexual reproduction, development and larval biology in scleractinian corals. Coral reefs 2: 129–150.
47. Richmond RH, Hunter CL (1990) Reproduction and recruitment of corals: Comparisons among the Caribbean, the Tropical Pacific, and the Red Sea. Mar Ecol Prog Ser 60: 185–203.
48. Nakamura E, Yokohama Y, Tanaka J (2004) Photosynthetic activity of a temperate coral *Acropora pruinosa* (Scleractinia, Anthozoa) with symbiotic algae in Japan. Phycol Res 52: 38–44.
49. Al-Horani FA (2005) Effects of changing seawater temperature on photosynthesis and calcification in the scleractinian coral *Galaxea fascicularis*, measured with O_2, Ca^{2+} and pH microsensors. Sci Mar 69: 347–354.
50. Rinkevich B (1989) The contribution of photosynthetic products to coral reproduction. Mar Biol 101: 259–263.
51. Ramirez-Llodra E (2002) Fecundity and life-history strategies in marine invertebrates. Adv Mar Biol 43: 87–170.
52. Hayward A, Gillooly JF (2011) The cost of sex: quantifying energetic investment in gamete production by males and females. PloS One 6: e16557.
53. Leuzinger S, Anthony KR, Willis BL (2003) Reproductive energy investment in corals: scaling with module size. Oecologia 136: 524–531.
54. Maltby L (1999) Studying stress: the importance of organism-level responses. Ecol Appl 9: 431–440.
55. Nespolo RF, Halkett F, Figueroa CC, Plantegenest M, Simon JC (2009) Evolution of trade-offs between sexual and asexual phases and the role of reproductive plasticity in the genetic architecture of aphid life histories. Evolution 63: 2402–2412.
56. Fischer B, Dieckmann U, Taborsky B (2011) When to store energy in a stochastic environment. Evolution 65: 1221–1232.
57. Leuzinger S, Willis BL, Anthony KR (2012) Energy allocation in a reef coral under varying resource availability. Mar Biol 159: 177–186.
58. Fantazzini P, Mengoli S, Evangelisti S, Pasquini L, Mariani M, et al. (2013) Time-Domain NMR study of Mediterranean scleractinian corals reveals skeletal-porosity sensitivity to environmental changes. Environ Sci Technol 47: 12679–12686.
59. Lueg JR, Moulding AL, Kosmynin VN, Gilliam DS (2012) Gametogenesis and spawning of *Solenastrea bournoni* and *Stephanocoenia intersepta* in southeast Florida, USA. J Mar Biol 2012.
60. Okubo N, Motokawa T, Omori M (2007) When fragmented coral spawn? Effect of size and timing on survivorship and fecundity of fragmentation in *Acropora formosa*. Mar Biol 151: 353–363.
61. Goffredo S, Mattioli G, Zaccanti F (2004) Growth and population dynamics model of the Mediterranean solitary coral *Balanophyllia europaea* (Scleractinia, Dendrophylliidae). Coral Reefs 23: 433–443.
62. Sagarin RD, Gaines SD, Gaylord B (2006) Moving beyond assumptions to understand abundance distributions across the ranges of species. Trends Ecol Evol 21: 524–530.
63. Zibrowius H (1980) Les Scléractiniaires de la Méditerranée et de l'Atlantique nord-oriental. Mémoires de l'Institut océanographique, Monaco 11.
64. Goffredo S, Mezzomonaco L, Zaccanti F (2004) Genetic differentiation among populations of the Mediterranean hermaphroditic brooding coral *Balanophyllia europaea* (Scleractinia, Dendrophylliidae). Mar Biol 145: 1075–1083.

OPEN ACCESS Freely available online

PLoS one

The Skeletal Organic Matrix from Mediterranean Coral *Balanophyllia europaea* Influences Calcium Carbonate Precipitation

Stefano Goffredo[2], Patrizia Vergni[1], Michela Reggi[2], Erik Caroselli[2], Francesca Sparla[3], Oren Levy[4], Zvy Dubinsky[4], Giuseppe Falini[1]*

1 Dipartimento di Chimica 'G. Ciamician', Alma Mater Studiorum Università di Bologna, Bologna, Italy, **2** Marine Science Group, Alma Mater Studiorum Università di Bologna, Bologna, Italy, **3** Dipartimento di Biologia Evoluzionistica Sperimentale, Alma Mater Studiorum Università di Bologna, Bologna, Italy, **4** The Mina and Everard Goodman Faculty of Life Sciences, Bar Ilan University, Ramat Gan, Israel

Abstract

Scleractinian coral skeletons are made mainly of calcium carbonate in the form of aragonite. The mineral deposition occurs in a biological confined environment, but it is still a theme of discussion to what extent the calcification occurs under biological or environmental control. Hence, the shape, size and organization of skeletal crystals from the cellular level through the colony architecture, were attributed to factors as diverse as mineral supersaturation levels and organic mediation of crystal growth. The skeleton contains an intra-skeletal organic matrix (OM) of which only the water soluble component was chemically and physically characterized. In this work that OM from the skeleton of the *Balanophyllia europaea*, a solitary scleractinian coral endemic to the Mediterranean Sea, is studied *in vitro* with the aim of understanding its role in the mineralization of calcium carbonate. Mineralization of calcium carbonate was conducted by overgrowth experiments on coral skeleton and in calcium chloride solutions containing different ratios of water soluble and/or insoluble OM and of magnesium ions. The precipitates were characterized by diffractometric, spectroscopic and microscopic techniques. The results showed that both soluble and insoluble OM components influence calcium carbonate precipitation and that the effect is enhanced by their co-presence. The role of magnesium ions is also affected by the presence of the OM components. Thus, *in vitro*, OM influences calcium carbonate crystal morphology, aggregation and polymorphism as a function of its composition and of the content of magnesium ions in the precipitation media. This research, although does not resolve the controversy between environmental or biological control on the deposition of calcium carbonate in corals, sheds a light on the role of OM, which appears mediated by the presence of magnesium ions.

Citation: Goffredo S, Vergni P, Reggi M, Caroselli E, Sparla F, et al. (2011) The Skeletal Organic Matrix from Mediterranean Coral *Balanophyllia europaea* Influences Calcium Carbonate Precipitation. PLoS ONE 6(7): e22338. doi:10.1371/journal.pone.0022338

Editor: Maria Gasset, Consejo Superior de Investigaciones Cientificas, Spain

Received March 5, 2011; **Accepted** June 24, 2011; **Published** July 22, 2011

Funding: The research leading to these results has received funding from the European Research Council under the European Union's Seventh Framework Programme (FP7/2007-2013)/ERC grant agreement n° [249930 - CoralWarm: Corals and global warming: the Mediterranean versus the Red Sea]. The funder had no role in study design, data collection and analysis, decision to publish, or preparation of the manuscript.

Competing Interests: The authors have declared that no competing interests exist.

* E-mail: giuseppe.falini@unibo.it

Introduction

Organisms exert an exceptional control over the polymorphism, orientation and morphology of their mineral components through a series of biochemical processes generally included under the term biomineralization [1–4]. It is generally recognised that the biomineralization process involves several steps: the fabrication of a hydrophobic solid organic substrate; the nucleation of crystalline materials associated with specific polyanionic macromolecules that cover the internal wall of the organic scaffold; the crystal growth, controlled by new secretions of polyanionic macromolecules; the termination of the process by secretion of inhibitory macromolecules [1,5].

Specific functions related to different types of molecules were shown for the organic matrix (OM) associated to the calcium carbonate polymorphs found in animal skeletal and shell elements: calcite, aragonite, vaterite or amorphous calcium carbonate (ACC). Pioneering *in vitro* experiments have shown the influence of acidic glycol-proteins on the morphological control of calcite deposition, highlighting an important role of the glycosidic regions in morphology modulation [6]. The capability of OM to determine the aragonite versus calcite polymorphic selection was determined in mollusc shells [7]. This organic control on the calcium carbonate polymorphism was also verified by the abrupt transition calcite-aragonite in abalone shells, accompanied by the synthesis of specific polyanionic proteins [8]. Acidic macromolecules associated with aragonite or vaterite from fish otoliths influence this polymorphic selection [9]. Families of mixed acidic macromolecules have always been used in all these studies. Only recently a specific protein, Pif1, able to selectively deposit aragonite on a chitin substrate was completely characterized [10]. The function of acid macromolecules can be triggered by the presence of magnesium ions. In a recent research was shown that ACC stabilized by magnesium ions can be converted into calcite by the addition of aspartic acid. The aspartic acid destabilizes the hydration of magnesium ions, thus favouring the precipitation of

calcite. This important observation was used to explain how organisms can control the phase transformation from ACC into calcite [11].

Among calcium carbonate depositing organisms, corals are of primary importance due to their dominance in shallow shores in the tropics. Corals give the opportunity of investigating many phenomena of geochemical, biochemical, mineralogical, ecological and paleontological interest [12,13]. Nowadays, corals relevance as calcium carbonate crystallizers is of extreme importance in view of the effects of global warming and ocean acidification [14,15].

The mineralogy of aragonitic skeleton of scleractinian corals was investigated in great detail [16,17]. The building blocks of the skeleton are formed of thin aragonite crystals or fibres (0.04–0.05 μm in diameter), which set up in a tri-dimensional structure. The fibres are preferentially orientated along the crystallographic *c*-axis of aragonite and are assembled as *spherulites*, grouped into fishead-shaped bundles. A building block grow into a vertical spine called *trabecula*; groups of trabeculae form the *septa*, the primary macroscopic structure of the coral skeleton, arranged inside the skeleton in a radial way, which is species specific [18]. At the centre of each spine there is the *centre* of *calcification* (COC, nucleation centre), from which the aragonite fibres growth. Inside the COCs granular sub-micronic crystals grouped in 2–4 μm nuclear packets are located [19,20].

The morphological relationship between OM and mineral phases in coral unit crystals is poorly understood. OM is synthesized by cells of the calicoblastic epithelium and then secreted into the adjacent subepithelial space in which calcification takes place [21]. The OM of scleractinian corals was investigated in detail in its structure and relation with the mineral phase [20,22–26]. The whole OM is made of glycoproteins in which the proteic regions assume preferentially a α-helical conformation in all the coral species studied, except in one case [26], where a β-sheet conformation was observed. The amino-acid analysis of OM from representative coral skeletons showed a similar composition characterized by a high content of Glu, Asp and Gly. Moreover, Gln, Ser, and Thr were demonstrated to act respectively as N- and O- linking sites for glucidic regions, which were found to be sulphated [24,27]. X-ray Absorption Near Edge Structure (XANES) mapping of the earliest COC and the fibrous zone, the two main structural entities of the coral skeleton, has shown the correspondence between S-polysaccharides and the spatial arrangement of mineral growth and have evidenced 1) a biochemical zonation that corresponds to the step by step growth, and 2) the general coordination by polyp physiology [20,22,24,26].

The calcium carbonate precipitation is influenced by environmental conditions [28,29]. It was suggested that seawater Mg/Ca molar ratio influences the polymorphism of calcium carbonate in coral skeletons. Corals should calcify calcite when the Mg/Ca molar ratio is below 2, and aragonite when the ratio is above 2. A cretaceous scleractinians had a calcitic skeleton, when the inferred Mg/Ca ratio of seawater was below 2 [30]. Current Mg/Ca molar ratio of seawater is around 5, then several studies claim that living scleractinians have aragonitic skeletons, due to a strong if not an exclusively environmental control on calcification [31–33]. Other researchers have suggested a minor, or indirect, role of the organism in the precipitation processes. In this case the biological control is directed towards the calcium carbonate supersaturation level [34,35]. However, this is in contrast with the observation of a high biological control on the kind of skeletal material produced in corals [20,22–26,36], gorgonians [37], molluscs [7,8], seastars [38] and fish otoliths [9].

Several clues support the existence of a biological influence over the mineral deposition. First, the ultra-structural organization of the aragonite crystals in coral skeleton shows differences from the one of aragonite precipitated abiologically and is species specific. Second, in the coral skeleton, COCs rich of biological macromolecules were identified, suggesting a controlled release of macromolecules in space and time by the organism [20,22–26,36]. Third, many organisms exert a tremendous biological control over the calcium carbonate polymorphic selection. Indeed, in several mineralized tissues aragonite, calcite and vaterite, the anhydrous calcium carbonate polymorphs, are present and localized in different regions and are never mixed together [1]. This high level of control is mainly due to specific families of acidic macromolecules [1–4], which are intimately associated with the mineral phases. Over the years this was demonstrated, mainly by *in vitro* experiments, for mollusc shells and fish otoliths among many (e.g. [7–9]).

In the present work, *in vitro* mineralization of calcium carbonate was conducted in presence of both water soluble and insoluble fractions of the intra-skeletal OM from the aragonitic skeleton of *Balanophyllia europaea* (Scleractinia) and magnesium ions at different concentrations. This research was done with the aim to explore the relative biological (OM) and environmental (Mg ions) influence on polymorphism and morphology of $CaCO_3$ in the biomineralization of *B. europaea*, an endemic Mediterranean coral living in shallow water (maximum population density at depth <10 m) [39], which has served as model organism and extensively studied in its main aspects of growth, population structure and dynamics, and reproductive biology [40].

Materials and Methods

Coral skeletons

Samples of *Balanophyllia europaea* were randomly collected during scuba diving at 5–7 m depth from two sites in the North-Western Mediterranean Sea: Calafuria 43°27′N, 10°21′E (CL) and Elba Island, 42°45′N, 10°24′E (LB). After collection the corals were dipped in a sodium hypochlorite solution (commercial) for 4 days until the polyp tissue was completely dissolved, then the remaining skeletons were washed with double distilled water and dried in oven at 37°C for 24 hr and stored. Each skeleton was analyzed under a binocular microscope to remove fragment of substratum and calcareous deposit produced by other organisms. Successively, the skeletons were ground in a mortar to obtain a fine and homogeneous powder. The obtained powder was further suspended (1% w/v) in a sodium hypochlorite solution (3% v/v) to remove traces of organic material eventually not removed from the first treatment.

Extraction of the organic components

5 ml of milliQ water, in which 2.5 g of powdered coral skeleton were dispersed, were poured in a 50 cm-long osmotic tube for dialysis (MWCO = 3.5 kDa; CelluSep®, MFPI). The sealed tube was put into 1 L of 0.1 M CH_3COOH (Riedel–de Haen) solution under stirring. The decalcification proceeded for 72 hr. At the end the tube containing the dissolved OM was dialysed against milliQ water until the final pH was about 6. The obtained aqueous solution containing the OM was centrifuged at 30 g for 3 min to separate the soluble (SOM) and the insoluble (IOM) organic matrix fractions, which were then lyophilized and weighted. The content of OM in the skeleton was gravimetrically determined.

Characterization of the organic matrix

SDS-PAGE was performed on 12.5% polyacrylamide gel in a vertical slab gel apparatus (Mini-PROTEAN®, Bio-Rad). Different sample volumes were applied for gel lane (10–20 μl). Samples

were prepared adding reduced sample buffer 1× (60 mM Tris-HCl pH 6.8; 2% SDS; 2.5% β-mercaptoethanol; 10% glycerol; 0.025% bromophenol blue) and then boiled at 100°C for 5 minutes. The gels ran at a constant voltage of 100 V for 1.5 hr at room temperature. Proteins were detected with Coomassie Brilliant Blue. In the stained procedure, the gel was immersed for 1 hr under shaking in Coomassie Brilliant Blue Staining Solution (0.1% Coomassie Blue R-250 in 1% acetic acid/40% MeOH) and then placed in destaining solutions (25% ethanol and 8% acetic acid) until band became evident. Aminoacid analysis was conducted by a chromatographic technique using an amino acid analyzer. The organic matrix material was weighed, then hydrolyzed at 110°C for 24 hr in 6 M HCl vapor, and analyzed using a Dionex BIOLC amino acid analyzer. Spectroscopic Fourier Transform Infra Red (FTIR) analyses were conducted by using a FTIR Nicolet 380 Thermo Electron Corporation working in the range of wave-numbers 4000–400 cm^{-1} at a resolution of 2 cm^{-1}. Disk was obtained by mixing little amounts (<1 mg) of SOM or IOM with 100 mg of KBr and applying a pressure of 48.6 tsi (670.2 MPa) to the mixture using a hydraulic press. UV/Vis analysis was conducted with a Cary UV/Vis 300BIO Varian instrument, in a range between 190 nm e 800 nm, using milliQ water as blank.

Calcium carbonate overgrowth experiments

Small pieces (about 3 mm) of coral skeleton were place in a Petri dish (d = 5.4 cm) in different orientations, as the overgrowth could not be uniform on all surfaces. The specimens were overlaid with 10.0 mL of 10 mM $CaCl_2$ solution. Calcium carbonate crystals were grown for one month. The overgrown specimens were then lightly rinsed with milliQ water, dried and examined in the scanning electron microscope (SEM) after coating with gold.

Calcium carbonate crystallization experiments

A 30×30×50 cm^3 crystallization chamber was used. Two 25 mL beakers half-full of $(NH_4)_2CO_3$ (Carlo Erba) covered with Parafilm 10 times holed and two Petri dishes (d = 8 cm) full of anhydrous $CaCl_2$ (Fluka) were put inside the chamber. Microplates for cellular culture (MICROPLATE 24 well with Lid, IWAKI) containing a round glass cover slip in each well were used. In each well, 750 µL of 10 mM $CaCl_2$ solutions having Mg/Ca ratio equal to 0, 3 or 5 ($CaCl_2.2H_2O$, Merck; $MgCl_2.6H_2O$, Sigma-Aldrich) were poured. SOM aliquots giving concentration 1.06 mg/mL, 0.44 mg/mL (hereafter reported as c_s) or 0.11 mg/mL were added for each Mg/Ca solution. In other experiments 0.5 mg of IOM (hereafter reported as c_i) were added at each Mg/Ca solution. SOM (c_s) and IOM (c_i) were added in each well in a third set of experiments. The micro-plate was covered with aluminium foil and a hole was made over every well. The experiment proceeded for 4 days. At the end of the crystallization experiment the pH of the solutions in each well was measured. The obtained crystals were washed two times with milliQ water and then analyzed. All the experiments were conducted at room temperature. The crystallization trials of calcium carbonate in the different conditions were replicate at least ten times starting from different batches of organic matrix fractions.

Characterization of $CaCO_3$ precipitates

X-ray powder diffraction patterns were collected using a PanAnalytical X'Pert Pro equipped with X'Celerator detector powder diffractometer using Cu Kα radiation generated at 40 kV and 40 mA. The diffraction patterns were collected within the 2θ range from 10° to 60° with a step size (Δ2θ) of 0.02° and a counting time of 1200 s. FTIR spectra of samples in KBr disks were collected at room temperature by using a FTIR Nicolet 380 Thermo Electron Corporation working in the range of wavenumbers 4000–400 cm^{-1} at a resolution of 2 cm^{-1}. A finely ground, approximately 1% (*w*/*w*) mixture of the sample in KBr was pressed into a transparent disk using a hydraulic press and applying a pressure of 48.6 tsi (670.2 MPa). The optical microscope (OM) observations were made with an Leika optical microscope equipped with a digital camera. The SEM observations were conducted in a scansion electronic microscope, Philips SEM-XL20 equipped with a CCD camera after specimens coating with gold and directly in a Phenom™ microscope (FEI).

Results

XRD and FTIR analyses of the powdered skeletal samples of *Balanophyllia europaea* showed that in the whole skeleton the main calcium carbonate polymorph is aragonite and that calcite sometimes appears in trace amounts. In the bigger skeletons (above 3 g), the ones used in our experiments, only aragonite was present (Fig. 1).

The percentage of the overall OM in the skeleton, gravimetrically determined, was around 0.3% (*w*/*w*). A water soluble (SOM) and insoluble (IOM) organic matrix fractions were obtained. The mass ratio of SOM and IOM, changed from one experiment to another and was not easy to accurately quantify, however, it was always above 1.5. The chemical-physical characterization of the OM fractions was performed by FTIR spectroscopy, polyacrylamide gel electrophoresis and amino-acidic analyses. In FTIR spectra of both SOM and IOM fractions, typical proteic and polysaccharidic adsorption bands were observable (Fig. 2). The proteic bands of the amide I (1612 cm^{-1} and 1637 cm^{-1} in SOM, and 1619 cm^{-1} and 1638 cm^{-1} in IOM) and II (1558 cm^{-1} in SOM and 1546 cm^{-1} in IOM) were present. The wave-number of the amide I bands at 1637/8 cm^{-1} is typical of a protein in a β-sheet conformation. The amide II band at 1558 cm^{-1} in the SOM and 1546 cm^{-1} in the IOM corresponds to a β-turn and are related to glutamic acid. The relative absorption of the amide II in the SOM fraction was higher than that in the IOM, with respect to the amide I bands; the 1735 cm^{-1} or 1732 cm^{-1} peak is characteristic of the carboxyl group and it is related to aspartic acid. The 1250 cm^{-1} (SOM spectra) and 1220 cm^{-1} (IOM spectra) absorption bands can be attributed to the O-sulphated group or to the amide III [22–26]. It was possible to note a shift of both 1558–1546 cm^{-1} and 1250–1220 cm^{-1} peaks from SOM to IOM. The region between 1467–1384 cm^{-1} presented some difference between SOM and IOM fraction: the SOM had peaks at 1467 cm^{-1} (carboxylate group), 1454 cm^{-1} (–CH_2 or to =CH_2 bending), 1420 cm^{-1} (carboxylate group), 1384 cm^{-1} (carbonyl group); all of them were of high intensities and were very well identifiable. The IOM had instead a very weak absorption in that range and only the 1463 cm^{-1} and 1384 cm^{-1} peaks were clearly identifiable. The sugar region (1030–1078 cm^{-1}) presented similar pattern of adsorption bands between the SOM and the IOM sample. In the IOM there was only a well resolved peak at 1078 cm^{-1}, while in the SOM one there were three evident peaks, 1030 cm^{-1}, 1052 cm^{-1} and 1078 cm^{-1}. The FTIR spectra also show absorption bands at 2956 cm^{-1}, 2923 cm^{-1}, and 2852 cm^{-1} that are due to the presence of lipids [41]. The macromolecules comprising the SOM and IOM fractions were also investigated by SDS-polyacrylamide gel electrophoresis. The gel revealed several macromolecular species with molecular masses ranging from ca. 14 to 66 kDa (Fig. 3). Both IOM and SOM fractions were characterized by the presence of the same macromolecular species, gathered around two main molecular weight distributions around 66 kDa and 14 kDa. The relative

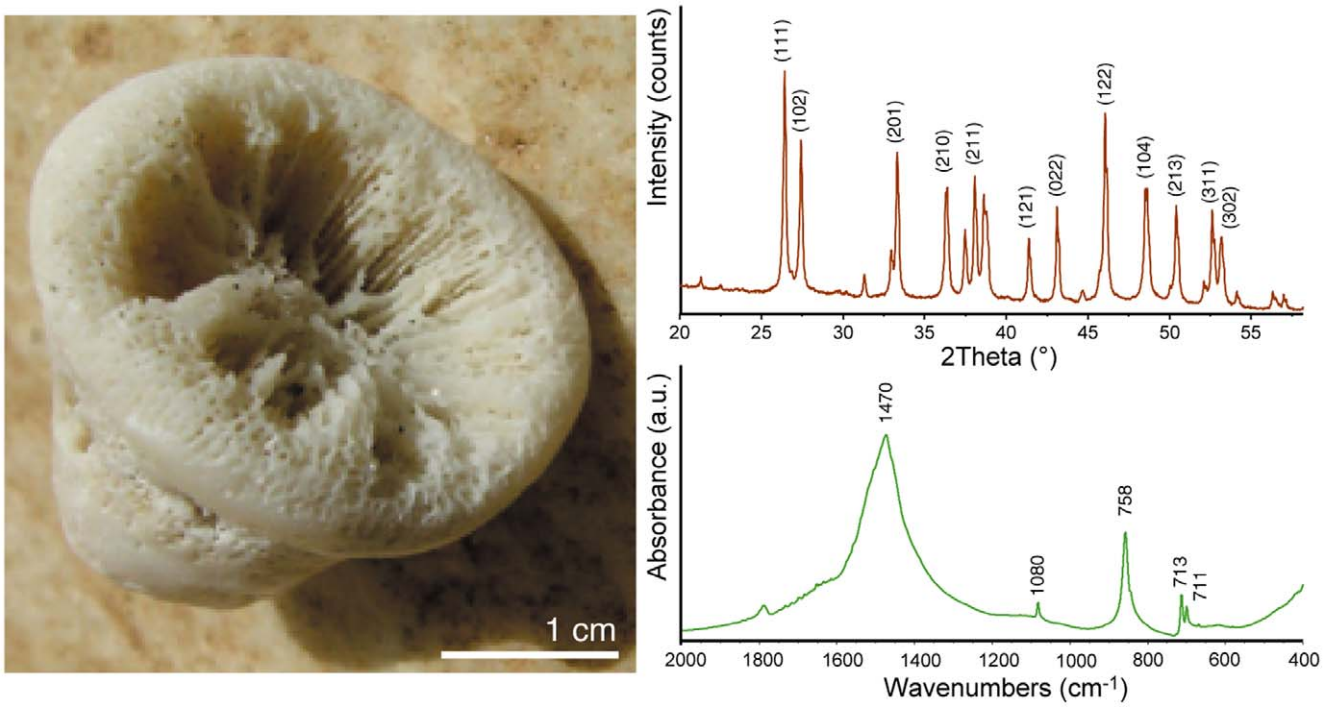

Figure 1. Skeleton of the coral *Balanophyllia europaea*. (A) Digital camera picture of the skeleton of the coral *Balanophyllia europaea* after digestion in a sodium hypochlorite solution to remove the soft organic tissues. (B) X-ray powder diffraction pattern from a powdered coral skeleton sample. Only the characteristic diffraction peaks from aragonite are observable. The main diffraction peaks of the Miller index are indicated according to the reference pattern PDF 98-006-0908 [60]. (C) FTIR spectrum from a powdered coral skeleton sample. Only the typical absorption bands from aragonite were detected. They were assigned as $\nu_2 = 858\ cm^{-1}$; $\nu_3 = 1470\ cm^{-1}$; $\nu_4 = 713\ cm^{-1}$ [42].
doi:10.1371/journal.pone.0022338.g001

intensity of the bands in these two regions changed between IOM and SOM, the former being richer of high molecular weight macromolecular species with respect to the latter. The amino acid composition of the proteic regions of IOM and SOM is reported in Table 1. The SOM was characterized by a high content of acidic residues, above 56 mol %: Asx (aspartate or aspargine residues) 50.0 mol %, and Glx (glutamate or glutamine residues) about 6 mol %. On the contrary in the IOM the content of acidic residues was low, about 20 mol%: Asx about 12 mol% and Glx about 8 mol%. The content of hydrophobic residues was higher in IOM than in SOM; in fact Gly, Ala, Val, Ile and Lue represented about 50 mol% and about 30 mol% in IOM and SOM, respectively. In IOM proline was present (about 4 mol%), which was absent in SOM.

The results of the calcium carbonate overgrown experiments on a coral skeleton fragment are illustrated in figure 4. Overgrowth of aragonite and calcite crystals occurred on the aragonitic skeleton surfaces (Fig. 4-A). The crystals were oriented in different directions, probably reflecting the topography of the substrate. The overgrown of needle like crystals of aragonite occurred in different locations of the skeleton septa as aggregates of different sizes (Fig. 4-B). They usually appeared organized clustered in bunch of fibers which locally exhibited preferential orientation (Fig. 4-C and inset). Organic matrix was observed among the crystals of aragonite (arrows in Fig. 3-B-inset and Fig. 4-C). The overgrown calcite crystals exhibit an additional group of faces other than the {104} set (Fig. 4-D and inset). Measurement of the overgrown calcite crystal faces show that that the new formed faces can be gathered in a family parallel to the crystallographic c-axis. The extension of the new family {hk0} of the crystal faces on the overgrowth calcite crystals changed with the location on the coral skeleton. In rare cases the calcite crystals did show only the {104} cleavage faces.

Calcium carbonate was also precipitated in solution in the presence SOM, IOM and/or magnesium ions. The deposited mineral phases were revealed by FTIR measurements and, in some cases, confirmed by XRD (Table 2), while their morphology was observed by optical and electron microscopes (Figures 5, 6, 7). These data summarize the results of more than ten calcium carbonate independent crystallization experiments using different batches of OM components. It is important to state that it was not possible to get a complete control over the crystallization process in the presence of OM fractions. Thus, the presented data represent the general trend of the crystallizations trials. Among the single experiment some difference could be present in the relative amount of polymorphs and the exposition of new crystalline faces in calcium carbonate crystals.

In the absence of additives, neither magnesium ions nor OM components, only the deposition of rhombohedral calcite crystals was observed from a 10 mM calcium chloride solution (Fig. 5-Ctrl). In the presence of a concentration of SOM equal to 0.11 mg/mL ($0.25c_s$), the precipitation of calcite occurred as in the absence of additives. With a concentration of SOM of 1.06 mg/mL, $2.5c_s$, the complete inhibition of the precipitation was observed. In the presence of c_s of SOM an aggregation of the crystals in spherulites that were rhombohedral capped was observed (Fig. 5-SOM inset). These aggregates formed on the surface of a shapeless precipitate (Fig. 5-SOM). The FTIR spectrum of this material showed the characteristic absorption bands of calcite, $\nu_2 = 875\ cm^{-1}$; $\nu_3 = 1432\ cm^{-1}$; $\nu_4 = 713\ cm^{-1}$ [42] plus broad bands at $1030\ cm^{-1}$ and $1082\ cm^{-1}$. These latter two bands could be associated to SOM and to ACC [43], respectively. In the presence of dispersed IOM ($c_i = 0.5$ mg) IOM the precipitation of calcite was detected by FTIR. In this case the broad bands around $1050\ cm^{-1}$ showed a weak absorption.

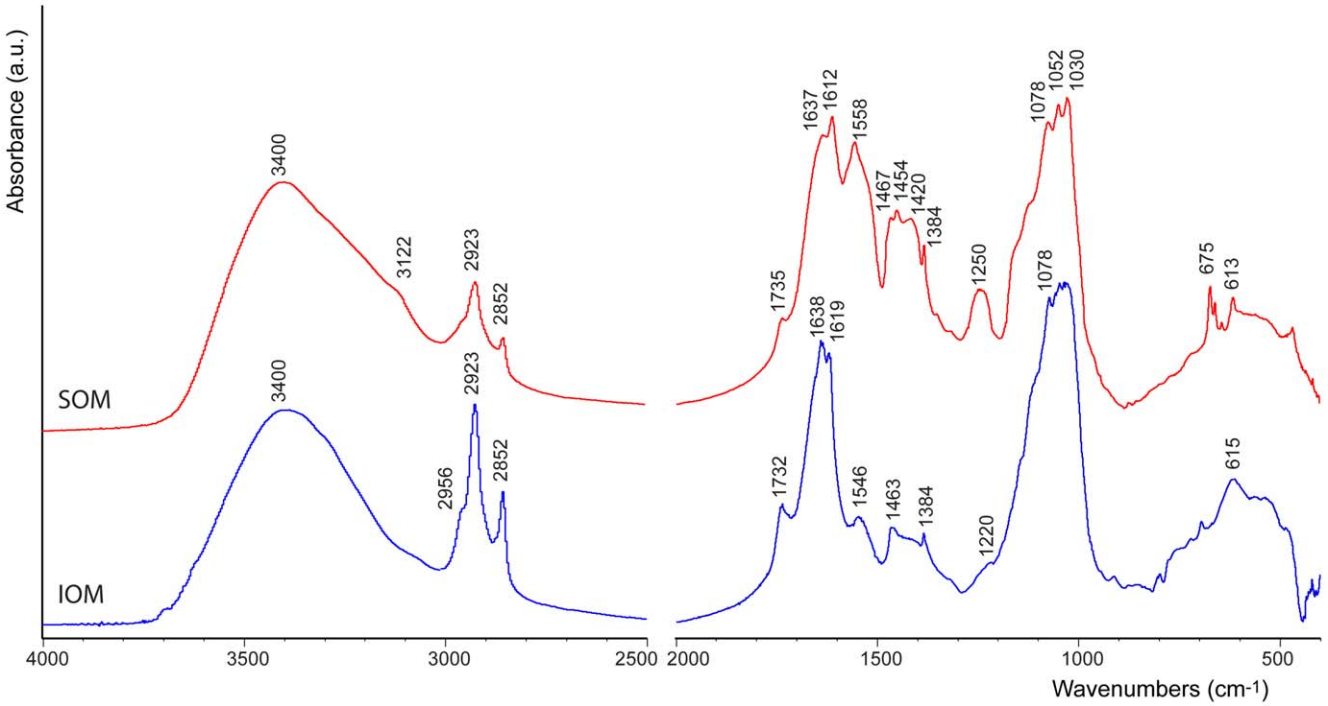

Figure 2. OM characterization. FTIR spectra of intra-skeletal soluble (SOM) and insoluble (IOM) organic matrix from the *Balanophyllia europaea* aragonitic skeleton. Typical absorption bands from protein molecules (around 1600 cm^{-1}), polysaccharides (around 1000 cm^{-1}) and lipids (around 2900 cm^{-1}) are indicated. The absorption due to the polysaccharidic regions appeared stronger than the one due to the proteic regions in both the IOM and SOM spectra.
doi:10.1371/journal.pone.0022338.g002

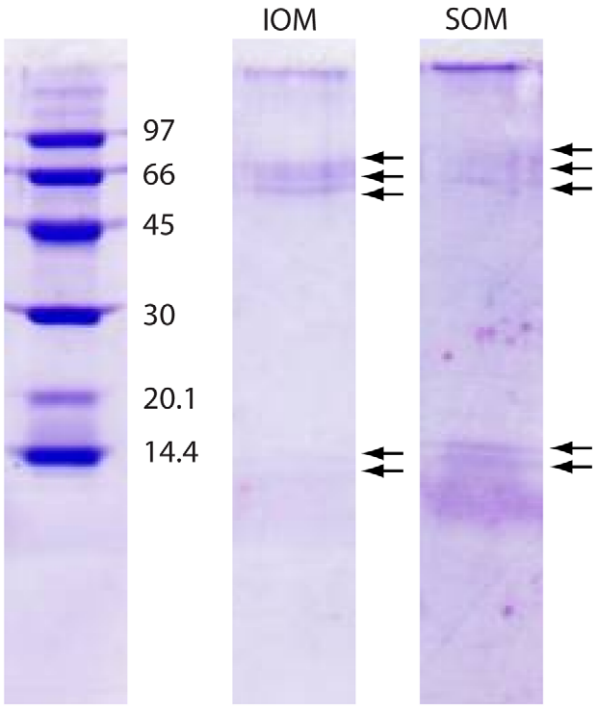

Figure 3. OM characterization. SDS-polyacrylamide gels electrophoresis of intra-skeletal insoluble (IOM) and soluble (SOM) organic matrix extracted from the *Balanophyllia europaea* skeleton. In the first lane the markers are reported. The arrows indicate the major proteic bands.
doi:10.1371/journal.pone.0022338.g003

Table 1. Amino acid compositions (relative mol %) of proteins extracted from the soluble (SOM) and insoluble (IOM) fractions of the *Balanophyllia europaea* skeleton intra-skeletal organic matrix.

	SOM	IOM
Cys	-*	-
Asx	50.0	12.6
Met	-	-
Thr	1.7	4.2
Ser	12.2	9.4
Glx	6.1	8.6
Pro	-	3.7
Gly	18.6	24.3
Ala	4.1	13.2
Val	2.6	4.8
Ile	1.5	4.6
Leu	2.0	5.3
Tyr	-	1.9
Phe	1.2	3.0
His	-	1.2
Lys	-	3.2

*- indicates a not detectable amount.
doi:10.1371/journal.pone.0022338.t001

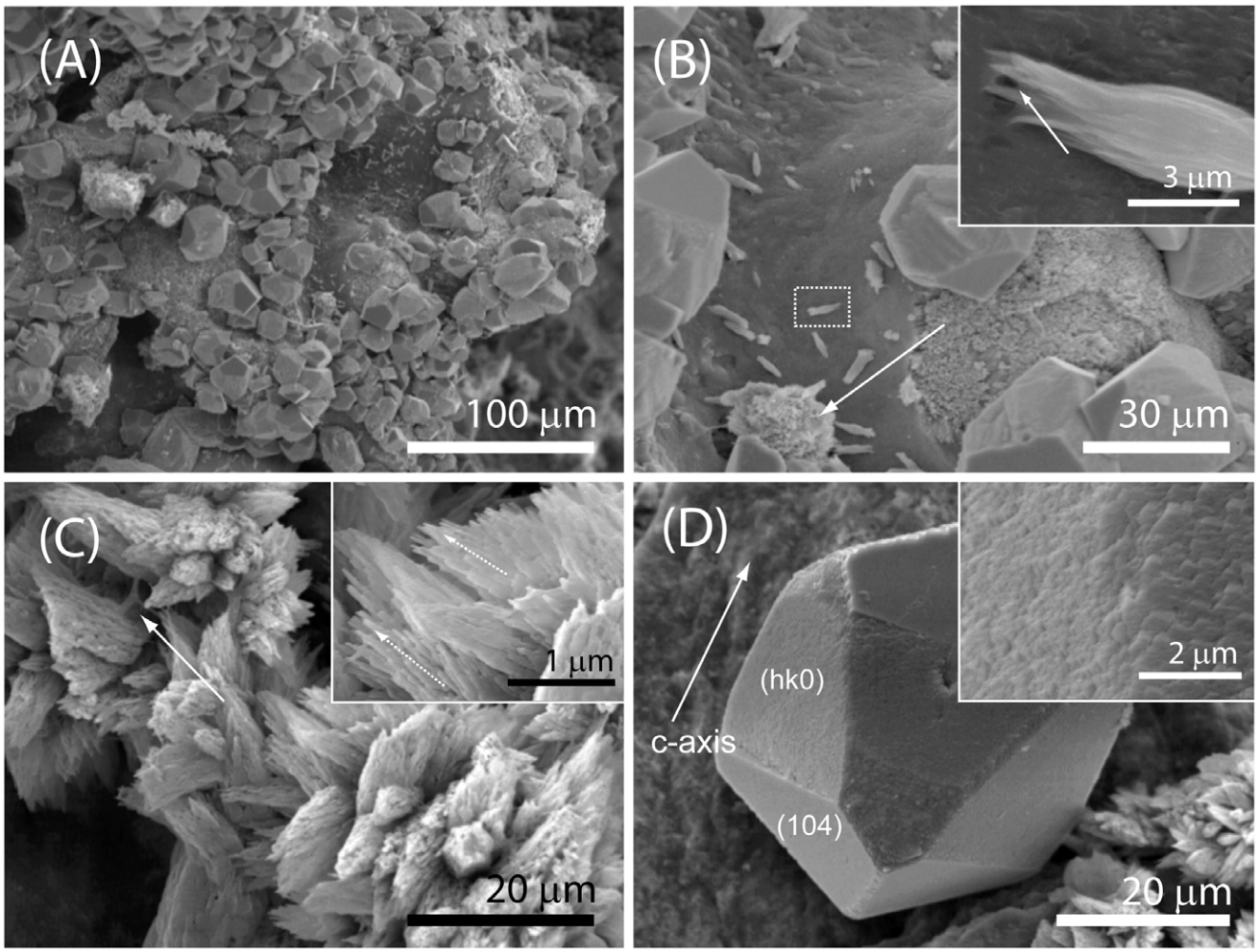

Figure 4. Calcium carbonate overgrowth experiments. (A–D) SEM pictures of a fragment of coral skeleton after the calcium carbonate overgrowth experiment. The overgrowth of calcite and aragonite crystals was observed as shown in (B). In (B) the arrow indicates an aggregate of crystals of aragonite and the dashed square the area illustrated at higher magnification in the inset. The crystals of aragonite appear clustered in bunch of fibers (C), which locally exhibited preferential orientation (arrows in the inset in C). Organic matrix is visible in contact with the crystals of aragonite (arrows in inset in B and in C). The crystals of calcite showed an additional group of {hk0} faces other than the {104} set (D). These new faces showed as smooth surface, typical of interaction with macromolecules (inset in D).
doi:10.1371/journal.pone.0022338.g004

Table 2. Crystalline phases precipitated at different amounts of magnesium ions in 10 mM calcium chloride solutions and in the presence of SOM ($c_s = 044$ mg/mL), IOM ($c_i = 050$ mg) or both of them, SOM+IOM (c_s SOM; c_i IOM).

$[Mg^{2+}]/[Ca^{2+}]$	Ctrl*	SOM	IOM	SOM+IOM
0	C	C	C	**C** A
3	C A	C	**C** A	C A
5	**A** C	**C** A	A C	**A** C

A and C indicate aragonite and calcite, respectively. When two phases are obtained the main phase is indicated in bold.[#]

[#]The reported data represent the trend observed from more than 10 independent replica of crystallization experiments using different batches of OM fractions. The presence of ACC is not indicated.

*Ctrl indicates mineralization experiment conducted in the absence of organic matrix.

doi:10.1371/journal.pone.0022338.t002

Calcite crystals were observed on the IOM and almost conserved the classical rhombohedral morphology (Fig. 4-IOM). The co-presence of SOM (c_s) and IOM (c_i) favoured the precipitation of small crystals that clustered in big aggregates. On their surface, big rounded precipitates formed (Fig. 5-SOM+IOM and inset). The FTIR spectrum of this material showed, together with the absorption bands observed in the presence of SOM, an additional band at 858 cm^{-1}, which is characteristic of aragonite (ν_2) [42]. The second ν_2 band (844 cm^{-1}) of aragonite, related to the substitution of strontium to calcium in the aragonite lattice, was not observed.

A second set of experiments was conducted in the presence of magnesium ions, with Mg/Ca molar ratio equal to 3 (Fig. 6). In this condition the only presence of magnesium ions was able to change the crystal morphology and the polymorphism of the precipitated calcium carbonate (Fig. 6-Ctrl3) with respect to the absence of additives. Indeed, crystals elongated along the c-axis (Fig. 6-Ctrl3, inset) and acicular spherulites (see inset in Fig. 7-Ctrl5) were observed. The corresponding FTIR spectrum showed the typical absorption bands of calcite ($\nu_2 = 875$ cm^{-1}) and

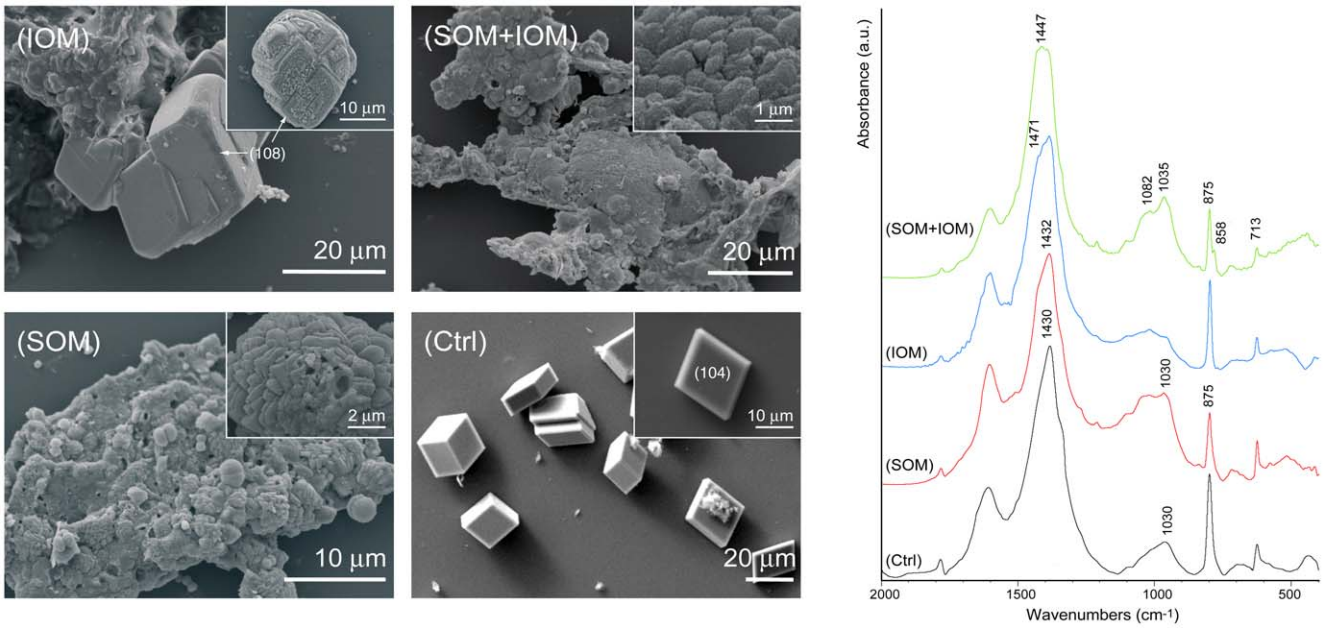

Figure 5. Calcium carbonate crystallization experiments. Crystallization experiments of calcium carbonate from 10 mM $CaCl_2$ solution in the absence of additives (Ctrl) and in the presence of soluble organic matrix (SOM), insoluble organic matrix (IOM) or both additives (IOM+SOM). The Miller indexes of calcite faces are indicated. *left* Scanning electron microscope images, the insets show sample details. *right* FTIR spectra of the precipitated. The main absorption bands of calcium carbonate are indicated.
doi:10.1371/journal.pone.0022338.g005

aragonite ($\nu_2 = 858\ cm^{-1}$), together with the no diagnostic ones. No strong IR absorption was present in the region around $1050\ cm^{-1}$. In the same conditions the addition of c_s of SOM provoked a strong aggregation of the elongated crystal of magnesium calcite (Fig. 6-SOM and inset), which almost lost the crystalline habitus. The FTIR spectrum of this material did not show the absorption band of aragonite ($\nu_2 = 858\ cm^{-1}$), while all those typical of calcite were present, although the band at $713\ cm^{-1}$ (ν_4) was very weak, in addition to two broad bands centred at about $1030\ cm^{-1}$ and $1082\ cm^{-1}$. In the presence of

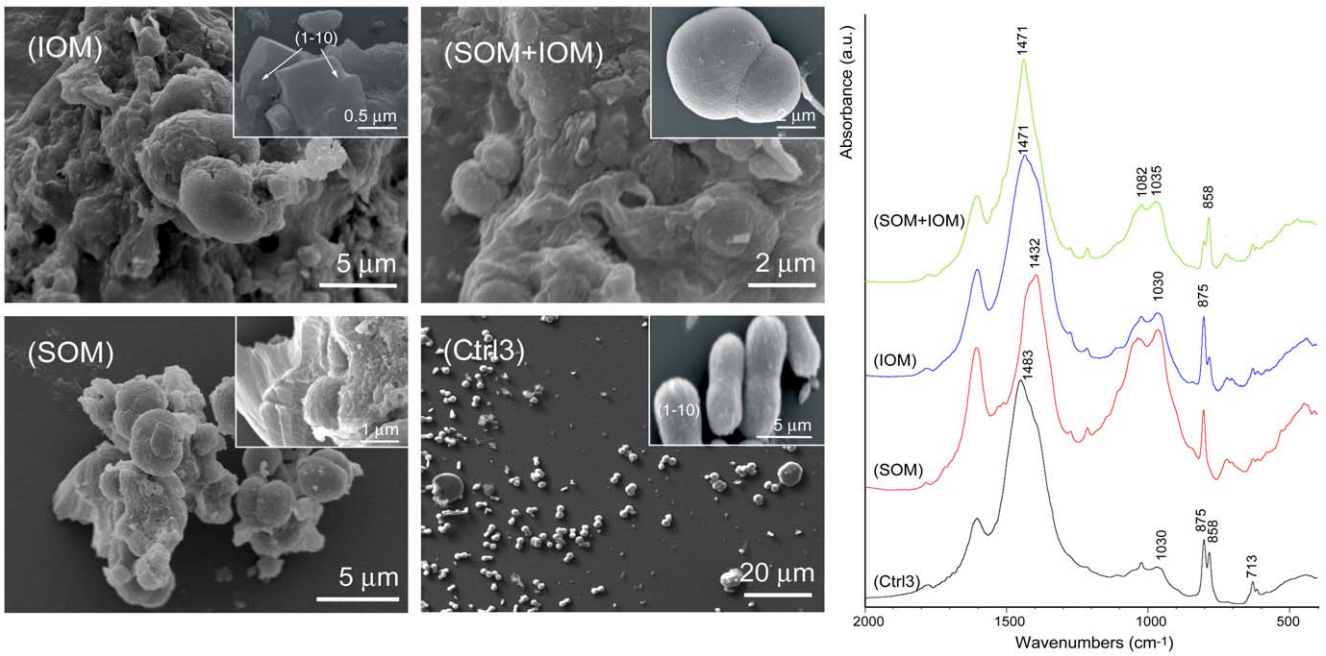

Figure 6. Calcium carbonate crystallization experiments. Crystallization experiments of calcium carbonate from 10 mM $CaCl_2$ solution with a Mg/Ca molar ratio equal to 3 (Ctrl3) and in the presence of soluble organic matrix (SOM), insoluble organic matrix (IOM) or both of these (IOM+SOM). The Miller indexes of calcite faces are indicated. *left* Scanning electron microscope images, the insets show sample's details *right* FTIR spectra of the precipitated. The main absorption bands of calcium carbonate are indicated.
doi:10.1371/journal.pone.0022338.g006

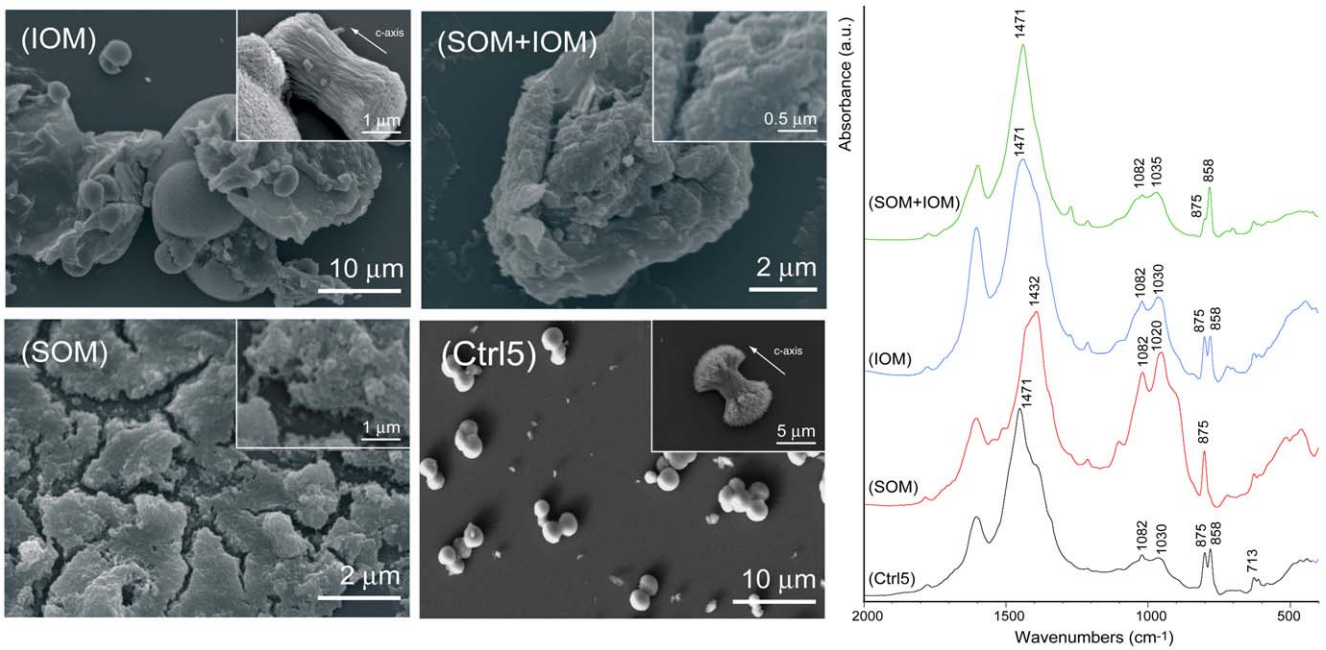

Figure 7. Calcium carbonate crystallization experiments. Crystallization experiments of calcium carbonate from 10 mM $CaCl_2$ solution with a Mg/Ca molar ratio equal to 5 (Ctrl5) and in the presence of soluble organic matrix (SOM), insoluble organic matrix (IOM) or both additives (IOM+SOM). The direction of the crystallographic *c*-axis of aragonite is indicated. *left* Scanning electron microscope images, the insets show samples details *right* FTIR spectra of the precipitated. The main absorption bands of calcium carbonate are indicated.
doi:10.1371/journal.pone.0022338.g007

IOM it was possible to observe the crystals grown on the insoluble matrix substrate and still presenting the typical morphology of magnesium calcite (inset in Fig. 6-IOM). The FTIR spectrum showed typical bands of calcite and aragonite, although acicular spherulites of aragonite were not observed. Also in this case the calcitic ν_4 (713 cm^{-1}) band was very weak compared to the ν_2 one. The co-presence of SOM and IOM provoked the deposition of surface smooth spherulites (Fig. 6-SOM+IOM and inset). The FTIR spectrum of this material showed the typical absorption bands of calcite ($\nu_2 = 875$ cm^{-1}) and aragonite ($\nu_2 = 858$ cm^{-1}). Broad absorption bands at 1030 cm^{-1} and 1082 cm^{-1} were also present.

The results of crystallization experiments of calcium carbonate from solutions with Mg/Ca molar equal to 5 is illustrated in figure 7. In the absence of SOM and IOM the precipitation of spherulitic aggregates of acicular crystals was mainly observed (Fig. 7-Ctrl5 and inset). The FTIR spectrum showed the typical absorption band of aragonite ($\nu_2 = 858$ cm^{-1}, stronger) and calcite ($\nu_2 = 875$ cm^{-1}, weaker), with weak absorption of the bands at 1030 cm^{-1} and 1082 cm^{-1}. The band ν_4 was centred at 715 cm^{-1} and although weak, was clearly visible. The ν_4 band of calcite shows a characteristic shift to higher wavenumber when magnesium substitute calcium in the calcite crystal lattice [42]. The addition of c_s of SOM provoked a strong effect on the morphology of the precipitate, which appeared as a layer formed by strongly aggregated micro-units (Fig. 7-SOM and inset). The FTIR spectrum of this material showed the adsorption bands of calcite ($\nu_2 = 875$ cm^{-1}; $\nu_3 = 1432$ cm^{-1}; $\nu_4 = 715$ cm^{-1}) and two strong broad absorption bands centred at 1020 cm^{-1} and 1082 cm^{-1}. In the presence of c_i of IOM the crystals deposited on the surface of the insoluble matrix substrate (Fig. 7-IOM). Some of them were formed by aggregation of acicular crystal, similar to those obtained in the same conditions in the absence of IOM or SOM, but missing the spherulitic shape being preferentially aggregated and aligned in one direction (Fig. 7-IOM inset). The FTIR spectrum showed a similar absorption of the bands at 858 cm^{-1} (ν_2, aragonite) and at 875 cm^{-1} (ν_2, calcite). The bands at 1030 cm^{-1} and 1082 cm^{-1} were also clearly visible. Figure 7-SOM+IOM shows the results of the precipitation in the presence of SOM and IOM. No typical crystalline habits were visible in the precipitate in which the mineral phase appeared completely embedded in the OM. The FTIR spectrum of this material showed the presence of a strong absorption band due to aragonite (ν_2 at 858 cm^{-1}) and a weak one due to calcite (ν_2 at 875 cm^{-1}). Weak absorption was also associated to the bands at 1030 cm^{-1} and 1082 cm^{-1}.

The FTIR spectra of the mineral phases obtained in the presence of c_s of SOM and magnesium ions suggested that ACC could be present in the precipitate. These precipitates were also investigated by XRD. In figure 8A, as example, the XRD patterns of the precipitate obtained in the presence of c_s of SOM and Mg/Ca molar ratio equal to 5 and of the material precipitated in the absence of additives are reported. In the diffraction profile (SOM+Mg5) a broad band spanning between 20° and 40° of 2theta was present, which is typical of amorphous material. In figure 8B–C SEM pictures of the precipitate from the SOM+Mg5 solution are shown. ACC forms a jagged layer on/into which crystals of magnesium calcite and aragonite are deposited (Fig. 8B). The ACC layer is formed by the random assembly of particles of about 100 nm in diameter (Fig. 8C).

Discussion

In this research the intra-skeletal OM associated to the whole skeleton, COC and fibrous regions, of a solitary Mediterranean coral, *B. europaea*, was studied. It represented about 0.3% (*w*/*w*); this value is far lower than the amount detected by means of thermo-gravimetric analyses, about 1.5% (*w*/*w*), in coral skeleton

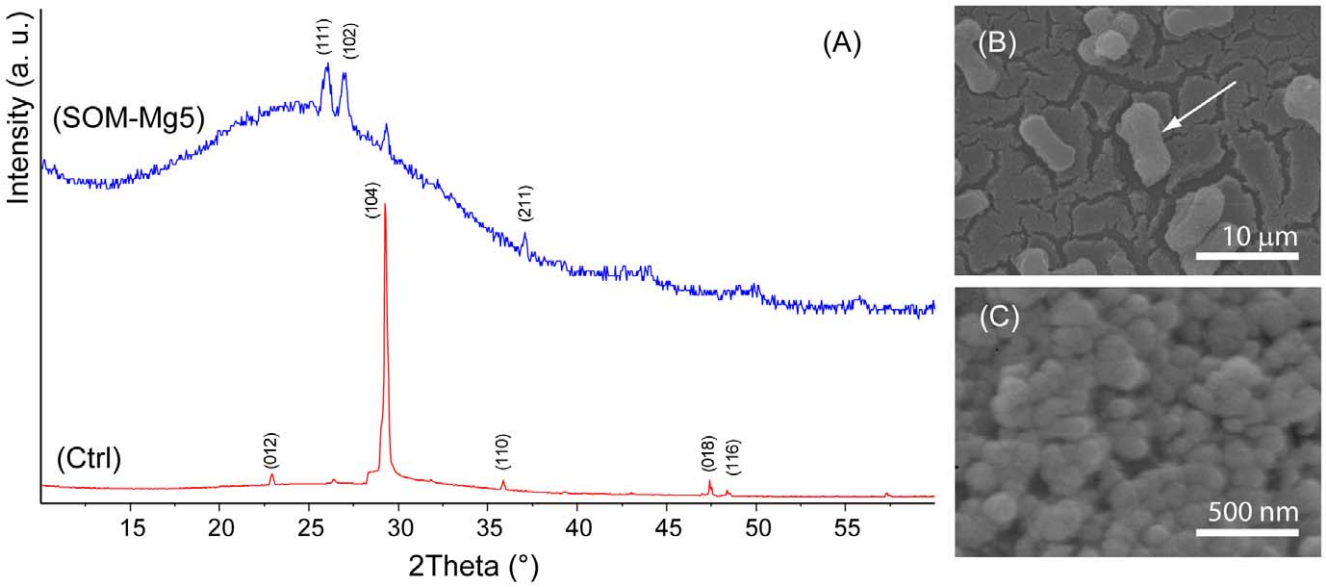

Figure 8. Calcium carbonate crystallization experiments. (A) X-ray powder diffraction patterns of the precipitates obtained from a 10 mM calcium chloride solution (Ctrl), from a 10 mM calcium chloride solution containing SOM and magnesium ions in Mg/Ca molar ratio equal to 5 (SOM-Mg5). In (Ctrl) only calcite is present, while in (SOM-Mg5) a mixture of calcite and aragonite is present. Moreover, in (SOM-Mg5) the broad band around between 20° and 40° suggests the presence of amorphous material. The calcite diffraction peaks, (012), (104), (110), (018) and (116), were indexed according to the reference pattern PDF 98-000-5342 [61], while the aragonite diffraction peaks, (111), (102) and (211), were indexed according to the reference pattern PDF 98-006-0908 [60]. (B and C) SEM pictures of the precipitate obtained from SOM-Mg5. Crystals of magnesium calcite (see arrow in (A)) and aragonite deposited on, and into, a jagged layer of ACC. In (B) is shown a magnification of the ACC layer, in it small particles of about 100 nm in diameter are visible.
doi:10.1371/journal.pone.0022338.g008

from other species [44]. The different evaluation method could be one of the reasons for this difference. Moreover, in the used OM extraction protocol a fraction OM is degraded by the powered skeleton treatment in the NaClO solution and the OM low molecular weight components are lost during the dialysis process. OM fractions, water soluble (SOM) and water insoluble (IOM), were investigated, differently from the previously reported studied which mainly focused on the soluble OM fraction [22,23,25,27,45]. This distinction allowed evidencing some important features. An important observation concerns the relative amount of SOM and IOM that does not appear constant, but changes from one experiment to another. A possible explanation could be the tendency of these macromolecules to undergo to partial denaturation, once extracted from the mineral phase, and then to aggregate when in solution [46]. Indeed it was observed an increase of the insoluble fraction as the amount of extracted material increased (data not reported). The gel electrophoresis of SOM and IOM showed that the same macromolecules, as molecular weight, are present in both fractions. This indicates that the solubility of the two fractions is probably related to their degree of cross-linking and/or association in water. Thus, it is possible to infer that in the studied coral the same macromolecules are assembled in different ways, both to build the matrix framework and to exert their function of control over the mineral deposition. This does not match with what reported for mollusc shells, where a clear compositional distinction occurs between the soluble and the insoluble macromolecules that compose the OM [1]. Moreover, the gel electrophoresis showed that the OM macromolecules were mainly gathered in a high and a low molecular weight families. The SOM fraction, richer of low molecular weight macromolecules (around 14 kDa), showed an amino acid composition characterised by a high content of acidic residues, above 50 mol %, mainly represented by Asx. On the contrary the IOM fraction, richer in high molecular weight macromolecules (around 66 kDa), is low acidic and contains more hydrophobic residues. Interestingly, the IOM contains proline, an amino acid usually associated to fibrous proteins. The amino acid analyses conducted on the soluble extract from several coral skeleton specie are in agreement with the above observation e.g. [22,23,25,27,45]]. SOM and IOM are mainly glycoproteins in which the glycosidic regions represent their major component, as shown by the FTIR spectra (Fig. 2). The absorption bands associated to the glycosidic regions have a similar pattern, suggesting that the sugars have the same structure in SOM and IOM. This observation matches with the above considerations, which suggest that IOM and SOM are made of the same macromolecules, but with a different distribution between two main families. A significant content of lipids was also detected by FTIR spectroscopy in both SOM and IOM (Fig. 2). They could have an influence in the mineralization process. They could be involved in the stabilization of ACC as final or transient phase. In particular phospholipids could play a double role in stabilizing ACC through the interaction with phosphate groups and isolating the mineral phase through the formation of vesicles [41,47].

A key to understanding the mechanisms and functions of biological macromolecules in mineralized tissues is the recognition between the macromolecules and the crystal faces and/or the stabilization of unfavoured mineral phases [1–3]. Overgrown experiments allow to study specific crystal-macromolecules interactions [48]. In these experimental conditions the acidic macromolecules-crystal interactions occur under conditions that minimally affect the macromolecules. Local dissolution of skeletal surface and release of acidic macromolecules into the overgrowth microenvironment must be involved in the mechanism of expression of new crystal faces and/or stabilization of unfavoured mineral phases. Dissolution and crystallization, which take place in

the same microenvironment, may be due to the lower thermodynamic stability of the biogenic mineral, which must be due to the presence of occluded acidic macromolecules. In overgrowth experiments, although the macromolecules are not in a native state, they are certainly more conducive to preserving their structure that after isolation and separation procedures, which often result in macromolecule denaturation. However, not all the intra-skeletal acidic macromolecules could be released by the skeletal elements or be able to interact with the overgrowing phases. The presence of overgrowth aragonite on the coral skeleton may indicate a capability of the organic matrix component to stabilize this polymorph, even in the absence of magnesium ions. The fact that aragonite was observed only on the surface of the skeletal elements and in contact with the OM suggests a role of IOM in aragonite stabilization. The calcite crystals overgrown on coral skeleton showed crystal faces {hk0} other than those of the stable cleavage {104} habit. These faces develop as a result of selective re-adsorption of the soluble acid macromolecules released from the coral skeleton, as also suggested by their smoothness [48]. Calcite crystals showing the new crystal faces were also observed in proximity of the coral skeleton and not in contact with it, indicating a diffusion of SOM components in solution. A different expression of the new crystal faces on the overgrowth crystals depending of the location on the coral skeleton was also noted. An explanation could be that the release of acidic macromolecules form any surface other than the plane of intercalation is hampered. This factor will cause differences in acidic macromolecules availability in various directions, depending on their orientation relative to the surface of the crystal. The above observations from the overgrowth experiments clearly suggest that the OM components from the coral skeleton are able to influence the calcium carbonate precipitation. Thus, calcium carbonate precipitation experiments were also conducted to evaluate the SOM and IOM fractions influence on the mineralization process. This was done using an *in vitro* model system of the crystallization process [49]. This model system is far from the real biological environment, but is able to simulate the mineralization process by increasing concentration of carbonate ions [1–3] and was widely used in all the recent literature. The experiments were conducted using as additives SOM, IOM and magnesium ions. The SOM was studied at different concentrations. It was observed that a low concentration of SOM ($0.25c_s$) does not affect the precipitation of calcium carbonate, while a high concentration ($2.5c_s$) provoked a complete inhibition of precipitation. A concentration of SOM, c_s was chosen with the criterion to compromise between the inhibition of precipitation and the need to assess its influence on the precipitation process. Interestingly, a c_s concentration of SOM favoured the precipitation of calcite, even in conditions where in its absence aragonite precipitated, i.e. from solution having Mg/Ca molar ratio equal to 3 or 5 (Table 2). This effect could be due to a preferential interaction with magnesium ions that may reduce their activity in solution. Indeed, it is reported that the precipitation of aragonite from solutions containing magnesium ions is due to an inhibition of the precipitation of calcite; magnesium ions poison crystal nuclei of calcite and stop their growth [28]. This mechanism of preferential interaction of acidic macromolecules with magnesium ions was also proposed to explain the switch off of ACC stabilization done by some specific aspartate rich macromolecules [11]. Another possibility is that the SOM inhibits the precipitation of aragonite, interacting with some specific crystalline planes and stopping the growth of the crystals in a process mediated by magnesium ions, as observed to occur in calcite as a consequence of mineral-macromolecules interaction [50]. This latter hypothesis is further supported by the observation that in the presence of SOM the morphology of the crystals, mainly the calcitic ones, is strongly modified (Figs. 5SOM and 7SOM). It was demonstrated that aragonitic macromolecules are able to interact with calcite crystals in analogous ways to what may occur with biogenic aragonite crystals [49]. Moreover, in the presence of SOM, and in minor extent in the presence of IOM, ACC appears to be present in the precipitates. This is indicated by the FTIR strong absorption band around 1080 cm^{-1}, which could also be due to the SOM itself, by the weak peak at 713 cm^{-1} [42] and by the XRD data. In fact, the precipitation of ACC is favoured by magnesium ions and molecules that inhibit calcium carbonate crystalline phases precipitation [29,51,52]. Interestingly the ACC precipitate forming aggregates of spheres showing a diameter of about 100 nm. The size of these particles, above the critical size (70 nm) of those formed in bulk, requires their stabilization by components of the organic matrix [53]. The existence of similar particles of ACC was observed to occur *in vivo* in molluscs. It was suggested that these particles had the role of calcium and carbonate ions reservoirs to feed the growing crystals of calcium carbonate [46,54]. This may suggest that AAC could be also involved in the precipitation of aragonite in corals, analogously to what observed in molluscs. However, differently from the molluscs, no direct observation of ACC in corals was so far reported [43,55–57]. A precipitation mechanism involving ACC similar to that observed during shell molt of crustaceans may occur also in corals. There a magnesium ions-aspartate-based calcium carbonate crystallization switch from ACC into calcite was demonstrated to occur. The ACC stabilizing role of magnesium ions is switched off by Asp-rich proteins. Thus, these proteins favour the polymorphic transition from ACC to a crystalline phase [11]. Although the OM macromolecules from coral skeleton have a high content of aspartate, this destabilization of the ACC has not been observed and the experimental data suggest an opposite effect. However, the involvement order of magnesium and aspartate is critical to compose the crystallization switch. No switch is observed if the ACC is first stabilized by aspartate, followed by the addition of magnesium ions. Since in the presented experiments there is the co-presence of aspartate rich acidic macromolecules and magnesium ions, the absence of a crystallization switch does not surprise. Nevertheless, it is conceivable that the biological system controlling the aragonite deposition in corals may use magnesium to stabilize ACC and the acidic macromolecules to address specifically the crystallization process.

The presence of IOM had a minor effect on the polymorphism of precipitated calcium carbonate. The polymorphic distribution as a function of the Mg/Ca molar ratio in solution was similar to that observed in its absence (Table 2). However, the morphology of the crystal was affected, suggesting that an interaction between the macromolecules released by the IOM and specific crystalline planes of calcite and aragonite occurred. The calcite crystals showed additional crystalline planes ({018} in the absence of magnesium ions and {1–10} in the presence of magnesium ions) with respect to the {104} rhombohedra obtained in the absence of additives. The aragonite crystals appeared cut along their main axis, c-axis, as a result of the presence of IOM and magnesium ions, suggesting an interaction between IOM macromolecules and {001} crystalline planes of aragonite, mediated by the presence of magnesium ions. This observation may have some implication with the zonal distribution of magnesium ions in the fibrous aragonite region of corals that could be mediated by OM molecules [50,58].

The precipitation experiments with the co-presence of IOM and SOM in the media should be the ones that better may symbolize

the *in vivo* system, being the OM components similar to those present in the coral skeleton. In this condition, even the absence of magnesium ions, the precipitation of aragonite, as minor phase, together with calcite was observed. It is important to note that the only presence of the single fractions of the OM, SOM or IOM, was unable to induce the precipitation of aragonite. The presence of magnesium ions strengthens the capability of the IOM+SOM mixture to favour the precipitation of aragonite, and at a Mg/Ca molar ratio equal to 5 aragonite is the main phase present. The presence of magnesium ions also influences the morphology of the precipitates and when increasing its concentration the precipitated mineral lost crystalline features and was completely entrapped in the dry OM (or xerogel). This outcome suggests that the mineralization process occurs in a gelling environment.

The fact that both, IOM and SOM, are necessary to exert a high influence on calcium carbonate crystal morphology and polymorphism was already reported for mollusc shells, since the acidic macromolecules extracted from aragonitic layers are able to precipitate aragonite only when absorbed in a specific gelling substrate made of chitin and silk fibroin or in synthetic analogous [7,8,10]. The precipitation of aragonite in the presence of the OM from coral may also occur in a gelling environment. Indeed, both IOM and SOM components are rich of polysaccharides that usually have strong tendency to entangle giving a gelling structure [5,59] on which the acidic macromolecules, mainly from SOM, could adsorb and exert their control on the calcium carbonate precipitation.

This research represents, to our knowledge, the first study on the influence of the intra-skeletal OM from coral skeletons on *in vitro* precipitation of calcium carbonate. The OM contains two main families of acidic glycoproteins that when extracted aggregates giving a water soluble and an insoluble fraction. The soluble fraction strongly interacts with aragonite and calcite crystals and favours the precipitation of calcite or the inhibition of aragonite. The co-presence of both fractions allows the co-precipitation of aragonite with calcite, even in the absence of magnesium ions, and strongly favours the precipitation of aragonite in the presence of magnesium ions. Thus, this research, although does not resolve the controversy of the weight between environmental or biological control on the deposition of calcium carbonate in coral skeletons, sheds a light on the role of the OM, which appears to be regulated by magnesium ions. In conclusion on the base of our results we may safely conclude that the OM composition and magnesium ions influence the fine scale characteristics of the crystals of which the coral skeleton is constructed.

Acknowledgments

GF and PV thank the Consorzio Interuniversitario di Ricerca della Chimica dei Metalli nei Sistemi Biologici (CIRC MSB) for the support. SG, EC and MR thank M. Cova, G. Gasparini and P. Bonzi for their underwater assistance in collecting the samples. The diving centre Sub Maldive supplied logistic assistance in the field. The experiments complied with current Italian law.

Author Contributions

Conceived and designed the experiments: GF SG ZD. Performed the experiments: PV MR FS. Analyzed the data: PV MR FS SG GF. Contributed reagents/materials/analysis tools: EC SG. Wrote the paper: GF. Gave conceptual advice: OL ZD.

References

1. Lowenstam HA, Weiner S (1989) On biomineralization. Oxford University Press: New York.
2. Estroff L (2008) Biomineralization. Chem Rev 108: 4329–4331.
3. Addadi L, Joester D, Nudelman F, Weiner S (2006) Mollusk shell formation: s source of new concepts for understanding biomineralization rocesses. Chem Eur J 12: 981A–987.
4. Mitterer RM (1978) Amino acid composition and metal binding capability of the skeletal protein of corals. Bull Mar Sci 28: 173–18.
5. Arias JL, Fernàndez MS (2008) Polysaccharides and proteoglycans in calcium carbonate-based biomineralization. Chem Rev 108: 4475–4482.
6. Addadi L, Weiner S, Albeck S (1996) Polysaccharides of intracrystalline glycoproteins modulate calcite crystal growth in vitro. Chem Eur J 2: 278–284.
7. Falini G, Albeck S, Weiner S, Addadi L (1996) Control of aragonite or calcite polymorphism by mollusk shell macromolecules. Science 271: 67–69.
8. Belcher AM, Wu XH, Christensen RJ, Hansma PK, Stucky GD, et al. (1996) Control of crystal phase switching and orientation by soluble mollusc-shell proteins. Nature 381: 56–58.
9. Falini G, Fermani S, Vanzo S, Miletic M, Zaffino G (2005) Influence on the formation of aragonite or vaterite by otolith macromolecules. Eur J Inorg Chem 1: 162–167.
10. Suzuki M, Saruwatari K, Kogure T, Yamamoto Y, Nishimura T, et al. (2009) An acidic matrix protein, Pif, is a key macromolecule for nacre formation. Science 325: 1338–1341.
11. Tao J, Zhou D, Zhang Z, Tang R (2009) Magnesium-aspartate-based crystallization switch inspired from shell molt of crustacean. Proc Natl Acad Sci USA 106: 22096–22101.
12. Cohen AL, McConnaughey TA (2003) Geochemical perspective on coral mineralization. Rev Mineral Geoch 54: 151–187.
13. Nakamura M, Ohki S, Suzuki A, Sakai K (2011) Coral larvae under ocean acidification: survival, metabolism, and metamorphosis. PLoS ONE 6: e14521.
14. Fine M, Tchernov D (2007) Scleractinian coral species survive and recover from decalcification. Science 315: 1811.
15. Hoegh-Guldberg O, Mumby PJ, Hooten AJ, Steneck RS, Greenfield P, et al. (2007) Coral reefs under rapid climate change and ocean acidification. Science 318: 1737–1742.
16. Ogilvie MM (1896) Microscopic and systematic study of madreporian type of corals. R Soc Lond Phil Trans 187B: 83–345.
17. Cuif JP, Dauphin Y (1998) Microstructural and physicochemical characterization of "centers of calcification" in septa of some recent scleratinian corals. Pal Zeit 72: 257–270.
18. Wells JW (1956) Scleractinia. In Moore RC, ed. Treatise on invertebrate palaeontology Part F Coelenterata. Geological Society of America University of Kansas Press USA. pp F328–F479.
19. Barnes DJ (1970) Coral skeletons: an explanation of their growth and structure. Science 170: 1305–1308.
20. Cuif JP, Dauphin Y (2005) The two-step mode of growth in the scleractinian coral skeletons from the micrometre to the overall scale. J Struct Biol 150: 319–331.
21. Muscatine L, Goiran CL, Jaubert J, Cuif JP, Allemand D (2005) Stable isotopes ($\delta^{13}C$, $\delta^{15}N$) of organic matrix from coral skeleton. Proc Natl Acad Sci USA 102: 1525–1530.
22. Dauphin Y (2001) Comparative studies of skeletal soluble matrices from some scleractinian corals and molluscs. Int J Biolog Macr 28: 293–304.
23. Wanatabe T, Fukada I, China K, Isa Y (2003) Molecular analyses of protein components of the organic matrix in the exoskeleton of two scleractinian coral species. Comp Biochem Physiol B 136: 767–774.
24. Cuif JP, Dauphin Y, Doucet J, Salome M, Susini J (2003) XANES mapping of organic sulfate in three scleractinian coral skeletons. Geoc Cosm Acta 67: 75–83.
25. Puverel S, Tambutté E, Periera-Mouriés L, Zoccola D, Allemand D, et al. (2005) Soluble organic matrix of scleractinian corals: partial and comparative analysis. Comp Biochem Physiol B 141: 480–487.
26. Dauphin Y, Cuif JP, Williams CT (2008) Soluble organic matrices of aragonitic skeletons of Merulinidae (Cnidaria, Anthozoa). Comp Biochem Phys B 150: 10–22.
27. Cuif JP, Dauphin Y, Freiwald A, Gautret P, Zibrowius H (1999) Biochemical markers of zooxanthellae symbiosis in soluble matrices of skeleton of 24 Scleractinia species. Comp Biochem Physiol A 123: 269–278.
28. Lipmann F (1973) Sedimentary carbonate minerals Springer-Verlag: Berlin.
29. Falini G, Fermani S, Tosi G, Dinelli E (2009) Calcium carbonate morphology and structure in the presence of sea water ions and humic acids. Cryst Growth Des 9: 2069–2075.
30. Stolarski J, Meibom A, Przeniosło R, Mazur M (2007) A cretaceous scleractinian coral with a calcitic skeleton. Science 318: 92–94.
31. Weber JN (1974) Skeletal chemistry of scleractinian reef corals; uptake of magnesium from seawater. Am J Sci 274: 84–93.
32. MacIntyre IG, Towe KM (1976) Skeletal calcite in living scleractinian corals: microboring fillings and not primary skeletal deposits. Science 193: 701–702.
33. Ries JB, Stanley SM, Hardie LA (2006) Scleractinian corals produce calcite, and grow more slowly, in artificial Cretaceous seawater. Geology 34: 525–528.

34. Constantz BR (1986) Coral skeleton construction: a physio-chemically dominated process. Palios 1: 152–157.
35. Holcomb M, Cohen AL, Gabitov RI, Hutter JL (2009) Compositional, morphological features of aragonite precipitated experimentally from sea water and biogenically by corals. Geochim Cosmochim Acta 73: 4166–4179.
36. Tambutté E, Allemand D, Zoccola D, Meibom A, Lotto S, et al. (2007) Observations of the tissue skeleton interface in the scleractinian coral *Stylophora pistillata*. Coral Reefs 26: 517–529.
37. Kaczorowska B, Hacura A, Kupka T, Wrzalik R, Talik E, et al. (2003) Spectroscopic characterization of natural corals. Anal Bioanal Chem 377: 1032–1037.
38. Gayathri S, Lakshminarayanan R, Weaver JC, Morse DE, Kini RM, et al. (2007) In vitro study of magnesium-calcite biomineralization in the skeletal materials of the seastar *Pisaster giganteus*. Chem Eur J 13: 3262–3268.
39. Goffredo S, Caroselli E, Mattioli G, Pienotti E, Zaccanti F (2008) Relationships between growth, population structure, sea surface temperature in the temperate solitary coral Balanophyllia europaea (Scleractinia, Dendrophylliidae). Coral Reefs 27: 623–632.
40. Goffredo S, Arnone S, Zaccanti F (2002) Sexual reproduction in the Mediterranean solitary coral *Balanophyllia europaea* (Scleractinia, Dendrophylliidae). Mar Ecol Prog Ser 229: 83–94.
41. Farre B, Cuif JP, Dauphin Y (2010) Occurrence and diversity of lipids in modern coral skeleton. Zoology 113: 250–257.
42. White WB (1974) The carbonate minerals. In Farmer VC, ed. Infrared Spectra of Minerals Mineralogical Society: London. pp 227–284.
43. Weiss IM, Tuross N, Addadi L, Weiner S (2002) Mollusc larval shell formation: amorphous calcium carbonate is a precursor phase for aragonite. J Exp Zool 293: 478–491.
44. Cuif JP, Dauphin Y, Berthet P, Jegoudez J (2004) Associated water and organic compounds in coral skeletons: quantitative thermogravimetry coupled to infrared absorption spectrometry. Geochem Geophys Geosyst 5: Q11011.
45. Constantz BR, Weiner S (1988) Acidic macromolecules associated with the mineral phase of scleractinian coral skeletons. J Exp Zool 248: 253–258.
46. Gotliv BA, Addadi L, Weiner S (2003) Mollusk shell acidic proteins: in search of individual functions. ChemBioChem 4: 522–529.
47. Tester CC, Brock RE, Wu CH, Krejci MR, Weigand S, et al. (2011) In vitro synthesis and stabilization of amorphous calcium carbonate (ACC) nanoparticles within liposomes. CrystEngComm 13: 3975–3978.
48. Aizenberg J, Albeck S, Weiner S, Addadi l (1994) Crystal-protein interactions studied by overgrowth of calcite on biogenic skeletal elements. J Cryst Growth 142: 156–164.
49. Addadi L, Moradian J, Shay E, Maroudas NG, Weiner S (1987) A chemical model for the cooperation of sulfates and carboxylates in calcite crystal nucleation: relevance to biomineralization. Proc Natl Acad Sci USA 9: 2732–2736.
50. Stephenson E, DeYoreo JJ, Wu KJ, Hoyer J, Dove PM (2008) Peptides enhance magnesium signature in calcite: insights into origins of vital effects. Science 322: 724–727.
51. Raz S, Weiner S, Addadi L (2000) Formation of high-magnesium calcite via an amorphous precursor phase: possible biological implication. Adv Mat 12: 38–42.
52. Wang DB, Wallace AF, De Yoreo JJ, Dove PM (2009) Carboxylated molecules regulate magnesium content of amorphous calcium carbonates during calcification. Proc Natl Acad Sci USA 106: 21511–21516.
53. Pouget EM, Bomans PHH, Goos J, Frederik PM, de With G, et al. (2009) The initial stages of template-controlled $CaCO_3$ formation revealed by cryoTEM. Science 323: 1555–1458.
54. Politi Y, Metzler RA, Abrecht M, Gilbert B, Wilt FH, et al. (2008) Transformation mechanism of amorphous calcium carbonate into calcite in the sea urchin larval spicule. Proc Natl Acad Sci USA 105: 17362–17366.
55. Nassif N, Pinna N, Gehrke N, Antonietti M, Jäger C, et al. (2005) Amorphous layer around platelets in nacre. Proc Natl Acad Sci USA 102: 12653–12655.
56. Baronnet A, Cuif JP, Farre DB, Nouet J (2008) Crystallization of biogenic carbonate within organo-mineral micro-domains. Structure of the calcite prisms of the pelecypod *Pinctada margaritifera* (Mollusca) at the submicron to nanometer ranges. Min Mag 72: 617–626.
57. Clode PL, Lema K, Saunders M, Weiner S (2011) Skeletal mineralogy of newly settling Acropora millepora (Scleractinia) coral recruits. Coral Reefes 30: 1–8.
58. Meibom A, Cuif JP, Hillion F, Constantz BR, Juillet-Leclerc A, et al. (2004) Distribution of magnesium in coral skeleton. Geophys Res Lett 31: L23306.
59. Estroff L, Hamilton AD (2004) Water gelation by small organic molecules. Chem Rev 104: 1201–1218.
60. Pilati T, Demartin F, Gramaccioli CM (1998) Lattice-dynamical estimation of atomic displacement parameters in carbonates: calcite and aragonite $CaCO_3$ and dolomite $CaMg(CO_3)_2$ and magnesite $MgCO_3$. Acta Cryst B 54: 515–523.
61. Chessin H, Hamilton WC, Post B (1965) Position and thermal parameters of oxygen atoms in calcite. Acta Cryst 18: 689–693.

nature climate change

LETTERS

PUBLISHED ONLINE: 25 MAY 2014 | DOI: 10.1038/NCLIMATE2241

Biomineralization control related to population density under ocean acidification

Stefano Goffredo[1]*, Fiorella Prada[1], Erik Caroselli[1], Bruno Capaccioni[2], Francesco Zaccanti[1], Luca Pasquini[3], Paola Fantazzini[3,4], Simona Fermani[5], Michela Reggi[5], Oren Levy[6], Katharina E. Fabricius[7], Zvy Dubinsky[6] and Giuseppe Falini[5]*

Anthropogenic CO_2 is a major driver of present environmental change in most ecosystems[1], and the related ocean acidification is threatening marine biota[2]. With increasing pCO_2, calcification rates of several species decrease[3], although cases of upregulation are observed[4]. Here, we show that biological control over mineralization relates to species abundance along a natural pH gradient. As pCO_2 increased, the mineralogy of a scleractinian coral (*Balanophyllia europaea*) and a mollusc (*Vermetus triqueter*) did not change. In contrast, two calcifying algae (*Padina pavonica* and *Acetabularia acetabulum*) reduced and changed mineralization with increasing pCO_2, from aragonite to the less soluble calcium sulphates and whewellite, respectively. As pCO_2 increased, the coral and mollusc abundance was severely reduced, with both species disappearing at pH < 7.8. Conversely, the two calcifying and a non-calcifying algae (*Lobophora variegata*) showed less severe or no reductions with increasing pCO_2, and were all found at the lowest pH site. The mineralization response to decreasing pH suggests a link with the degree of control over the biomineralization process by the organism, as only species with lower control managed to thrive in the lowest pH.

Several studies on the influence of pH on crystallography and texture of calcified regions are *ex situ*, short-term experiments on isolated organisms[5], providing important information, but unrepresentative of natural ecosystems and failing to assess long-term effects[6]. There is a great need for long-term analyses on ocean acidification effects on marine ecosystems acclimated to high pCO_2, as found around CO_2 vents. Vents are not perfect predictors of future oceans, owing to pH variability, proximity of unaffected populations, and co-varying environmental parameters[7]. However, vents acidify sea water on sufficiently large temporal and spatial scales to integrate ecosystem processes[6], acting as 'natural laboratories'. In Papua New Guinea vents, reductions in coral diversity, recruitment and abundance, and shifts in competitive interactions, are found[8]. In Mediterranean vents, decreased diversity, biomass, trophic complexity and abundance in many calcifying and non-calcifying organisms, and increases in macroalgae and seagrasses, are observed[7,9,10].

We assessed, along a natural pH gradient, the effect of pCO_2 on the mineralization and abundances of the aragonitic scleractinian *B. europaea*, the aragonitic tube-forming gastropod *V. triqueter*, the brown alga *P. pavonica*, which deposits aragonite on the thalli surface, the green alga *A. acetabulum*, whose cups' outer surfaces are calcified with aragonite and a small amount of whewellite (calcium oxalate), and the non-mineralized brown alga *L. variegata*. The mineralization is biologically controlled in *V. triqueter* (that is, mineral is deposited in confined nucleation sites under complete biological control with minimal environmental effects), biologically induced in *P. pavonica* and *A. acetabulum* (that is, it is strongly affected by the environment with minimal biological control), whereas *B. europaea* may represent an intermediate and still controversial situation[11]. We aimed to assess changes in the mineralization and abundance of species along a pCO_2 gradient in relation to their control over biomineralization.

Mean pH, CO_2, saturation of calcite (Ω_{calc}), and of aragonite (Ω_{arag}) differed among Sites (Kruskal–Wallis test/analysis of variance, $p < 0.001$). The median pH values were 8.1 (Site 1), 7.9 (Site 2), 7.8 (Site 3) and 7.7 (Site 4), with increasing variability towards Site 4 (Fig. 1 and Supplementary Fig. 1 and Table 1).

Aragonite was the only mineral phase in *B. europaea* skeletons (Supplementary Fig. 2). Organic matrix content was homogeneous among Sites (Kruskal–Wallis test, $p > 0.05$; Supplementary Fig. 3 and Table 1). Skeletal texture exhibited fibres evolving from a centre of calcification (Supplementary Fig. 4), but the morphology of these centres, and fibre thickness (600 ± 200 nm), were not related to pCO_2 (Supplementary Fig. 5). Hardness was homogeneous among sample regions and study Sites (5100 ± 600 MPa). The elastic Young's modulus decreased (that is, the skeleton became less stiff) along the aboral to oral direction and was lower at Sites 2 and 3 than at Site 1 (Supplementary Table 2). Crystal quality and fibre thickness usually increases when crystallization occurs under lower supersaturation[12]. Although a reduction of precipitation rate with pCO_2 could increase crystal quality, other mechanisms could involve organic matrix molecules. Corals seem to maintain a high pH at the nucleation sites within the calicoblastic layer, possibly expending a significant amount of energy[13]. This is supported by the lack of increase in aragonite fibre thickness with decreasing seawater Ω_{arag}, which would be expected if Ω_{arag} of the calcification site decreased[12]. The reduction of skeletal stiffness with declining pH is probably associated with an increase in porosity, as confirmed by preliminary

[1]Marine Science Group, Department of Biological, Geological and Environmental Sciences, Section of Biology, Alma Mater Studiorum — University of Bologna, Via F. Selmi 3, 40126 Bologna, Italy, [2]Department of Biological, Geological and Environmental Sciences, Section of Geology, Alma Mater Studiorum — University of Bologna, Piazza di Porta S. Donato 1, 40127 Bologna, Italy, [3]Department of Physics and Astronomy, Alma Mater Studiorum — University of Bologna, Viale Berti Pichat 6/2, 40127 Bologna, Italy, [4]Centro Enrico Fermi, Piazza del Viminale 1, 00184 Rome, Italy, [5]Department of Chemistry 'G. Ciamician', Alma Mater Studiorum — University of Bologna, Via F. Selmi 2, 40126 Bologna, Italy, [6]The Mina and Everard Goodman Faculty of Life Sciences, Bar-Ilan University, 52900 Ramat-Gan, Israel, [7]Australian Institute of Marine Science, PMB 3, Townsville 4810, Queensland, Australia.
*e-mail: s.goffredo@unibo.it; giuseppe.falini@unibo.it

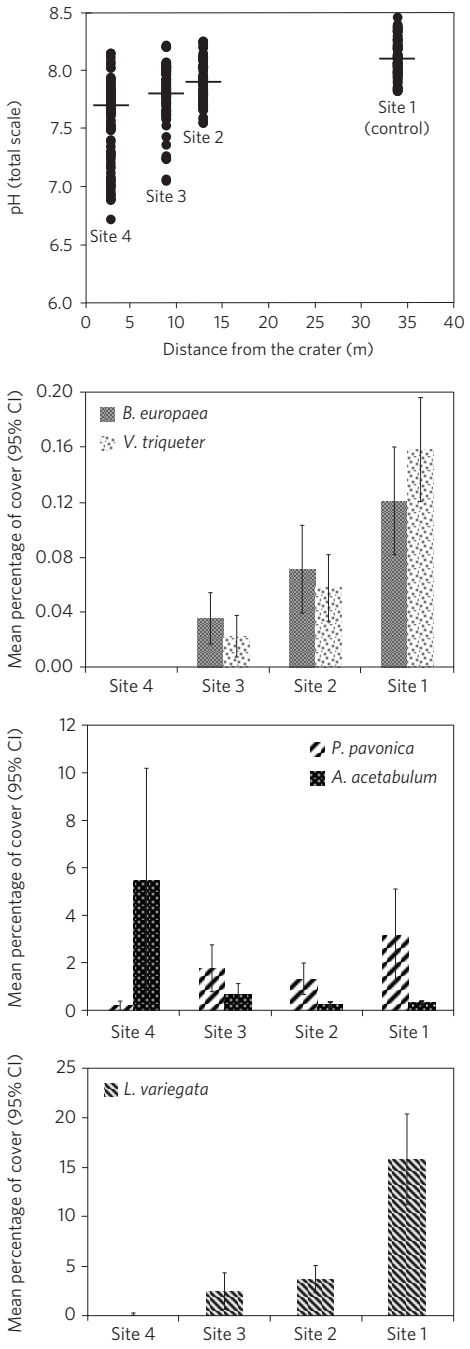

Figure 1 | Range in pH total scale and mean percentage of cover for *Balanophyllia europaea, Vermetus triqueter, Padina pavonica, Acetabularia acetabulum* and *Lobophora variegata* along the pCO_2 gradient. pH measures were 103–110 per site. Horizontal bars indicate the median pH. Error bars are 95% confidence intervals (CI).

nuclear magnetic resonance analyses. *B. europaea* skeletons have already been found to increase their porosity in stress conditions, such as increasing temperature[14].

The apical regions of *V. triqueter* shell-tubes of similar diameter (~5 mm) were analysed. Aragonite was the only mineral phase (Supplementary Fig. 2). Shell-tubes from Site 1 had four layers with different crystal texture and variable relative thickness among samples (Fig. 2). The first two layers were prismatic, with the second one made of regular prisms with a square section (500 nm side). The third was cross-lamellar with regular fibres 500 nm thick. The fourth external layer was spherulitic, with several bores and channels (Fig. 2). In one of six samples from Site 2, and in four of six from Site 3, the two internal layers were not present. Different hardnesses and elastic Young's moduli were associated with different textures, without significant variations among Sites (Supplementary Table 2). Organic matrix content was homogeneous among Sites (Kruskal–Wallis test, $p > 0.05$; Table 1 and Supplementary Fig. 3). The unaffected mineralogy of *V. triqueter* shell-tubes is possibly due to the exquisite control of biological macromolecules on mollusc mineralization, which occurs in confined sites resulting in complex crystalline textures (Fig. 2). During shell-tube growth, the external layers are the first to be deposited, followed by the internal ones[11]. A pH reduction can reduce the growth rates (calcification) of mollusc shells[15], which probably explains the absence of the internal layers in shell-tubes from the most acidic Sites.

Padina pavonica thallus tips from Site 1 were mainly aragonitic with traces of hydrate calcium sulphate salts (CSh). Aragonite concentration decreased with increasing pCO_2, and almost only CSh was observed at Site 4 (Supplementary Fig. 2). The presence of CSh was investigated in detail by further tests and considerations (Supplementary Information). The overall mineral content differed among Sites (Kruskal–Wallis test, $p < 0.05$; Table 1 and Supplementary Fig. 3), and declined with increasing pCO_2 (Spearman's rho of the correlation with pH = 0.592, $p < 0.01$). In all samples, many aragonite needle-like crystals were aggregated or merged forming bundles. CSh crystals appeared as prisms or tablets (Fig. 3 and Supplementary Fig. 6). The decalcification left the thalli free of mineral deposits (Supplementary Fig. 6). In *P. pavonica*, CSh increased with increasing pCO_2. Some stabilization of CSh salts by algal molecules[16,17], probably polysaccharides, is expected, as in sea water CSh converts to gypsum.

Acetabularia acetabulum was mainly aragonitic, with minor presence of whewellite (Supplementary Fig. 2). All samples contained about 10% (w/w) of water. The content of mineral phases, estimated after pyrolysis and release of water, differed among Sites (Kruskal–Wallis test, $p < 0.01$; Table 1 and Supplementary Fig. 3) and declined with increasing pCO_2 (Spearman's rho of the correlation with pH = 0.555, $p < 0.01$). The aragonite/whewellite ratio decreased with increasing pCO_2. Globular granules of amorphous material rich in Ca and S were observed on the surface of needle-like aragonite aggregates at Sites 1–4 (Fig. 3 and Supplementary Fig. 6). Whewellite was the only phase detected at Site 4 (Fig. 3 and Supplementary Fig. 2), where it appeared as prisms. After decalcification, the cup surface was free of mineral deposits (Supplementary Fig. 6). In line with a mainly chemical mineralization control[17], increasing pCO_2 did not affect deposition of whewellite in *A. acetabulum*. The persistence of amorphous globular particles rich in calcium and sulphur was unexpectedly observed when aragonite disappeared. This phase, soluble in acetic acid solution, may be the result of interactions between Ca ions and the sulphonated groups of polysaccharides.

Within each sample, *P. pavonica* and *A. acetabulum* showed a marked reduction of mineralized areas with increasing pCO_2 (Fig. 4). Their aragonite content decreased with decreasing Ω_{arag}. At a Ω_{arag} of 1.5, aragonite was not observed, probably because this saturation level is too low to sustain its nucleation process. The observed changes in morphology of aragonite crystals (Fig. 3) are associated with seawater chemistry[18].

The percentage of cover for all species, except *A. acetabulum*, differed among Sites (Kruskal–Wallis test, $p < 0.001$), and decreased with increasing pCO_2 (Supplementary Table 3). *B. europaea* and *V. triqueter* were not found at Site 4 (pH = 7.7, $\Omega_{arag} = 1.5$; Fig. 1). Densities of *A. acetabulum* were homogeneous among Sites (Kruskal–Wallis test, $p > 0.05$). This suggests that *P. pavonica* and *A. acetabulum* are not obligate calcifiers, persisting in high pCO_2 where also the non-calcifying species *L. variegata* survives (Fig. 1).

Table 1 | Summary of the main effects of ocean acidification on the mineral distribution and content in the calcified organisms with increasing proximity to the CO_2 seep (declining pH).

			Balanophyllia europaea		*Vermetus triqueter*		*Padina pavonica*		*Acetabularia acetabulum*	
	Median pH	Median Ω_{arag}	Mineral phase	Mineral phase (%)†	Min phase	Mineral phase (%)†	Mineral phases	Mineral phases (%)	Mineral phases*	Mineral phases (%)
Site 1	8.1	3.6	A	97.4 ± 0.4	A	98.0 ± 0.5	**A** CSh‡	73.9 ± 8.3	**A** Wh	42.9 ± 3.9
Site 2	7.9	2.4	A	97.80 ± 0.04	A	98.3 ± 0.2	A CSh	71.5 ± 10.6	**A** Wh	24.2 ± 6.9
Site 3	7.8	2.1	A	97.8 ± 0.2	A	98.1 ± 0.1	A **CSh**	59.6 ± 4.9	A **Wh**	22.7 ± 7.6
Site 4	7.7	1.5	-	-	-	-	A‡ **CSh**	61.6 ± 4.5	Wh	25.4 ± 8.0

Uncertainties are one standard deviation. A, Wh and CSh indicate aragonite, whewellite and monohydrate calcium sulphate salts. The percentage of mineral phase(s) is reported as mass ratio. *Amorphous globular particles were also detected. †The content of organic matrix is the complement to 100 in *B. europaea* and *V. triqueter* where no significant amounts of water were detected in the skeletons and shell-tubes. *P. pavonica* and *A. acetabulum* contained a significant amount of bounded water and their percentage of organic matrix significantly increased with pCO_2. ‡This phase was detected in traces. When two phases were present, the most abundant one is indicated in bold.

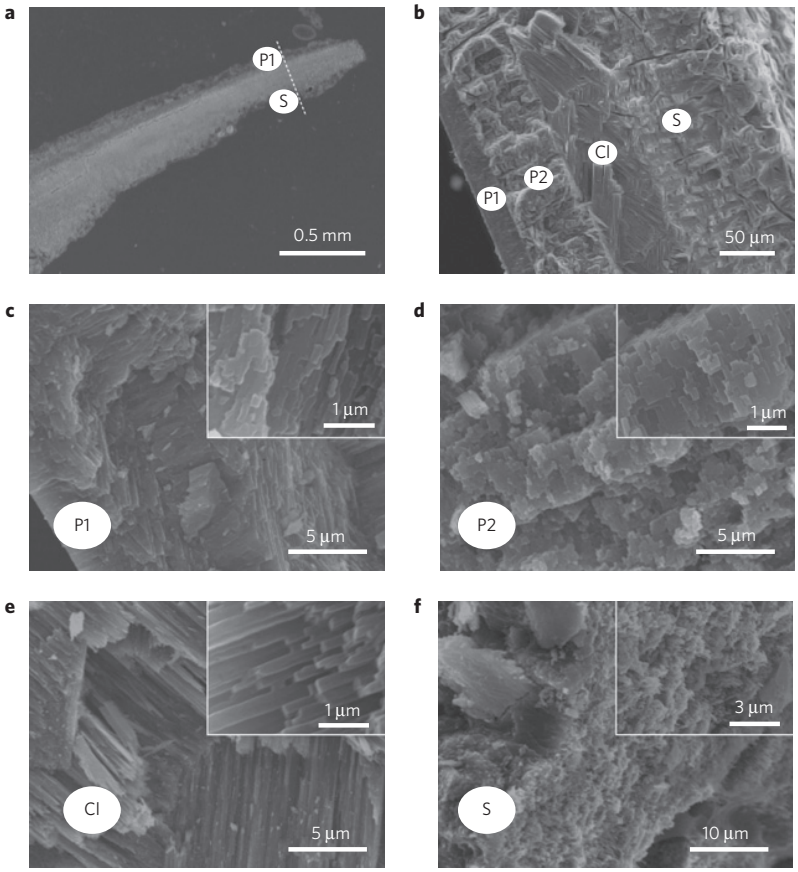

Figure 2 | Scanning electron microscope images of a longitudinal section of *Vermetus triqueter* shell-tube. a, Apical region of shell-tube. High-magnification images were taken along the dotted line from inside (P1) to outside (S) the tube. **b**, Shell-tubes in Site 1 consisted of four layers (P1, P2, Cl, S). **c**, First prismatic layer (P1). **d**, Second prismatic layer (P2), with square cross-sections. **e**, Cross-lamellar layer (Cl). **f**, Spherulitic layer (S) containing bores and channels. The first two layers were not present in one sample from Site 2 and in most of the samples from Site 3.

A changing benthic community was associated with the pCO_2 gradient (Supplementary Video). The coverage of a coral, a mollusc, and two macroalgae, one of which is a calcifier, declined with increasing pCO_2 (Fig. 1). This is in agreement with previous investigations at CO_2 vents, documenting marked reductions in calcifying macroalgal abundance[7,8]. Calcifying organisms seem the most sensitive to elevated pCO_2 (ref. 19), even if their response is not consistent[8,15,20]. *A. acetabulum*, *B. europaea* and *V. triqueter* were previously found only outside vent areas, at a pH_{TS} of 8.14 (ref. 7). Instead, in our survey *B. europaea* and *V. triqueter* survived up to pH_{TS} 7.8 and algal species up to pH_{TS} 7.7 (Fig. 1). The response of macroalgae to pCO_2 is expected to vary among species. As an example, increased cover with decreasing pH was observed for *Padina* spp. at CO_2 seeps in Vulcano and Papua New Guinea[21], and for *L. variegata* at CO_2 seeps in Ischia[10], which contrasts with our data. The response of non-calcifying macroalgae to elevated pCO_2 is variable[22], depending on energy availability[23]. The nature of CO_2-induced shifts in macroalgal community structure is likely to vary depending on other environmental factors, such as nutrient availability, temperature and solar radiation[24]. For instance, *L. variegata* were sampled in Ischia at 1 m depth and in our study at 8–12 m. Growth of the brown alga *Dictyota ciliolata* decreases with decreasing light intensity[25]. In the brown alga *Fucus vesiculosus*, photosynthesis and growth decrease with increasing depth[26] from

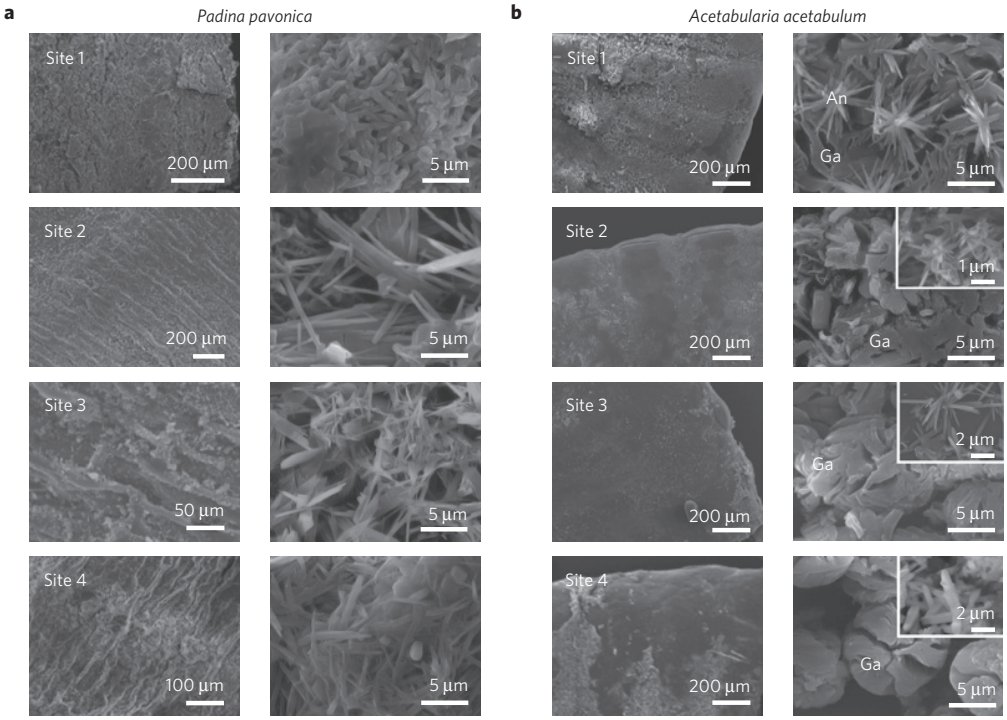

Figure 3 | Scanning electron microscope images of *Padina pavonica* thalli and *Acetabularia acetabulum* cups. a,**b**, Low-magnification (left column) and high-magnification (right column) images. *P. pavonica* (**a**) became less mineralized with increasing pCO_2. The aggregation and shape of aragonite crystals was lightly affected by pCO_2. In *A. acetabulum* (**b**), needle-like crystals of aragonite (An) were above and among the globular aggregates (Ga). The amount of biomineralized material was reduced with increasing pCO_2, whereas the centre of the cup became more populated by spherical aggregates. Aragonite needles are shown in the inset for Site 2 and 3, and whewellite is shown in the inset for Site 4.

1 to 6 m. At the high light of the shallow Ischia site, *L. variegata* may compensate for the negative effect of lowered pH through enhanced growth.

We related the biological control over biomineralization with changes in the abundance of organisms along natural pCO_2 gradients. The content of biomineralized products decreased with increasing pCO_2 only in the two calcifying algal species (with a weak control over their biomineralization), but the two species with stronger biomineralization control (*B. europaea* and *V. triqueter*) tolerated less severe pCO_2 increases (pH 7.8) than the algae (pH $\leq$ 7.7). Moreover, the more tolerant algae continued to grow despite their biomineralization products being profoundly altered by pCO_2. Even if biomineralization in algae is only induced[17], we cannot exclude that the switch from aragonite to other biominerals may represent a phenomenon of phenotypic plasticity[27], which is increasingly being found to strongly contribute to persistence in the face of climate change[28]. The control over biomineralization may not be the only cause of the observed differences, because the coral and the mollusc have a biology completely dependent on calcification, whereas the algae do not. Moreover, the algae may benefit from pCO_2 increase in terms of photosynthesis, whereas the coral may be less dependent on the photosynthetic process and the mollusc does not photosynthesize. This study adds new evidence to field studies on ocean acidification effects[4,9,29,30], all indicating major ecological shifts as CO_2 rises. It documented that the mineralization response to ocean acidification seems connected with the organisms' control of biomineralization, increasing pCO_2 profoundly affects the abundance of many benthic organisms, and only the species with weaker control were observed at the lowest pH.

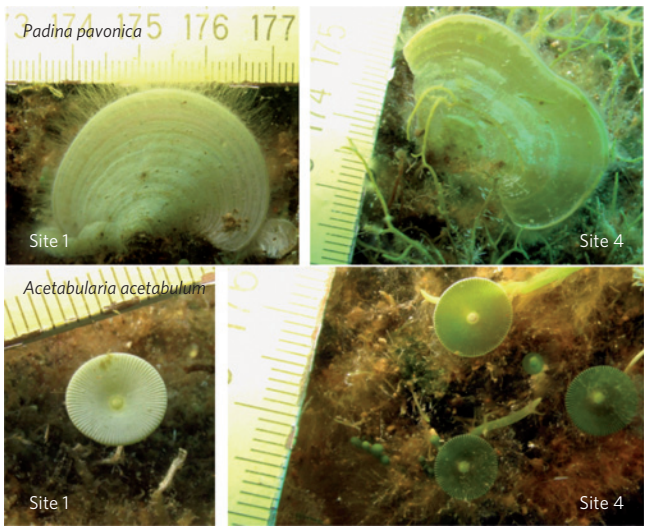

Figure 4 | *In situ* pictures of *Padina pavonica* and *Acetabularia acetabulum* at Sites 1 and 4, showing the reduction of calcified material (white areas) with increasing pCO_2. A ruler is included in each image to show scale. The smallest tick marks indicate a length of 1 mm.

Methods

Study site. Fieldwork was conducted at Panarea, Italy (Supplementary Video and Fig. 1), where hydrothermally stable CO_2 emissions acidify sea water, generating a pH gradient (see Supplementary Information for details).

Carbonate chemistry. Four sampling Sites were selected (Fig. 1 and Supplementary Fig. 1): a control site (Site 1), two intermediate pCO_2 sites (Site 2 and Site 3), and a high pCO_2 site (Site 4). pH (NBS scale), temperature and salinity were measured at each Site during several surveys between July 2010 and May 2013 with a multi-parametric probe (600R, YSI Incorporated) powered from a small boat and operated by SCUBA divers. Bottom-water samples for determination of total alkalinity were collected and analysed using standard methods

(see Supplementary Information for details). Further temperature data were recorded every three hours by sensors (Thermochron iButton, DS1921G, Maxim Integrated Products) attached in each Site from July 2010 to May 2013. Measured pH was converted to the total scale using CO2SYS software. Median pH (back-transformed hydrogen ion concentrations) were calculated for each Site. The pH, total alkalinity, salinity and temperature were used to calculate other carbonate system parameters using the software CO2SYS (Supplementary Information).

Benthic survey. Photographs of benthos (5 to 10 per Site, 50 × 50 cm for the animals, 21.0 × 29.7 cm for the algae) were used to measure the percentage of cover for *B. europaea*, *V. triqueter*, *P. pavonica*, *A. acetabulum* and *L. variegata* at each Site. See Supplementary Information for details.

Vent gas. Gas was sampled during five surveys (June 2011–May 2013) and analysed at the Laboratory of Fluid and Rock Geochemistry of the University of Florence using standard methods (Supplementary Information). Water samples were collected and tested for dissolved H_2S (Supplementary Information).

Statistical analyses. Analysis of variance and the *post hoc* Fisher least significant difference test were used to test for differences among Sites using arcsine and log-transformation for percentage of cover and environmental data, respectively, when necessary. Otherwise, the non-parametric Kruskal–Wallis and Spearman's rank correlation coefficients were used. All analyses were performed using SPSS v.20.

Biomineralization. Samples were randomly collected by SCUBA divers at all Sites and were prepared for analyses with standard methods (Supplementary Information). Microscopic observations and mechanical and spectroscopic measurements required the preparation of cross-sections of the samples (Supplementary Information). X-ray powder diffraction and Fourier transform infrared spectroscopy patterns on small amounts of powdered samples were collected using standard methods (Supplementary Information). Attenuated total reflection Fourier transform infrared spectra of sample cross-sections were acquired with standard methods (Supplementary Information). The organic matter content in the sample was determined by thermogravimetric analysis (Supplementary Information). Microstructures were observed using optical and scanning electronic microscopes (SEM; Supplementary Information). The mechanical properties of shell-tubes and skeletons were measured with standard nano-indentation techniques (Supplementary Information).

Received 12 December 2013; accepted 7 April 2014; published online 25 May 2014

References

1. IPCC, *IPCC Special Report on Renewable Energy Sources and Climate Change Mitigation* (Cambridge Univ. Press, 2011).
2. Orr, J. C. *et al.* Anthropogenic ocean acidification over the twenty-first century and its impact on calcifying organisms. *Nature* **437,** 681–686 (2005).
3. Fabry, V. J., Seibel, B. A., Feely, R. A. & Orr, J. C. Impacts of ocean acidification on marine fauna and ecosystem processes. *ICES J. Mar. Sci.* **65,** 414–432 (2008).
4. Rodolfo-Metalpa, R., Martin, S., Ferrier-Pages, C. & Gattuso, J. P. Response of Mediterranean corals to ocean acidification. *Biogeosciences Discuss.* **6,** 7103–7131 (2010).
5. Hahn, S. *et al.* Marine bivalve shell geochemistry and ultrastructure from modern low pH environments: environmental effect versus experimental bias. *Biogeosciences* **9,** 1897–1914 (2012).
6. Barry, J. P., Hall-Spencer, J. M. & Tyrrell, T. Guide to Best Practices for Ocean Acidification Research and Data Reporting (Publications Office of the European Union, 2010).
7. Hall-Spencer, J. M. *et al.* Volcanic carbon dioxide vents show ecosystem effects of ocean acidification. *Nature* **454,** 96–99 (2008).
8. Fabricius, K. E. *et al.* Losers and winners in coral reefs acclimatized to elevated carbon dioxide concentrations. *Nature Clim. Change* **1,** 165–169 (2011).
9. Cigliano, M., Gambi, M. C., Rodolfo-Metalpa, R., Patti, F. P. & Hall-Spencer, J. M. Effects of ocean acidification on invertebrate settlement at volcanic CO_2 vents. *Mar. Biol.* **157,** 2489–2502 (2010).
10. Porzio, L., Buia, M. C. & Hall-Spencer, J. M. Effects of ocean acidification on macroalgal communities. *J. Exp. Mar. Biol. Ecol.* **400,** 278–287 (2011).
11. Lowenstam, H. A. & Weiner, S. *On Biomineralization* (Oxford Univ. Press, 1989).
12. Holcomb, M., Cohen, A. L., Gabitov, R. I. & Hutter, J. L. Compositional and morphological features of aragonite precipitated experimentally from seawater and biogenically by corals. *Geochim. Cosmochim. Acta* **73,** 4166–4179 (2009).
13. Venn, A. A. *et al.* Impact of seawater acidification on pH at the tissue–skeleton interface and calcification in reef corals. *Proc. Natl Acad. Sci. USA* **110,** 1634–1639 (2013).
14. Fantazzini, P. *et al.* A time-domain nuclear magnetic resonance study of Mediterranean scleractinian corals reveals skeletal-porosity sensitivity to environmental changes. *Environ. Sci. Technol.* **47,** 12679–12686 (2013).
15. Ries, J. B., Cohen, A. L. & McCorkle, D. C. Marine calcifiers exhibit mixed responses to CO_2-induced ocean acidification. *Geology* **37,** 1131–1134 (2009).
16. McCandless, E. L. & Craigie, J. S. Sulfated polysaccharides in red and brown algae. *Ann. Rev. Plant Physiol.* **30,** 41–53 (1979).
17. Mann, S., Webb, J. & Williams, R. J. P. *Biomineralization: Chemical and Biochemical Perspectives* (VCH Verlagsgesellschaft, 1989).
18. Robbins, L. L., Knorr, P. O. & Hallock, P. Response of *Halimeda* to ocean acidification: field and laboratory evidence. *Biogeosci. Discuss.* **6,** 4895–4918 (2009).
19. Kroeker, K. J., Kordas, R. L., Crim, R. N. & Singh, G. G. Meta-analysis reveals negative yet variable effects of ocean acidification on marine organisms. *Ecol. Lett.* **13,** 1419–1434 (2010).
20. Fabry, V. J. Marine calcifiers in a high-CO_2 ocean. *Science* **320,** 1020–1022 (2008).
21. Johnson, V. R., Russell, B. D., Fabricius, K. E., Brownlee, C. & Hall-Spencer, J. M. Temperate and tropical brown macroalgae thrive, despite decalcification, along natural CO_2 gradients. *Glob. Change Biol.* **18,** 2792–2803 (2012).
22. Cornwall, C. E. *et al.* Carbon-use strategies in macroalgae: Differential responses to lowered pH and implications for ocean acidification. *J. Phycol.* **48,** 137–144 (2012).
23. Hofmann, L. C., Straub, S. & Bischof, K. Competition between calcifying and noncalcifying temperate marine macroalgae under elevated CO_2 levels. *Mar. Ecol. Prog. Ser.* **464,** 89–105 (2012).
24. Sarker, M. Y., Bartsch, I., Olischläger, M., Gutow, L. & Wiencke, C. Combined effects of CO_2, temperature, irradiance and time on the physiological performance of *Chondrus crispus* (Rhodophyta). *Bot. Mar.* **56,** 63–74 (2013).
25. Cronin, G. & Hay, M. E. Effects of light and nutrient availability on the growth, secondary chemistry, and resistance to herbivory of two brown seaweeds. *Oikos* **77,** 93–106 (1996).
26. Rohde, S., Hiebenthal, C., Wahl, M., Karez, R. & Bischof, K. Decreased depth distribution of *Fucus vesiculosus* (Phaeophyceae) in the Western Baltic: Effects of light deficiency and epibionts on growth and photosynthesis. *Eur. J. Phycol.* **43,** 143–150 (2008).
27. Munday, P. L., Warner, R. R., Monro, K., Pandolfi, J. M. & Marshall, D. J. Predicting evolutionary responses to climate change in the sea. *Ecol. Lett.* **16,** 1488–1500 (2013).
28. Anderson, J. T., Inouye, D. W., McKinney, A. M., Colautti, R. I. & Mitchell-Olds, T. Phenotypic plasticity and adaptive evolution contribute to advancing flowering phenology in response to climate change. *Proc. R. Soc. B* **279,** 3843–3852 (2012).
29. Dias, B. B., Hart, M. B., Smart, C. W. & Hall-Spencer, J. M. Modern seawater acidification: The response of foraminifera to high-CO_2 conditions in the Mediterranean Sea. *J. Geol. Soc.* **167,** 843–846 (2010).
30. Calosi, P. *et al.* Distribution of sea urchins living near shallow water CO_2 vents is dependent upon species acid-base and ion-regulatory abilities. *Mar. Pollut. Bull.* **73,** 470–484 (2013).

Acknowledgements

I. Berman-Frank helped with alkalinity measurements. B. Basile, F. Sesso, and Eolo Sub diving centre assisted in the field. F. Gizzi and G. Polimeni helped during preparation and participated in field surveys. The Scientific Diving School supplied scientific, technical and logistical support. The research leading to these results has received funding from the European Research Council under the European Union's Seventh Framework Programme (FP/2007-2013)/ERC Grant Agreement no. [249930 - CoralWarm].

Author contributions

S.G., Z.D. and G.F. conceived and designed research. S.G., F.P., E.C. and B.C. collected the samples and performed the diving fieldwork. L.P., S.F., M.R. and G.F. performed the laboratory experiments. S.G., F.P., E.C., B.C., L.P., P.F., M.R., K.E.F. and G.F. analysed the data. All authors wrote the manuscript and participated in the scientific discussion.

Additional information

Supplementary information is available in the online version of the paper. Reprints and permissions information is available online at www.nature.com/reprints. Correspondence and requests for materials should be addressed to S.G. or G.F.

Competing financial interests

The authors declare no competing financial interests.

nature COMMUNICATIONS

ARTICLE

Received 30 Dec 2014 | Accepted 10 Jun 2015 | Published 17 Jul 2015

DOI: 10.1038/ncomms8785 OPEN

Gains and losses of coral skeletal porosity changes with ocean acidification acclimation

Paola Fantazzini[1,2], Stefano Mengoli[3], Luca Pasquini[1], Villiam Bortolotti[4], Leonardo Brizi[1,2], Manuel Mariani[1,2], Matteo Di Giosia[5], Simona Fermani[5], Bruno Capaccioni[6], Erik Caroselli[7], Fiorella Prada[7], Francesco Zaccanti[7], Oren Levy[8], Zvy Dubinsky[8], Jaap A. Kaandorp[9], Pirom Konglerd[9], Jörg U. Hammel[10], Yannicke Dauphin[11], Jean-Pierre Cuif[11], James C. Weaver[12], Katharina E. Fabricius[13], Wolfgang Wagermaier[14], Peter Fratzl[14], Giuseppe Falini[5] & Stefano Goffredo[7]

Ocean acidification is predicted to impact ecosystems reliant on calcifying organisms, potentially reducing the socioeconomic benefits these habitats provide. Here we investigate the acclimation potential of stony corals living along a pH gradient caused by a Mediterranean CO_2 vent that serves as a natural long-term experimental setting. We show that in response to reduced skeletal mineralization at lower pH, corals increase their skeletal macroporosity (features $>10\,\mu m$) in order to maintain constant linear extension rate, an important criterion for reproductive output. At the nanoscale, the coral skeleton's structural features are not altered. However, higher skeletal porosity, and reduced bulk density and stiffness may contribute to reduce population density and increase damage susceptibility under low pH conditions. Based on these observations, the almost universally employed measure of coral biomineralization, the rate of linear extension, might not be a reliable metric for assessing coral health and resilience in a warming and acidifying ocean.

[1] Department of Physics and Astronomy, University of Bologna, Viale Berti Pichat 6/2, 40127 Bologna, Italy. [2] Centro Enrico Fermi, Piazza del Viminale 1, 00184 Rome, Italy. [3] Department of Management, University of Bologna, Via Capo di Lucca 34, 40126 Bologna, Italy. [4] Department of Civil, Chemical, Environmental, and Materials Engineering, University of Bologna, Via Terracini 28, 40131 Bologna, Italy. [5] Department of Chemistry 'G. Ciamician', University of Bologna, Via F. Selmi 2, 40126 Bologna, Italy. [6] Department of Biological, Geological and Environmental Sciences, Section of Geology, University of Bologna, Piazza di Porta S. Donato 1, 40126 Bologna, Italy. [7] Marine Science Group, Department of Biological, Geological and Environmental Sciences, Section of Biology, University of Bologna, Via F. Selmi 3, 40126 Bologna, Italy. [8] The Mina and Everard Goodman Faculty of Life Sciences, Bar-Ilan University, Ramat-Gan 52900, Israel. [9] Section Computational Science, Faculty of Science, University of Amsterdam, Science Park 904, room C3.147, 1090 GE Amsterdam, The Netherlands. [10] Institute of Materials Research, Helmholtz-Zentrum Geesthacht, Outstation at DESY, Building 25c Notkestr. 85, D-22607 Hamburg, Germany. [11] Micropaléontologie, UFR TEB Université P. & M. Curie, 75252 Paris, France. [12] Wyss Institute for Biologically Inspired Engineering at Harvard University, 60 Oxford Street, Cambridge, Massachusetts 02138, USA. [13] Australian Institute of Marine Science, PMB 3, Townsville, 4810 Queensland, Australia. [14] Department of Biomaterials, Max Planck Institute of Colloids and Interfaces, 14424 Potsdam, Germany. Correspondence and requests for materials should be addressed to P.F. (email: paola.fantazzini@unibo.it) or to G.F. (email: giuseppe.falini@unibo.it) or to S.G. (email: s.goffredo@unibo.it).

Climate change is among the biggest threats to the health of marine ecosystems. Rising atmospheric carbon dioxide partial pressure (pCO_2)[1] increases ocean surface pCO_2 due to CO_2 diffusion across the air-water interface, leading to ocean acidification (OA)[2]. Since global warming and OA are coupled and are predicted to act synergistically[3,4], the future health of marine ecosystems and their corresponding long-term economic impacts on human coastal populations remain uncertain[5–7]. It is therefore of great interest to understand how increasing atmospheric CO_2 concentrations will affect these marine habitats and the species that inhabit them.

Since the early 1800s, ocean pH has decreased from 8.2 by *ca.* 0.1 U[8] and, if CO_2 emissions continue at their current rates, the average sea surface pH is predicted to drop to 7.8 by the year 2100 (ref. 1). The Mediterranean Sea, with its closed circulation patterns and limited water exchange with the adjacent Atlantic Ocean, has already undergone a larger decrease in surface pH compared with the global average[9], making it an ideal site for OA studies[10–13].

Near Panarea Island, off the southwestern coast of Italy, lies a series of active volcanic vents in the seabed releasing CO_2 emissions that acidify the surrounding seawater, making this location an ideal natural laboratory for OA studies. The underwater CO_2 emissions generate a stable pH gradient with levels matching several Intergovernmental Panel on Climate Change (IPCC) sea surface pH predictions associated with different atmospheric CO_2 emission scenarios for the end of the century[1].

The present study investigates the effects of environmental pH on skeletal structures and growth at multiple length scales in the solitary scleractinian coral *Balanophyllia europaea* living along the pH gradient. We studied 74 corals of similar age (mean age of 12 years) that had spent their lives at the CO_2-pH gradient. Using a combination of scanning electron microscopy (SEM), atomic force microscopy (AFM), small-angle X-ray scattering (SAXS), micro computed tomography (μCT), nanoindentation, hydrostatic weight measurement and time-domain nuclear magnetic resonance (TD-NMR), we document the skeletal mass, bulk volume, pore volume, porosity, biomineral density, bulk density, hardness, stiffness (ratio between elastic stress and strain), biometry data, net calcification rate and linear extension rate for each coral. Weight measurements combined with TD-NMR data represent a non-destructive technique for quantifying skeletal porosity over length scales spanning from tens of nanometres to tens of micrometres[14,15], whereas μCT analysis permits a detailed large-scale quantitative 3D analysis of skeletal architecture, including the interseptal regions.

We show that in response to depressed calcification at lower pH, corals increase their skeletal porosity maintaining constant linear extension rate, which is important for reaching critical size at sexual maturity. However, higher skeletal porosity and reduced bulk density and stiffness may contribute to reduced mechanical strength, increasing damage susceptibility, which could result in increased mortality in an acidic environment.

Results

Study site and seawater carbonate chemistry. The four sites around the main vent are reported in Fig. 1. Site 1 (S1) has an

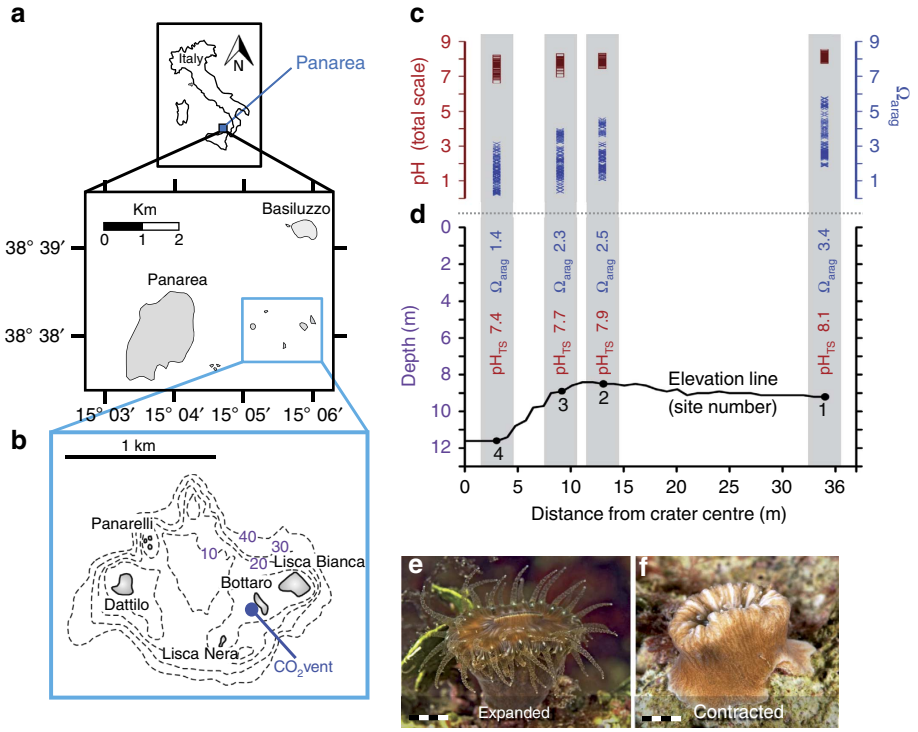

Figure 1 | Study location. Located off the southwestern coast of Italy (**a**), near Panarea Island (**b**), there are underwater volcanic vents releasing persistent gaseous emissions (98–99% CO_2 without instrumentally detectable toxic compounds), resulting in a stable pH gradient. Four sites at various distances from the primary vent were initially selected for study. No temperature difference exists among the four study sites throughout the year. (**c**) Ranges of measured pH_{TS} (number of observations [*n*] = 103–110 per site) and Ω_{arag} (*n* = 96–104 per site) values at the four sites, showing consistent increases in both pH_{TS} and Ω_{arag} from the vent crater to its periphery. (**d**) Bathymetric profile of the sites with associated mean pH_{TS} and Ω_{arag} values. No corals were found at Site 4, characterized by the lowest pH (mean pH_{TS} 7.4). Living specimens of *Balanophyllia europaea*, photographed at night with expanded tentacles (**e**) and during the day with contracted tentacles (**f**); marker 5 mm.

average total scale pH (pH_{TS}) of 8.1, equivalent to the average surface pH of modern oceans. S2's average pH_{TS} of 7.9 aligns with IPCC's predictions of a conservative CO_2 emissions scenario (Representative Concentration Pathway (RCP6.0)), and the average pH_{TS} of 7.7 for S3 fits the predictions of the 'business-as-usual' CO_2 emissions scenario (RCP8.5). Since no corals were found at S4 (within the vent crater, pH_{TS} 7.4), only S1–3, which had growing coral populations and pH_{TS} values ranging from 8.1 to 7.7, were included in the present study. Of the measured parameters at the three sites along the pH gradient (pH_{TS}, total alkalinity, temperature and salinity), only pH_{TS} differed significantly across sites ($N = 103$–110; $P < 0.001$, Kruskal–Wallis χ^2-test). The changing pH was accompanied by significant shifts in carbonate–bicarbonate equilibria, with aragonite saturation (Ω_{arag}) decreasing by >30% from S1 to S3 (Fig. 1, Supplementary Table 1, Supplementary Note 1).

Multi-scale analysis of coral skeletal properties. Combined results of SEM, µCT, AFM and TD-NMR skeletal analyses of corals growing at each study site revealed the detailed, multi-scale structural organization of the skeletons of *B. europaea* (Fig. 2, Supplementary Figs 1–3).

At the macroscale (relating to feature sizes >10 µm), linear extension rate (averaging *ca.* 1 mm per year) did not vary among sites (Supplementary Table 2), whereas net calcification rate ($N = 44$; $P < 0.01$, robust *t*-statistics test) and skeletal bulk density ($N = 44$, $P < 0.001$, robust *t*-statistics test) significantly declined (Fig. 3, Supplementary Table 3) and skeletal porosity and macroscale porosity increased ($N = 44$; $P < 0.001$, robust *t*-statistics test, Fig. 3, Supplementary Fig. 1, and Supplementary Table 3). The differences between S1 and S3 were *ca.* −18% for net calcification rate, *ca.* −7% for bulk density, *ca.* +21% for porosity and *ca.* +30% for macroscale porosity (Supplementary Table 2). The corallite interseptal volume fraction from µCT (Supplementary Fig. 4) showed a difference among sites ($N = 30$; $P < 0.05$, F and Kruskal–Wallis χ^2-tests, Supplementary Table 4) but no significant dependence on pH (Supplementary Fig. 5). The biometric data for the corallites (Supplementary Table 5) did not vary among sites.

At the micro/macroscale, skeletal stiffness significantly declined with decreasing pH ($n = 122$; $P < 0.001$, robust *t*-statistics test, Fig. 3, Supplementary Fig. 6, Supplementary Tables 4 and 6), whereas skeletal microscale porosity did not vary among sites (Supplementary Table 2 and Supplementary Fig. 1).

At smaller length scales (at the micro and nanoscales), SEM and AFM showed that the organization of the aragonite fibre bundles (Fig. 2c,g,k) and the morphology and packing of the constituent mineral grains (Fig. 2d,h,l) appeared similar among corals from the three different sites, confirming that the basic biomineralization products were not affected by reduced pH[13] (Fig. 2 and Supplementary Fig. 2). Skeletal biomineral hardness did not change among sites (Supplementary Fig. 7, Supplementary Table 4). Also, skeletal biomineral density values were similar across sites and consistent with those measured in previous studies[16] (Supplementary Table 2). Similar results were obtained from both SAXS and TD-NMR analyses, which revealed that nanoscale porosity did not change significantly with changing pH (Supplementary Figs 1e and 8–10 and Supplementary Tables 2 and 4).

The principal component analysis identified three major components: growth, skeletal porosity and biomineral density (Supplementary Tables 7 and 8). Only the first two components depended significantly on pH (Supplementary Table 9).

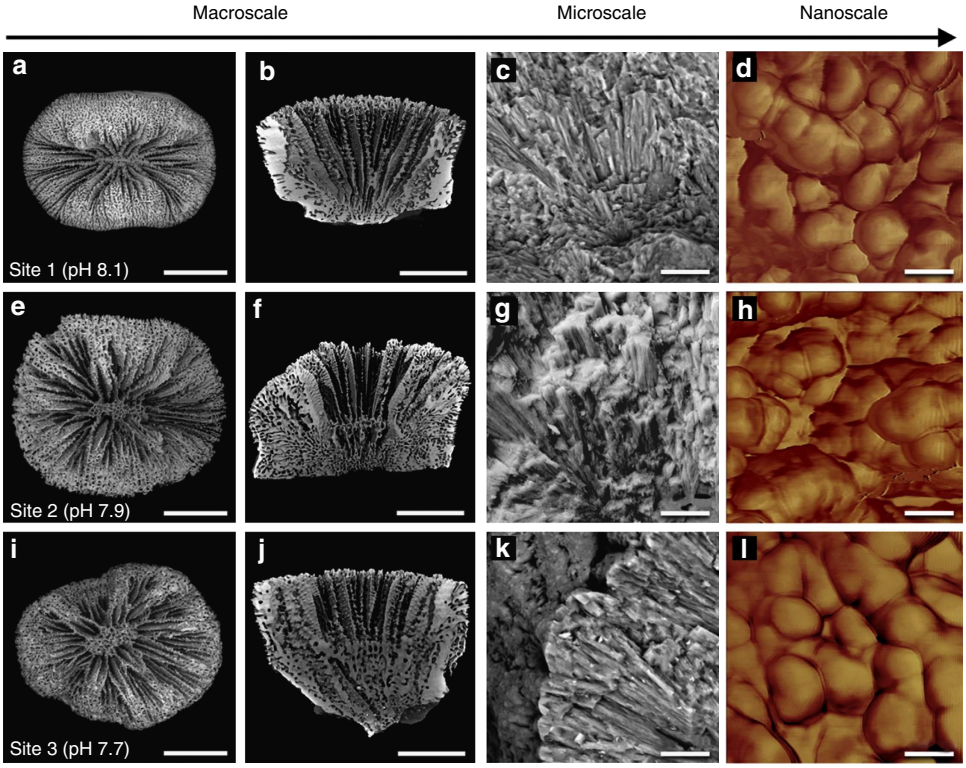

Figure 2 | Skeletal morphology of *Balanophyllia europaea* growing under different pH conditions from the macroscale to the nanoscale. Each row in the figure corresponds to a different study site and sample age is 9–11 years. Images are representative of all observed skeletons. (**a**,**e**,**i**) Low magnification SEM images of coral skeletons, marker 5 mm. (**b**,**f**,**j**) Internal sections of corallites from µCT images, marker 5 mm. (**c**,**g**,**k**) SEM images of entire skeletal fibres from fractured septae, marker 10 µm. (**d**,**h**,**l**) AFM images of mineral grains on the skeletal fibre surfaces, marker 50 nm.

In summary, skeletal nano and microstructural features, linear extension rate, interseptal volume fraction and corallite biometry of *B. europaea* did not change significantly with decreasing pH, despite a clear reduction in net calcification rates. This reduction in net calcification rate was accompanied by an increase in skeletal porosity (Fig. 3f, $N=44$; $P<0.001$, robust *t*-statistics test) and a consequent decrease in skeletal bulk density and stiffness.

Discussion

Results of the present study complement previous research on *B. europaea* at this same vent site, which revealed no changes in skeletal calcium carbonate polymorph, organic matrix content, aragonite fibre thickness and skeletal hardness in corals growing along the pH gradient[13]. There was, however, a significant reduction in population density along the pH gradient, decreasing by a factor of 3 with increasing proximity to the vent crater centre (that is, from S1 to S3)[13].

Figure 4 summarizes these results at the ocean, population, macro, micro and nanoscales for *B. europaea*. At the macroscale, increasing acidity was associated with a reduction in net calcification rate and a parallel increase in skeletal porosity, coupled with a decrease in skeletal bulk density. Linear extension rate and corallite shape (biometry and interseptal volume fraction) did not depend on pH, probably as a result of the compensation of reduced net calcification rate by increased skeletal porosity. At the micro/macroscale, the declining skeletal stiffness with decreasing pH could be coupled to an increased volume fraction of pores having a size comparable to the indentation area (that is, at the border between the micro and macroscales). At the nanoscale, porosity, biomineral hardness and density were not significantly affected by pH. These results, bolstered by qualitative SEM and AFM analyses, suggest that the 'building blocks' produced by the biomineralization process are substantially unaffected, but the increase in skeletal porosity is both a gain and a loss for the coral. In fact, in an acidic

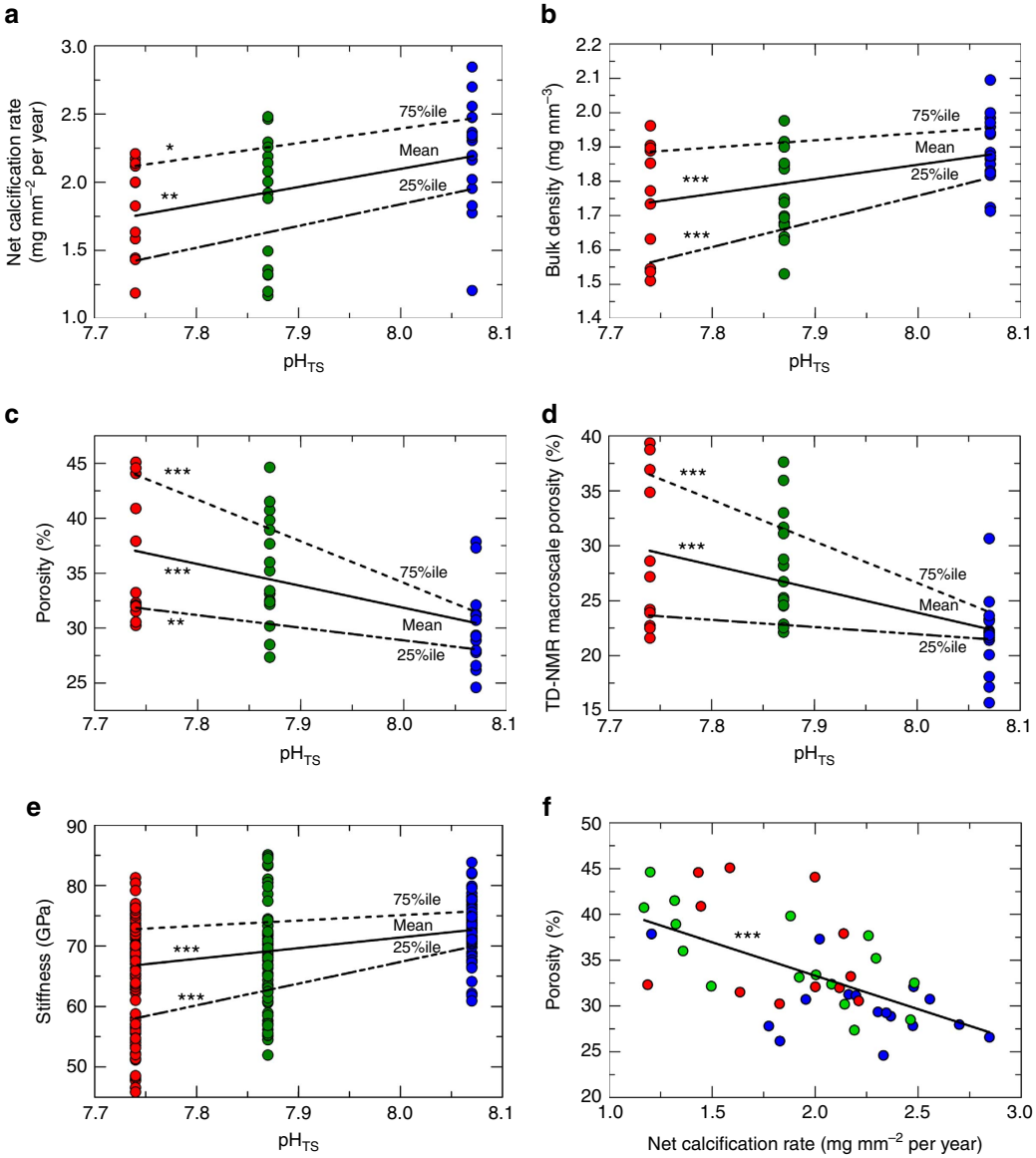

Figure 3 | Scatterplots of skeletal parameters, and correlation analysis between porosity and net calcification rate. Site 1 = blue, Site 2 = green, Site 3 = red. Straight lines represent the best-fit linear regression (mean, solid line), 25% quantile and 75% quantile (dashed lines). (**a**–**e**) Skeletal parameters (*y*-axes) plotted against pH_{TS}. (**f**) Scatterplot of porosity (P_A) versus net calcification rate in corals from Sites 1 to 3. For **a**–**d**,**f** $N=44$; for **e** $n=122$. ***$P<0.001$; **$P<0.01$; *$P<0.05$, robust *t*-statistics test.

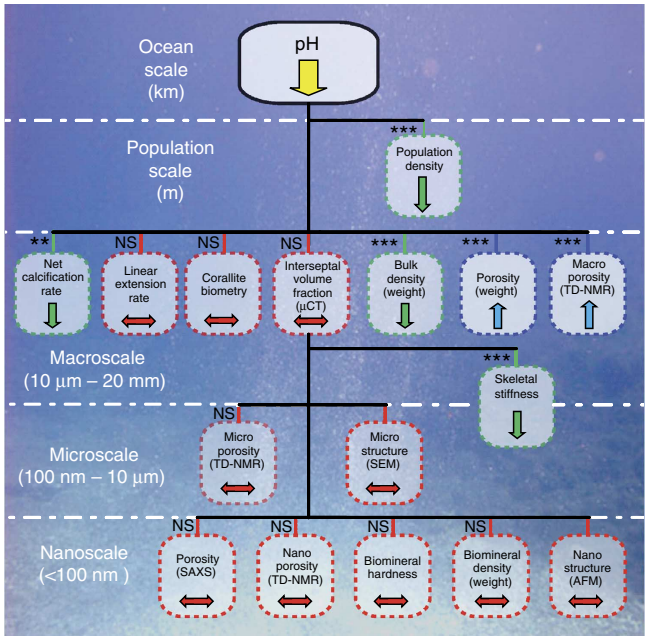

Figure 4 | Summary of responses in *Balanophyllia europaea* skeletal parameters as a function of pH from the ocean to the nanoscale. The significant decline in population density with pH was measured in previously published research[13]. Net calcification rate and bulk density decrease with decreasing pH, whereas porosity (P_A) increases, preserving the linear extension rate and corallite shape (biometry and interseptal volume fraction as measured by µCT do not correlate with pH). The increase in porosity is associated with a decrease in skeletal stiffness. At the nanoscale, the 'building blocks' (the fundamental structural components of the coral skeleton, aragonite fibre bundles and their constituent mineral grains) produced by the biomineralization process are substantially unaffected by increased acidity. Green boxes denote parameters found to have a direct relationship with pH, blue boxes denote parameters that have an inverse relationship and red boxes denote parameters found to have no relationship with pH. The significances of the regression of each parameter (dependent variable) with pH (independent variable) are indicated; $***P<0.001$; $**P<0.01$; NS indicates no significance. Micro and nanoscale structure observations by SEM and AFM represent qualitative data.

environment, where the net calcification is depressed, enhanced macroporosity keeps linear extension rate constant, potentially meeting functional reproductive needs (for example, the ability to reach critical size at sexual maturity); however, it also reduces the mechanical strength of the skeletons, increasing damage susceptibility, which could result in increased mortality and the observed population density decline[13].

While the results reported here for *B. europaea* may not be representative of the generalized response of all coral species to OA, they are consistent with field observations made on other reef-building scleractinians. For example, while maintaining constant skeletal linear extension, decreased rates of calcification and losses in bulk skeletal density as a function of reduced aragonite saturation have been observed in *Montastraea annularis*[17] and *Porites astreoides*[18]. While low aragonite saturation as a sole driver for the observed reduction in coral calcification has been discussed[19], our conclusions regarding a balance between reduced net calcification rate and increased macroporosity to maintain constant linear extension can explain the outcomes of those studies[17,18]. In fact bulk density depends both on biomineral density and porosity. Our multi-scale analysis shows that all the skeletal features at the nano and microscales, including biomineral density, are unchanged. The decrease of bulk density with decreasing pH depends on the increase of macroporosity, leaving the linear extension rate constant.

Our findings, together with the well-described detrimental effects of heat stress on the scleractinian zooxanthellate coral *B. europaea*[16,20–23], provide several independent and consistent clues regarding the sensitivity of this species to global climate change predicted for the coming decades. Together with results from previous studies[24], we demonstrate that the almost universally employed measure of coral biomineralization, namely the rate of linear extension, might not be a reliable metric for assessing coral health and resilience in a warming and acidifying ocean. Indeed, although the coral's ability to maintain linear extension rate and gross skeletal morphology under conditions of decreasing oceanic pH could allow it to reach sexual maturity, it could reduce skeletal resistance to environmental challenges, affecting the long-term survivability of the species.

Methods

Study site. Off the southwestern coast of Italy, near the island of Panarea, an area delimited by the islets of Dattilo, Bottaro, Lisca Nera and Lisca Bianca (Fig. 1) is characterized by underwater volcanic CO_2 vents. The main vent, a crater measuring 20 m × 14 m and ~10-m deep, generates a persistent column of CO_2 bubbles that rise from the seabed to the sea surface. In this hydrothermally stable setting with ambient temperature, CO_2 emissions establish a pH gradient that extends ~34 m from the centre of this crater to its periphery[13]. Three sites along this pH gradient were chosen for study. Distances (d) from the main crater centre and mean pH_{TS} values of the three sites from which corals were collected are: S1 (the control site), $d=34$ m, $pH_{TS}=8.07$; S2, $d=13$ m, $pH_{TS}=7.87$; S3, $d=9$ m, $pH_{TS}=7.74$. Water depth varies from 11.6 m within the crater to 8.8 m at the crater edge (S2) to 9.2 m at the outer margins (S1), where the local pH matches that of the surrounding seawater. The study site has stable hydrothermal–chemical properties[25].

The corals. *B. europaea* (Fig. 1) is a solitary zooxanthellate scleractinian coral endemic to the Mediterranean Sea found at depths ranging from 0 to 50 m[26]. Specimens of *B. europaea* were randomly collected by SCUBA diving at the three study sites along the pH gradient (26 from S1, 26 from S2 and 22 from S3) between November 2010 and May 2013. This sample size was chosen to limit damage on the natural population, which significantly diminishes in the most acidic sites[13], and was considered suitable for properly describing the skeletal properties, as shown in previous studies[13,14]. Biometric data were recorded for the specimens (that is, width-to-length, width-to-height and height-to-length ratios, Supplementary Table 5). Nanoindentation, hydrostatic weight measurement, SEM, AFM, SAXS, µCT and TD-NMR analyses were performed on a subsample of specimens from each site.

Coral sample cleaning. Coral skeletons were submerged in 1% solution of sodium hypochlorite for 3 days to dissolve polyp tissue. After washing with deionized water and drying at 50 °C for 3–4 days, each coral was examined under a binocular microscope to remove fragments of sediment, rock and encrusting organisms[16].

Weight measurements. The buoyant method, usually applied for corals[27–29], was used to measure the total volume occupied by the coral skeleton (called bulk volume, V_B), the bulk density (d_b, ratio of the mass to V_B), the biomineral density (d_r, ratio of the biomineral mass to biomineral volume, excluding pore volume connected to the external surface, also called real density or micro-density) and the apparent porosity (or effective or connected porosity, P_A)[30] (ratio of the pore volume connected to the external surface (V_A) to V_B). This method is based on the Archimedean principle applied to a specimen after full saturation with the same fluid in which it is submerged (water in our case). It is worth to underline that the pore volume (V_A) measured by the buoyant method is only the volume of the pores that can be saturated with water, that is, connected with the external surface. Pores inside the biomineral that are not connected to the external surface (occluded pores) are not measured. An estimate of the occluded porosity gave a negligible maximum value of ~3% (in porosity units) (Supplementary Note 2), which was homogeneous among sites. For coherence with coral literature, for the apparent porosity we use the term porosity.

The skeletons were weighed with a precision balance to determine the dry mass (m) and then placed inside a dryer chamber and evacuated with a rotary mechanical pump down to a vacuum of 10^{-2} mbar. After 6 hours, water was gently introduced to fully saturate the samples. The pump was switched off, the chamber was vented to the ambient atmosphere, and the masses of the fully water-saturated samples (m_s) determined. With a hydrostatic balance, the masses of saturated samples fully immersed in water (m_h) were determined. The skeletal parameters were calculated (Supplementary Table 2) by means of the following operational definitions: ρ_w = water density, $V_A=(m_s-m)/\rho_w$; $V_B=(m_s-m_h)/\rho_w$; $P_A=V_A/V_B=(m_s-m)/(m_s-m_h)$; $d_b=m/V_B$; $d_r=m/(V_B-V_A)$.

After weight measurement, the fully saturated samples were removed from the water container and rapidly placed on wet paper to remove excess water on the external surface. Each specimen was then placed in the bottom of a glass tube, which was then sealed for TD-NMR measurements.

TD-NMR method and parameter definitions. This technique (Supplementary Note 3) was applied to obtain skeletal 'pore-size' distributions by the analysis of quasi-continuous distributions of the transverse relaxation time T_2 (ref. 14) by means of the algorithm UPEN[31], implemented in the UpenWin software[32]. Supplementary Figure 1a shows examples of T_2 distributions for specimens of *B. europaea*. In all cases, the slope of the distribution presented a strong increase at a specific T_2 value, the 'cutoff', revealing a sharp boundary between two distinct pore classes. This point was chosen as the boundary between smaller (shorter T_2) and larger (longer T_2) pores. The ratio of the area under the distribution for T_2 larger than the cutoff to the total area under the distribution, called 'macroscale pore volume fraction' (Supplementary Fig. 1b), indicates the fraction as a percentage of the pore volume in the macroscale. On the basis of the comparison with mercury intrusion porosimetry data, the sizes of pores in the macroscale pore volume fraction, corresponding to the major fraction of pores, are >10–$20\,\mu m$. The tail in the distribution is about 3 orders of magnitude long and should correspond to smaller pore sizes up to tens of nanometres[14]. The distribution with $T_2 < 3$ ms was chosen to identify the signal corresponding to water in the smallest pores or size-scale, which we refer to here as 'nanoscale pore volume fraction'. The remaining fraction of the distribution is called 'microscale pore volume fraction'. The nano, micro and macroscale pore volume fractions multiplied by the skeletal porosity (Supplementary Table 2) produced the TD-NMR nano, micro and macroscale porosities, respectively.

TD-NMR apparatus and data acquisition. A homebuilt relaxometre based on a 0.2 T permanent magnet operating at 8 MHz was used for acquisition of the transverse relaxation curve of the ^{1}H nuclei of water molecules saturating the cleaned coral skeletons. The relaxometer was equipped with a coil $\sim$2 cm in diameter to analyse the entire coral and a Spinmaster console (Stelar, Mede, Pavia, Italy) for automatic pulse sequence transmission and data acquisition. The transverse relaxation data were acquired by using the Carr–Purcell–Meiboom–Gill sequence[33] with a 200 µs echo time. Sixteen corals from S1, 16 corals from S2 and 12 corals from S3 were analysed.

SEM images. To investigate the meso and macroscale organization of the aragonite fibre bundles, SEM analyses were performed. The cleaned coral skeletons were mounted (uncoated) to conductive carbon tape and examined with a Tescan Vega3 GMU (Czech Republic) variable pressure scanning electron microscope. Three corals per site were analysed.

Evaluation of net calcification rate. The age of each coral was determined based on growth band analysis via computerized tomography[22,34]. The linear extension rate was obtained by dividing the length of each sample (maximum axis of the oral disc) by its age. The net calcification rate was calculated as: net calcification rate = bulk density × linear extension rate[21,35] (Supplementary Table 2).

µCT analysis. To compute the corallite interseptal volume fraction (ratio of the total pore space volume inside the corallite to the total volume occupied by the corallite itself), µCT analyses were acquired and the convex hull approach was followed. µCT scans of coral skeletons were performed with a GE phoenix X-ray Nanotom S. The voxel sizes in the scans varied from 2.91 to 13.25 µm depending on the actual size of the investigated coral sample. All image processing steps in the analysis were performed with the open source software FIJI[36]. Supplementary Fig. 3 shows different views of the 3D volume renderings obtained from three corals of the same age from each of the three study sites. Ten corals from each site were analysed.

Nanoindentation. To analyse mechanical properties of the coral skeletons, skeletal stiffness (Young's modulus) and hardness were determined by Oliver–Pharr analysis of load-depth curves[37], using a Nanoindentation Tester, model NHT-TTX by CSM Instruments, Switzerland, equipped with a Berkovich diamond tip (opening angle = 142.3°). On each sample, a minimum of 10 indentation tests were carried out, in the oral region, with a minimum distance of 30 µm between two tests (the total number of tests for each site is reported in Supplementary Table 4). To avoid influence from the embedding resin, a minimum distance of 100 µm from the skeleton/resin boundaries was always maintained.

SAXS analysis. To obtain information on skeletal porosity at the nanoscale, SAXS analyses (Supplementary Note 4) were performed on three corals per site. Sections were mounted onto a laboratory SAXS apparatus with a rotating anode X-ray generator (Bruker, AXS, Karlsruhe, Germany) operating with a copper anode. Light microscopy images of the three specimens are shown in Supplementary Fig. 8 together with X-ray radiographies taken with the SAXS instrument.

AFM analysis. To study the morphology and packing of skeletal mineral grains at the nanoscale, AFM images were acquired. Samples were lightly polished using diamond paste, cleaned with milli-Q water and observed using a Veeco AFM Dimension 3100 Nanoscope III, Plainview, NY. The probe consisted of a cantilever with an integrated silicon nitride tip. Samples were imaged at room temperature and in air using tapping mode phase contrast imaging.

Statistical analysis. Statistical analyses (analysis of variance, multivariate, principal components and quantile analysis) were performed using the Statistical Package STATA 9.0 (StataCorp LP). To test the significance of the differences among sites, parametric (F) or non-parametric (Kruskal–Wallis χ^2) tests were run. Non-parametric tests were performed for data that did not assume normal distributions. Multivariate regression analyses were performed to investigate the relationships between one dependent and one or several independent variables, using ordinary least squares robust to outliers. The model is described by the equation (1):

$$y_i = a + \sum_{j=1}^{M} b_j x_{i,j} + \varepsilon_i \quad (1)$$

where the index i refers to the i-observation, x_j is an independent variable, y_i is the value of the dependent variable and ε_i is the corresponding error. The constants a, b_j ($j = 1, M$) are the best-fit parameters, to be determined by the best fit. Quantile analysis was performed to study the previous relationships for homogeneous groups of values of the dependent variable. This analysis was used to give a more comprehensive picture of the effect of the independent variable (pH) on the dependent variables of Fig. 3 and Supplementary Fig. 1, as it can show different effects of the independent variable in different ranges of the dependent variable.

References

1. Stocker, T. F. *et al.*in *Climate Change 2013: The Physical Science Basis* (Cambridge Univ. Press, 2013).
2. Sabine, C. L. *et al.* The oceanic sink for anthropogenic CO_2. *Science* **305,** 367–371 (2004).
3. Six, K. D. *et al.* Global warming amplified by reduced sulphur fluxes as a result of ocean acidification. *Nat. Clim. Change* **3,** 975–978 (2013).
4. Rodolfo-Metalpa, R. *et al.* Coral and mollusc resistance to ocean acidification adversely affected by warming. *Nat. Clim. Change* **1,** 308–312 (2011).
5. Hoegh-Guldberg, O. *et al.* Coral reefs under rapid climate change and ocean acidification. *Science* **318,** 1737–1742 (2007).
6. Dove, S. *et al.* Future reef decalcification under a business-as-usual CO_2 emission scenario. *Proc. Natl Acad. Sci. USA* **110,** 15342–15347 (2013).
7. Pandolfi, J. M., Connolly, S. R., Marshall, D. J. & Cohen, A. L. Projecting coral reef futures under global warming and ocean acidification. *Science* **333,** 418–422 (2011).
8. Orr, J. C. *et al.* Anthropogenic ocean acidification over the twenty-first century and its impact on calcifying organisms. *Nature* **437,** 681–686 (2005).
9. Touratier, F. & Goyet, C. Impact of the Eastern Mediterranean transient on the distribution of anthropogenic CO_2 and first estimate of acidification for the Mediterranean Sea. *Deep-Sea Res. I* **58,** 1–15 (2011).
10. Yilmaz, A. *et al.* Impact of acidification on biological, chemical and physical systems in the Mediterranean and Black Sea Mediterranean. *Mediterranean Sci. Committee (CIESM), Monograph Ser.* **36,** 124 (2008).
11. Calvo, E. *et al.* Effects of climate change on Mediterranean marine ecosystems: the case of the Catalan Sea. *Climate Res.* **50,** 1–29 (2011).
12. Ziveri, P. Research turns to acidification and warming in the Mediterranean Sea, IMBER (Integrated Marine Biogeochemistry and Ecosystem Research). http://www.imber.info/index.php/News/Newsletters/Issue-n-20-May-2012 (2012).
13. Goffredo, S. *et al.* Biomineralization control related to population density under ocean acidification. *Nat. Clim. Change* **4,** 593–597 (2014).
14. Fantazzini, P. *et al.* Time-Domain NMR study of Mediterranean scleractinian corals reveals skeletal-porosity sensitivity to environmental changes. *Environ. Sci. Technol.* **47,** 12679–12686 (2013).
15. Laine, J., Labady, M., Albornoz, A. & Yunes, S. Porosities and pore sizes in coralline calcium carbonate. *Mater. Charact.* **59,** 1522–1525 (2008).
16. Caroselli, E. *et al.* Environmental implications of skeletal micro-density and porosity variation in two scleractinian corals. *Zoology* **114,** 255–264 (2011).
17. Carricart-Ganivet, J. P. Sea surface temperature and the growth of the West Atlantic reef-building coral *Montastraea annularis*. *J. Exp. Marine Biol. Ecol.* **302,** 249–260 (2004).
18. Crook, E. D., Cohen, A. L., Rebolledo-Vieyra, M., Hernandez, L. & Paytan, A. Reduced calcification and lack of acclimatization by coral colonies growing in areas of persistent natural acidification. *Proc. Natl Acad. Sci. USA* **110,** 11044–11049 (2013).
19. Iglesias-Prieto, R., Galindo-Martinez, C. T., Enriquez, S. & Carricart-Ganivet, J. P. Attributing reductions in coral calcification to the saturation state of

aragonite, comments on the effects of persistent naturals acidification. *Proc. Natl Acad. Sci. USA* **111,** E300–E301 (2014).
20. Goffredo, S., Caroselli, E., Mattioli, G., Pignotti, E. & Zaccanti, F. Variation in biometry and demography of solitary corals with environmental factors in the Mediterranean Sea. *Mar. Biol.* **152,** 351–361 (2007).
21. Goffredo, S. *et al.* Inferred level of calcification decreases along an increasing temperature gradient in a Mediterranean endemic coral. *Limnol. Oceanogr.* **54,** 930–937 (2009).
22. Goffredo, S., Caroselli, E., Mattioli, G., Pignotti, E. & Zaccanti, F. Relationships between growth, population structure and sea surface temperature in the temperate solitary coral *Balanophyllia europaea* (Scleractinia, Dendrophylliidae). *Coral Reefs* **27,** 623–632 (2008).
23. Airi, V. *et al.* Reproductive efficiency of a Mediterranean endemic zooxanthellate coral decreases with increasing temperature along a wide latitudinal gradient. *PLoS ONE* **9,** e91792 (2014).
24. Wooldridge, S. A. Assessing coral health and resilience in a warming ocean: Why looks can be deceptive. *Bioessays* **36,** 1041–1049 (2014).
25. Capaccioni, B., Tassi, F., Vaselli, O., Tedesco, D. & Poreda, R. Submarine gas burst at Panarea Island (southern Italy) on 3 November 2002: A magmatic versus hydrothermal episode. *J. Geophys. Res.* **112,** B05201 (2007).
26. Zibrowius, H. Les scleractiniaires de la Méditerranée et del'Atlantique nord-oriental. *Mem. Inst. Oceanogr* **11,** 1–284 (1980).
27. Jokiel, R. L., Maragos, J. E. & Franzisket, L. In: *Coral Reef Research Methods.* (eds Stoddart, D. R. & Johannes, R. E.) **5** 529–542 (UNESCO, 1978).
28. Davies, P. S. Short-term growth measurements of corals using an accurate buoyant weighing technique. *Mar. Biol.* **101,** 389–395 (1989).
29. Walsh, S.-J. in Proceedings of 12th International Coral Reef Symposium, Cairns, Australia, 9–13 July 2012.
30. Manger, G. E. Porosity and bulk density of sedimentary rocks. *Geol. Survey Bull.* **1144–E** (1963).
31. Borgia, G. C., Brown, R. J. S. & Fantazzini, P. Examples of marginal resolution of NMR relaxation peaks using UPEN and diagnostics. *Magn. Reson. Imaging* **19,** 473–475 (2001).
32. Bortolotti, V., Brown, R. J. S. & Fantazzini, P. *UpenWin: a Software to Invert Multi-Exponential Decay Data;* http://wwwunibo.it/PortaleEn/Research/Services + for + companies/UpenWin.htm (2009).
33. Cowan, B. *Nuclear Magnetic Resonance and Relaxation* (Cambridge Univ. Press, 1997).
34. Goffredo, S., Mattioli, G. & Zaccanti, F. Growth and population dynamics model of the Mediterranean solitary coral *Balanophyllia europaea* (Scleractinia Dendrophylliidae). *Coral Reefs* **23,** 433–443 (2004).
35. Lough, J. M. & Barnes, D. J. Environmental controls on growth and of the massive coral *Porites*. *J. Exp. Mar. Biol. Ecol.* **245,** 225–243 (2000).
36. Schindelin, J. *et al.* Fiji: an open-source platform for biological-image analysis. *Nat. Methods* **9,** 676–682 (2012).
37. Oliver, W. C. & Pharr, G. M. An improved technique for determining hardness and elastic modulus using load and displacement sensing indentation experiments. *J. Mater. Res.* **7,** 1564–1583 (1992).

Acknowledgements

The research leading to these results has received funding from the European Research Council under the European Union's Seventh Framework Programme (FP7/2007–2013)/ERC grant agreement n° 249930—CoralWarm: Corals and global warming: the Mediterranean versus the Red Sea. Bartolo Basile, Francesco Sesso and Eolo Sub diving center assisted in the field. Francesca Gizzi and Giorgia Polimeni helped during preparation and participated in field surveys. The Scientific Diving School collaborated with the underwater activities. We are grateful to Ingrid Zenke (MPI Potsdam) for help with the SAXS measurements, Michela Reggi for sample preparation, Gianni Neto and Francesco Sesso for the images in the Panarea site.

Author contributions

S.G., G.F., P.F., L.P. and Z.D. conceived and designed the research. E.C., F.P., S.G. and B.C. collected the samples and performed the diving field work. L.B., M.M., M.D.G., E.C., F.P., P.K., J.U.H., Y.D., J-P.C., J.C.W., W.W. and G.F. performed the laboratory analyses. P.F., S.M., L.P., V.B., L.B., M.M., E.C., F.P., J.A.K., P.K., J.U.H., Y.D., J-P.C., J.C.W., W.W., P.F., G.F. and S.G. analysed the data. All authors wrote the manuscript and participated in the scientific discussion.

Additional information

Supplementary Information accompanies this paper at http://www.nature.com/naturecommunications

Competing financial interests: The authors declare no competing financial interests.

Reprints and permission information is available online at http://npg.nature.com/reprintsandpermissions/

How to cite this article: Fantazzini, P. *et al.* Gains and losses of coral skeletal porosity changes with ocean acidification acclimation. *Nat. Commun.* 6:7785 doi: 10.1038/ncomms8785 (2015).